

DESIGN INVESTIGATION OF CYLINDRICAL
STRUCTURES OTHER THAN HONEYCOMB

FINAL REPORT

1 JUNE 1965 TO 30 NOVEMBER 1965

CONTRACT NO. NAS8-20009

CONTROL NO. DCN 1-5-53-01082-01 (IF)

GPO PRICE \$ _____

CFSTI PRICE(S) \$ _____

Hard copy (HC) 46.00

Microfiche (MF) 41.50

653 July 65

FACILITY FORM 602

N66-19133

(ACCESSION NUMBER)

264

(PAGES)

CR 70373

(NASA CR OR TMX OR AD NUMBER)

(THRU)

(CODE)

32

(CATEGORY)



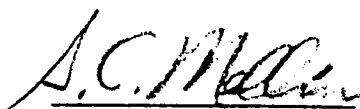
NORTH AMERICAN AVIATION, INC. / LOS ANGELES DIVISION

DESIGN INVESTIGATION OF CYLINDRICAL
STRUCTURES OTHER THAN HONEYCOMB

FINAL REPORT
1 JUNE 1965 TO 30 NOVEMBER 1965

CONTRACT NO. NAS8-20009
CONTROL NO. DCN 1-5-53-01082-01(1F)

PREPARED BY



S. C. MELLIN
STRUCTURES RESEARCH

APPROVED BY



A. L. KOLOM
PROGRAM MANAGER

DATE 31 December 1965

NO. OF PAGES 226



NORTH AMERICAN AVIATION, INC. / LOS ANGELES DIVISION
INTERNATIONAL AIRPORT • LOS ANGELES, CALIFORNIA 90009

FOREWORD

This report was prepared by North American Aviation, Inc, Los Angeles Division under Contract No. NAS8-20009, "Design Investigation of Cylindrical Structures Other Than Honeycomb," for the George C. Marshall Space Flight Center Administration. The work was administered under the technical direction of the Propulsion and Vehicle Engineering Laboratory, George C. Marshall Space Flight Center, with James B. Dalton II and Lester Katz acting as Project Managers.

ABSTRACT

19133

Increasingly demanding aerospace missions require continued advancement in all pertinent technical disciplines. The value of increased payload is evident from the major efforts in miniaturization of electronics and sophistication of subsystems. Comparable payload increases are attainable through improvements of structures by exploiting recent developments in materials and producibility technologies.

The objective of this program is a minimum weight design investigation of unconventional structures/materials concepts for large diameter unpressurized booster shells. A unique concept, the double-wall structure, is developed in this investigation. The double-wall concept offers a significant weight advantage over conventional designs in a wide range of load levels.

A two-phase program is employed to achieve lightweight structural concepts. The first phase involves a parametric theoretical study of unpressurized cylindrical shells. A matrix of over 10,000 structural/material/design points is developed. An optimization screening of the resulting designs is performed. The second phase of the program is a detailed evaluation of six selected concepts. Final data is obtained for over 300 design points.

The theoretical basis of this investigation is small deflection analysis. A large deflection analysis is conducted for the most attractive detailed designs.

Presentation of final data in the form of design drawings and design charts provides direct utilization of program accomplishments.



ACKNOWLEDGEMENTS

Mr. Stanley C. Mellin was the principal investigator, responsible for technical direction and coordination of the program. Mr. Aaron L. Kolom provided general program direction.

Recommendations and guidance were provided by MSFC/P&VE Structures Division personnel.

NAA personnel contributing to the program include: D. H. Emero, R. V. Cimino, C. E. Conn, V. W. Alvey from LAD and S. M. Gee and A. M. Bickham from S&ID.

TABLE OF CONTENTS

	Page
FOREWORD	i
ABSTRACT	ii
ACKNOWLEDGEMENTS	iii
TABLE OF CONTENTS	iv
LIST OF ILLUSTRATIONS	vii
LIST OF TABLES	x
NOTATION	xi
INTRODUCTION	1
CONCEPTUAL DESIGN	4
Importance of Unpressurized Segments of Booster Shells	4
Evolution of Double-Wall Concept	4
Design Investigation Technical Approach	5
DESIGN CRITERIA	9
Load Levels	9
Shell Diameter and Length	9
Candidate Materials	11
Candidate Cover Panel and Substructure Concepts	17
Load/Geometry/Material/Concept Matrix	20
SUMMARY OF PARAMETRIC STUDY AND DETAILED DESIGN	21
Design Principles	21
Six Selected First Phase Design Concepts	22
Practical Design Considerations	40
Design Drawings and Charts	42
Optimum Structural Concept/Material Matrix	42
General Comments on Optimum Designs	52
Use of Design Drawings, Graphs, and Summary Tables	54
Double-Wall Truss Core Sandwich Cover Panels With Sine-wave Shear Web Substructure	55

	Page
Double-wall Trapezoidal Corrugation Cover Panels With Sine-wave Shear Web Substructure	66
Double-wall Truss Core Semisandwich Cover Panels With Truss Web Substructure	76
Double-wall Integrally Stiffened Cover Panels With Truss Rib Substructure	86
Double-wall Integrally Zee Stiffened Cover Panels With Truss Rib Substructure	96
Ring Stiffened Trapezoidal Cover Concept	105
STRUCTURAL OPTIMIZATION ANALYSIS	112
Ring Stiffened Cylinder	112
Shanley Stability Criterion	112
Arie VanderNeut Stability Criterion	114
Summary of Results	115
Double-wall Cylinders	122
Method of Analysis	122
General Cylinder Stability	122
Panel Stability	126
Verification of Attainment of Simple Panel Support	127
Non-optimum Structure	132
Balanced Design Procedure	133
Honeycomb Sandwich Cylinders	141
Significance of Length/Diameter	158
Background	158
Ring Stiffened Cylinder Analysis	159
Double-wall Cylinder Analysis	160
Comparison of Structural Stiffness of Optimum Concepts	165
Large Deflection Analysis	165
Introduction	165
Honeycomb and Double-wall Cylinders	169
Results of Large Deflection Analysis	171
Increased General Stability Safety Factor	171

	Page
COST ANALYSIS	186
FOLLOW-ON TESTING PROGRAM	205
Introduction	205
Proposed Follow-on Program Plan	205
Test Program Scope	205
Short Column Tests	206
Panel Tests	207
Substructure Tests	209
Joint Tests	210
Double-wall Concept Tests	210
Final Report	210
Alternate Experimental Analyses	211
Objectives of Experimental Analyses	211
REFERENCES	212

LIST OF ILLUSTRATIONS

Figure No.	Title	Page
1	Typical Launch Vehicle Skirt Segments (Saturn V)	2
2	Evolution of the Double-wall Concept.	6
3	Range of Cylinder Diameters and Lengths Investigated.	10
4	Stress-Strain Curves in Compression	13
5	Stress-Strain Curves in Compression	14
6	Candidate Cover Panel Concepts.	18
7	Candidate Substructure Concepts	19
8	Weight Versus Load for 400-inch Diameter Cylinders (State-of-the-Art Materials)	24
9	Weight Versus Load for 200-inch Diameter Cylinders (State-of-the-Art Materials)	25
10	Weight Versus Load for 400-inch Diameter Cylinders - Comparison of Truss Web and Sine-Wave Shear Web Substructures	26
11	Weight Versus Load for 400-inch Diameter Cylinders - Comparison of Truss Web and Biaxial Truss Substructures	27
12	Weight Versus Load for 400-inch Diameter Cylinders (Advanced Materials).	28
13	Weight Versus Load for 200-inch Diameter Cylinders (Advanced Materials).	29
14	Weight Versus Load for 400-inch Diameter Cylinders - Comparison of Truss-Web and Sine-Wave Shear Web Substructures	30
15	Selected Concept - Double-wall Truss Core Sandwich.	34
16	Selected Concept - Double-wall Trapezoidal Corrugation.	35
17	Selected Concept - Double-wall Truss Core Semisandwich.	36
18	Selected Concept - Double-wall Integrally Stiffened Panel	37
19	Selected Concept - Double-wall Zee Stiffened Panel.	38
20	Selected Concept - Ring Stiffened Cylinder.	39
21	Final Weight Versus Load Diagrams for 400-inch Diameter (State-of-the-Art Materials).	44
22	Final Weight Versus Load Diagrams for 200-inch Diameter (State-of-the-Art Materials).	45
23	Final Weight Versus Load Diagrams for 400-inch Diameter (Advanced Materials).	46
24	Final Weight Versus Load Diagrams for 200-inch Diameter (Advanced Materials).	47
25	Optimum Concepts for State-of-the-Art Materials - Load Versus Diameter	48

Figure No.	Title	Page
26	Optimum Concepts for Advanced Materials - Load Versus Diameter.	49
27	Cost/Weight Trade Study Chart 5,000 lb/in..	50
28	Cost/Weight Trade Study Chart 15,000 lb/in.	51
29	Illustration of the Use of Design Graphs.	54
30	Design Drawing - Double-wall Truss Core Sandwich.	58
31	Design Graph - Double-wall Truss Core Sandwich.	59
32	Panel Weight Versus Load - Truss Core Sandwich.	65
33	Design Drawing - Double-wall Trapezoidal Corrugation.	68
34	Design Graph - Double-wall Trapezoidal Corrugation.	69
35	Panel Weight Versus Load - Trapezoidal Corrugation.	75
36	Design Drawing - Double-wall Truss Core Semisandwich.	78
37	Design Graph - Double-wall Truss Core Semisandwich.	79
38	Panel Weight Versus Load - Truss Core Semisandwich.	85
39	Design Drawing - Double-wall Integrally Stiffened	88
40	Design Graph - Double-wall Integrally Stiffened Panel	89
41	Panel Weight Versus Load - Integrally Stiffened Panel	95
42	Design Drawing - Double-wall Zee Stiffened Panel.	97
43	Design Graph - Double-wall Zee Stiffened Panel.	98
44	Panel Weight Versus Load - Zee Stiffened Panel.	104
45	Design Drawing - Trapezoidal Ring Stiffened Cylinder.	107
46	Design Graph - Trapezoidal Ring Stiffened Cylinder.	108
47	Panel Weight Versus Load-Ring Stiffened Trapezoidal Corrugation	111
48	Ring Stiffened Construction Comparison Various Types of Construction (State-of-the-Art Materials)	117
49	Ring Stiffened Construction Comparison - Various Types of Construction (Advanced Materials)	118
50	Ring Stiffened (Trapezoidal Corrugation R = 100 Inches.	119
51	Ring Stiffened Trapezoidal Corrugation R = 200 Inches	120
52	Ring Stiffened Trapezoidal Corrugation - Optimum Material	121
53	Buckling Coefficient for Sandwich Cylinders	124
54	Minimization of Buckling Coefficient.	125
55	Stability of 3 Bay Plate.	129
56	Buckling Curves - Column With Infinite Number of Spans.	130
57	Illustration of Symmetrical and Antisymmetrical Buckling Terms	131
58	Definition of Panel Geometry Terms.	139
59	Typical Weight-load Variation (R = 100 Inches).	143
60	Typical Weight-load Variation (R = 200 Inches).	144
61	Weight Versus Load - 400-inch Diameter - State-of-the-Art Materials (Wide Column)	145
62	Weight Versus Load - 400-inch Diameter - Advanced Materials (Wide Column)	146
63	Weight Versus Load - 400-inch Diameter - State-of-the-Art Materials (Plate)	147

Figure No.	Title	Page
64	Weight Versus Load - 400-inch Diameter - Advanced Materials (Plate)	148
65	Weight Versus Load - Full Depth Honeycomb Cylinders	149
66	Envelope of Optimum Materials for Honeycomb	150
67	Weight Versus Load - Envelope of Constrained Parameters (Honeycomb)	151
68	Variation of K_{MIN} With Shell Buckling Parameters.	162
69	Comparison of Primary Bending Stiffness of Selected Concepts to Honeycomb (D = 400).	166
70	Comparison of Primary Bending Stiffness of Selected Concepts to Honeycomb (D = 200).	167
71	Postbuckling Response of Isotropic Cylinders With Initial Imperfections	168
72	K versus V_x for Large Deflection Analysis	172
73	Weight Comparison Large Deflection Theory Versus Small Deflection Theory	174
74	Weight Comparison Large Deflection Theory Versus Small Deflection Theory	177
75	Weight Comparison Large Deflection Theory Versus Small Deflection Theory	179
76	Margin of Safety Effect Integrally Stiffened Wide Column Beaded Truss Substructure Aluminum X7106.	185
77	Effect of Quantity on Cost of Various Design Concepts (P = 2000 lb/in.)	188
78	Effect of Quantity on Cost of Various Design Concepts (P = 5000 lb/in.)	189
79	Effect of Quantity on Cost of Various Design Concepts (P = 15000 lb/in.)	190
80	Cost/Weight Trade Study Chart (P = 5000 lb/in.)	191
81	Cost/Weight Trade Study Chart (P = 15000 lb/in.)	192
82	Test Values Versus Theory	208

LIST OF TABLES

Table No.	Title	Page
I	Design Load Levels.	9
II	Shell Diameters Considered for Design Investigations.	11
III	Candidate Materials With Minimum Gage Restraints.	12
IV	Definition of Material Categories	12
V	Summary of State-of-the-Art Materials Properties.	15
VI	Summary of Advanced Material Properties	16
VII	Six Selected Optimum Concepts	32
VIII	Optimum Materials for Selected Concepts	43
IX	Double-wall Truss Core Sandwich Geometry and Weight Summary	61
X	Double-wall Trapezoidal Corrugation Geometry and Weight Summary	72
XI	Double-wall Truss Core Semisandwich Geometry and Weight Summary	82
XII	Double-wall Integrally Stiffened Panel Geometry and Weight Summary.	92
XIII	Double-wall Zee Stiffened Panel Geometry and Weight Summary	101
XIV	Trapezoidal Ring Stiffened Cylinder Geometry and Weight Summary	109
XV	Ring Stiffened Cylinder Coefficients.	116
XVI	Integrally Stiffened Panel Geometry Versus Column Length. . .	134
XVII	Column Length Versus Panel Weight	134
XVIII	Computer Output Data - Substructure Properties.	136
XIX	Integrally Stiffened Wide-column Double Wall Computer Summary	142
XX	Summary of Honeycomb Geometry (P = 2000 lb/in.)	153
XXI	Summary of Honeycomb Geometry (P = 5000 lb/in.)	154
XXII	Summary of Honeycomb Geometry (P = 8000 lb/in.)	155
XXIII	Summary of Honeycomb Geometry (P = 12000 lb/in.)	156
XXIV	Summary of Honeycomb Geometry (P = 15000 lb/in.)	157
XXV	Cylinder Lengths.	158
XXVI	Minimum K Values.	161
XXVII	Circumferential Half-wave Lengths	163
XXVIII	Number of Longitudinal Half-waves	164
XXIX	Longitudinal Half-wave Lengths.	164
XXX	Weight and Configuration Comparison - Full Depth Honeycomb Shell	173
XXXI	Weight and Configuration Comparison - Integrally Stiffened Wide Column With Beaded Truss Substructure.	175
XXXII	Weight and Configuration Comparison - Full Depth Honeycomb Sandwich Shell.	176

Table No.	Title	Page
XXXIII	Weight and Configuration Comparison.	178
XXXIV	Weight and Configuration Comparison.	180
XXXV	Weight Increments Caused by Variation In M.S..	183
XXXVI	Weight Increase Versus Panel Height for Varing M.S..	184
XXXVII	Summary of Dash Numbered Parts in Assembly = 1 5000 =/in. - Truss Core, Sine Weld.	193
XXXVIII	Summary of Dash Numbered Parts in Assembly = 1 15000=/in. - Truss Core, Sine Weld.	194
XXXIX	Summary of Dash Numbered Parts in Assembly = 2 5000 =/in. - Semi-Sand, Bead Truss.	195
XL	Summary of Dash Numbered Parts in Assembly = 2 15000 =/in. - Semi-Sand, Bead Truss.	196
XLI	Summary of Dash Numbered Parts in Assembly = 3 5000 =/in. - Trap. Core-Sine Weld	197
XLII	Summary of Dash Numbered Parts in Assembly = 3 15000 =/in. - Trap. Core-Sine Weld	198
XLIII	Summary of Dash Numbered Parts in Assembly = 4 5000 =/in. - Integral Skin-Sine 2	199
XLIV	Summary of Dash Numbered Parts in Assembly = 4 15000 =/in. - Integral Skin-Sine 2	200
XLV	Summary of Dash Numbered Parts in Assembly = 5 5000 =/in. - Zee Stiff, Sine Zee.	201
XLVI	Summary of Dash Numbered Parts in Assembly = 5 15000 =/in. - Zee Stiff, Sine Zee.	202
XLVII	Summary of Dash Numbered Parts in Assembly = 6 2000 =/in. - Ring Stiff Trapezoid	203
XLVIII	Summary of Dash Numbered Parts in Assembly = 6 5000 =/in. - Ring Stiff Trapezoid	204

NOTATION

a	Length of cylinder (in.)
b	Plate support spacing (in.)
b _s	Stiffener spacing (in.)
b _w	Stiffener height (in.)
b _f	Stiffener flange width (in.)
b _d	Stiffener diagonal dimension (in.)
C	Panel width in circumferential direction (in.)
C _f	Ring stiffener coefficient
D	Cylinder diameter (in.)
E _c	Compression modulus of elasticity (lb/in. ²)
E _s	Secant modulus of elasticity (lb/in. ²)
E _t	Tangent modulus of elasticity (lb/in. ²)
e	Strain (in./in.)
F _{cy}	Compressive yield stress (lb/in. ²)
F _{PL}	Proportional limit stress (lb/in. ²)
F _{su}	Ultimate shear stress (lb/in. ²)
F _{bru}	Ultimate bearing stress (lb/in. ²)
F _{.7}	Reference stress .7E _c e (lb/in. ²)
F _{.85}	Reference stress .85E _c e (lb/in. ²)
G	Shear modulus of elasticity (lb/in. ²)
f _{cr}	Critical buckling stress (lb/in. ²)
G _{xz}	Longitudinal core shear modulus (lb/in. ²)
G _{yz}	Circumferential core shear modulus (lb/in. ²)
h	Distance between cover panel centers of gravity (in.)
h _f	Ring stiffener height (in.)
I	Moment of inertia of ring (in. ⁴)
I _x	Moment of inertia in axial direction (in. ⁴ /in.)
I _y	Moment of inertia in circumferential direction (in. ⁴ /in.)
k _c	Buckling coefficient
L	Panel length in longitudinal direction (in.)
l	Ring spacing, cover support spacing (in.)
m	Number of half-waves in axial direction
N _x	Axial load intensity (lbs/in.)
n	Number of waves in circumferential direction
R	Cylinder radius (in.)
t	Total equivalent shell thickness (in.)
t _{sp}	Splice thickness (in.)
t _s	Skin thickness (in.)
t _w	Stiffener thickness (in.)
t _f	Ring stiffener thickness (in.)
t _{fr}	Equivalent frame thickness (in.)

\bar{t}	Equivalent thickness of skin, also effective thickness of single cover
t_1	Outer wall area (in. ² /in.)
t_2	Inner wall area (in. ² /in.)
V_x	Core shear parameter
WGT.	Shell weight (lbs/ft ²)
W_{pen}	Weight penalty (lb/ft ²)
W_{spl}	Splice weight (lb/ft ²)
W_{att}	Splice attachment weight (lb/ft ²)
W_{cap}	Shear web cap weight (lb/ft ²)
W_{pad}	Cover pad weight (lb/ft ²)
W_{attp}	Substructure fastener weight (lb/ft ²)
W_{bond}	Substructure bond weight (lb/ft ²)
W_{LJ}	Weight of longitudinal splice (lb)
W_{CJ}	Weight of circumferential splice (lb)
W	Splice width (in.)
μ	Poisson's ratio
ρ	Material density, radius of gyration
σ_a	Applied stress (lb/in. ²)
σ_e	Euler wide column allowable stress (lb/in. ²)
σ_{cr}	Local plate element allowable buckling stress (lb/in. ²)
η_s	$= \frac{E_s}{E}$
η_t	$= E_t/E$
η_c	Plasticity - reduction factor
ϵ	Structural efficiency coefficient
θ	$= \frac{G_{xz}}{G_{yz}}$
ξ	$= \left(\frac{na}{m\pi r} \right)^2$
η	$= \frac{a^2 \sqrt{1 - \mu^2} (t_1 + t_2)}{2 m^2 n^2 r h \sqrt{t_1 t_2}}$
$\bar{\eta}$	$\eta_T^{3/4}$
η_T	Ramberg Osgood plasticity correction factor
ψ	Structural load index

INTRODUCTION

Achievement of increasingly demanding aerospace missions requires continued advancement in all technical disciplines involved. The value of increased payload and/or improved mission performance is evident from the major efforts in miniaturization of electronics and sophistication of subsystems. Comparable payload increases are attainable through improvement of structures by exploiting recent developments in materials and producibility technologies.

The objective of this program is the design investigation of unconventional structures/materials concepts to minimize structural weight of large diameter unpressurized booster shells. Unpressurized segments offer a significant area for weight savings. The importance of advancing the state-of-the-art in this field becomes evident, for example, in view of the fact that 27 percent of the structural weight of Saturn V goes into skirt structures. (Reference 1). This report summarizes the design investigation performed to achieve practical lightweight structures described generally as "other-than-honeycomb."

A unique concept, the double-wall structure, is developed in this investigation. Efficient double-wall configurations and typical areas of applicability are shown in figure 1. The double-wall concept offers a significant weight advantage over conventional designs in a wide range of load levels.

Double-wall structure evolves from the honeycomb sandwich concept. The double-wall structural arrangement replaces delicate honeycomb core with more rugged, more widely spaced, cover panel supporting substructure elements. In order to carry high stress levels, the isotropic honeycomb facing sheet is replaced with a built-up plate element. In comparison with full-depth honeycomb, double-wall substructure is lighter and the facings or cover panels are heavier. Thus, areas of shell diameter and load level exist where each concept has a weight advantage.

A two-phase program is employed to achieve lightweight structural concepts. The general approach is considered to be complementary application and blending of advanced manufacturing and advanced structural design technologies into improved reliable structures. Considerations include new material and composite developments coupled with fabrication technique improvements.

The first phase involves a parametric theoretical study of unpressurized cylindrical shells. A matrix of over 10,000 structural/material/design points is developed and an optimization screening of the resulting designs is performed. The matrix results from the consideration of approximately thirty concepts; ten materials, four diameters, five N_x load levels, and certain manufacturing variations. The analytical evaluation and progressive elimination includes strength, weight, and producibility factors. Full-depth honeycomb, analyzed by consistent theory, is the basis of weight comparison.

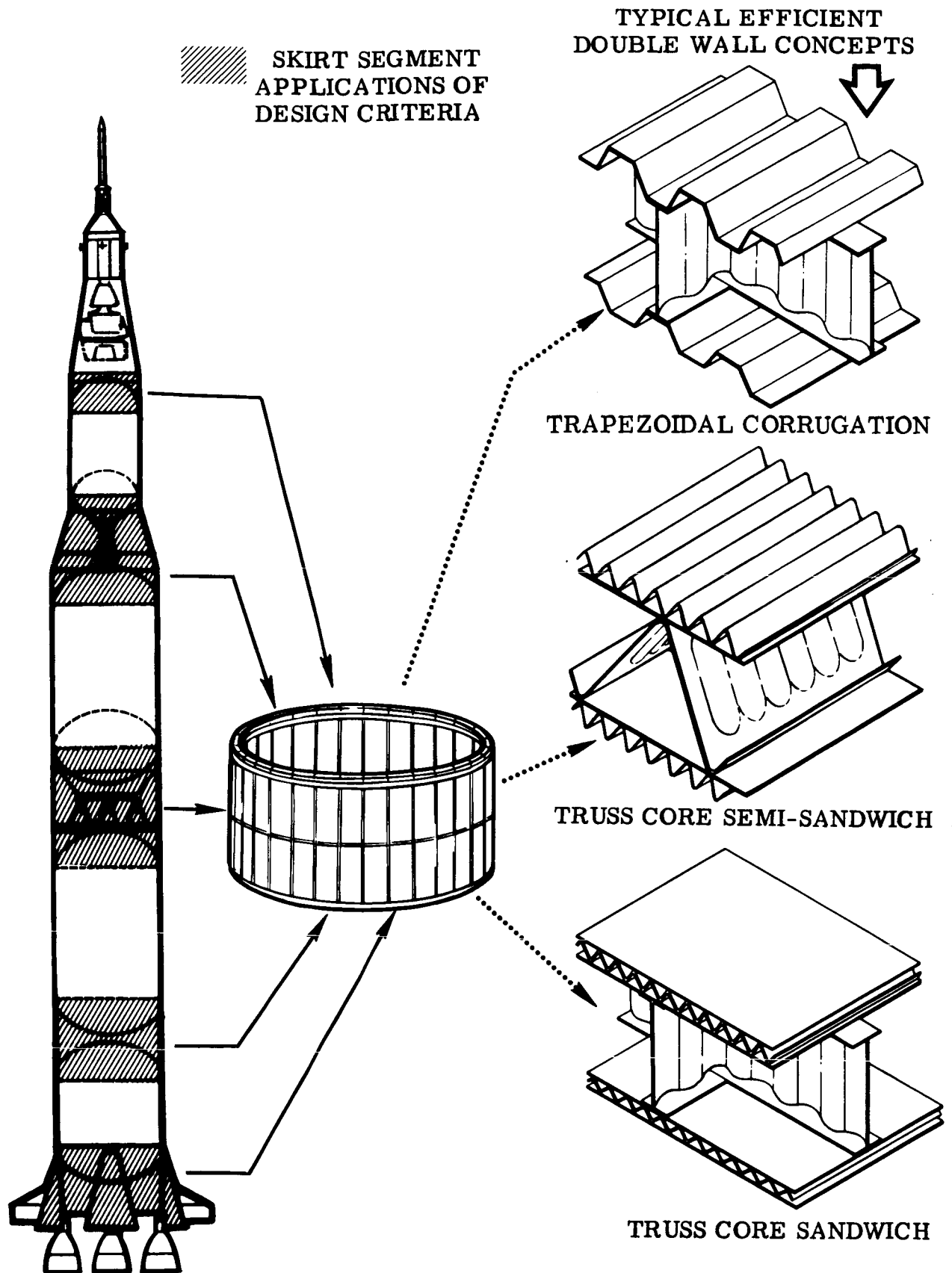


Figure 1. Typical Launch Vehicle Skirt Segments (Saturn V)

Detailed design evaluation of six selected concepts is performed in the second phase of this investigation. These optimum concepts are carried to completion for most promising candidate materials. Final data is obtained for over 300 design points.

In practical structural design applications cost considerations are paramount. A structural cost-effectiveness analysis is performed in the second phase, which permits selection of the optimum design concept in accordance with cost/weight trade-off values. This approach employs the value of weight saving as a common denominator. The optimum design concept varies for different applications; for a payload stage an exotic approach to weight reduction is justified, for a booster stage a simpler, low-cost structure is applicable. Value engineering provides greatest benefits as a selection guide for initial design, rather than after-the-fact product improvement.

The basis of this comparative evaluation is small-deflection analysis. A large deflection analysis is conducted for the most attractive detailed design concepts and design ramifications of the more conservative post-buckling theory are established.

Presentation of final data in the form of design drawings and design charts provides direct utilization of program accomplishments.

CONCEPTUAL DESIGN

IMPORTANCE OF UNPRESSURIZED SEGMENTS OF BOOSTER SHELLS

The objective of this program is the investigation of advanced structures/materials design concepts to minimize structural weight of large diameter unpressurized booster shells. The Saturn V configuration illustrates utilization of unpressurized shell segments in large launch vehicle technology (figure 1). Important unpressurized connecting booster structures include:

1. Thrust structure
2. Intertank structure
3. Interstage structure

Unpressurized segments of boosters offer a significant area for weight savings. The importance of advancing the state-of-the-art in this field becomes evident, for example, in view of the fact that 27 percent of the structural weight of Saturn V goes into skirt structures (Reference 1).

Increased performance of existing systems is attainable directly by replacing segments of existing boosters with more efficient, i.e., lighter weight unpressurized structure. Application of advanced structural concepts has further advantages when applied in the preliminary design stage. The percentage allocation of total structural weight to unpressurized versus pressurized tank segments results from compromises between intertank skirt design and tank design. Lightweight unpressurized structure permits greater latitude in tank design parameter trade-offs and, therefore, offers potential for further decreases in structural weight.

EVOLUTION OF DOUBLE-WALL CONCEPT

Unpressurized booster designs, currently in production, utilize two basic types of construction:

1. Conventional (skin-stringers supported by ring frames)
2. Honeycomb

This study investigates unconventional structures/materials arrangements to establish competitive practical designs for varying load levels and shell diameters.

The double-wall concept is shown to be a most competitive design for a wide range of load levels. The double-wall structure is a development of the

honeycomb concept. The double-wall concept replaces delicate honeycomb substructure with more rugged, more widely spaced, cover panel supporting elements. In order to carry high stress levels efficiently, the isotropic honeycomb facing sheet is replaced with a built-up plate element. In comparison with full-depth honeycomb, double-wall substructure is lighter and the facing structure or skin plate elements are heavier. Thus, areas of shell diameter and load level exist where each concept has a weight advantage.

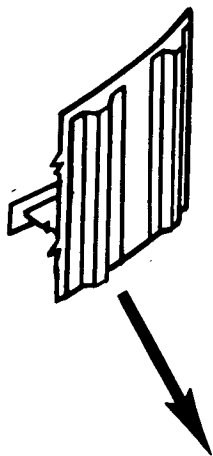
The evolution of the unconventional double-wall structural concept is shown in figure 2. Conventional aluminum construction provides reliable low-cost structure, which is efficient at low load levels and "small" cylinder radii. As loadings and radii increase, the ring-stiffened shell is not competitive because each of the ring frames is a significant weight item that does not carry load. Honeycomb sandwich increases structural efficiency over a certain load/diameter region but has a limitation in minimum practical core density. Core weight and face sheet-to-core bonding agent weight become excessive. Double-wall composite structure, with various panel concepts and substructure arrangements, provides an efficient cylindrical shell structure in the 2,000 to 15,000 lb/in. range of loads and the 200-400-inch diameters investigated. Qualities of double-wall structure contributing to minimum weight design are:

1. All cover panel material carries axial load.
2. Panel material simultaneously provides shell stiffness and eliminates weight penalty associated with nonload-carrying ring frames.
3. Lightweight substructure permits large increases in shell general stability:
 - a. Bending rigidity increased by a deeper section
 - b. Shear rigidity increased by reinforcement of substructure
4. Selective directional placement of materials in cover panels and substructure provides most efficient configuration for a particular design application.

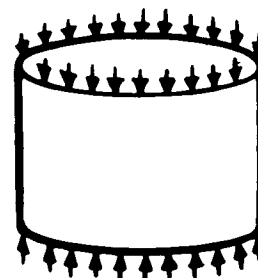
DESIGN INVESTIGATION TECHNICAL APPROACH

A technical program, divided into four major tasks, is employed to develop efficient double-wall structural configurations:

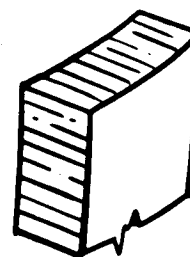
1. Establishment of potentially attractive design concepts and a load/geometry/material/concept matrix
2. Parametric evaluation and progressive screening of concept matrix

CYLINDRICAL SHELL
AXIAL LOADSCONVENTIONAL DESIGN

- MATERIAL - ALUMINUM
- SKIN - STRINGERS
DESIGN STRESS - 45 KSI
- FRAME STABILIZATION - 25% SKIN WEIGHT

HONEYCOMB SANDWICH

- HIGH STRESS - REDUCED SKIN WEIGHT
- CORE STABILIZES SKINS PROVIDES GENERAL STABILITY
- CORE WEIGHT LIMITS
EFFICIENCY FOR LARGE SHELLS &
HIGH LOAD INDICES

DOUBLE-WALL CONCEPTS

- MAXIMUM PANEL EFFICIENCY
- SUBSTRUCTURE PROVIDES
GENERAL (BENDING & SHEAR)
STABILITY AT MINIMUM WEIGHT

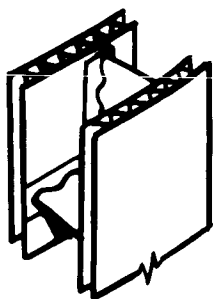


Figure 2. Evolution of the Double-wall Concept

3. Design trade-off studies of selected concepts

4. Presentation of study parameters as design charts

Steps 1 and 2 are considered as the first phase of this program. Steps 3 and 4 constitute the second phase. The first phase evaluation is performed with a minimum of restraints, such as minimum element thickness. This approach is used to show true potential without the influence of arbitrary restraints. The second phase effort is directed toward practical design details, such as minimum gages and practical attachment and joint provisions. Final design emphasis is on feasibility and reliability of selected concepts.

The load/geometry/material/concept matrix developed in the first phase is summarized in the section entitled "Design Criteria." The concept matrix comprises over 10,000 design points. Parametric evaluation and progressive screening of the concept matrix includes an evaluation of the strength/weight relation coupled with producibility/design. Feasibility, fabrication, attachment, and assembly considerations yield a number of most promising designs.

The first reduction in the matrix of designs is accomplished by qualitative evaluation of materials, their mechanical properties, and producibility. A second screening reduction establishes optimum configuration types. It is noted that the suitability of the wall concepts to efficient panel splice design and substructure to cover panel attachment is a most important factor in selecting optimum configurations. Splices and joints are investigated to ensure realism in practical concept selection. Further preliminary screening includes first-order structural efficiency evaluations of the two primary components of the wall structure: the load-carrying cover panels and the stabilizing substructure. A number of configurations were carried beyond the tentative screening point for a numerical check of the screening procedure and to ascertain that attractive concepts were not overlooked.

Six optimum concepts are selected at the conclusion of first phase effort for detailed design and analysis in the second phase.

The second phase design trade-off studies develop feasible designs for the six selected concepts. The transition from unrestrained configurations to feasible designs involves two primary factors: minimum material gages and penalties associated with panel splices and cover panel to substructure attachments. Maximum panel dimensions are established. All designs are based on a consistent one material cover panel/substructure arrangement. Thus, the results have a greater applicability and flexibility. For instance, alternate methods of attachment are equally applicable with similar materials, whereas, dissimilar materials limit available joining methods.

A cost analysis is performed in the second phase, which permits selection of the optimum design concept in accordance with established guidelines of cost/weight trade-off values. This approach employs the value of weight saving as a common denominator. The optimum design concept varies for different applications. For a payload stage an exotic approach to weight reduction is justified, while for a booster stage a simpler low cost structure is applicable. Value engineering provides a selection guide for initial design rather than "after-the-fact" product improvement.

A large-deflection analysis is conducted for the most attractive detailed design concepts. Recommendations are made as to design ramifications of the post-buckling theory.

Presentation of data in the form of design drawings and design charts summarizes program accomplishments.

DESIGN CRITERIA

LOAD LEVELS

The design loadings for unpressurized booster structure are imposed by launch loads, wind shear, steering, staging operations, ground gusts, prelaunch fueling, and ground handling. The principal loads are circumferentially distributed compressive forces due to engine thrust reacted by inertia. Incremental forces due to cylinder bending moments are super-imposed upon the axial forces. In this investigation the summation of compressive and bending forces is considered as an equivalent axial load per inch.

Load level restraint limits evaluated are 2,000 pounds/inch and 15,000 pounds/inch. Evaluations are performed in five increments: 2,000, 5,000, 8,000, 12,000, and 15,000 pounds per inch (table I). The applied loads are considered to be ultimate loads.

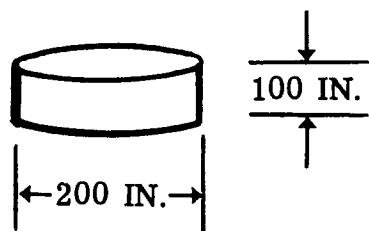
Table I
DESIGN LOAD LEVELS
(ULTIMATE LOADS)

Item	Axial Load
	Lb/in.
1	2,000
2	5,000
3	8,000
4	12,000
5	15,000

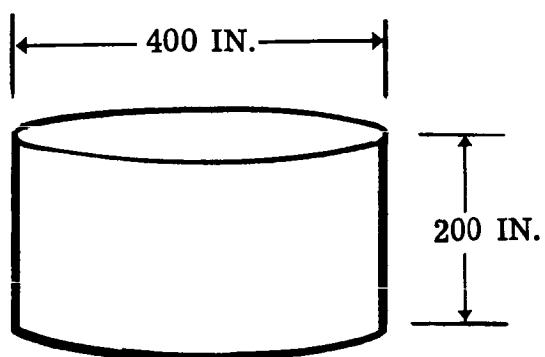
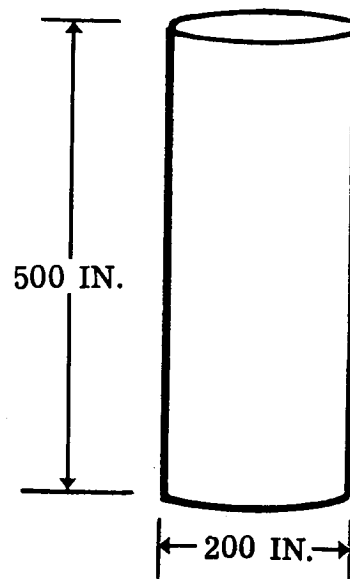
SHELL DIAMETER AND LENGTH

The effect of cylinder diameter on optimum design due to the general stability requirement is investigated in this study. The parametric design screening of the load/geometry/material/concept matrix will consider four diameters: 200 inches, 267 inches, 333 inches, and 400 inches (table II).

The effect of length of the cylindrical shell is investigated for length to diameter ratios varying from 0.5 to 2.5. Resulting ranges of lengths for the given diameters are shown in figure 3. Analyses are conducted in appropriate ranges.



A) MINIMUM DIAMETER



B) MAXIMUM DIAMETER

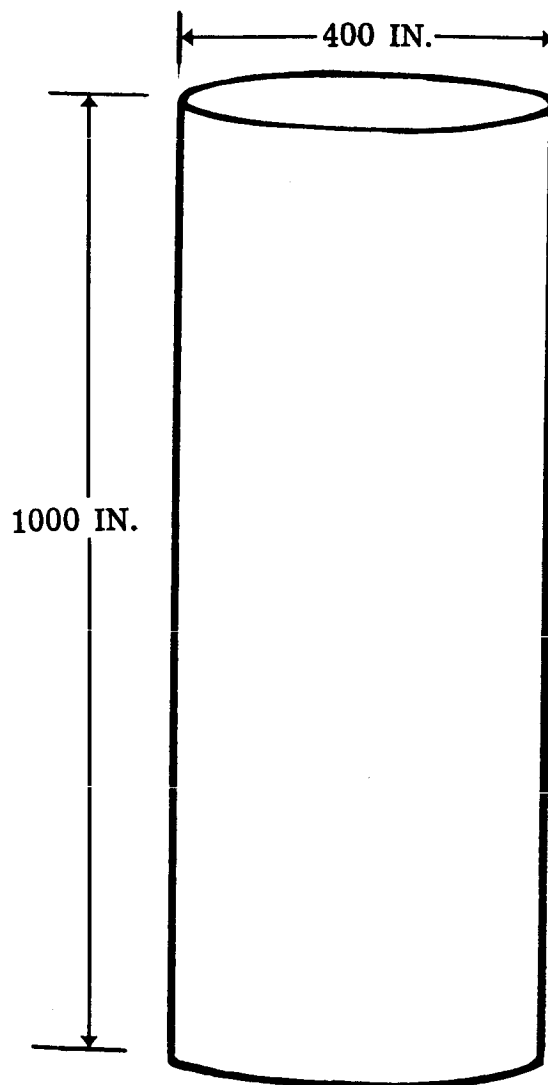


Figure 3. Range of Cylinder Diameters and Lengths Investigated

Table II
SHELL DIAMETERS CONSIDERED
FOR DESIGN INVESTIGATION

Item	Diameter (Inches)
1	200
2	267
3	333
4	400

CANDIDATE MATERIALS

A wide range of structural alloys were considered as candidate materials in the first phase of the design investigation. Metallic load-carrying materials and composite load-carrying materials which have high strength-to-weight ratios, and which show adaptability to a variety of optimum design concepts and fabrication methods are evaluated. The goal of the first phase material selection is the screening of alloys showing the greatest potential with respect to the cost/weight and related parameters. Potential materials selected in the first phase are listed in table III. These materials are considered to be representative alloys of the candidate materials. Compressive stress-strain curves for these representative alloys are presented in figures 4 and 5.

Fabricability and producibility are primary considerations in the practical design application of materials to lightweight structures. A most important criterion in evaluating lightly-loaded structure is the minimum practical material thickness. Minimum gages for the representative materials are shown in table III. It is noted that the tabulated multiwall gages entitled inner and outer refer to the primary structural members of the cover panels and substructure, respectively.

A great variation exists in the level of technology required for fabrication of design concepts from different candidate materials. Screening selection is, therefore, divided into two basic categories: state-of-the-art materials and advanced materials (refer to table IV).

Material properties for each of the representative alloys are summarized in tables V and VI. Minimum guaranteed values are used to establish material allowables.

Table III

CANDIDATE MATERIALS WITH MINIMUM GAGE RESTRAINTS

Material		Minimum Gages		
		Multiwall		Single -Wall
		Inner	Outer	
1	Aluminum (X7106-T6)	.010	.015	.020
2	Titanium (6Al-4V)	.010	.010	.010
3	Stainless Steel (PH15-7Mo)	.010	.010	.010
4	Maraging Steel (18 Ni)	.010	.010	.010
5	Beryllium	.020	.020	.020
6	Beryllium 62%/Aluminum 38% Alloy	.015	.015	.020
7	Boron 30%/Titanium (6Al-4V) 70% Composite	.020	.020	.020
8	Magnesium (AZ31-H24)	.020	.020	.020
9	S-994 Glass Fiber	.015	.015	.015
10	Aluminum/Polyethylene Composite	.010 A1	.010 A1	.010 A1

Table IV

DEFINITION OF MATERIAL CATEGORIES

State-of-the-art Materials	Advanced Materials
Aluminum	Beryllium
Titanium	Beryllium/Aluminum Alloy
Stainless Steel	Boron/Titanium Composite
Maraging Steel	S-994 Glass Fiber
Magnesium	Aluminum/Polyethylene Composite

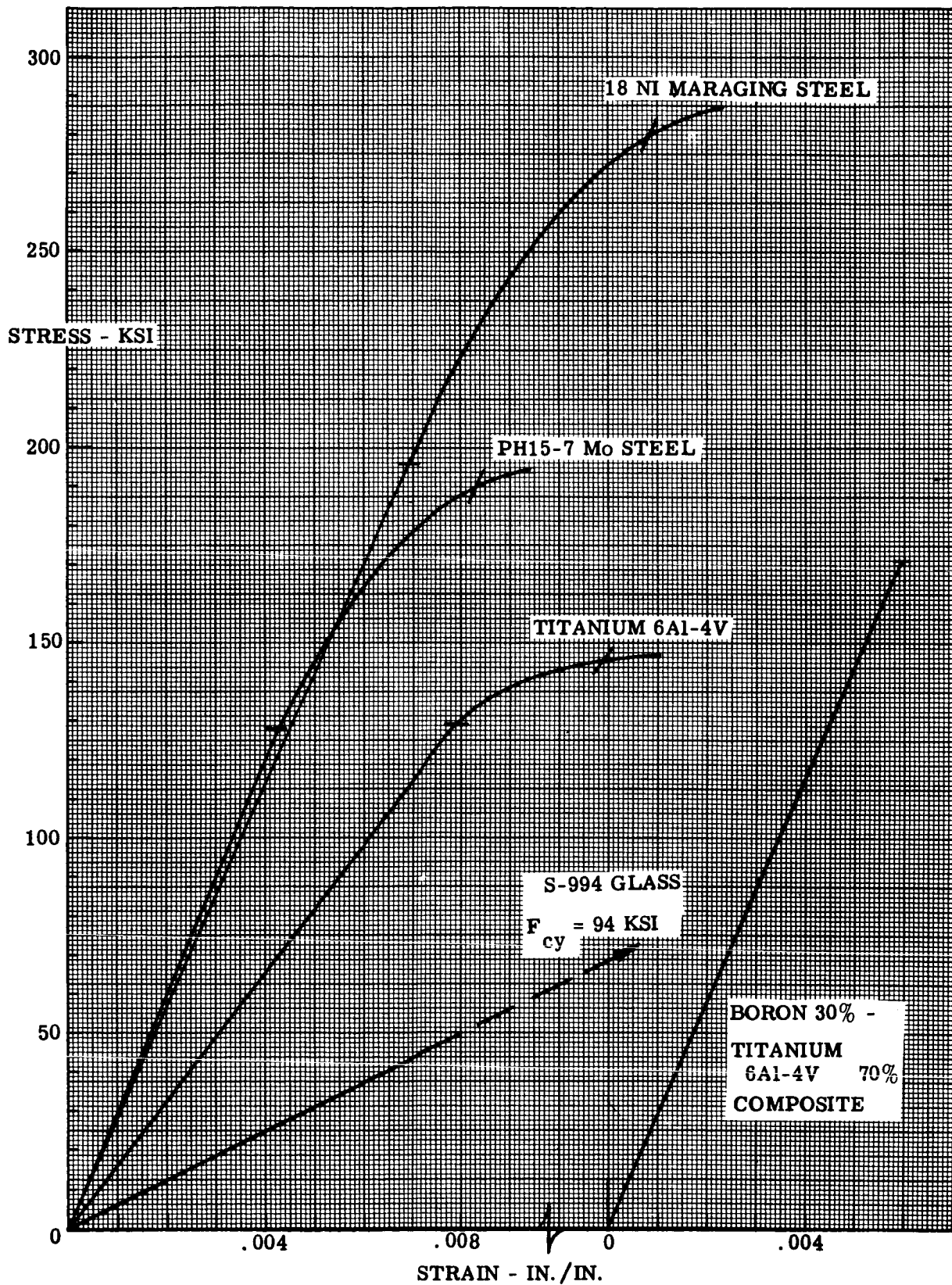


Figure 4. Stress-strain Curves in Compression

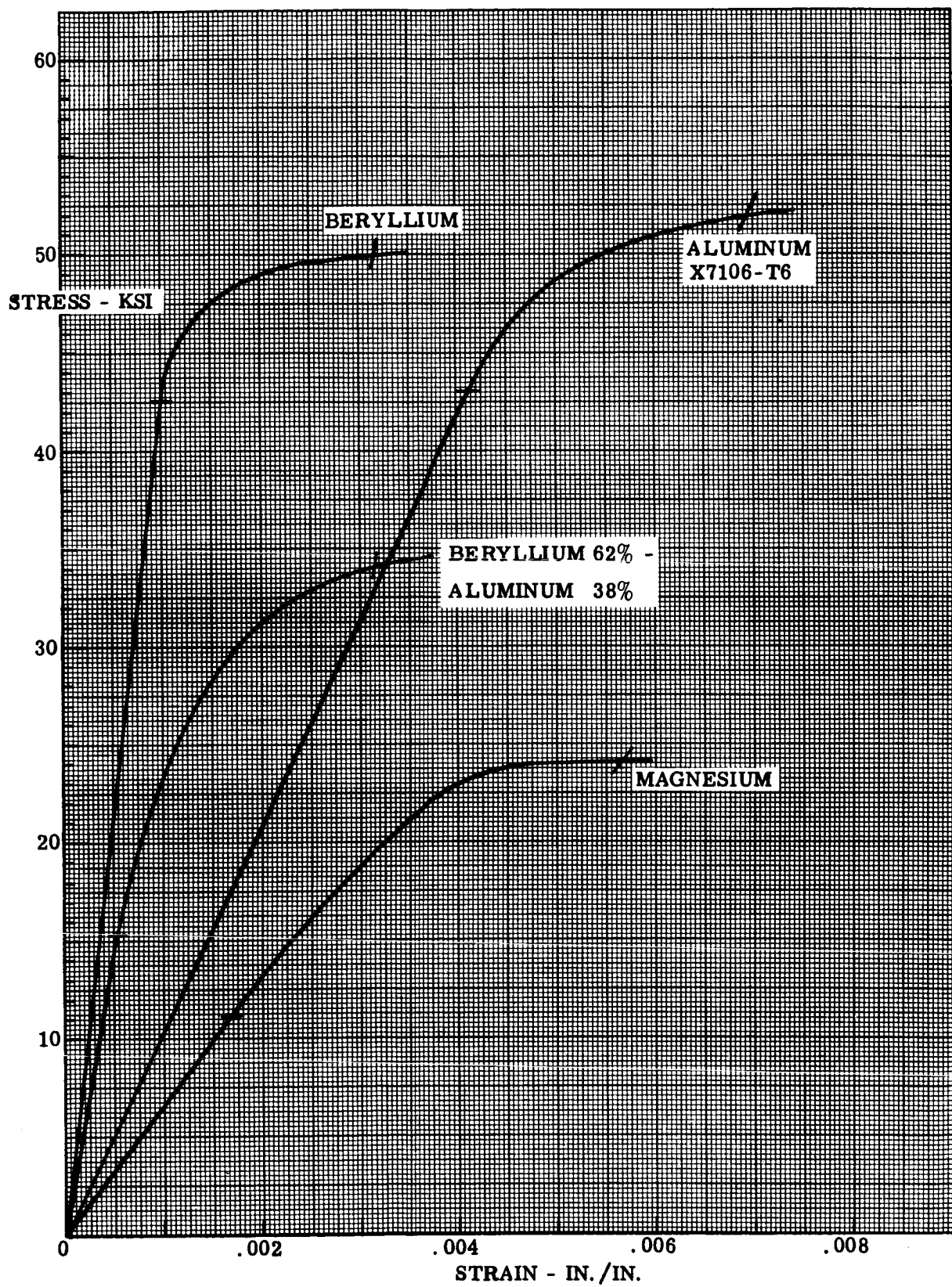


Figure 5. Stress-strain Curves in Compression

Table V

SUMMARY OF STATE-OF-THE-ART MATERIAL PROPERTIES

ROOM TEMPERATURE VALUES

		Aluminum X7106-T6	Titanium 6Al-4V	Stainless Steel PH15-7Mo	Maraging Steel 18 Ni	Magnesium AZ31-H24
F_{cy}	$\frac{LB}{IN.^2}$	52,000	145,000	190,000	280,000	24,000
F_{PL}	$\frac{LB}{IN.^2}$	43,000	129,000	128,000	195,000	11,000
F_{su}	$\frac{LB}{IN.^2}$	34,000	99,000	126,000	155,000	18,000
F_{bru}	$\frac{LB}{IN.^2}$	105,000	286,000	383,000	480,000	68,000
E_c	$\frac{LB}{IN.^2}$	10.5×10^6	16.3×10^6	30.0×10^6	28.3×10^6	6.5×10^6
G	$\frac{LB}{IN.^2}$	3.9×10^6	6.17×10^6	11.41×10^6	10.2×10^6	2.4×10^6
μ		.32	.32	.280	.30	.35
$F_{.7}$	$\frac{LB}{IN.^2}$	52,000	147,000	194,500	288,000	24,000
$F_{.85}$	$\frac{LB}{IN.^2}$	50,200	143,500	178,000	276,000	23,500
ρ	$\frac{LB}{IN.^3}$.099	.160	.277	.289	.0639
F_{cy}/ρ		505×10^3	906×10^3	686×10^3	969×10^3	376×10^3
$E_c^{1/2}/\rho$		32.7×10^3	25.2×10^3	19.8×10^3	18.4×10^3	40.0×10^3

Table VI
SUMMARY OF ADVANCED MATERIAL PROPERTIES
ROOM TEMPERATURE VALUES

		Beryllium	Beryllium Aluminum Alloy	Boron/ Titanium Composite	S-994 Glass Fiber
F_{cy}	$\frac{LB}{IN.^2}$	50,000	34,000	170,000	94,000
F_{PL}	$\frac{LB}{IN.^2}$	42,500	15,000	None	None
F_{su}	$\frac{LB}{IN.^2}$	40,000	30,600	76,000	12,000
F_{bru}	$\frac{LB}{IN.^2}$	140,000	91,800	212,000	None
E_c	$\frac{LB}{IN.^2}$	42.0×10^6	28.5×10^6	28.0×10^6	4.9×10^6
G	$\frac{LB}{IN.^2}$	20.0×10^6	12.4×10^6	11.8×10^6	1.1×10^6
μ		.030	.15	.14	.100
$F_{.7}$	$\frac{LB}{IN.^2}$	48,000	26,000	None	None
$F_{.85}$	$\frac{LB}{IN.^2}$	47,000	20,500	None	None
ρ	$\frac{LB}{IN.^3}$.066	.0756	.139	.070
F_{cy}/ρ		758×10^3	450×10^3	1225×10^3	1340×10^3
$E_c^{1/2}/\rho$		98.0×10^3	70.5×10^3	38.1×10^3	31.6×10^3

NOTE: Aluminum polyethylene material properties tabulated in Reference 2.

CANDIDATE COVER PANEL AND SUBSTRUCTURE CONCEPTS

A most important facet in the establishment of the load/geometry/material/concept matrix is the selection of candidate cover panel concepts and candidate substructure concepts.

Eight candidate cover panel concepts are investigated in the first phase study (figure 6):

1. Integrally stiffened
2. Zee stiffened
3. Truss core semisandwich
4. Trapezoidal corrugation
5. Truss core sandwich
6. Honeycomb (brazed or bonded)
7. Honeycomb (diffusion bonded)
8. Waffle grid

Four substructure concepts are investigated in the first phase investigation (figure 7):

1. Sine-wave shear web
2. Truss web
3. Biaxial truss
4. Conventional ring frame

The principal orientation of the candidate substructures may be longitudinal or circumferential. Each of the eight cover panel concepts, therefore, has the potential of acting as a long simply supported plate or as a wide column. The optimization screening considers both configurations.

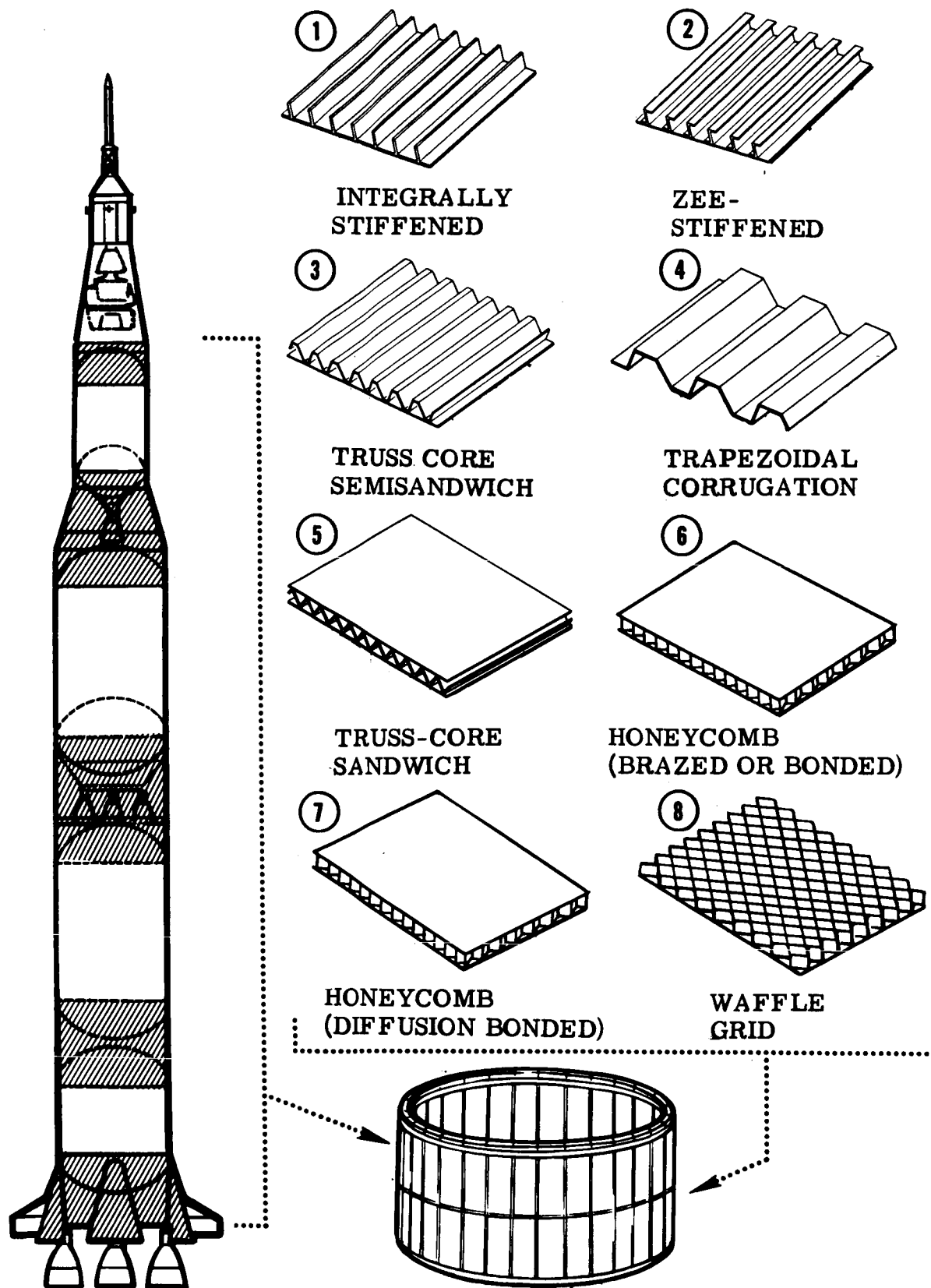


Figure 6. Candidate Cover Panel Concepts

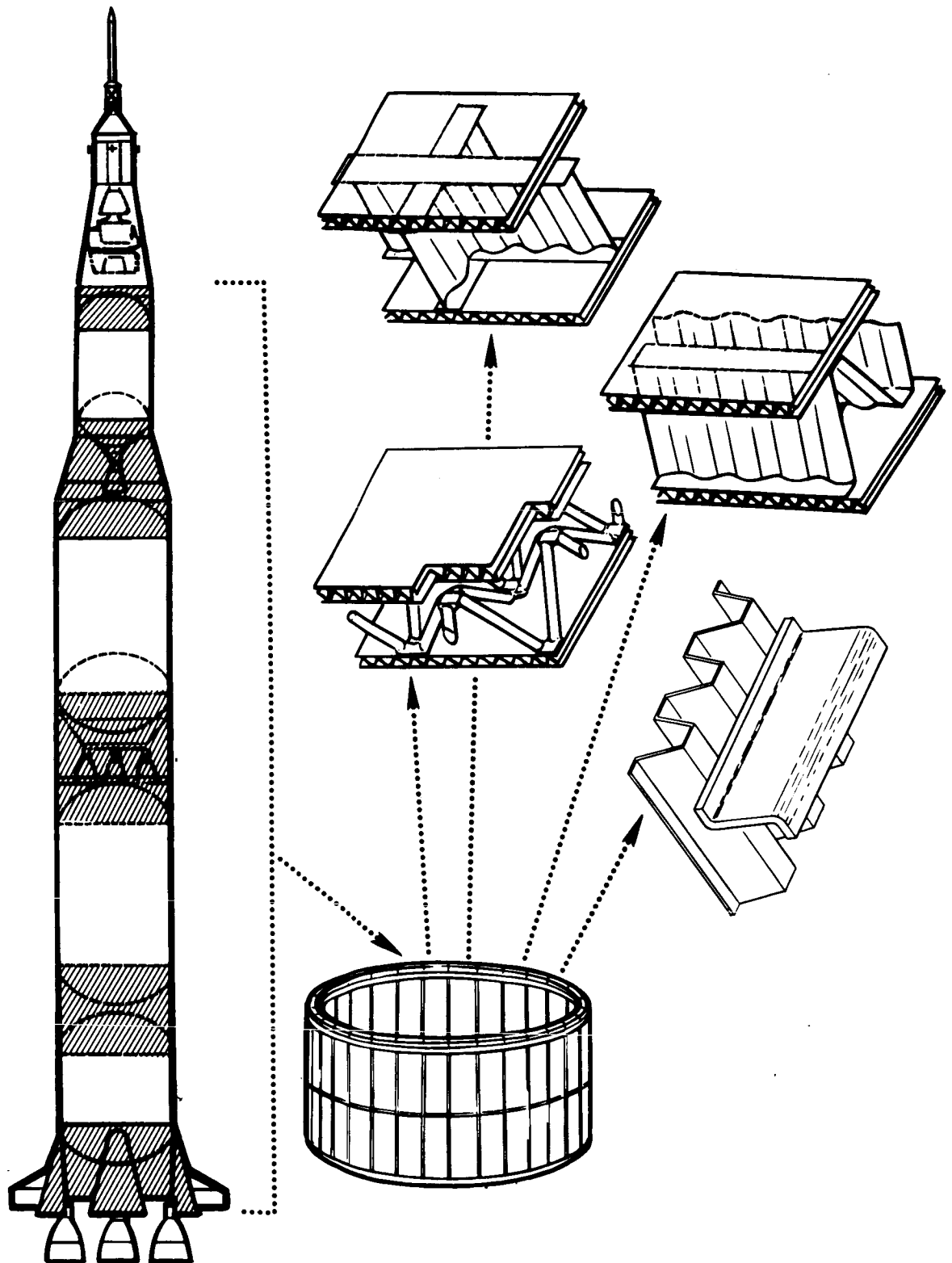


Figure 7. Candidate Substructure Concepts

LOAD/GEOMETRY/MATERIAL/CONCEPT MATRIX

The matrix of candidate design concepts resulting from the preceding design criteria comprises over 10,000 design points. The total matrix of potential candidate concepts is the product of the number of selections in each of the variables. In the three double-wall substructure arrangements, the cover panel may be designed as a plate or a wide column design. Thus, the eight cover panel concepts and four substructure concepts must be multiplied by a factor of $(3 \times 2 + 1 \times 1)/4 = 7/4$ to obtain the actual number of potential design points considered. The total matrix of design points evaluated is, therefore:

	10 materials
x	5 loads
x	4 diameters
x	8 cover panel concepts
x	4 substructure concepts (3 double-wall, one ring frame)
x	$\frac{7}{4}$ plate versus wide column
	11,200 Summation of design points.

This matrix of design points coupled with the geometry and properties summarized previously in this section form the criteria for this design investigation.

SUMMARY OF PARAMETRIC STUDY AND DETAILED DESIGN

DESIGN PRINCIPLES

The primary goal of this design investigation is the development of reliable structural concepts that are lighter in weight than conventional ring-stiffened cylinders and honeycomb sandwich cylinders. This objective is achieved by designing structure which inherently possesses maximum wall stiffness for a given weight of material. Application of this guideline results in configurations which have a substantial portion of the material placed as far from the neutral axis of the section as possible.

In general, increased efficiency is attainable through selective orientation of the load carrying material in the axial and circumferential directions. Similarly, supporting substructure preferential orientation in the axial and circumferential directions shows promise of weight savings. The directionality depends upon fabrication potentials or difficulties, as complements to structural efficiency.

The first phase effort in developing the load/geometry/material concept matrix and in performing the parametric screening is directed to determining true potential of candidate concepts with a minimum of design restraints. A continuous convergence toward most advantageous concepts is accomplished in the first phase. Selection of optimum configurations is based upon coupled minimum weight and producibility considerations. In this manner, the second phase development of practical designs is facilitated by concentration on realism in design.

Efficient design of compressive cylinders is measured by the attainment of high stress levels and low structural weight. At high load indices the compressive yield stress versus density is the important measure of efficient design. As the loading index is reduced, the modulus of elasticity versus density is the criterion of efficient design. Further, it becomes increasingly difficult to design efficient structures. Factors that limit structural efficiency at low load levels are evaluated in detail in the second phase design investigation.

Conventional design of large shell structures under the predominantly compression forces has resulted in a basic configuration of load-carrying skin-stringers, stabilized by large frames which are non-load-carrying. This concept is the ring stiffened configuration. Stringer configurations vary, depending upon load and geometry parameters of the design problem. The function of the frames is to provide support for the column skin-stringer elements, and to provide sufficient circumferential moment of inertia to preclude general stability failure of the complete shell. Considering the shell as an

orthotropic structure, it is apparent that the difficulty in attaining truly efficient structure is the lack of interaction of rigidity factors in the axial and circumferential directions. This is true for both membrane stiffness and bending stiffness. A closely related aspect of the ring frame design is the significant weight increment demanded for the ring, which contributes nothing to actual load carrying structure. The important benefits of the ring stiffened cylinder concept are the favorable fabrication and cost considerations.

Honeycomb sandwich cylindrical shells provide an efficient and low cost construction which is competitive from the weight standpoint in a wide range of load levels. Minimum practical core density, and face sheet to core bond weight cause limitations in honeycomb applicability.

The double-wall cylinder concept achieves minimum weight by utilizing the load-carrying material as self-stabilizing to ensure general stability. The evolution of the double-wall structural concept is outlined in figure 2. This illustration shows how the weight of the non-load-carrying material is reduced to a minimum. The double-wall design approach is the placement of a maximum amount of structural material in the load-carrying and cylinder-stiffening cover panels with a minimum of material, consistent with structural integrity, in the supporting substructure. Thus, the cover panels are designed to operate at a maximum stress level for a given load level. The concept provides lightweight stabilizing substructure, due to the efficient burn-through welded sine-wave shear webs, beaded truss-core webs, or biaxial trusses. Structural efficiency of this configuration is attained from the strong interaction between the axial and circumferential stiffness parameters.

Directionality of double-wall cover panels is established by the optimum proportions of the respective structural concepts. Directionality of the substructure, in general, offers more latitude in design. The first phase structural optimization includes consideration of both longitudinally and circumferentially oriented substructure. Wide column panel allowable stresses are used with circumferential substructure and plate allowable stresses control in longitudinally oriented substructure.

These design principles result in the selection of six optimum concepts at the end of the first phase effort. The screening process is summarized in the following section.

SIX SELECTED FIRST PHASE DESIGN CONCEPTS

The first phase parametric screening of the matrix of structural/material/design points is summarized in this section. Details of the first phase study are reported in Reference 2. The first phase evaluation is

performed with a minimum of design restraints, such as minimum element thickness, to show concept potential. The exception to this rule is the necessity of establishing minimum substructure thickness in the doublewall concept and minimum core density in the honeycomb concept. These data are used as input to the optimization programs. In the range of substructure gages and core densities considered the optimum design occurs at, or very near, the minimum value.

Eight cover panel concepts and the four substructure concepts, with longitudinal and circumferential orientation, are considered for five load levels, four diameters, and ten materials. The truss-web and ring frame substructures are evaluated on the basis of axial load versus cylinder wall weight for the entire portion of the load/geometry/material matrix applicable to these substructure concepts (Reference 2). These concepts represent the lowest cost configurations of the competing concepts. The sine-wave shear web substructure is analyzed in portions of the design matrix promising greatest weight saving potential. The most attractive materials are evaluated for the biaxial truss substructure concept.

Graphs of panel weight versus axial load for competitive concepts are prepared to facilitate first phase screening and selection of optimum concepts. Summaries the truss-web substructure for the state-of-the-art materials category are shown in figures 8 and 9 for the range of diameters considered. A comparison of the truss-web and the sine-wave shear web substructures is shown in figure 10 for the 400-inch diameter shell. A comparison of the truss-web and biaxial truss substructures is shown in figure 11.

Summaries of the truss-web substructure for the advanced materials category are shown in figures 12 and 13 for the range of diameters considered. A comparison of the truss-web and sine-wave shear web substructures is shown in figure 14 for the 400-inch diameter shell.

It is noted that the panel weight figures are theoretical optimum values designed with like materials for cover panels and substructure. Cover panel weight is added to substructure weight for total cylinder wall panel weight. Penalties for panel splices and cover panel to substructure attachment are not included. Minimum material gage restraints for cover panel elements are not included. The results, therefore, indicate the lightest weight potential of the candidate concepts. The second phase detailed design effort evaluates the impact of such nonoptimum factors.

The most efficient double-wall configuration for state-of-the-art materials is the truss core sandwich plate. Figures 8 and 9 show that the truss core sandwich is optimum when aluminum 7106 and titanium 6-4 materials are employed with the truss-web substructure. This optimum weight concept has several close competitors in the truss-core semisandwich, and integrally

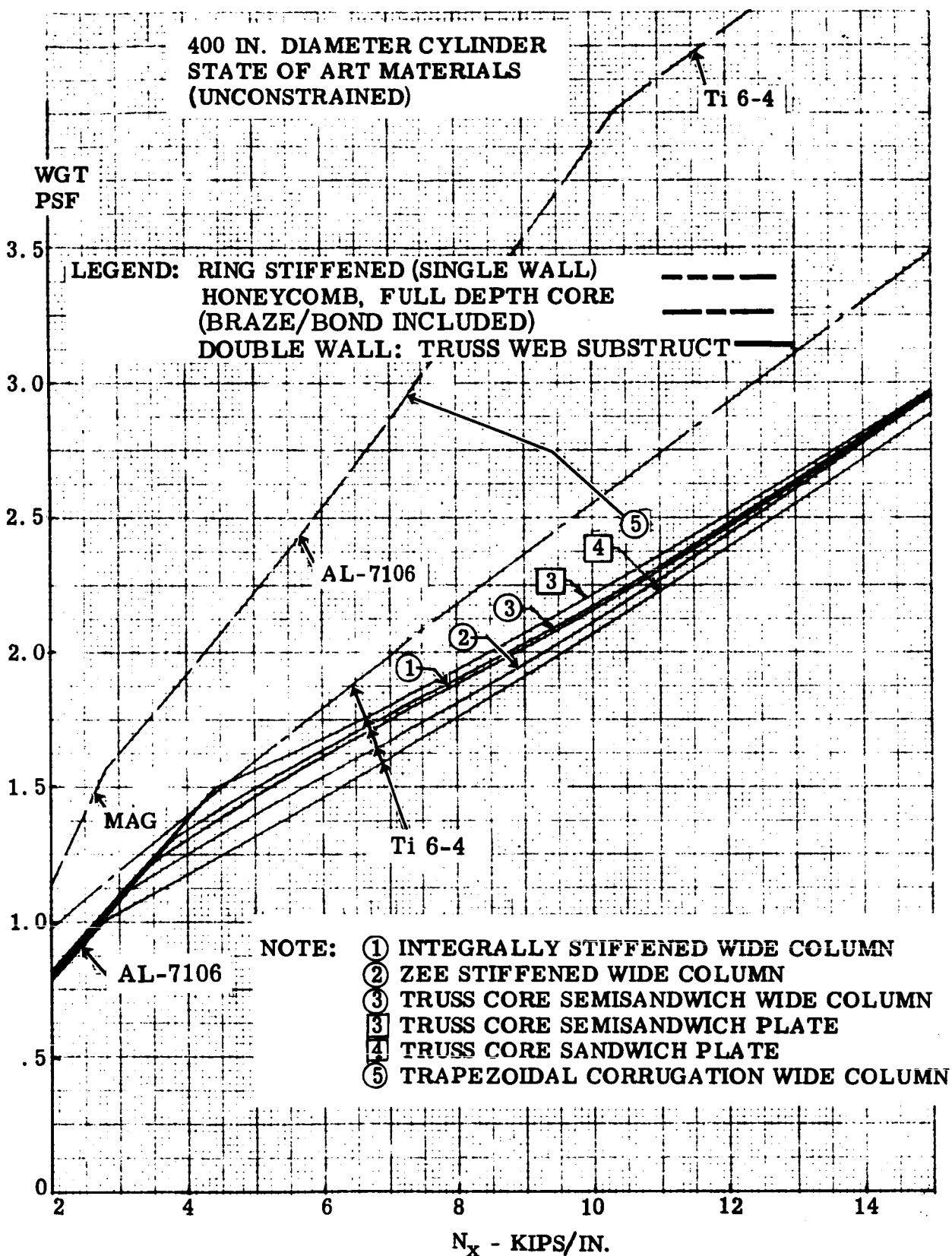


Figure 8. Weight Versus Load for 400-inch Diameter Cylinders
(State-of-the-Art Materials)

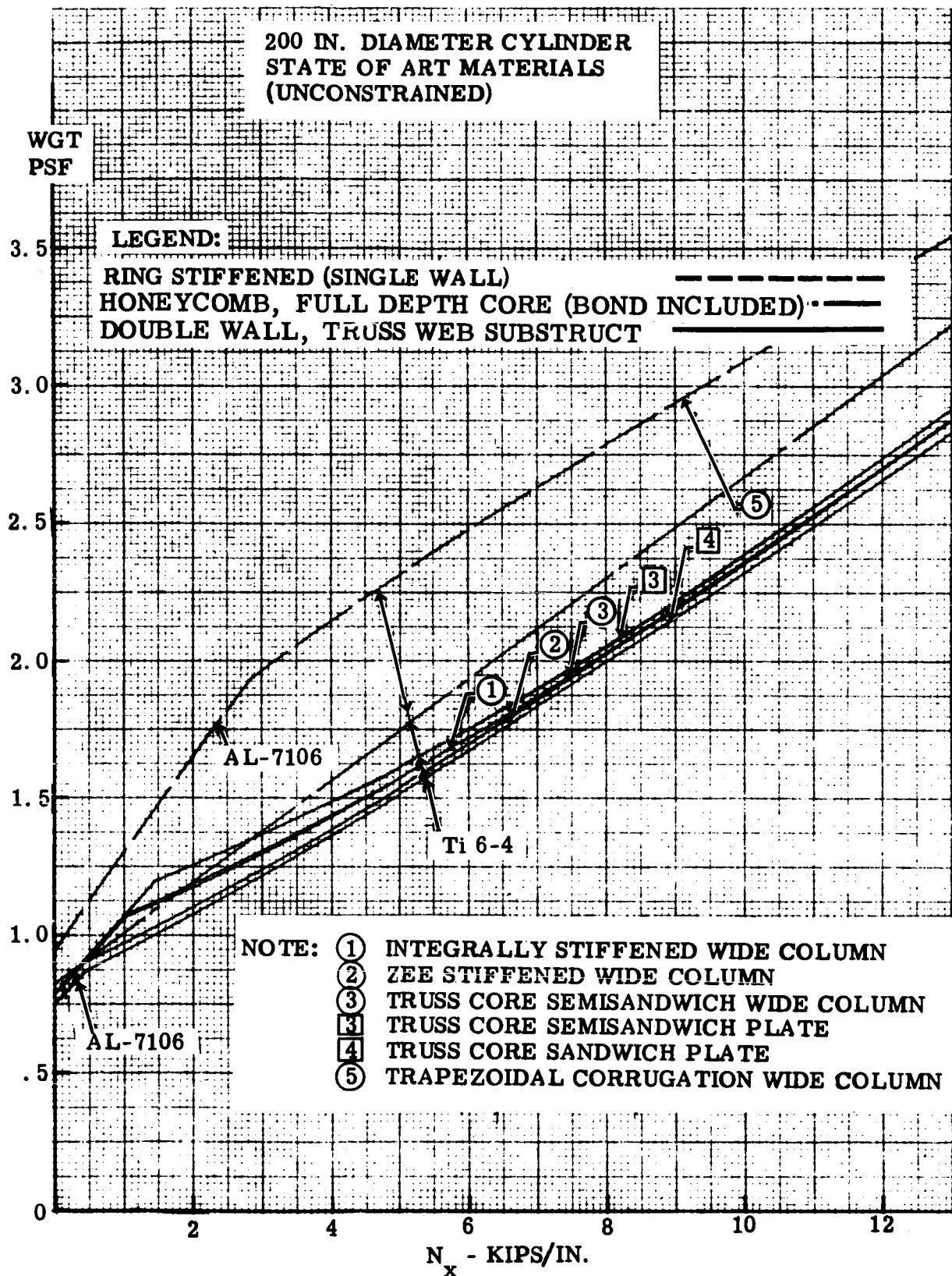


Figure 9. Weight Versus Load for 200-inch Diameter Cylinders
(State-of-the-Art Materials)

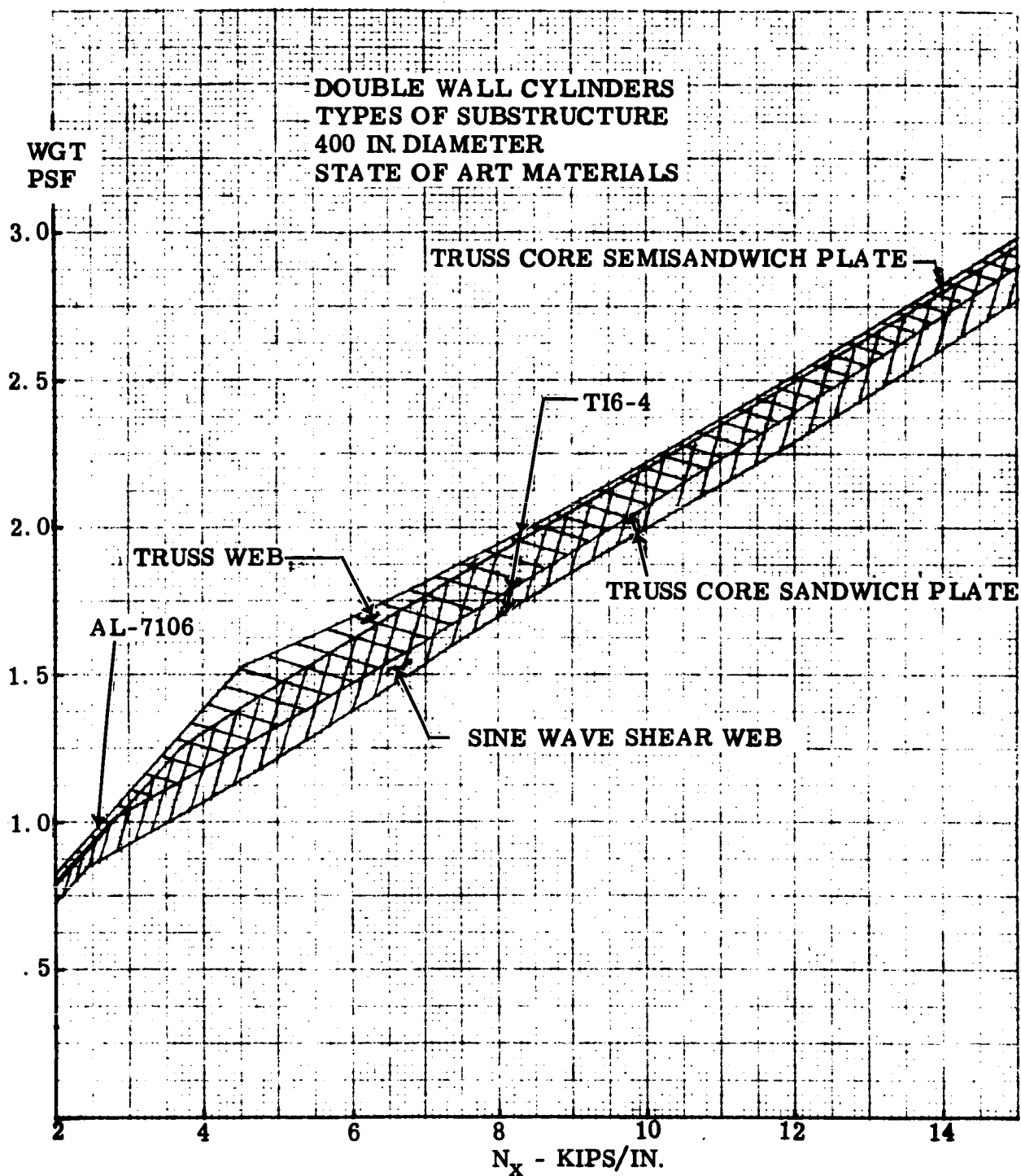


Figure 10. Weight Versus Load for 400-inch Diameter Cylinders-Comparison of Truss Web and Sine-Wave Shear Web Substructures

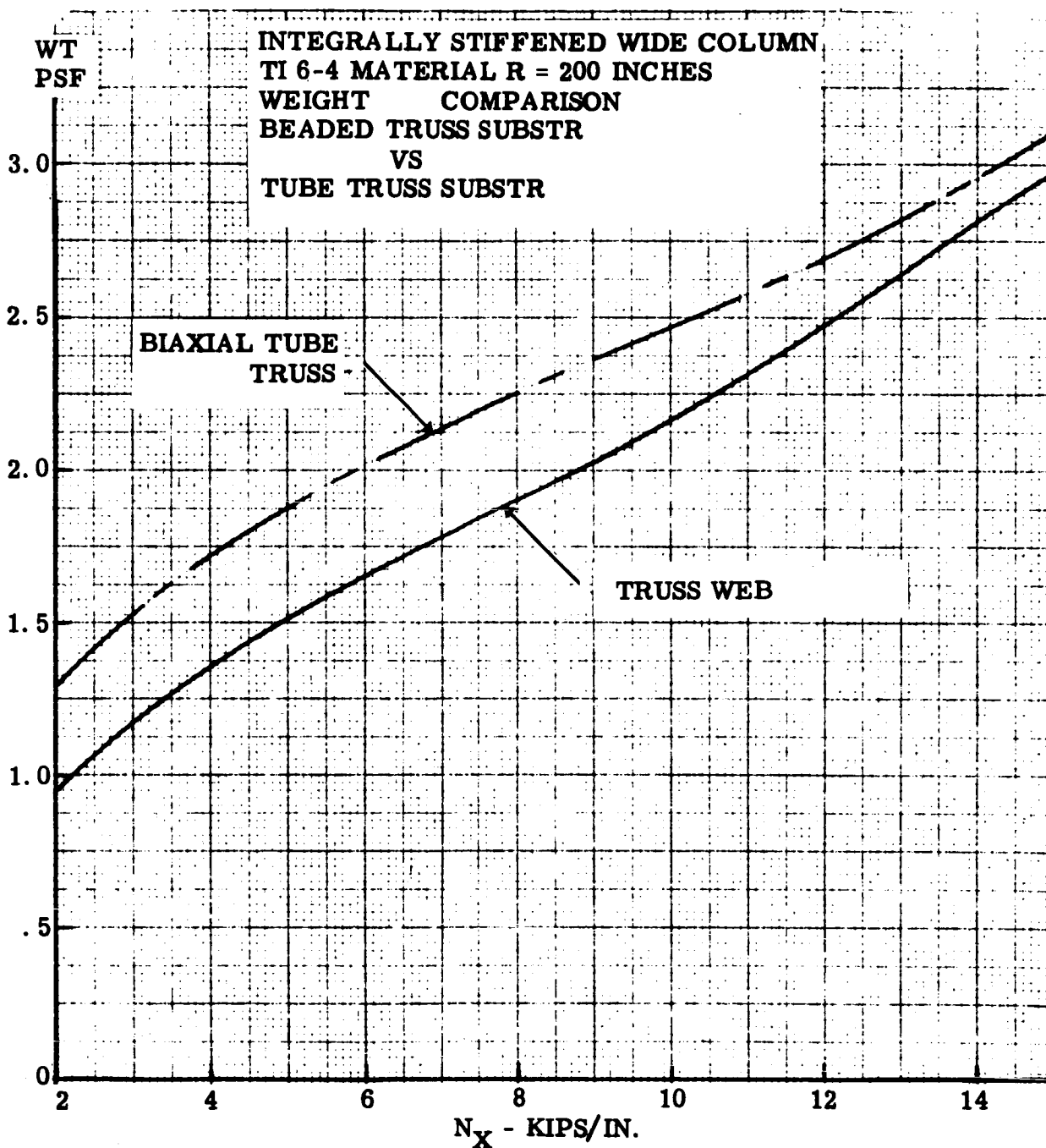


Figure 11. Weight Versus Load for 400-inch Diameter Cylinders - Comparison of Truss Web and Biaxial Truss Substructures

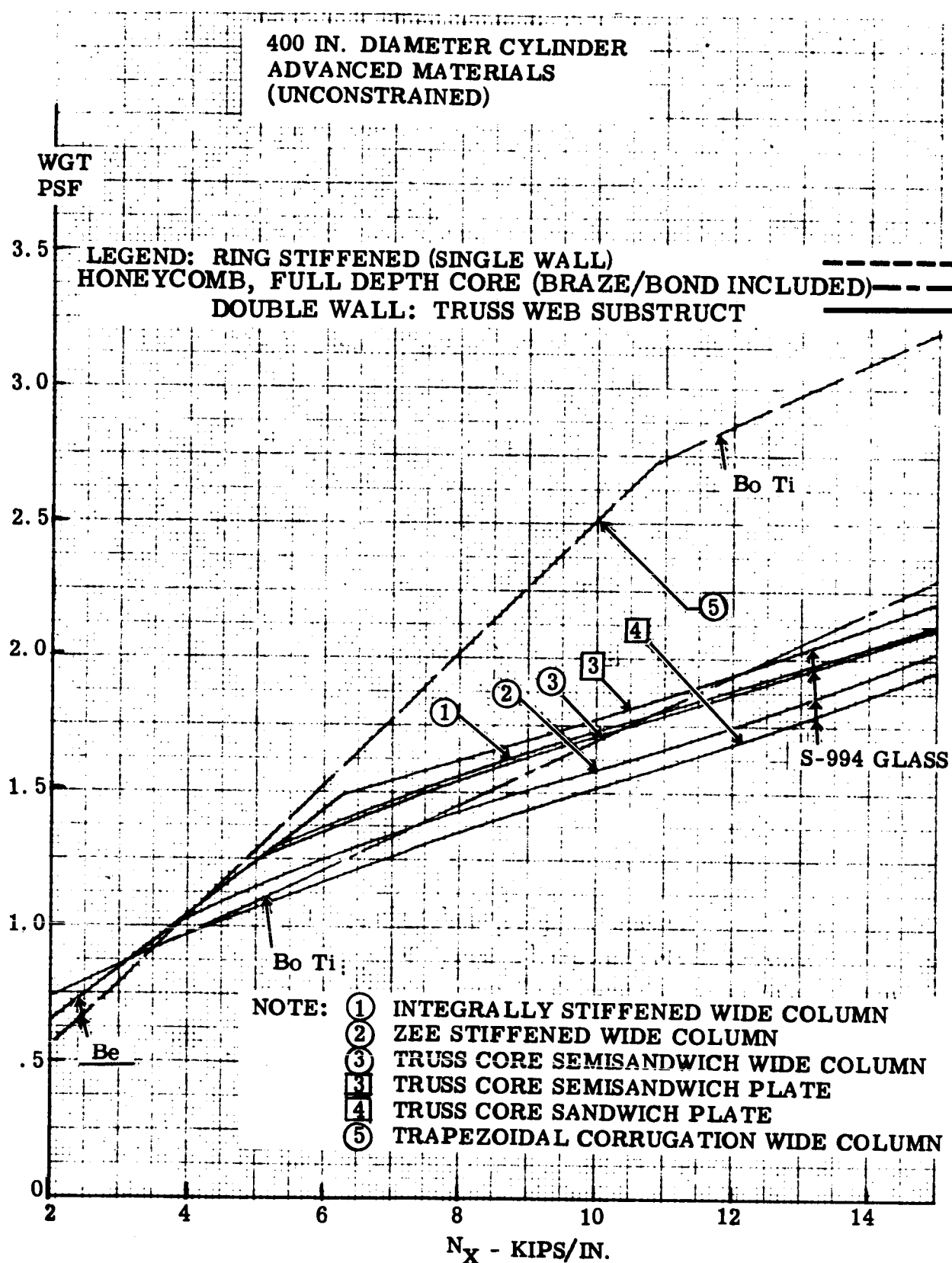


Figure 12. Weight Versus Load for 400-inch Diameter Cylinders
(Advanced Materials)

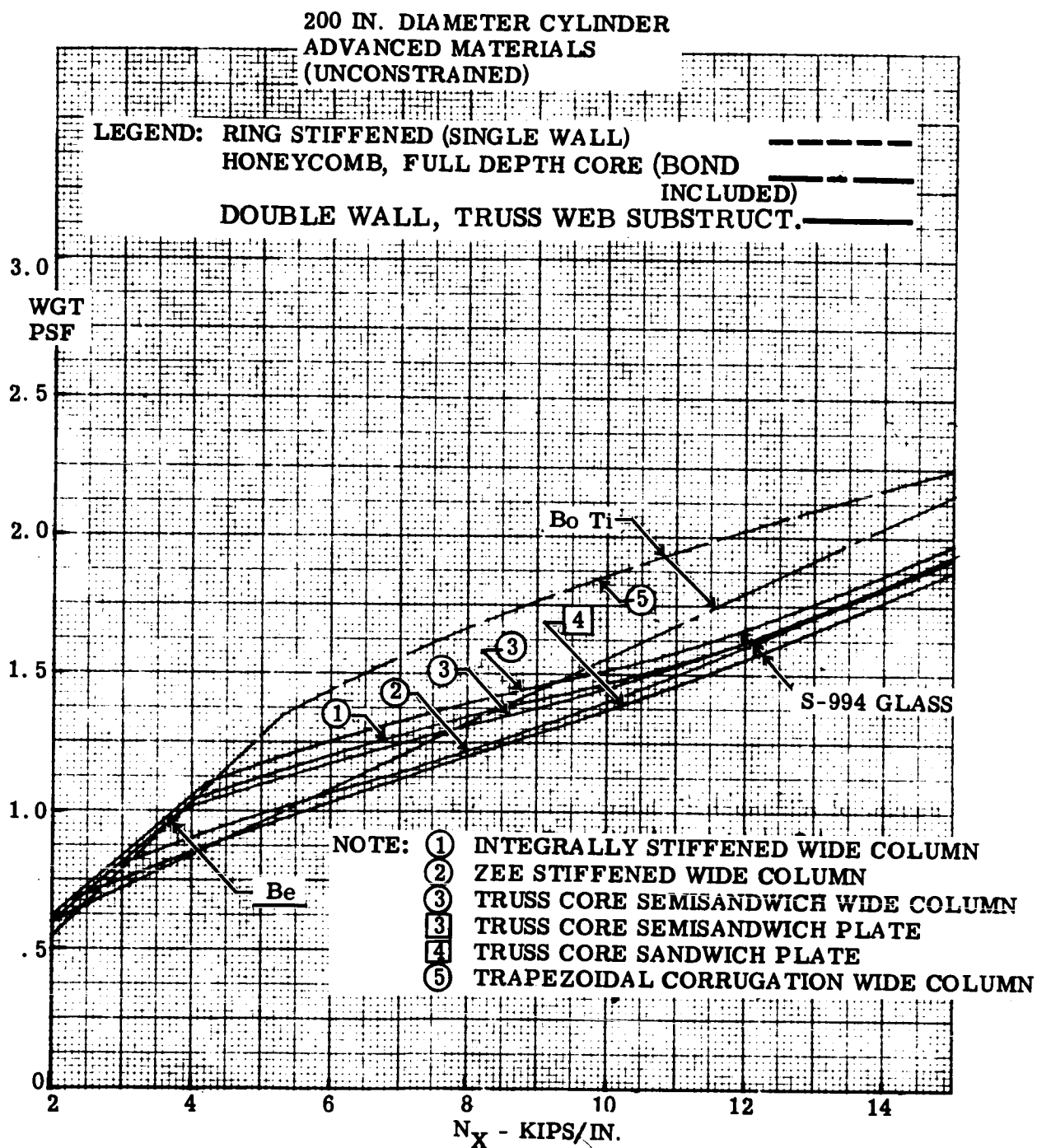


Figure 13. Weight Versus Load for 200-inch Diameter Cylinders
(Advanced Materials)

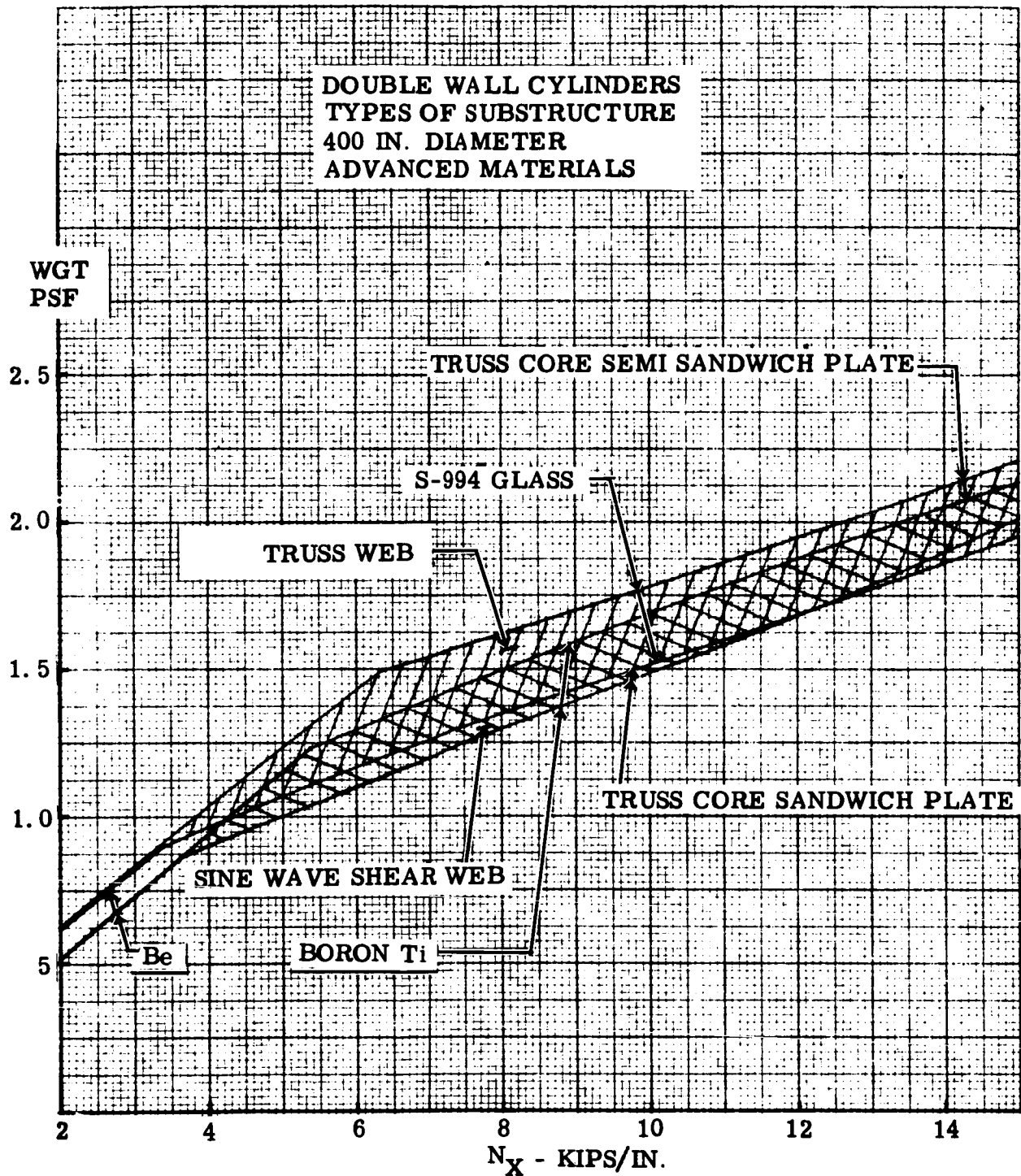


Figure 14. Weight Versus Load for 400-inch Diameter Cylinders - Comparison of Truss-web and Sine-wave Shear Web Substructures

stiffened cover panels. The truss-core semisandwich plate concept with the truss-web substructure establishes an upper bound for this band of double-wall configurations. The full depth honeycomb shell (braze/bond weight included) and the ring frame stiffened shell do not show a weight advantage, in the first phase, over the double-wall concepts for these materials of construction. It is noted that a variation in shell diameters has little impact on cylinder weight. Selection of materials is a most important factor in cylinder weight.

The load-weight variations of the truss web and sine-wave shear web substructure showed the weight bands with both concepts are essentially equal, but slightly favoring the shear web substructure (Reference 2).

For the advanced materials of construction, a similar trend is evidenced by the composite graphs of figures 12, 13, and 14. Examination of the 200-inch diameter graph, figure 12, shows that the weight trends of the various double-wall cover panel concepts follow the trends established with state-of-the-art materials. The optimum material of construction, S-994 fiberglass, is examined in more detail in the second phase design investigation. Optimum configuration analyses employing S-994 glass material are augmented in the second phase by analyses of Boron-Titanium material, which is almost identical in weight to S-994 glass construction.

All first phase honeycomb analysis is based upon utilization of like materials for facing sheets and core. It is recognized that many of the candidate materials cannot be fabricated into honeycomb core. The second phase evaluation utilizes aluminum core, in most cases. In many cases the resulting design is lighter than the comparable one-material design. In the remaining cases, a direct comparison of panel weights is available to assess the importance of core weight to total weight.

The full depth honeycomb shell of boron-titanium material facings and core is lighter from first phase investigation, in a certain range of loads, than the double-wall shell concepts. Such a concept is far from being producible with boron-titanium honeycomb core, however, the favorable load/weight comparison is attainable with boron-titanium facings and an aluminum metallic core. Therefore, this structural/material configuration is investigated in the second phase effort.

The ring frame stiffened shell is not competitive in the state-of-the-art materials. The ring frame stiffened shell of beryllium material is a **contender** in the lower load regime, and is examined in the second phase effort.

The optimum concepts selected for detailed evaluation in the second phase are shown in Table VII. Full depth honeycomb is carried through as a basis for weight comparison.

Table VII

SIX SELECTED OPTIMUM CONCEPTS

	Cylinder Concept	Cover Concept	Substructure Concept	Cover Stability Criterion
1	Double Wall	Truss Core Sandwich	Sine Wave Shear Web	Plate
2	Double Wall	Trapezoidal Corrugation	Sine Wave Shear Web	Wide Column
3	Double Wall	Truss Core Semisandwich	Beaded Truss Web	Wide Column
4	Double Wall	Integrally Stiffened	Beaded Truss Web	Wide Column
5	Double Wall	Zee Stiffened	Beaded Truss Web	Wide Column
6	Ring Stiffened	Trapezoidal Corrugation	Ring Frame	Wide Column

Six candidate materials appear most attractive for the second phase detailed analyses. These materials, and others of the original ten materials, are considered where they appear competitive. First phase optimum state-of-the-art materials selected include magnesium, aluminum, and titanium. First phase optimum advanced materials selected include beryllium, boron-titanium composite, and S-994 glass fiber.

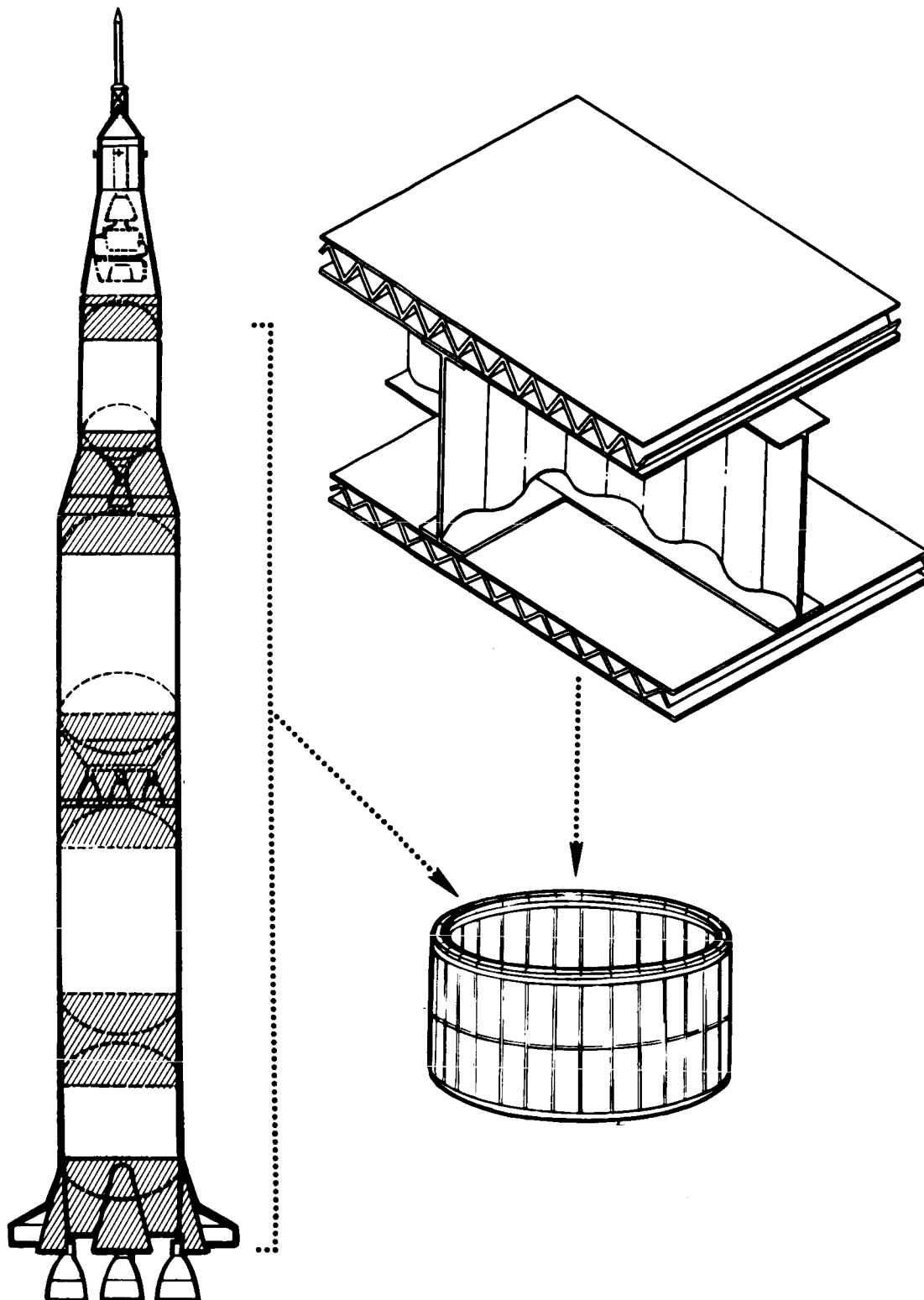


Figure 15. Selected Concept - Double Wall Truss Core Sandwich

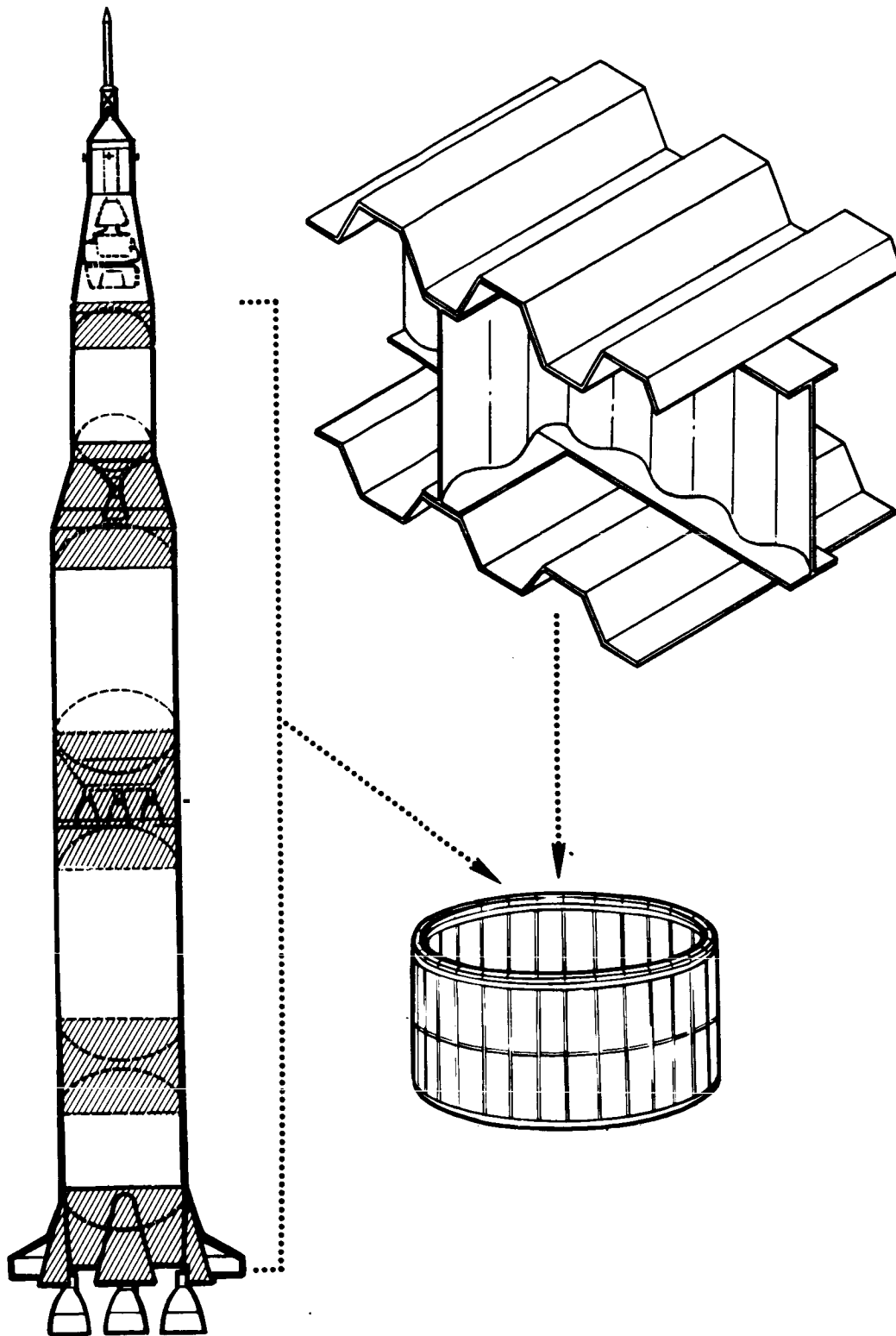


Figure 16. Selected Concept - Double Wall Trapezoidal Corrugation

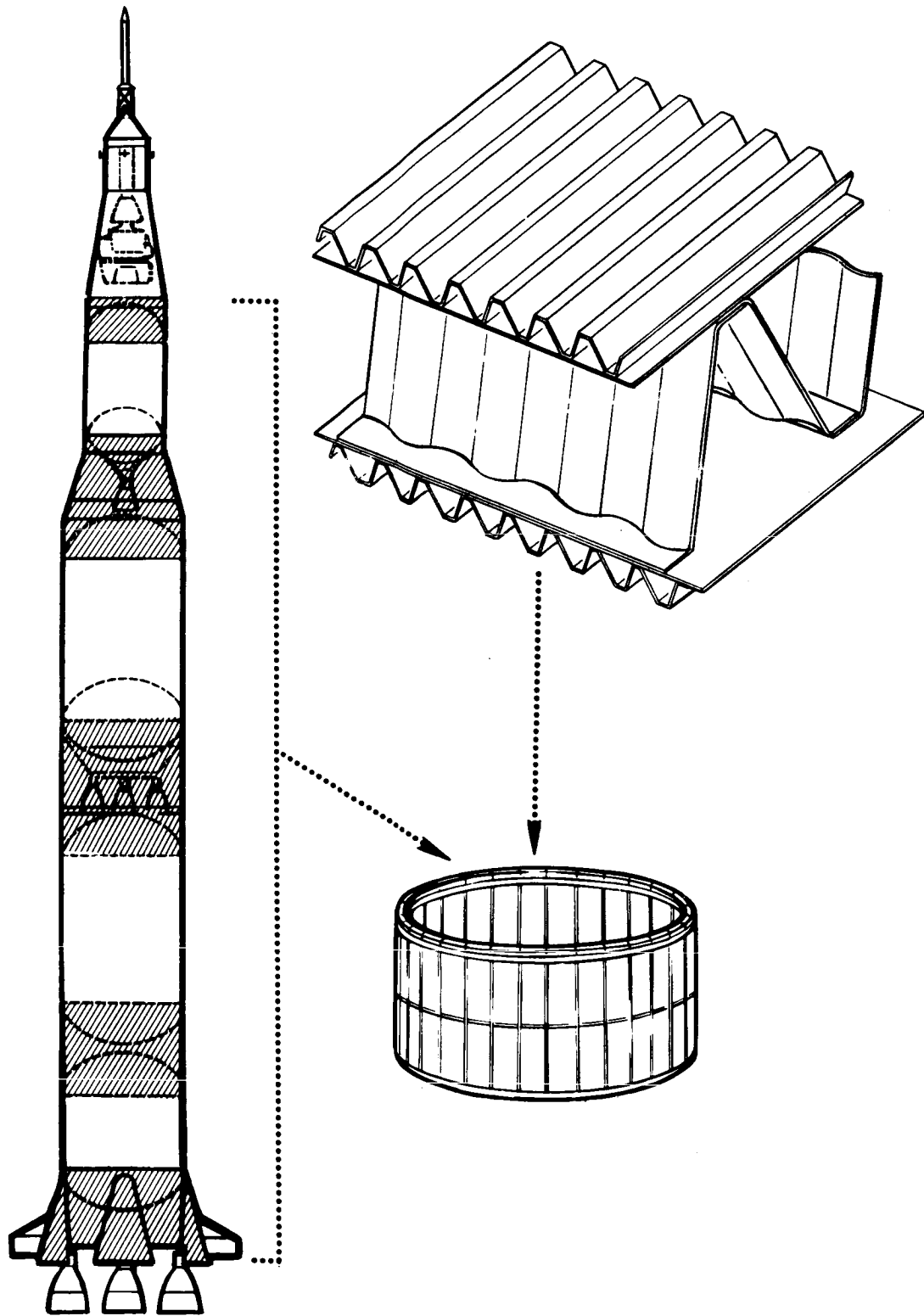


Figure 17. Selected Concept - Double Wall Truss Core Semisandwich

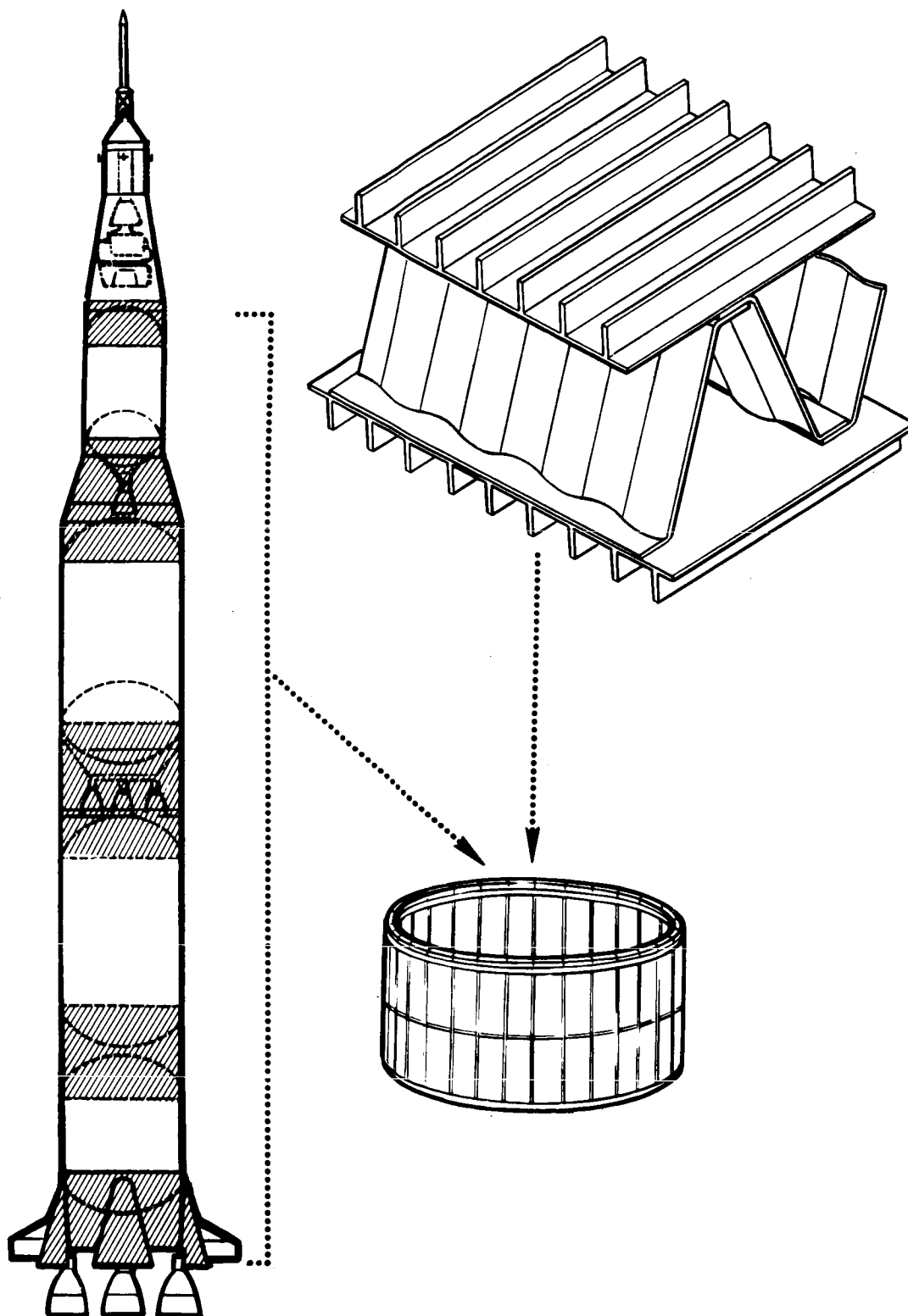


Figure 18. Selected Concept - Double Wall Integrally Stiffened Panel

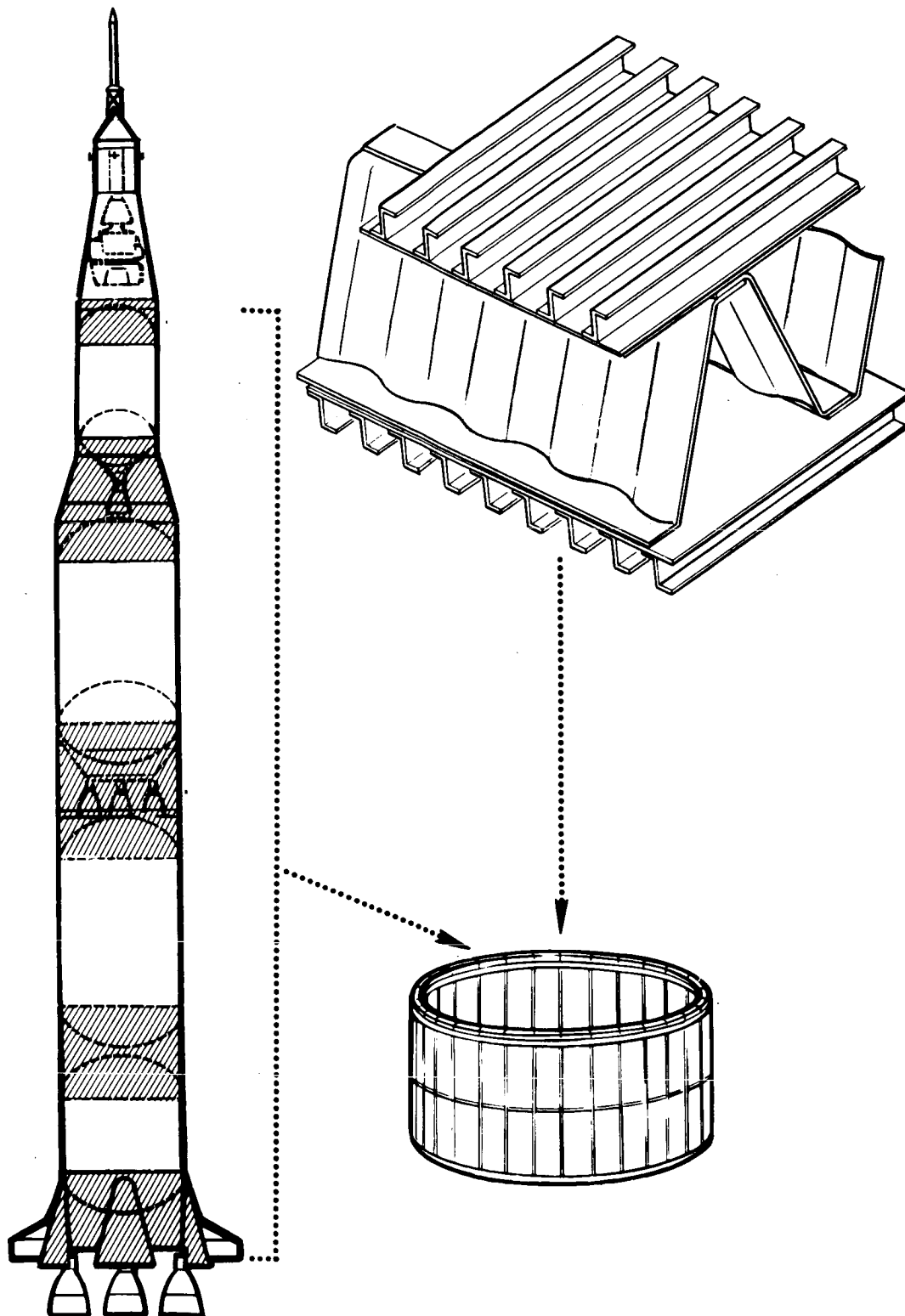


Figure 19. Selected Concept - Double Wall Zee Stiffened Panel

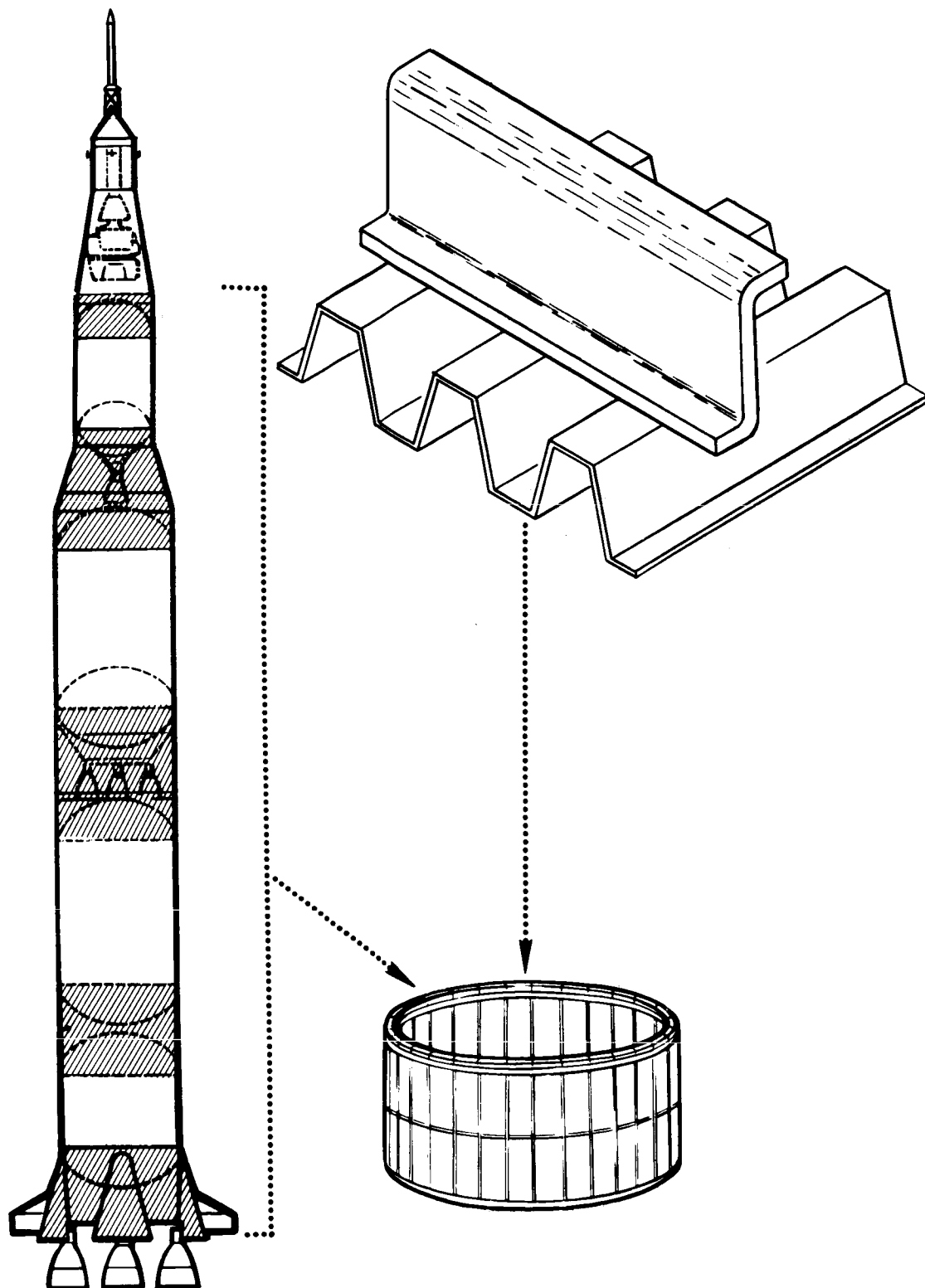


Figure 20. Selected Concept - Trapezoidal Ring Stiffened Cylinder

PRACTICAL DESIGN CONSIDERATIONS

The first phase parametric screening effort is directed toward convergence to most advantageous concepts. The second phase design investigation emphasizes feasibility and reliability of the six selected concepts. Careful attention to detailed design is necessary to exploit potentials developed in the first phase effort.

Efficient design is measured by the attainment of high stress levels and low structural weight. At high load indices the compressive yield stress versus density is the important measure of efficient design. At lower load indices, the modulus of elasticity versus density is the criterion of efficient design. Further, at lower load indices it becomes increasingly difficult to design efficient structures. Factors that limit structural efficiency at low load levels are:

1. Minimum gage limitations make optimum designs unworkable.
2. Minimum practical support spacing.
3. Difficulty in maintaining favorable b/t ratios for elements.
4. Material tolerance allowances.
5. Weight penalties associated with joints and splices.

Double-wall cylinder wall concepts possess flexibility in important design parameters. This inherent advantage makes the double-wall concepts adaptable to a wide variety of design variations. Many methods of fabrication are applicable to the cover panels, substructure, and the composite wall sections. Panel geometry can be varied with little penalty. For instance, a 1 to 3 percent weight increase, as compared to the optimum structural weight, provides great latitude in design dimensions. Panel depth, substructure spacing, and substructure thickness are basic design elements which can be adjusted for particular design requirements.

The producibility analysis performed in the first phase provides fabrication limitations for the selected material/concept structural arrangements (Reference 3). These limitations have been included in both the cover panel and substructure designs. Material size limits, equipment limits, material gages available, manufacturing methods, tolerances, and the level of technology necessary to fabricate the material into structure are listed. Minimum forming bend radii and spotwelding clearance requirements are established.

The impact of the transition from first phase unrestrained configurations to feasible designs depends upon the axial load level. There is no change in

relative efficiencies of competing concepts in the high load region. The minimum gage restraint results in substantial revisions in concept relative efficiencies in the intermediate and low load ranges. The absolute value of total panel weight, including joint and attachment penalties, requires additions of approximately 7 percent to 20 percent to first phase weight values. The second phase weight values include the penalty consideration. Summaries of panel weight versus axial load for each of the six concepts are included in the appropriate design section.

Minimum gage restraints for primary structural members are established in the section entitled "Design Criteria." The optimum sizing of certain elements to gages thinner than the nominal minimum is desirable from the design standpoint. In particular, thinner corrugated elements in the truss-core sandwich and semisandwich concepts are beneficial to two important problem areas.

The first is the proportion of total axial load in the corrugated elements, as compared to the facing sheets, resulting from design stress level. The axial load in the corrugations must be transferred to the facings at circumferential splice discontinuities. This causes local stress concentration in the facing sheets and load transfer problems at the corrugation-facing sheet interface. This problem is compounded when the facing sheets are relatively light, and alleviated when the facing sheets are relatively heavy. The second problem area occurs if forming of such elements is necessary. Large bend radii resulting from thick elements invalidate the theoretical design in less ductile materials. Small bend radii provide the truss action needed to yield a feasible design.

Primary cover panel design problems evaluated and resolved within the producibility limitations are:

1. Minimum feasible element dimensions.
2. The ability to fabricate a cross section which provides appropriate directional stiffnesses because of minimum bend radii limitations or necessary structural discontinuities.
3. The capability of reinforcement for panel splices and cover panel to substructure attachments.
4. Adaptability to one, or more, cover panels-to-substructure attachment methods, preferably blind attachments.
5. Provision for rivet gun or spot welder clearances. Close stiffener spacing resulting from certain optimum concepts is a particular problem for this consideration.

6. Alleviation of local cover panel flexibility due to offsets and eccentricities in the cover panel to substructure attachment.
7. Design of truss action elements in such a manner that the lines of action (c.g.'s) of the segments intersect at a point. The truss-web substructure is particularly sensitive in this regard.

First phase study shows the truss-web substructure and the sine-wave shear web substructures to be prime contenders for booster design. Both substructures result in essentially equal weights. Detailed design of the substructure to cover panel attachment and substructure to substructure splices, therefore, is the determining factor in selecting the optimum concept for a particular design application.

The truss-web substructure has an important inherent advantage in that one sheet of metal simultaneously provides both longitudinal and circumferential shear rigidity. Substructure to substructure splices are necessary only at the periphery of the largest material stock available. Gaps occurring between the intersection of truss web lines of action and the c.g. of the cover panel result in a secondary bending deformation. This problem results in a loss of effective shear stiffness and is minimized by careful design in the second phase designs.

The sine-wave shear web substructure has an important inherent advantage in that a definite shear path is provided in both longitudinal and circumferential directions. A practical design problem results from the large number of necessary substructure splices. Large panel dimensions alleviate this problem.

The preceding design considerations form the guideposts by which selected theoretical concepts are transformed into efficient practical designs.

DESIGN DRAWINGS AND CHARTS

OPTIMUM STRUCTURAL CONCEPT/MATERIAL MATRIX

Final detailed design of the six selected concepts is summarized in this section of the report. Three hundred sixty designs are developed in the second phase of the program. The matrix of design points is derived from the product of alternatives in each of the design variables:

Concepts	6
Load levels	X 5
Diameters	X 4
Materials	X 3
Summation of design points	360

The concepts, load levels, and diameters are delineated in preceding sections of this report. Materials selected as optimum for each of the six optimum concepts are shown in table VIII. Two "state-of-the-art" materials and one "advanced" material are chosen for each concept.

The final panel weight versus load diagrams include joint penalties and minimum gage restraints. These diagrams, developed for the second phase concept/material matrix, are shown in figures 21 through 24. Optimum concept/material arrangements are plotted as a function of cylinder diameter and axial load level in figures 25 and 26. These figures direct the designer to the appropriate concept design section for any design application within the ranges of variables considered. A summary of panel weight versus panel cost for optimum material configurations is included in figures 27 and 28.

Table VIII

OPTIMUM MATERIALS FOR SELECTED CONCEPTS

Concept	State-of-the-Art Materials		Advanced Materials
Truss Core Sandwich Double-wall	Titanium	15-7 steel	Beryllium
Trapezoidal Corrugation Double-wall	Titanium	Aluminum	S-994 glass
Truss Core Semisandwich Double-wall	Titanium	Maraging steel	Beryllium
Integrally Stiffened Panel Double-wall	Titanium	Aluminum	S-994 glass
Zee Stiffened Panel Double-wall	Titanium	Aluminum	S-994 glass
Ring Stiffened Trapezoidal Corrugation	Aluminum	Magnesium	Beryllium

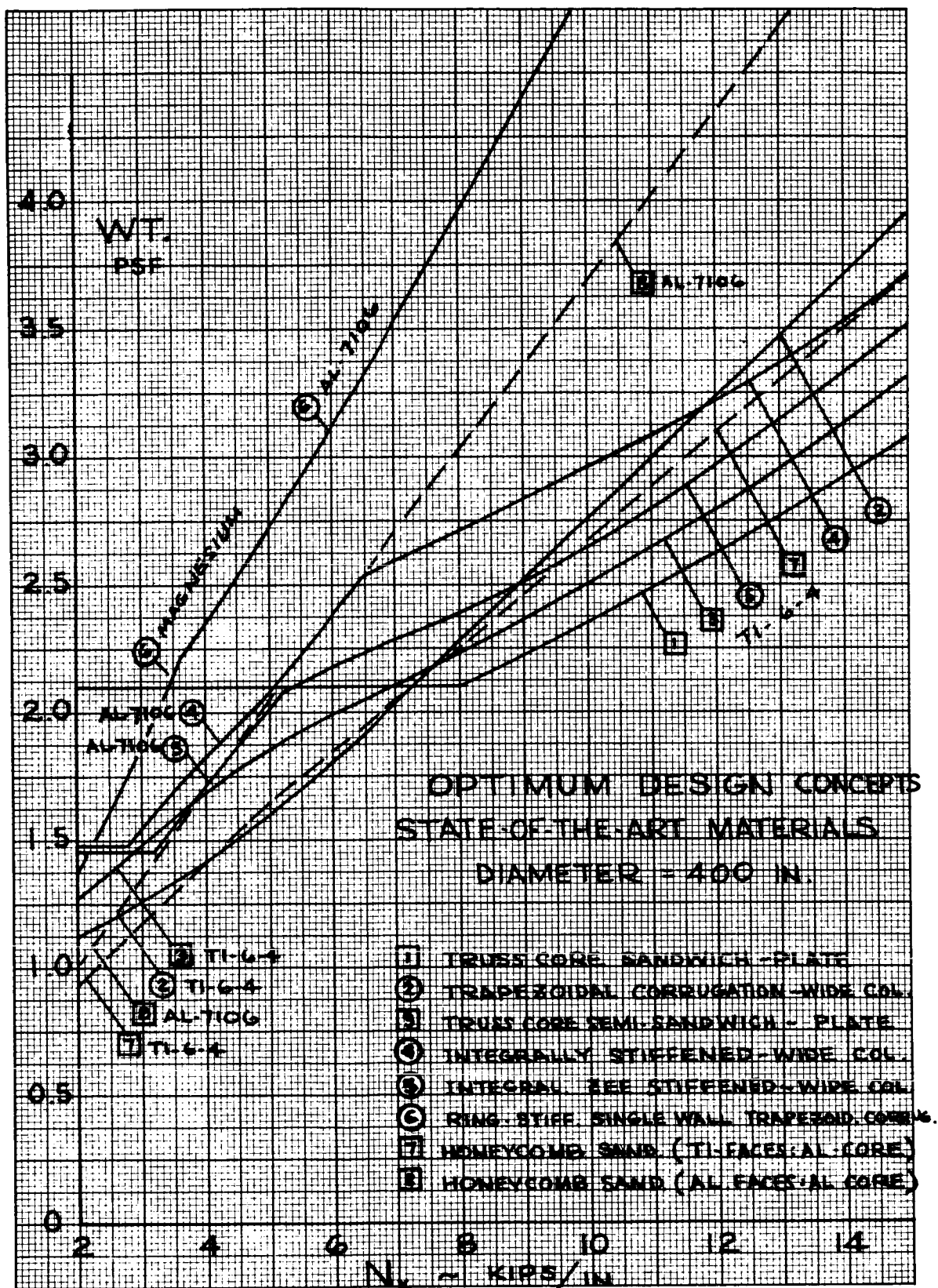


Figure 21. Final Weight Versus Load Diagrams for 400-Inch Diameter
(State-of-the-Art Materials)

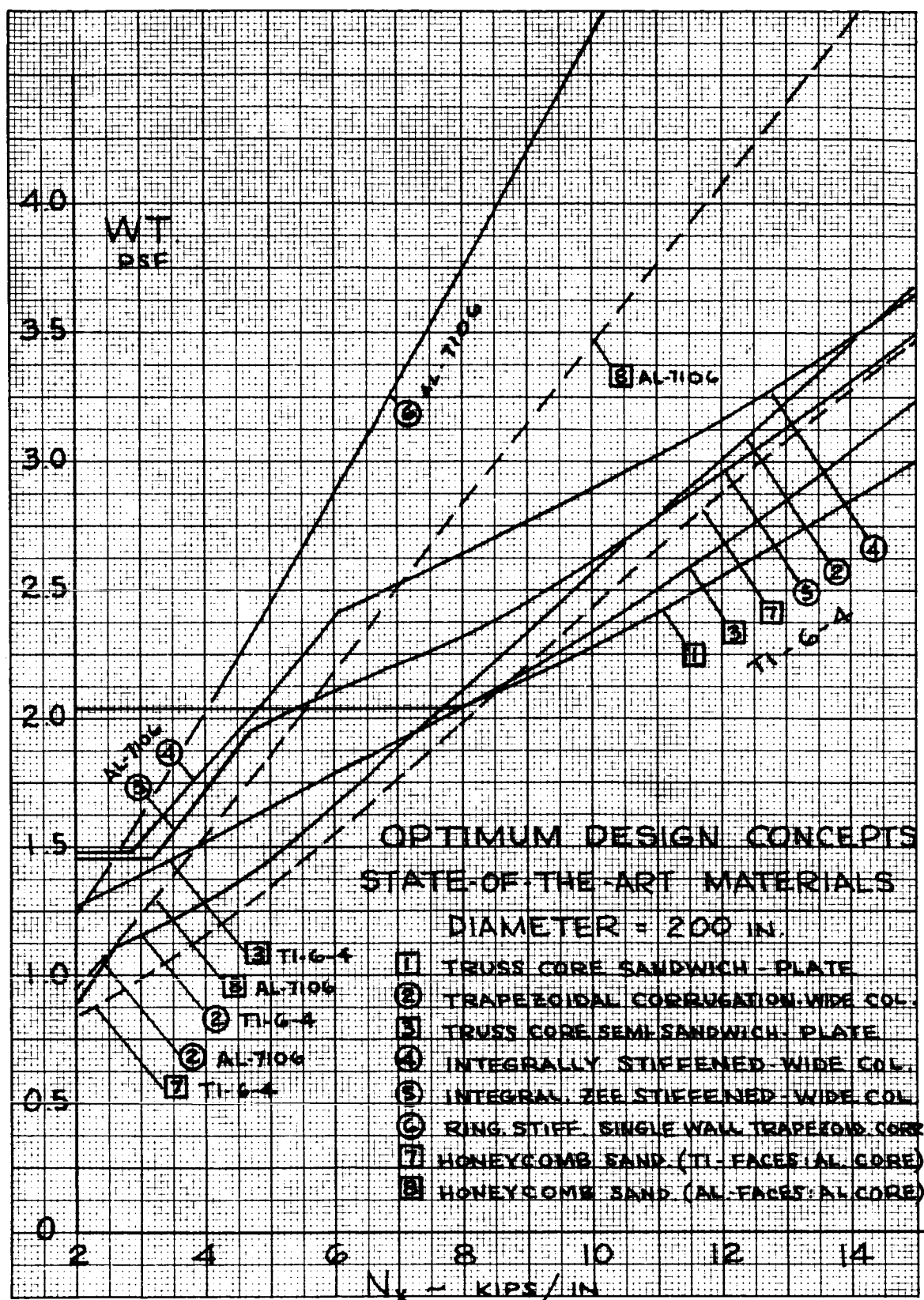


Figure 22. Final Weight Versus Load Diagrams for 200-Inch Diameter
(State-of-the-Art Materials)

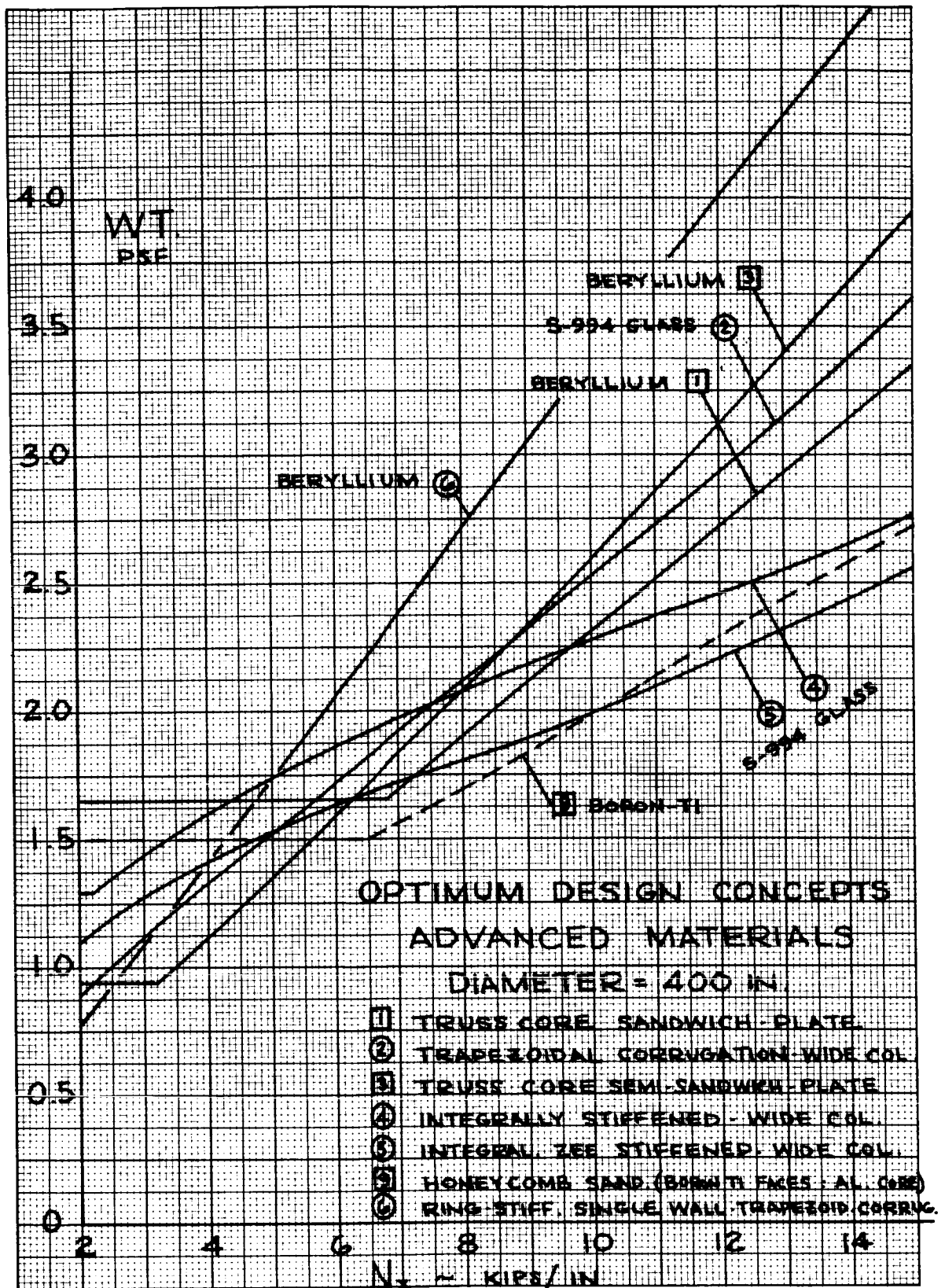


Figure 23. Final Weight Versus Load Diagrams for 400-Inch Diameter
(Advanced Materials)

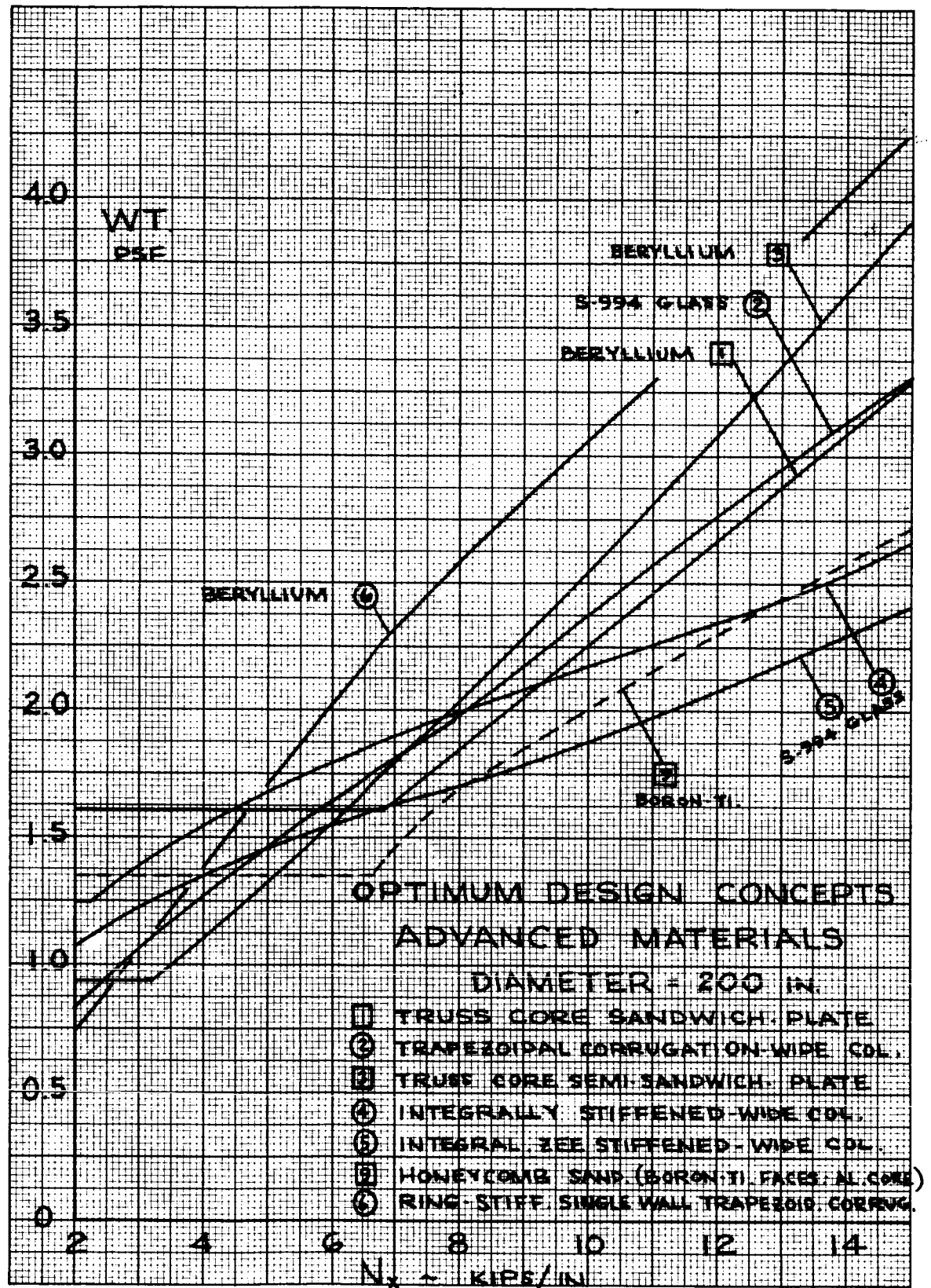


Figure 24. Final Weight Versus Load Diagrams for 200-Inch Diameter
(Advanced Materials)

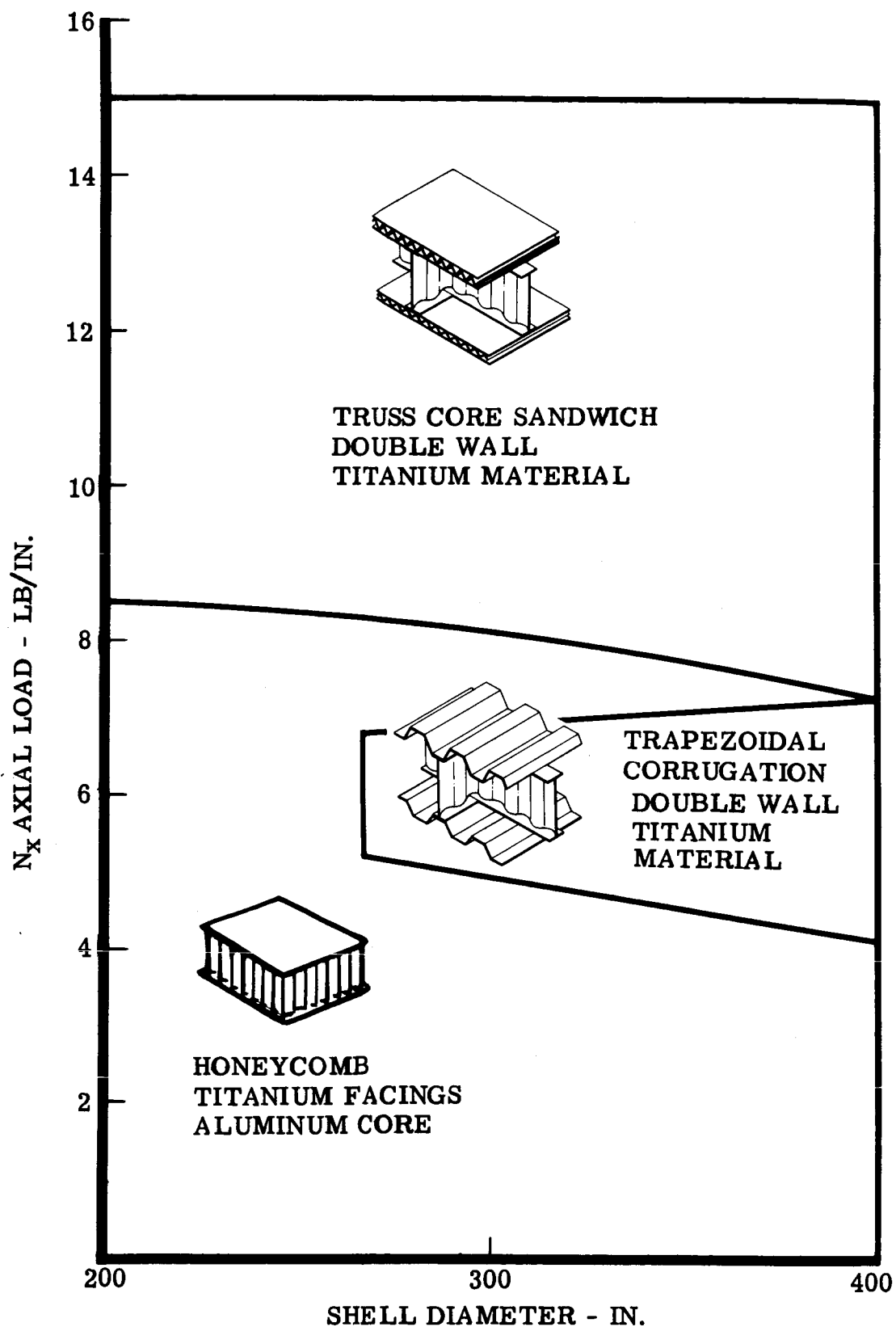


Figure 25. Optimum Concepts for State-of-the Art Materials - Load Versus Diameter

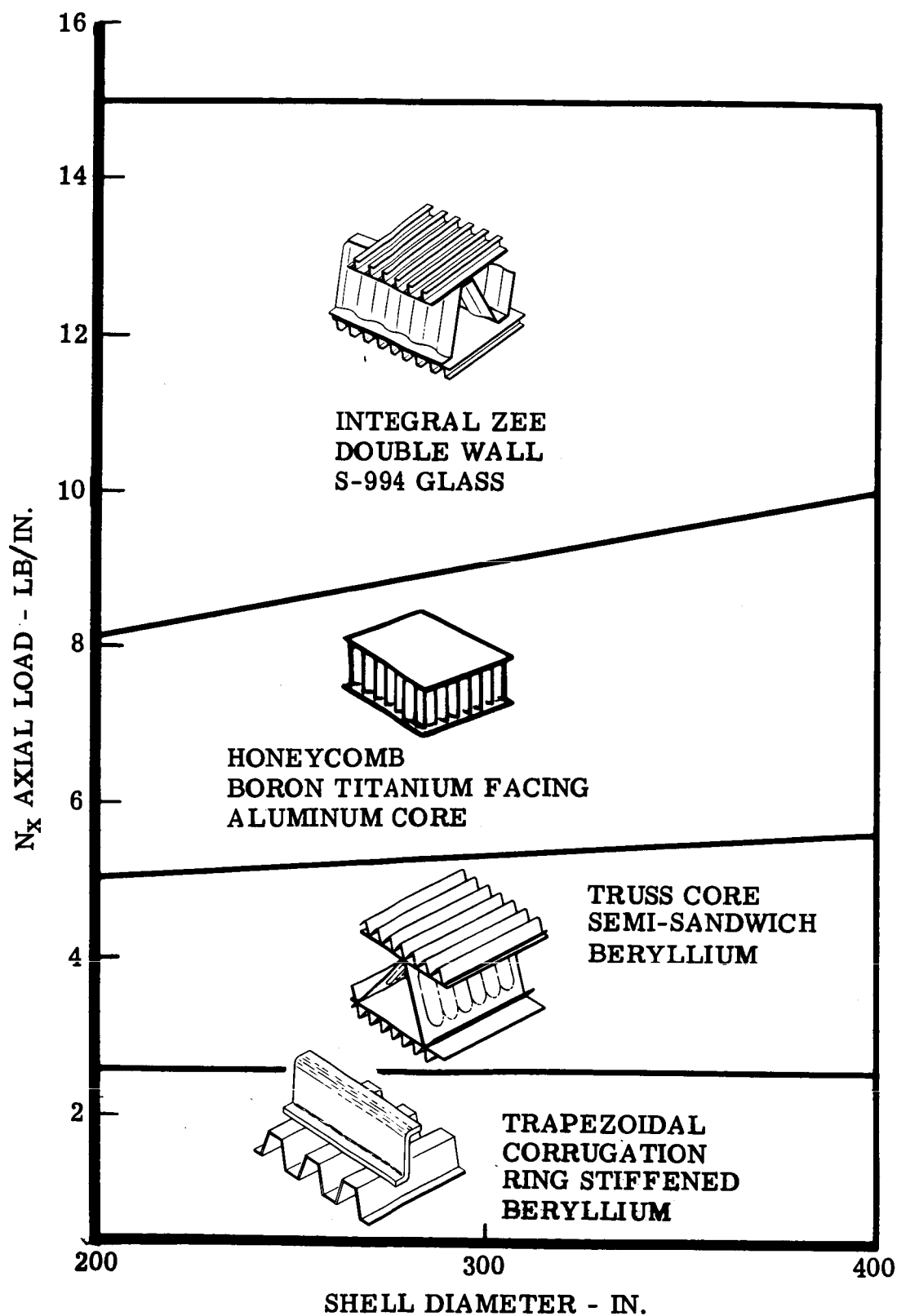


Figure 26. Optimum Concepts for Advanced Materials Load Versus Diameter

LOAD LEVEL = 5,000 LB/IN
50 UNIT COST

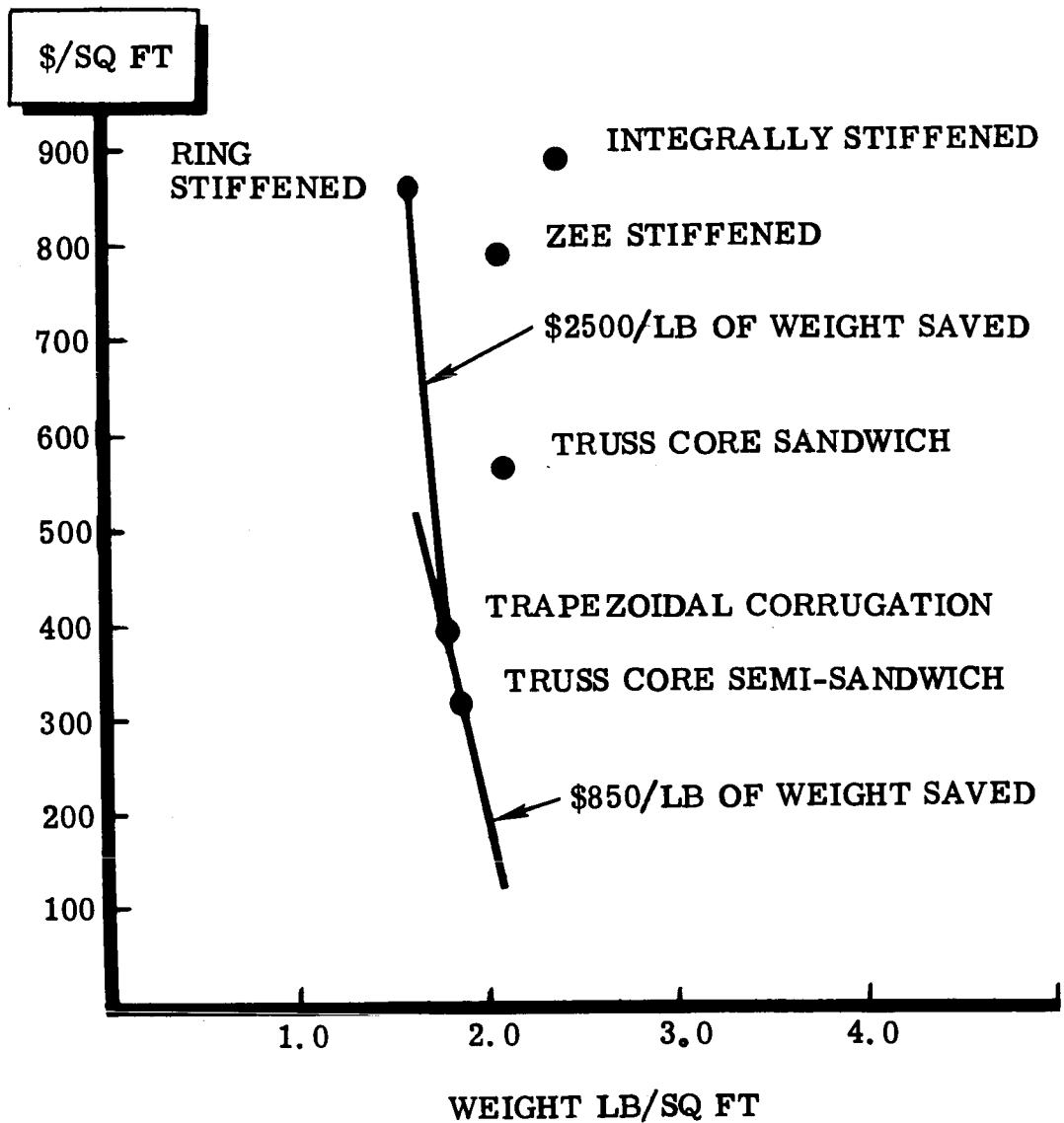


Figure 27. Cost/Weight Trade Study Chart - 5000 lb/in.

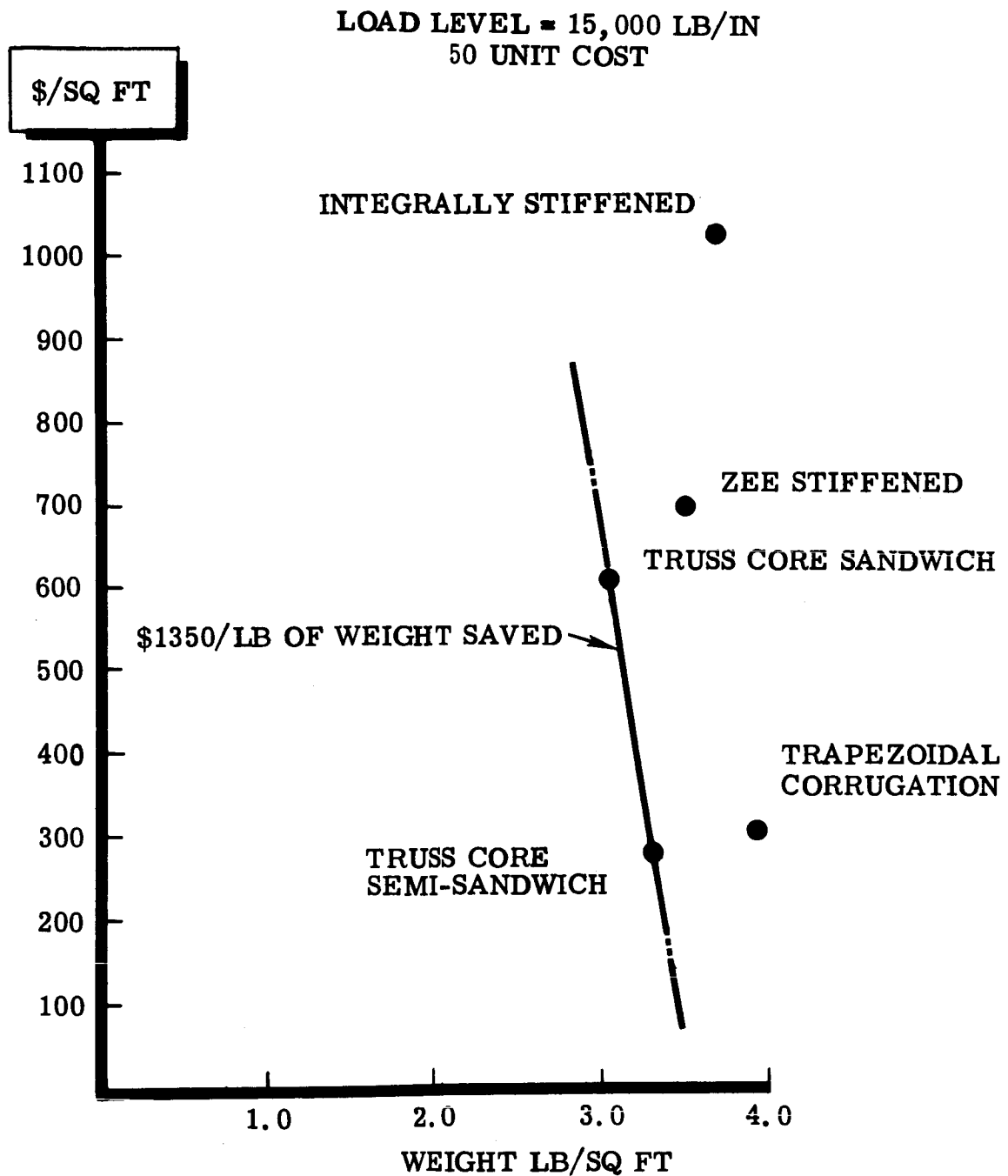


Figure 28. Cost/Weight Trade Study Chart - 15,000 lb/in.

GENERAL COMMENTS ON OPTIMUM DESIGNS

The ability to fabricate the selected concepts into reliable flight hardware has been the most important design criterion throughout the program. A producibility evaluation of the concept/material matrix shows that all designs can be fabricated into complete double-wall shell structure. The following manufacturing sequence is visualized:

1. The inner skin structural panels are assembled and spliced together completing the inner cylindrical shell.
2. The substructure is assembled to the inner shell and all substructure splices completed.
3. Closing out the outer panel of the shell completes the double-wall structure.

The cover panels and substructure form the primary weight increments in cylinder wall design. For efficient design, the minimum gage and attachment reinforcement considerations should be secondary items from a weight standpoint. However, these factors are often the controlling element in determining optimum concepts and optimum materials.

The basis on which the three materials are selected for each of the concepts is discussed next. Since the cutoff values change relative concept efficiencies significantly in the middle and low load regions, the selection of the optimum material is, in many cases, a design decision. The selection determines which material is optimum in the load region where the concept considered shows most promise. For instance, the truss-core sandwich double-wall concept is clearly superior in the higher load regions. Materials selected for the truss-core sandwich concept are those most attractive in high load regions. The trapezoidal corrugation double-wall concept is most competitive in lower load level applications. Materials selected for the trapezoidal corrugation concept are those most attractive in low load regions. Even with this ground rule it is difficult to narrow the field of candidate materials to the screening goal of three for each concept.

Production of titanium, magnesium, and aluminum structural concepts are all well within existing manufacturing capabilities. The PH15-7Mo and 18Ni maraging steel configurations (truss-core sandwich and truss-core semisandwich, respectively) can be formed by current manufacturing techniques. However, the flat required at the core to face spotweld line results in a deviation from the perfect truss desired for optimum design. Structural testing is recommended to evaluate the weight penalty resulting from this detailed design problem.

The advanced materials category is, by definition, an investigation into material potentials. The beryllium concepts appear to be producible based on preliminary fabrication development work being carried on in this country. However, major manufacturing development programs would be required to scale up fabrication processes now being used under research laboratory conditions. Joining of beryllium appears to be one of its major fabrication problems. The S-994 glass fiber concepts do not pose any difficulties from a general processing or manufacturing standpoint. However, fabrication of the selected configurations would be slow and costly.

It is noted that the boron-titanium composite was penalized by the 0.020 inch minimum gage. The high structural efficiency of this composite could be utilized only in the 15,000 lb/in. load region and was, therefore, eliminated from final evaluations. This composite and others, such as boron-resin composites under current development, offer significantly high properties and should be re-evaluated as production capabilities increase.

Detailed design of panel joints and cover to substructure attachments is the keystone to development of concept potential. Attainment of weight, producibility, and reliability requirements is a direct result of effective joint design. In order to achieve a feasible design weight as near the theoretical optimum as possible, eccentricities and offsets are minimized. Overlapping and duplicated structure is eliminated, where possible. Longitudinal joints must provide sufficient transverse shear and moment stiffness for shell stability requirements. Circumferential joints must be capable of transmitting structural loads to adjoining segments beside providing the required shear and moment stiffness.

All designs are based on a one material cover panel/substructure arrangement. Thus, the designs have greater applicability and flexibility. For instance, alternate methods of attachment are applicable with similar materials, whereas dissimilar materials limit available joining methods.

Maximum size of material available does not permit manufacture of the complete finished product, due to the extremely large cylinder sizes investigated. Thus, the shell wall must be fabricated in segments and joined together to form the complete assembly. Nominal panel sizes of the selected configurations are shown in the engineering drawings of each concept.

The engineering drawings for each concept, which follow, show a specific design for each material selected. A basic design is included for one load level and one diameter. Variations to this basic configuration necessary for diameter and load variations are included. These quantities are shown on the drawings and as tabulations in the geometry weight summaries for each concept. Longitudinal and circumferential splices are detailed. Substructure to cover attachments are shown.

All necessary information for the design of each concept/material arrangement is arranged in the following manner:

1. Explanatory remarks
2. Design drawing
3. Design graph
4. Geometry and weight summary

USE OF DESIGN DRAWINGS, GRAPHS, AND SUMMARY TABLES

For a particular uniaxial compression load level and shell diameter, use figure 25 or 26 to determine the optimum material/design concept. The appropriate layout drawing may be consulted to view the design details of the selected concept. The associated summary table lists the pertinent geometry data from which the weight, optimum substructure spacing, and shell thickness values may be determined. Knowing the load level (N_X) and the optimum support spacing (L_{OPT} or b_{OPT}), the design graph may be interpreted for the appropriate cover panel dimensions as follows:

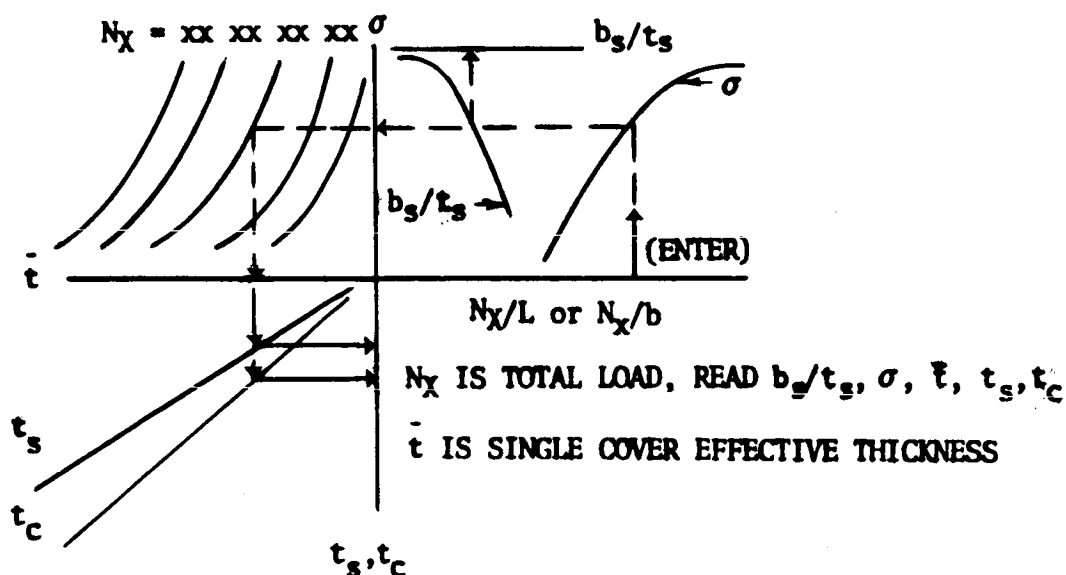


Figure 29. Illustration of the Use of Design Graphs

DOUBLE-WALL TRUSS-CORE SANDWICH COVER PANELS WITH SINE-WAVE SHEAR WEB SUBSTRUCTURE

The truss-core sandwich concept is a most promising double-wall configuration in the moderate to high load level range. The cover design concept combines the advantages of sandwich construction with efficient load carrying core. The structural elements of the core are arranged predominantly in the longitudinal direction to provide full advantage of cover panel axial load capability. The cross sectional view of the cover panel shows core elements forming diagonal truss members sufficiently rigid that the required transverse shear stiffness is obtained. The substructure concept was established with the sine wave web arranged in the longitudinal direction to provide efficient "plate type" support structure.

The three candidate materials providing the best potential designs for this concept on a minimum weight and producibility basis are titanium, stainless steel, and beryllium. The roll diffusion bonding process has been successfully achieved with titanium material. With minimum gage constraints applied to this concept, considerable weight savings over existing designs can be obtained in relatively high load levels (8500 to 13,000 lb/in.). The truss-core cover concept can also be fabricated by using spotwelding processes. However, with spot-welding a loss in structural efficiency may result if flats are required in the core to accommodate joints with the facing sheet. Lands on the facing sheets are chem-milled to provide reinforcement material at splices and substructure attachment lines.

Shear webs are predominantly longitudinal, with circumferential webs spaced 20 inches apart. The substructure consists of arc seam welded sine wave shear webs/caps. Commercially pure titanium is utilized, in lieu of 6Al-4V Ti, to meet shear rigidity design requirements with lower cost and more formability. The sine wave webs for both longitudinal and circumferential shear members are produced on multistage form tools. After the caps are arc seam welded to the webs, the subassemblies are stress relieved in a fixture.

Assembly of the panel wall sections is accomplished by the use of blind fasteners with room temperature adhesive applied along all joints to guarantee joint stiffness.

Panel sizes are based upon NAA in-house furnace capacity for solution heat treating and heat treat aging of the roll diffusion bonded panels. Panels are fabricated using a 60 percent reduction in the starting height of the pack layup. The fabrication sequence employs a layup of the material (annealed condition) in a retort, roll diffusion bonding of the panels, warm rolling of the pack to a contour, removal of the retort, solution heat treating, leaching of the mandrels, fusion welding of two panels to make a larger panel, and heat treat aging in a fixture. Fusion welding would be utilized to reduce the number of mechanical joints in order to save weight. Postbond chemical milling of the skin surface would be used as another weight saving operation.

Reliability of a high order can be obtained for the roll diffusion bonded panels by X-ray, ultrasonic, and/or proof pressure testing techniques. Combined with standard inspection techniques for process and control of other manufacturing operations, a highly reliable assembly can be obtained.

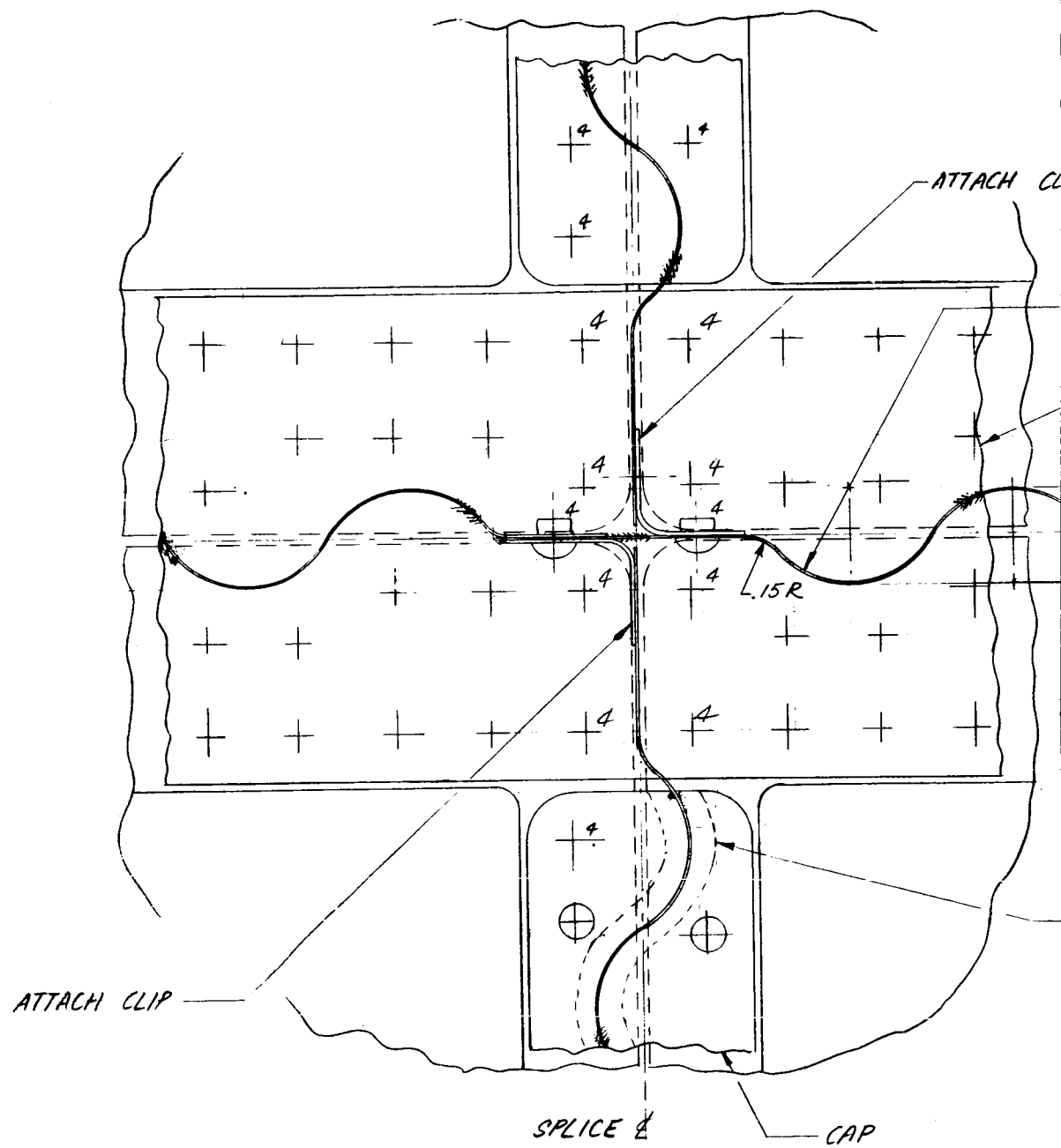
For the truss-core sandwich of PH15-7Mo stainless steel alloy, the spot-welding process becomes most favorable from the manufacturing standpoint. The material is not effected by the minimum gage constraint at high load levels (above 13,000 lb/in.). However, resistance welding of the core to the face sheet, requires sufficient flat at the node of the corrugation to prevent expulsion of the weld nugget. Providing a flat node corrugation may reduce the structural efficiency of the design. A structural test is recommended to assess the importance of this design problem.

The diffusion bonding manufacturing technique offers an attractive configuration approaching the theoretically desirable perfect truss cross-section. Parameters for diffusion bonding Ph15-7Mo truss-core are not fully established.

From the overall design standpoint, the PH15-7Mo steel configuration is similar in construction to the titanium design. Covers are joined to sine wave shear webs by organic bond and rivets. Splices are the same as for the titanium design, and are attached with A286 rivets. The shearwebs are fillet welded to the caps.

The best potential for the truss core sandwich concept with the efficient beryllium material is to use the diffusion bonding process. This material provides the best potential at intermediate load levels (5000 to 8500 lb/in.). Extensive development is required to obtain a method of fabricating beryllium sheet material by roll bonding into the truss core configuration. The attachment of the corrugations to the face sheet may be achieved by electron beam welding. Again, a major development program is required. The fabrication of detail parts, i.e., forming, trimming, etc., are well within the current state-of-the-art. Sheet stock can be formed at 1000°F to 1400°F.

Sine-wave shear webs are joined to the caps by electron beam welding. The splices appear the same as those illustrated for the titanium except more generous edge distances are provided, and monel rivets are utilized. To join the substructure to the covers, adhesive bonding and monel rivets are necessary.



570

IP

.50 R

CAP

SPLICE

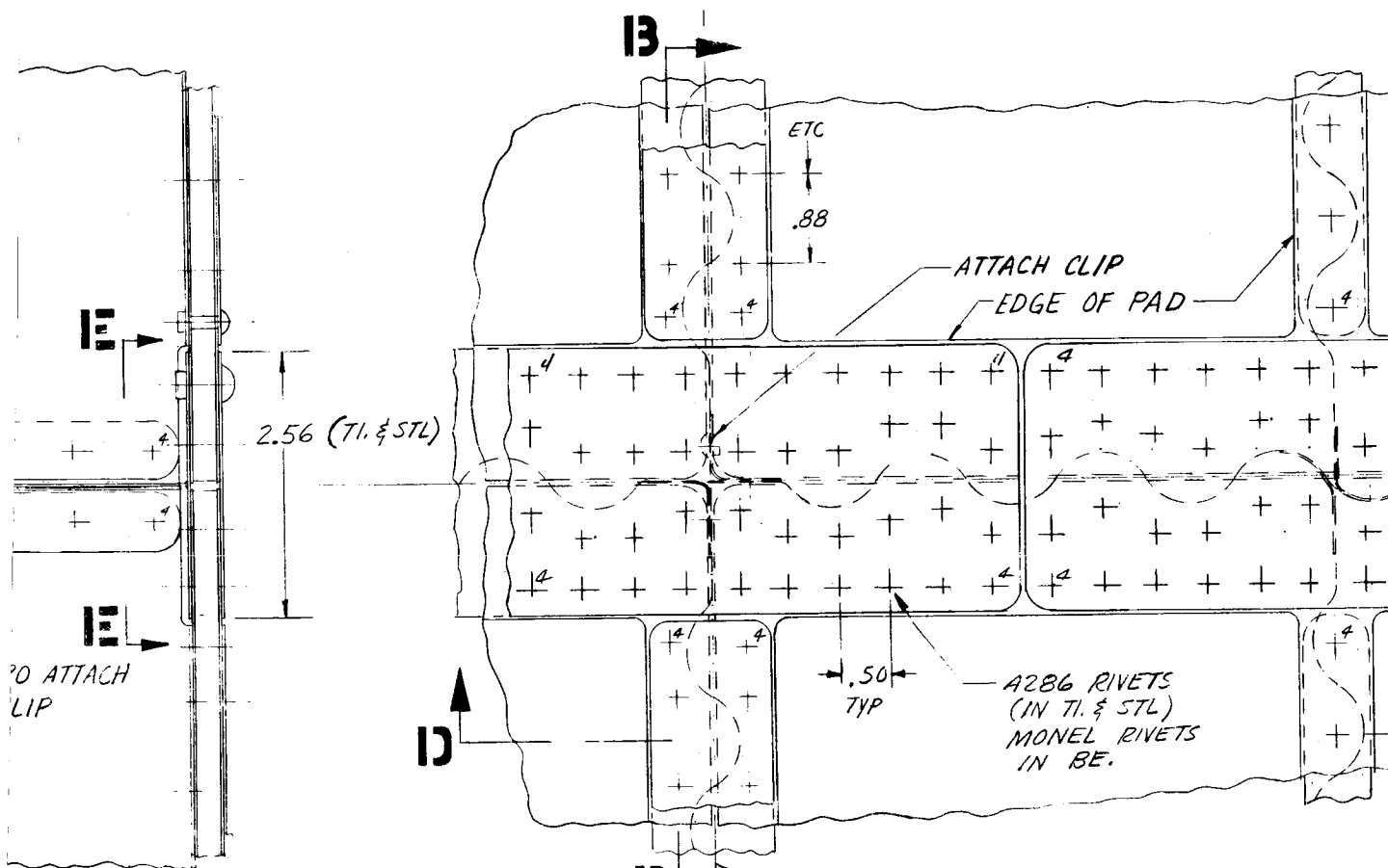
.50

WELD FILLET

TYP .090

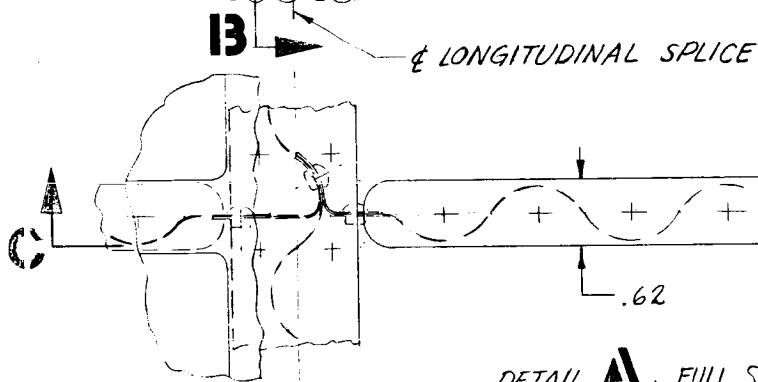
SECTION

57-②



TO ATTACH
CLIP

IN **B-B**



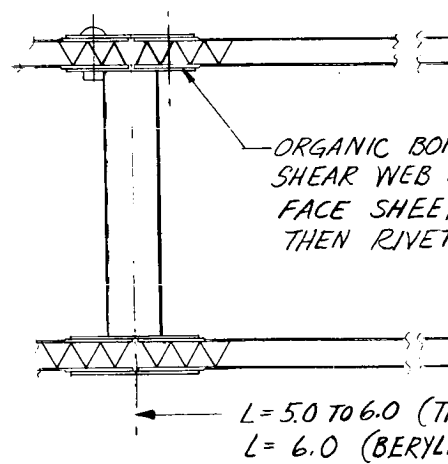
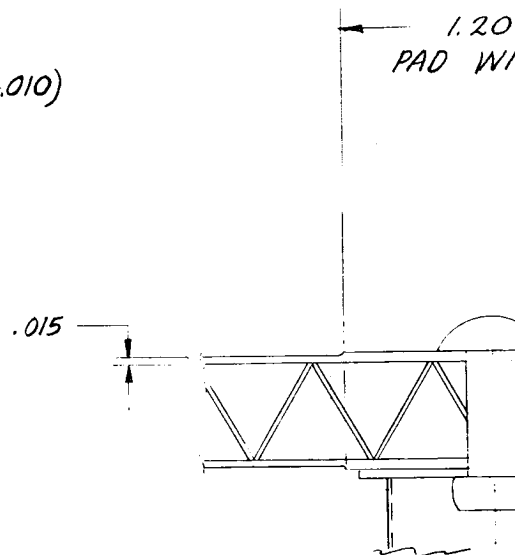
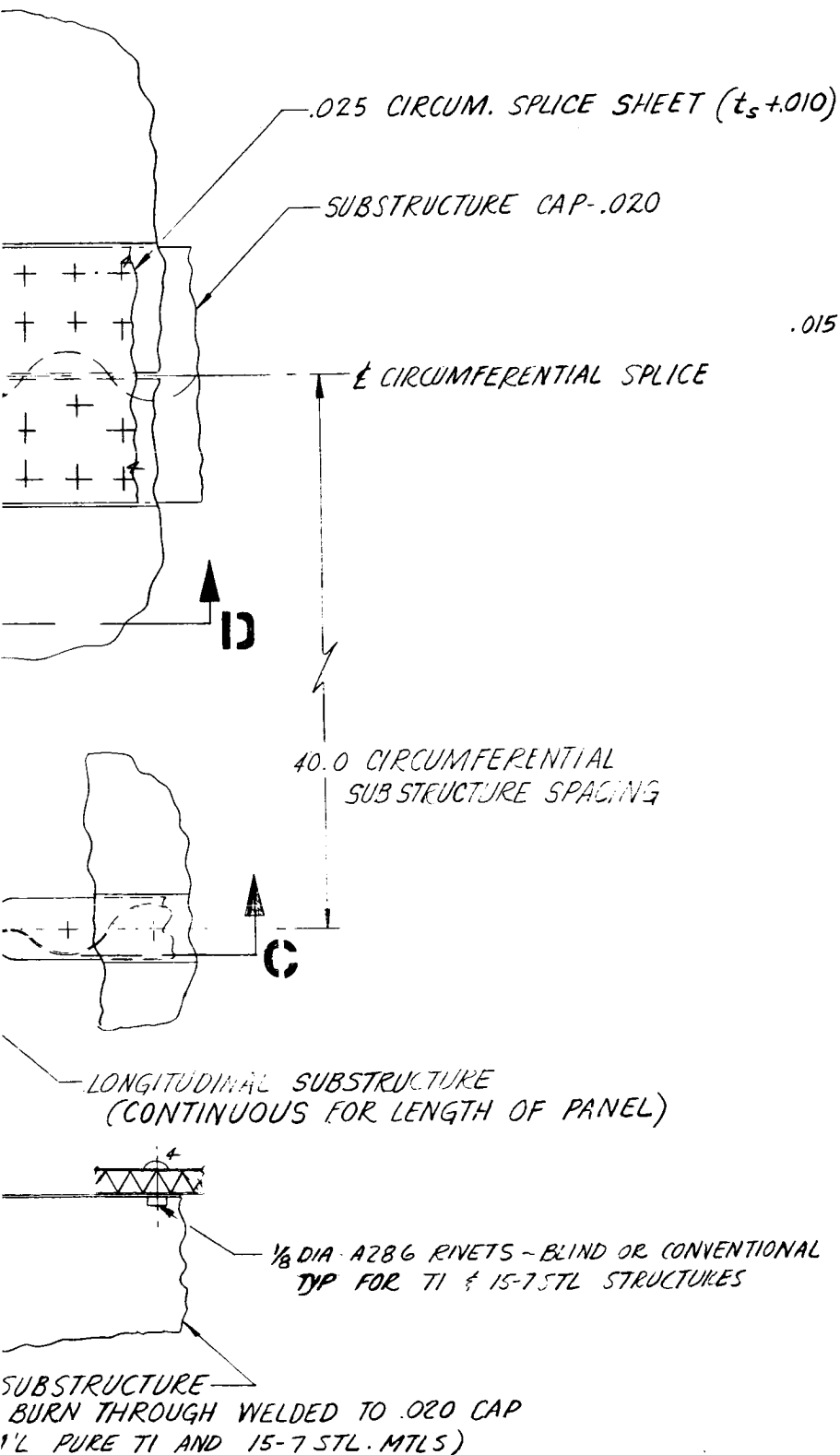
DETAIL **A**, FULL SCALE
 MTL TL ~ NR = 2000 TO 15000 LB/IN
 15,000 LB/IN, 200R SHOWN
 TYP FOR 15-7 STL & BE. EXCEPT AS NOTED.

(TL & 15-7 STL).020 ATTACH CLIP

SECTION **C-C**

CIRCUM.
 (.010 WEB
 FOR CON

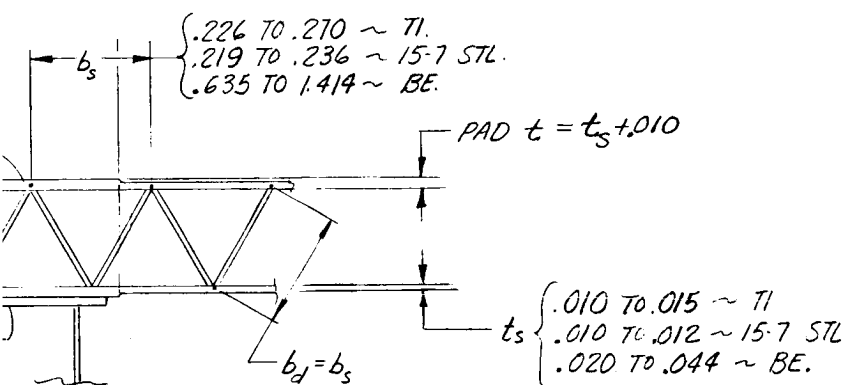
57-③



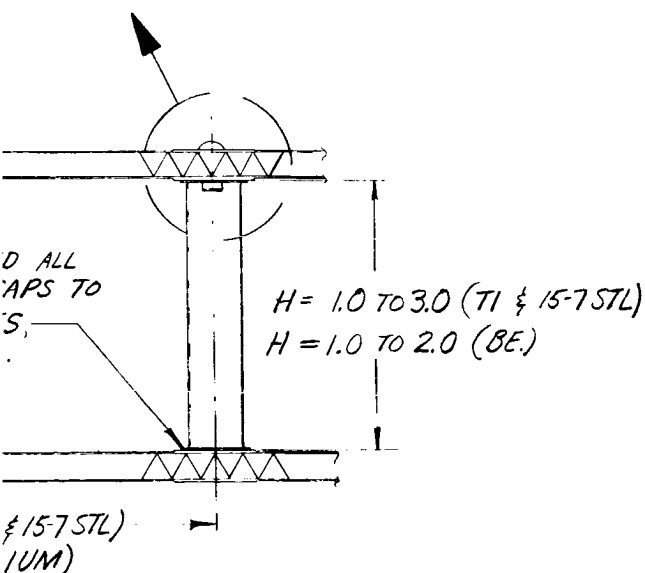
SECTION ID

57(4)

0TH



1/2 PAD CROSS SECTION

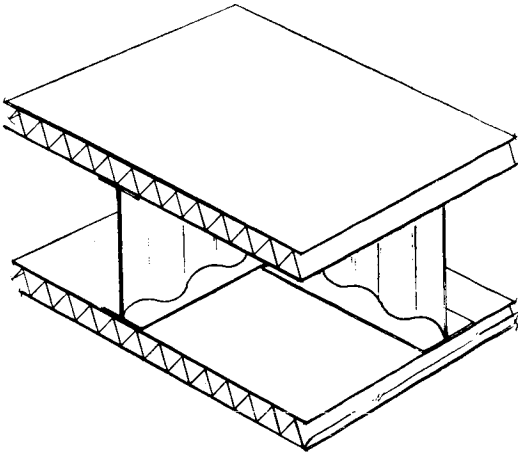


MAX PANEL WID
ROLLED DIFF BO
SPOT WELDED:

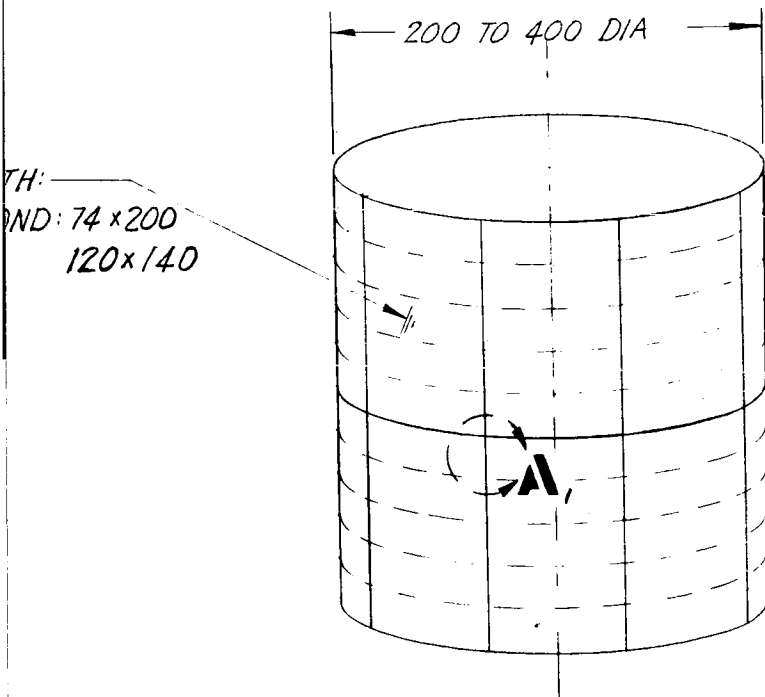
-13

57-5

Figure



DESIGN DWG-DOUBLE WALL TRUSS CORE SANDWICH
FIG. 30



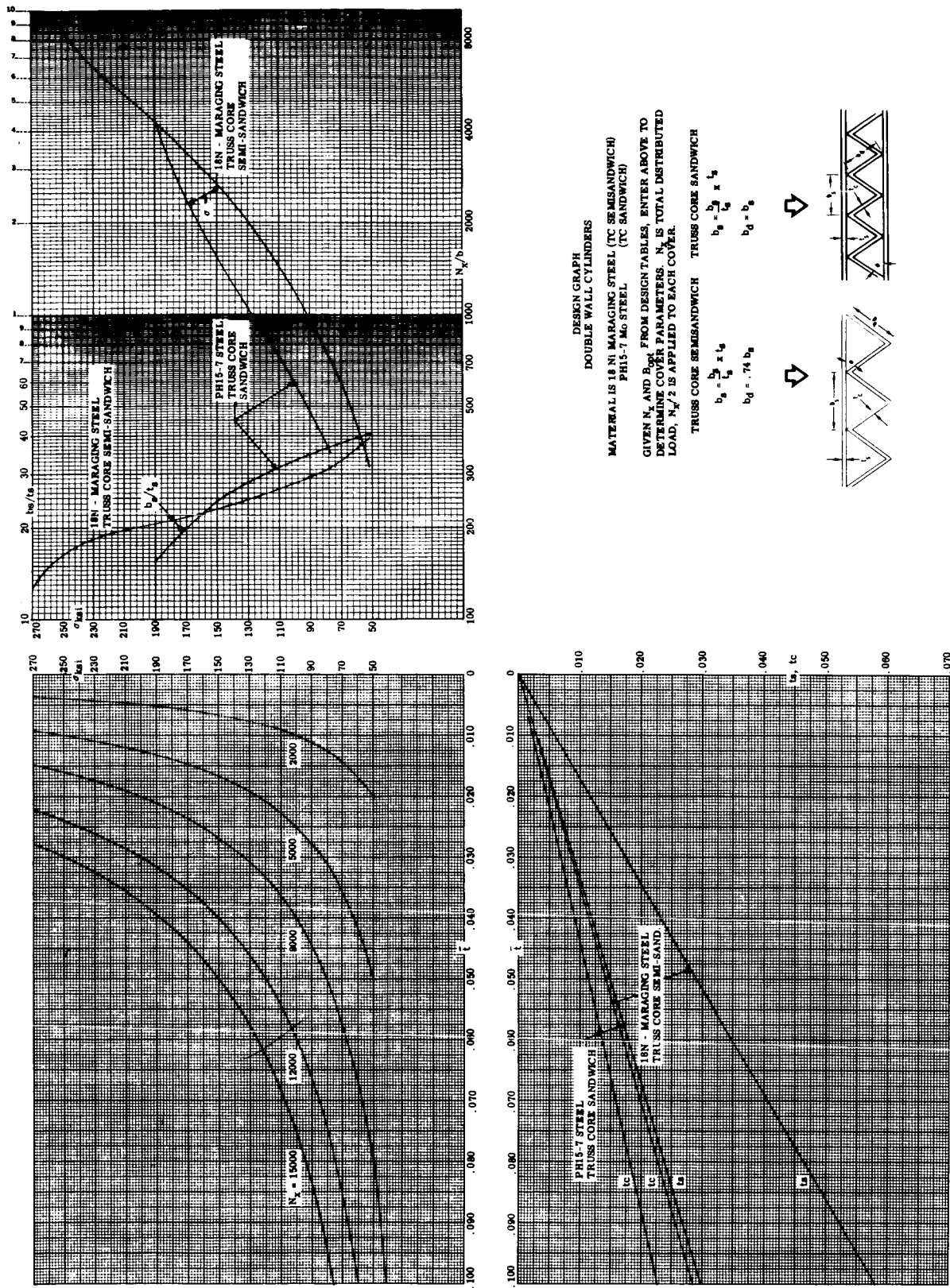


Figure 31. Design Graph - Double-wall Truss Core Sandwich

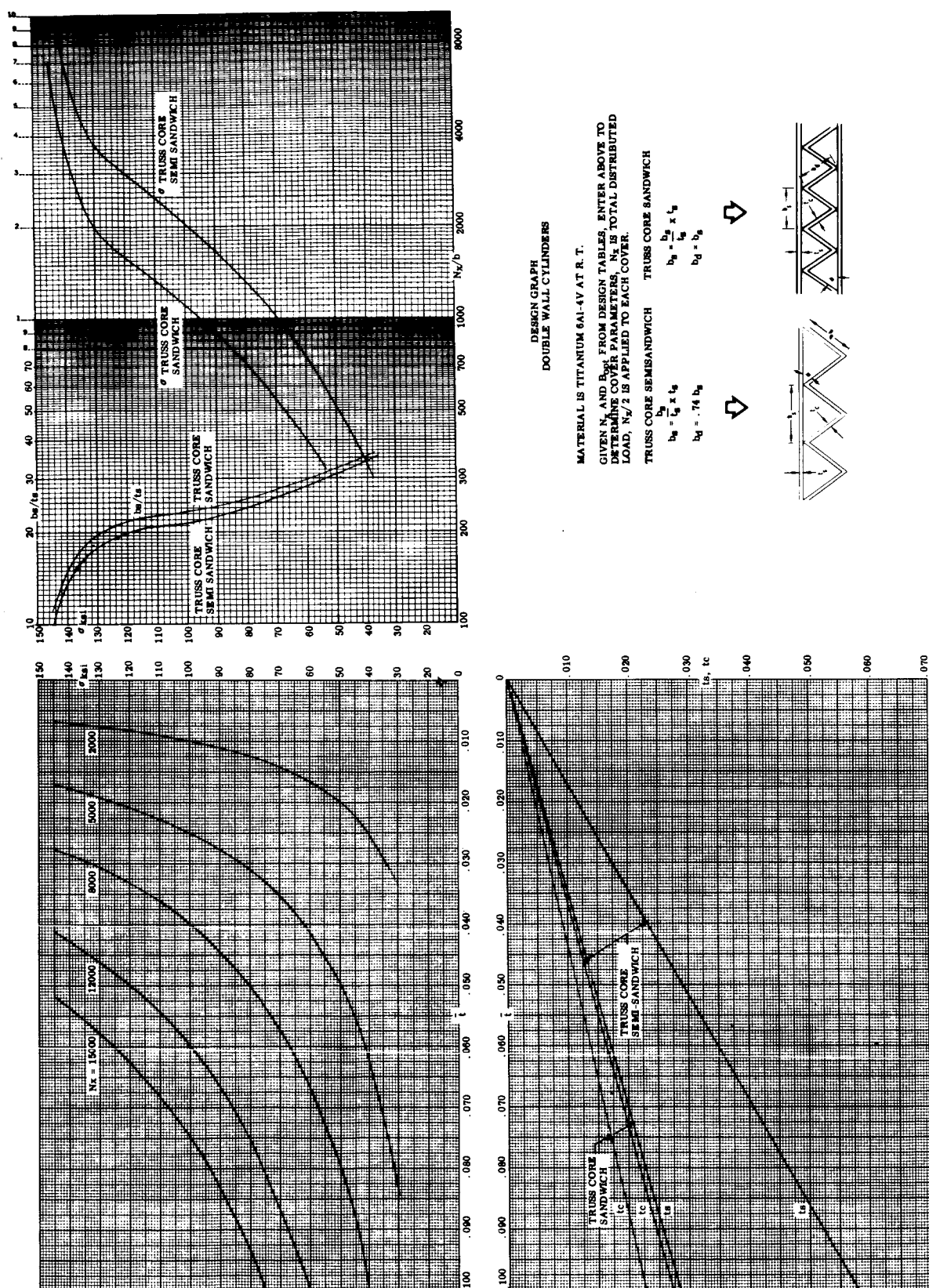


Figure 31. Design Graph - Double-wall Truss Core Sandwich

DESIGN GRAPH

DOUBLE WALL - TRUSS CORE SANDWICH
BERYLLIUM AT ROOM TEMPERATURE

ALL DESIGNS OPERATING AT 47000 PSI STRESS LEVEL

$$\bar{t} = \frac{N_x}{2\sigma}$$

$$b_s / t_s = 32.0$$

$$t_s = .273 \bar{t}$$

$$t_c = .227 \bar{t}$$

$$b_d = b_s$$

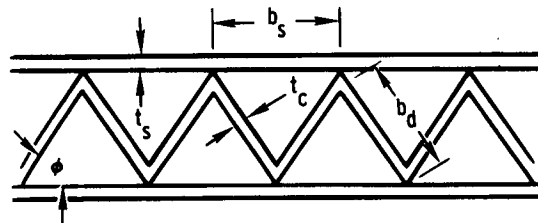


Figure 31. Design Graph - Double-wall Truss Core Sandwich (Cont)

Table IX

TRUSS CORE SANDWICH PLATE COVERS
SINE WAVE SHEAR WEB SUBSTRUCTURE

MTL.	N _x LB/IN.	RADIUS IN.	SUPPORT SPACING IN.	SHELL THICK. IN.	SUBSTR. WEB THICK. IN.	SUBSTR. WT. PSF	COVER WT. PSF	PENALTY WT. PSF	TOTAL WT. PSF
Ti 6-4	8000	100.	6.0	1.0	0.011	0.067	1.680	0.291	2.038
		133	6.0	2.0	0.010	0.122	1.680	0.291	2.093
		167	6.0	2.0	0.010	0.122	1.680	0.291	2.093
	8000	200	6.0	2.0	0.010	0.122	1.680	0.291	2.093
	12000	100	5.0	2.0	0.010	0.141	2.058	0.352	2.550
		133	5.0	2.0	0.010	0.141	2.058	0.352	2.550
		167	6.0	2.0	0.010	0.122	2.122	0.311	2.555
	12000	200	6.0	3.0	0.010	0.183	2.122	0.311	2.616
	15000	100	6.0	2.0	0.010	0.122	2.557	0.328	3.007
		133	6.0	2.0	0.013	0.158	2.557	0.328	3.043
		167	6.0	3.0	0.010	0.183	2.557	0.328	3.067
	15000	200	6.0	3.0	0.010	0.183	2.557	0.328	3.067

Table IX (Cont)

TRUSS CORE SANDWICH PLATE COVERS
SINE WAVE SHEAR WEB SUBSTRUCTURE

MTL	Nx LB/IN	RADIUS IN.	SUPPORT SPACING IN.	SHELL THICK. IN.	SUBSTR WEB THICK. IN.	SUBSTR WT. PSF	COVER WT. PSF	PENALTY WT. PSF	TOTAL WT. PSF
BE	6800	100	6.0	1.0	0.020	0.050	1.393	0.159	1.602
		133	6.0	1.0	0.020	0.050	1.393	0.159	1.602
		167	6.0	1.0	0.020	0.050	1.393	0.159	1.602
	6800	200	6.0	2.0	0.020	0.100	1.393	0.159	1.652
	8000	100	6.0	1.0	0.020	0.050	1.618	0.166	1.834
		133	6.0	1.0	0.020	0.050	1.618	0.166	1.834
		167	6.0	1.0	0.020	0.050	1.618	0.166	1.834
	8000	200	6.0	2.0	0.020	0.100	1.618	0.166	1.884
	12000	100	6.0	1.0	0.020	0.050	2.427	0.190	2.666
		133	6.0	1.0	0.020	0.050	2.427	0.190	2.666
		167	6.0	1.0	0.020	0.050	2.427	0.190	2.666
	12000	200	6.0	2.0	0.020	0.100	2.427	0.190	2.717

Table IX (Cont)

TRUSS CORE SANDWICH PLATE COVERS
SINE WAVE SHEAR WEB SUBSTRUCTURE

[illegible]

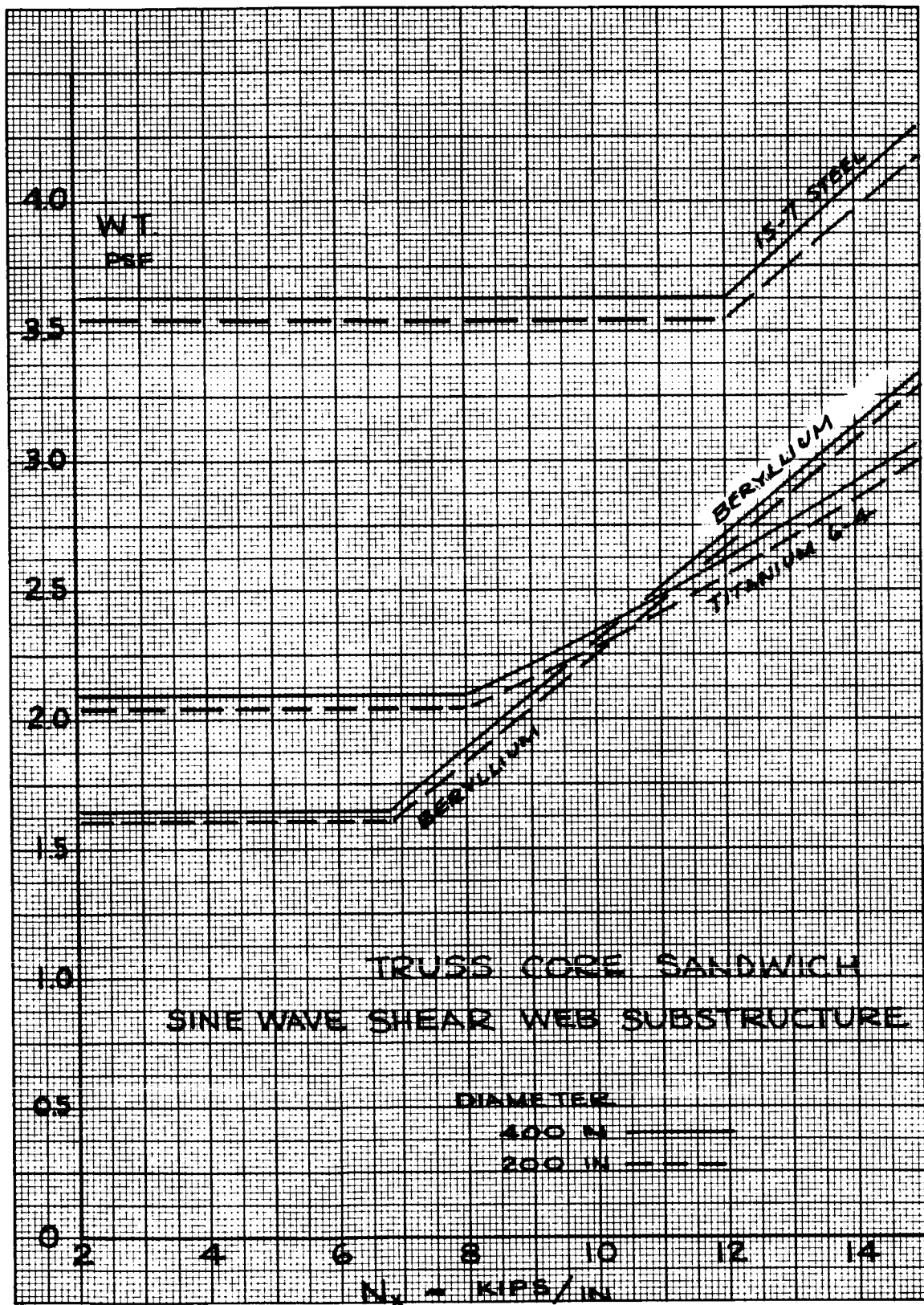


Figure 32. Panel Weight Versus Load - Truss Core Sandwich

DOUBLE-WALL TRAPEZOIDAL CORRUGATION COVER PANELS WITH SINE-WAVE SHEAR WEB SUBSTRUCTURE

This design concept offers an efficient load-carrying structure and fabrication simplicity, and shows an advantage over other concepts in the low and moderate load ranges. Titanium, aluminum, and fiber glass materials are selected for the trapezoidal corrugation configuration. In general, there are no major problems of fabrication or assembly. All three of these structures/material configurations have a high degree of reliability. All fabrication procedures are easily reproducible and inspectable, thus guaranteeing structural conformance to engineering design requirements.

The trapezoidal corrugation - sine-wave substructure concept is a double-wall cylinder having inner and outer longitudinally oriented corrugated panels separated by a substructure network of sine wave shear webs. These substructure stiffeners are spaced 4 to 6 inches apart longitudinally and 20 inches apart circumferentially. These members consist of a sine wave formed web with welded on caps. The corrugated covers are joined to the substructure caps by organic bonding and rivets. Splice sheets are flat, in most cases, and the circumferential cover splice is corrugated to match. The cover longitudinal splices are made by overlapping one corrugation and riveting.

The titanium sine-wave shear webs are fabricated by burn-through welding the web to the caps. The circumferential shear webs are segmented between the longitudinals and joined to them with shear clips. The longitudinal shear web splices are made by continuing the web past the caps and riveting to the continuous circumferential splice directly under a cover circumferential splice. These joints are made before the outer close-out panel is attached. Then the closeout panel attachment is accomplished by blind A286 rivets. Where required, radius washers are used under rivet heads.

The titanium configuration uses commercially pure titanium for substructure application. Pure titanium was selected because stiffness is the primary structural requirement. Alloyed titanium offers no advantage and is higher in cost than commercially pure titanium material. The use of arc seam welding to fabricate the substructure is a common production practice at NAA/LAD. Many thousands of feet of this type of welding have been used for similar applications on the XB-70.

The corrugated covers are fabricated by standard brake forming techniques using multi-stage brake forming dies. The corrugation is then hot sized in matching dies to final size and tolerance. This procedure, again, is a routine fabrication technique at NAA. The hot-sizing procedure was developed by NAA and used on the F-100, X-15, and XB-70 vehicles.

Joining of the substructure to the panels and panel-to-panel splices is accomplished with conventional and blind rivets. Drilling of holes in titanium present no problems when the proper drill point configuration is used. The

large amount of production fabrication experience on the F-100 through the XB-70 vehicles has shown the reliability of riveted titanium structure. A recent rehabilitation program on F-100 vehicles, which has a complete tail section fabricated from titanium, showed that these sections required little or no structural repair after thousands of hours of flight time.

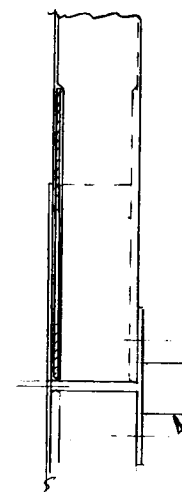
The aluminum structure design is, for all practical purposes, identical to the titanium. The aluminum structural configuration is conventional in all respects except that a relatively new alloy is being used. However, it is expected that only a limited fabrication development is required.

The general fabrication procedure for the aluminum is the same as for the titanium except in two areas: (1) no hot sizing is required after forming, and (2) the sine wave substructure is fabricated by fillet welding rather than the arc seam welding techniques.

The sine wave substructure is fabricated using .050 gage material and then chem-milled to the thickness required for strength. The .050 gage is selected as a reasonable minimum gage for production fillet welding.

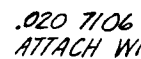
The S-994 glass version of this trapezoidal corrugation - sine wave shear web concept will be joined and spliced in a manner similar to the titanium version. The substructure segments are joined through web shear clips with all joints organic bonded and riveted. In the area of the circumferential splice an aluminum doubler sheet is sandwiched between layers of glass to provide cover bearing strength. The splice is accomplished with 2024-T3 aluminum corrugated flat sheet stock segments. This splice is designed to carry the total axial load via rivets. In all cases where bonding is required on assembly, a room temperature curing adhesive is utilized. Each shear web substructure is made by laying up the caps and web separately, then bonding together with organic adhesive.

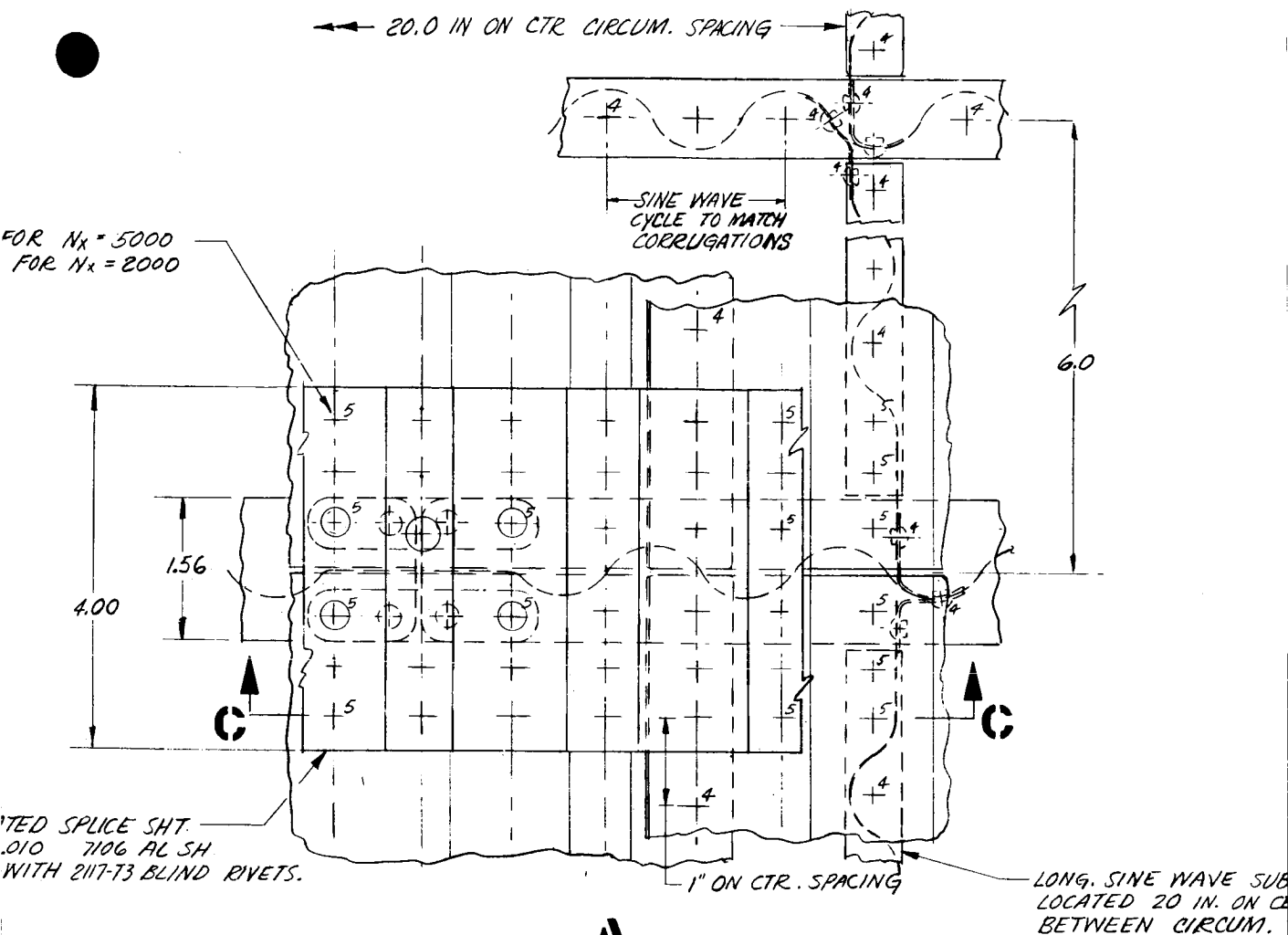
The S994 fiber glass configuration layup uses a two-ply layup with a 90 degree orientation. A preimpregnated tape is used which has uniaxial fiber direction. From a fabrication standpoint there are no problems. Detail parts are fabricated by current techniques utilizing matched heated dies, autoclave, or ovens. However, the local joining and splicing require careful detailed design.



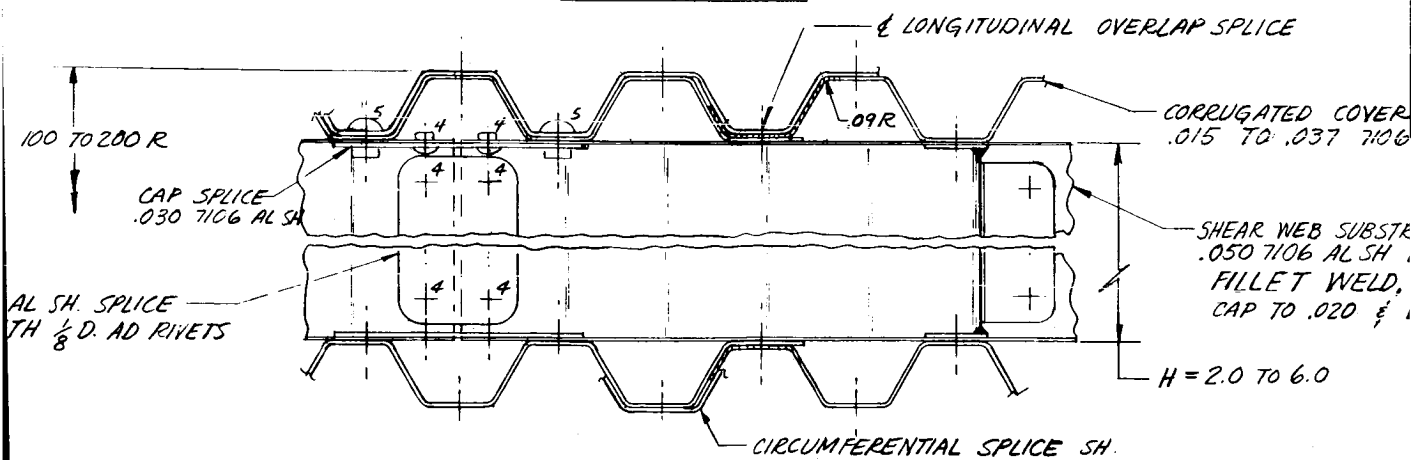
—SINE WAVE SUBSTR
BONDED TO PANEL

CORRUGA
t = t_s +
ATTACH





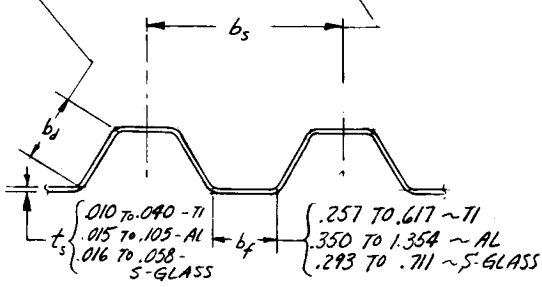
DETAIL A2 FULL SIZE
 MTL: 7106 AL - $N_x = 2000-15000$ LB/IN
 5000 LB/IN. SHOWN



SECTION C-C FULL SCALE

{ .303 TO .727 ~ TI
 .411 TO 1.596 ~ AL
 .346 TO .838 ~ S-GLASS

{ .818 TO 1.966 ~ TI.
 1.110 TO 4.333 ~ AL
 .935 TO 2.266 ~ S-GLASS



DETAIL OF PANEL CROSS SECTION ~ NO SCALE

LONGITUDINAL SUBSTRUC.
 SPACED 20 INCHES ON CENTER.
 ATTACH TO FACE SHEET & CORRUG. SHT.
 WITH 1/8 DIA A286 BLIND RIVETS

SHEAR WEB ATTACH CLIPS
 .020 COML PURE TI SH
 ATTACH WITH 1/8 DIA A286
 BLIND RIVETS

Nx	W	N & RIV. DIA.
3000	2.50	2 - 1/8
5000	2.75	2 - 5/32
8000	3.75	3 - 5/32
12000	4.12	3 - 3/16
15,000	5.35	4 - 3/16

SPLICE WIDTH W

NO. RIVETS N PER NODE EACH

STRUC.
 INTER
 SUBSTR.

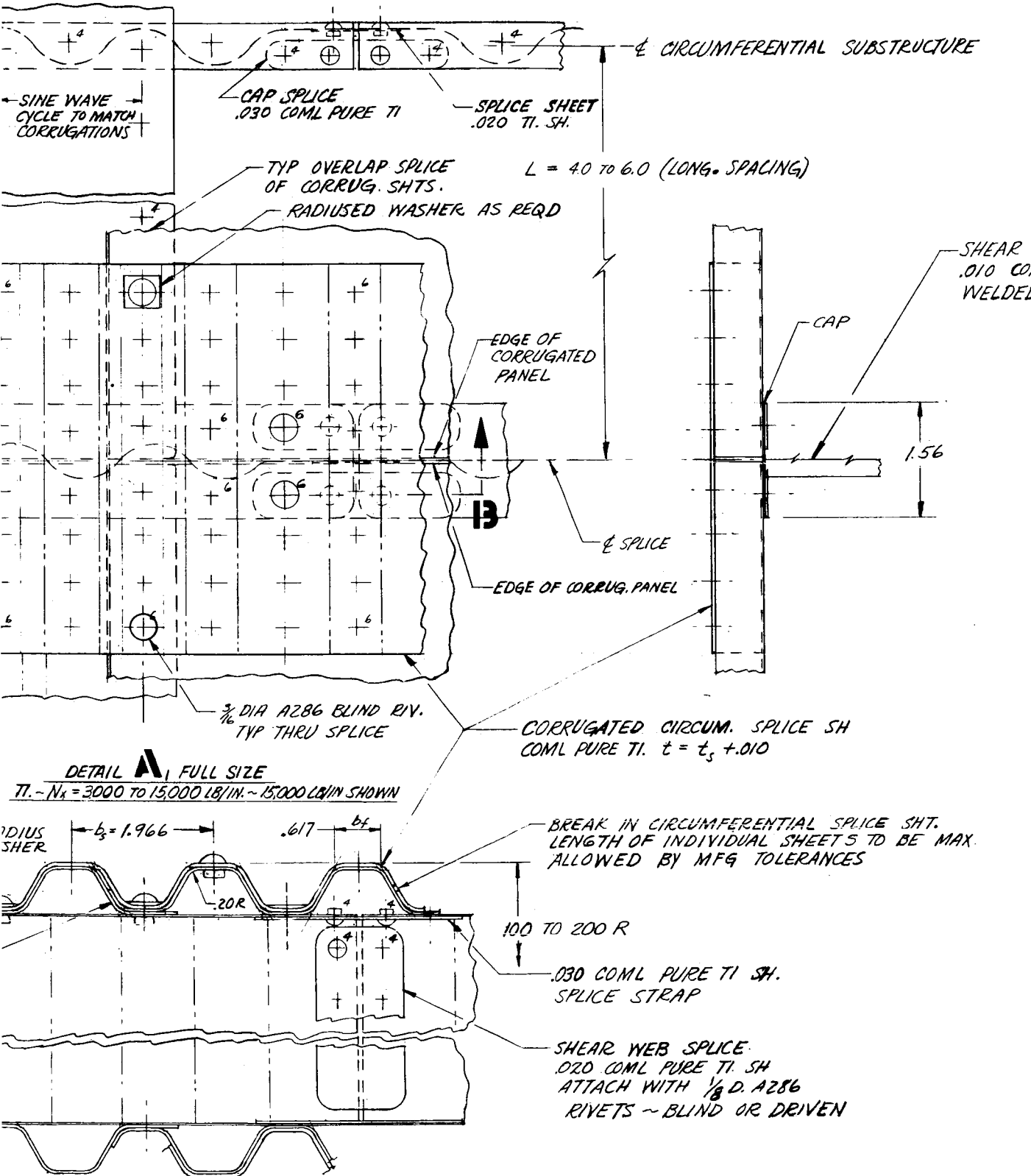
AL SH

WEB & CAP.
 CHEM MILL
 WEB TO .010

TYP OVERLAP SPLICE OF COVER SHEETS.
 JOIN WITH A286 1/8 D. RIVETS OUTSIDE
 OF CIRCUMFERENTIAL SPLICE

H = 2.0 TO 6.0

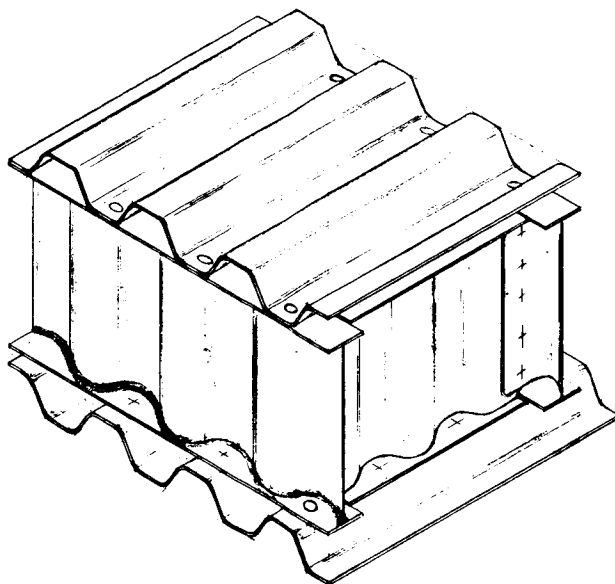
20.0 IN CTR. CIRCUM. SPACING



SECTION B-B FULL SCALE

68-2

WEB SUBSTR AT SPLICE.
 ML PURE TI BURN-THRU
 TO .020 OML PURE TI CAP



DESIGN DRAWING—DOUBLE-WALL TRAPEZOIDAL CORRUGATION

FIG. 33

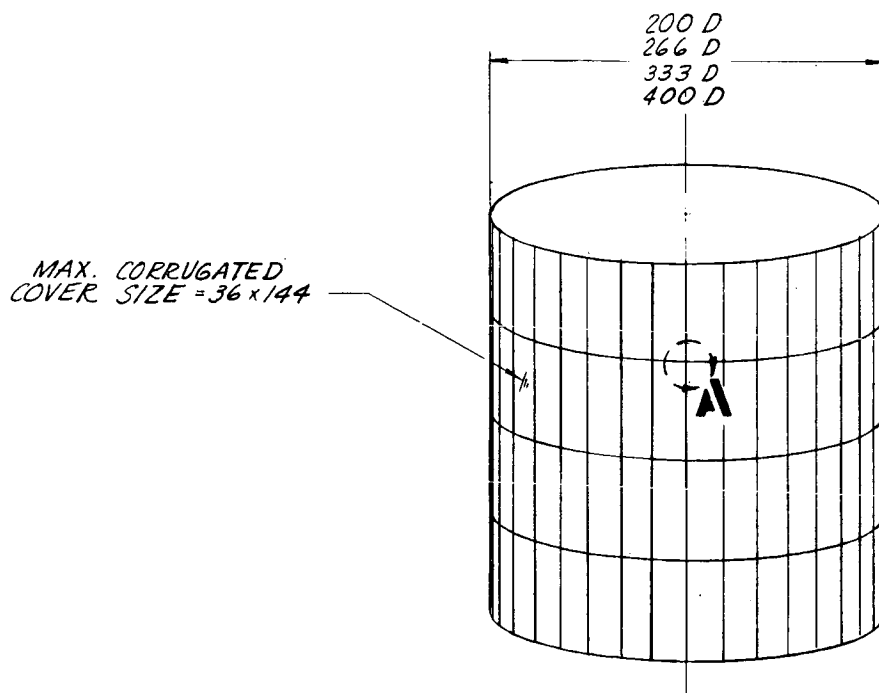


Figure 33. Design Drawing - Double-wall Trapezoidal Corrugation

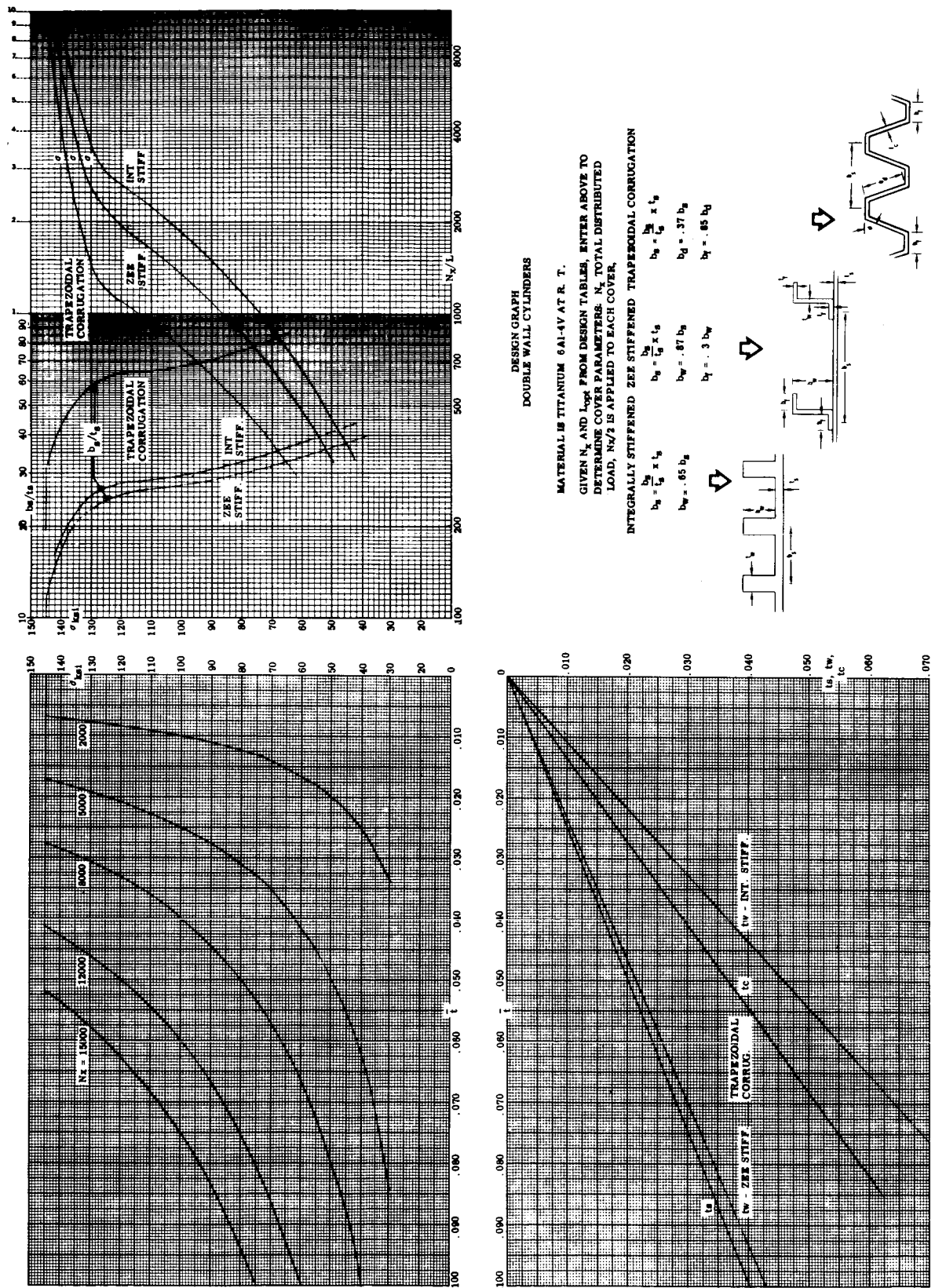


Figure 34. Design Graph - Double-wall Trapezoidal Corrugation

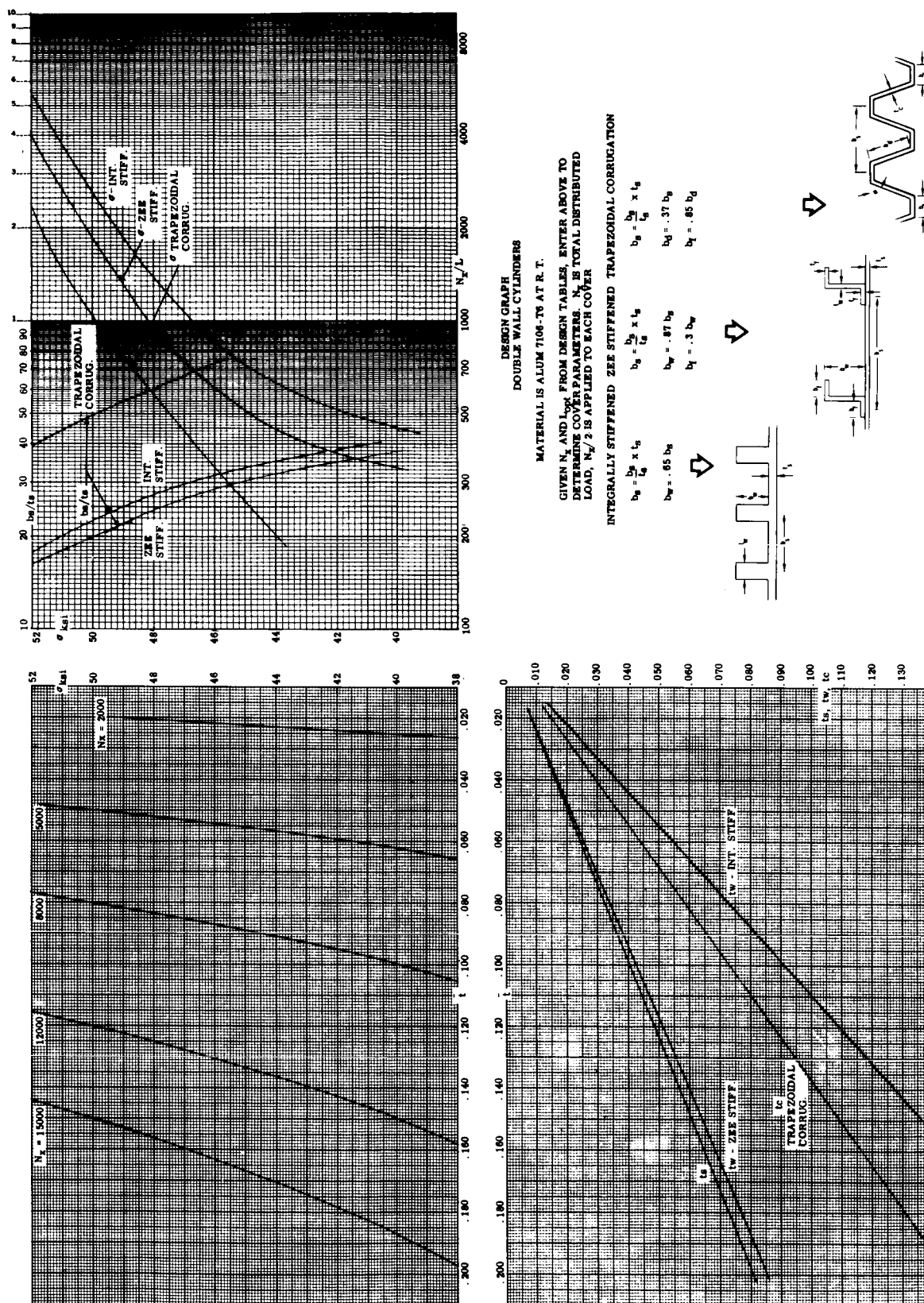
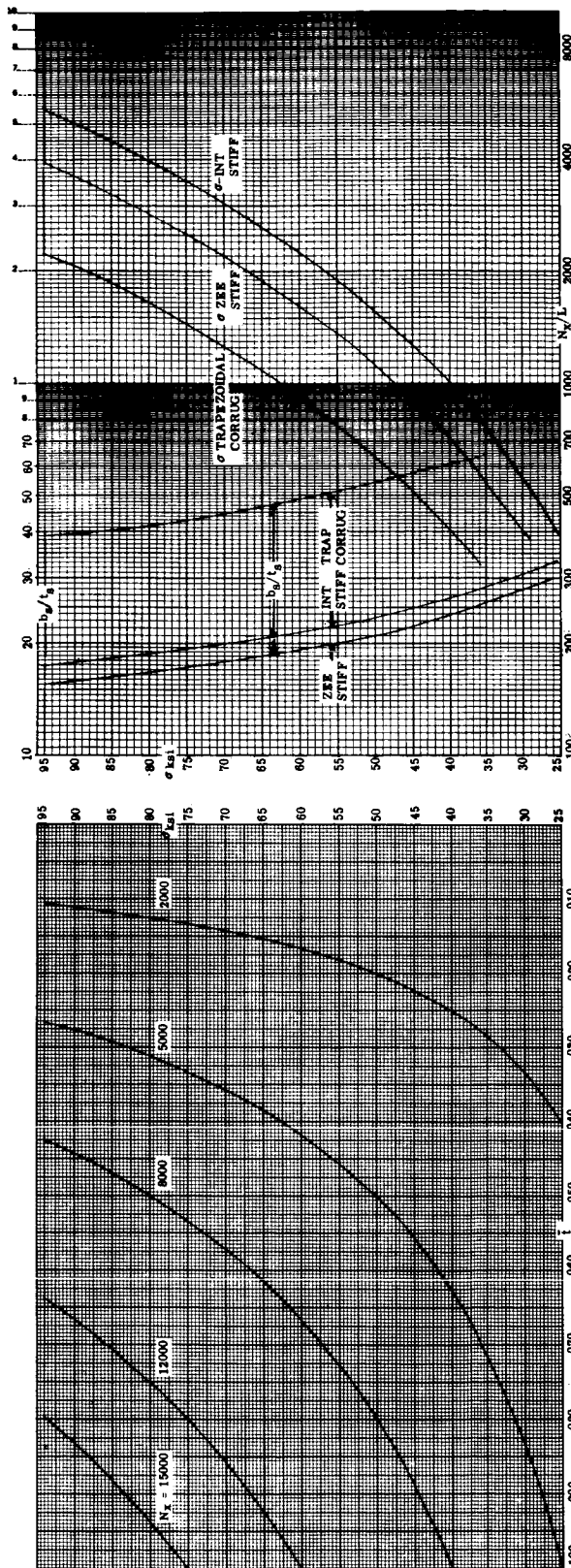


Figure 34. Design Graph - Double-wall Trapezoidal Corrugation (Cont)



DESIGN GRAPH
DOUBLE WALL CYLINDERS

MATERIAL IS 9-994 FIBERGLASS AT R. T.
GIVEN N_x AND L_{opt} FROM DESIGN TABLES, ENTER ABOVE TO
DETERMINE COVER PARAMETERS. N_x IS TOTAL DISTRIBUTED
LOAD. $N_x/2$ IS APPLIED TO EACH COVER.

INTEGRALLY STIFFENED ZEE STIFFENED TRAPEZOIDAL CORRUGATION

$$\begin{aligned} b_w &= \frac{b_f}{L_{opt}} \times L_{opt} & b_w &= \frac{b_f}{L_{opt}} \times L_{opt} \\ b_w &= .87 b_f & b_w &= .37 b_f \\ b_w &= .85 b_f & b_w &= .85 b_f \end{aligned}$$

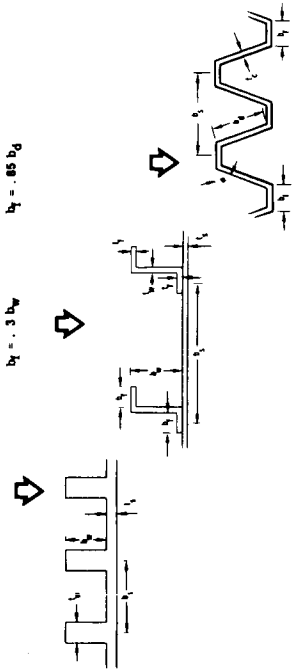


Figure 34. Design Graph - Double-wall Trapezoidal Corrugation (Cont)

Table X

TRAPEZOIDAL CORRUGATION WIDE COLUMN
SINE WAVE SHEAR WEB SUBSTRUCTURE

MTL.	N _x LB/IN	RADIUS IN.	SUPPORT SPACING IN.	SHELL THICK IN.	SUBSTR WEB THICK. IN.	SUBSTR WT. PSF	COVER WT. PSF	PENALTY WT. PSF	TOTAL WT. PSF
T16-4	2000	100	5.0	2.0	0.010	0.141	0.638	0.280	1.058
		133		2.0		0.141		0.280	1.058
		167		3.0		0.211		0.280	1.129
	2000	200	5.0	3.0	0.010	0.211	0.638	0.280	1.129
	5000	100	4.0	2.0	0.010	0.169	0.902	0.356	1.427
		133	5.0	2.0	0.010	0.141	1.009	0.311	1.460
		167	4.0	5.0	0.010	0.422	0.902	0.356	1.680
	5000	200	4.0	6.0	0.010	0.506	0.902	0.356	1.765
	8000	100	6.0	3.0	0.011	0.201	1.434	0.474	2.109
		133		4.0	0.010	0.244	1.434	0.474	2.152
		167		4.0	0.010	0.244	1.434	0.474	2.152
	8000	200	6.0	6.0	0.010	0.365	1.434	0.474	2.274
	12000	100	6.0	3.0	0.016	0.292	2.058	0.653	3.003
		133		5.0	0.010	0.305	2.058	0.653	3.015
		167		5.0	0.010	0.305	2.058	0.653	3.015
	12000	200	6.0	5.0	0.010	0.305	2.058	0.859	3.221
	15000	100	6.0	3.0	0.020	0.365	2.528	0.789	3.683
		133		6.0	0.010			0.789	3.683
		167		6.0	0.010			1.042	3.935
	15000	200	6.0	6.0	0.010	0.365	2.528	1.042	3.935

Table X (Cont)

TRAPEZOIDAL CORRUGATION WIDE COLUMN
SINE WAVE SHEAR WEB SUBSTRUCTURE

MTL.	N _x LB/IN	RADIUS IN.	SUPPORT SPACING IN.	SHELL THICK IN.	SUBSTR WEB THICK. IN.	SUBSTR WT. PSF	COVER WT. PSF	PENALTY WT. PSF	TOTAL WT. PSF
7106	2600	100	6.0	2.0	0.010	0.075	0.780	0.240	1.095
AL. ALLY		133		6.0		0.226	0.780	0.240	1.246
		167		6.0		0.226	0.780	0.289	1.295
	2600	200	6.0	6.0	0.010	0.226	0.780	0.313	1.319
	5000	100	6.0	4.0	0.010	0.151	1.446	0.461	2.057
		133		4.0		0.151		0.461	2.057
		167		4.0		0.151		0.605	2.202
	5000	200	6.0	5.0	0.010	0.188	1.446	0.605	2.240
	8000	100	6.0	5.0	0.010	0.188	2.251	0.919	3.358
		133		5.0	0.010	0.188		0.919	3.358
		167		6.0	0.020	0.452		1.144	3.847
	8000	200	6.0	6.0	0.023	0.520	2.251	1.369	4.140
	12000	100	6.0	6.0	0.013	0.294	3.307	1.331	4.932
		133			0.040	0.904		1.993	6.204
		167			0.054	1.221		2.654	7.181
	12000	200	6.0	6.0			3.307		
	15000	100	6.0	6.0	0.042	0.950	4.112	2.057	7.119
		133			0.053	1.198		2.879	8.190
		167			0.051	1.153		4.113	9.378
	15000	200	6.0	6.0			4.112		
	2000	100	6.0	2.0	0.010	0.075	0.622	0.184	.881
	2000	200	6.0	6.0	0.010	0.226	0.690	0.184	1.100

Table X (Cont)

TRAPEZOIDAL CORRUGATION WIDE COLUMN
SINE WAVE SHEAR WEB SUBSTRUCTURE

MTL.	N _x LB/IN	RADIUS IN.	SUPPORT SPACING IN.	SHELL THICK IN.	SUBSTR WEB THICK. IN.	SUBSTR WT. PSF	COVER WT. PSF	PENALTY WT. PSF	TOTAL WT. PSF
S-994	2000	100	4.0	3.0	0.015	0.166	0.455	0.198	0.819
GLASS	2000	133	4.0	3.0	0.015	0.166	0.455	0.198	0.819
	2000	167	6.0	3.0	0.015	0.120	0.558	0.212	0.890
	2000	200	6.0	3.0	0.015	0.120	0.558	0.212	0.890
	5000	100	4.0	5.0	0.022	0.415	0.720	0.306	1.441
		133	5.0	5.0	0.022	0.346	0.805	0.318	1.469
		167	4.0	5.0	0.022	0.415	0.720	0.378	1.513
	5000	200	4.0	6.0	0.019	0.432	0.720	0.378	1.529
	8000	100	5.0	4.0	0.045	0.553	1.018	0.411	1.983
		133	4.0	6.0	0.030	0.664	0.911	0.483	2.058
		167	4.0	6.0	0.030	0.664	0.911	0.483	2.058
	8000	200	6.0	6.0	0.030	0.480	1.115	0.543	2.138
	12000	100	6.0	4.0	0.066	0.703	1.366	0.686	2.755
		133	6.0	6.0	0.045	0.719	1.366	0.686	2.771
		167	6.0	6.0	0.045	0.719	1.366	0.686	2.771
	12000	200	6.0	6.0	0.061	0.983	1.366	1.232	3.581
	15000	100	6.0	5.0	0.066	0.879	1.609	0.811	3.299
		133	6.0	5.0	0.066	0.879	1.609	0.811	3.299
		167	6.0	6.0	0.069	1.103	1.609	1.455	4.166
	15000	200	6.0	6.0	0.072	1.151	1.609	1.610	4.375

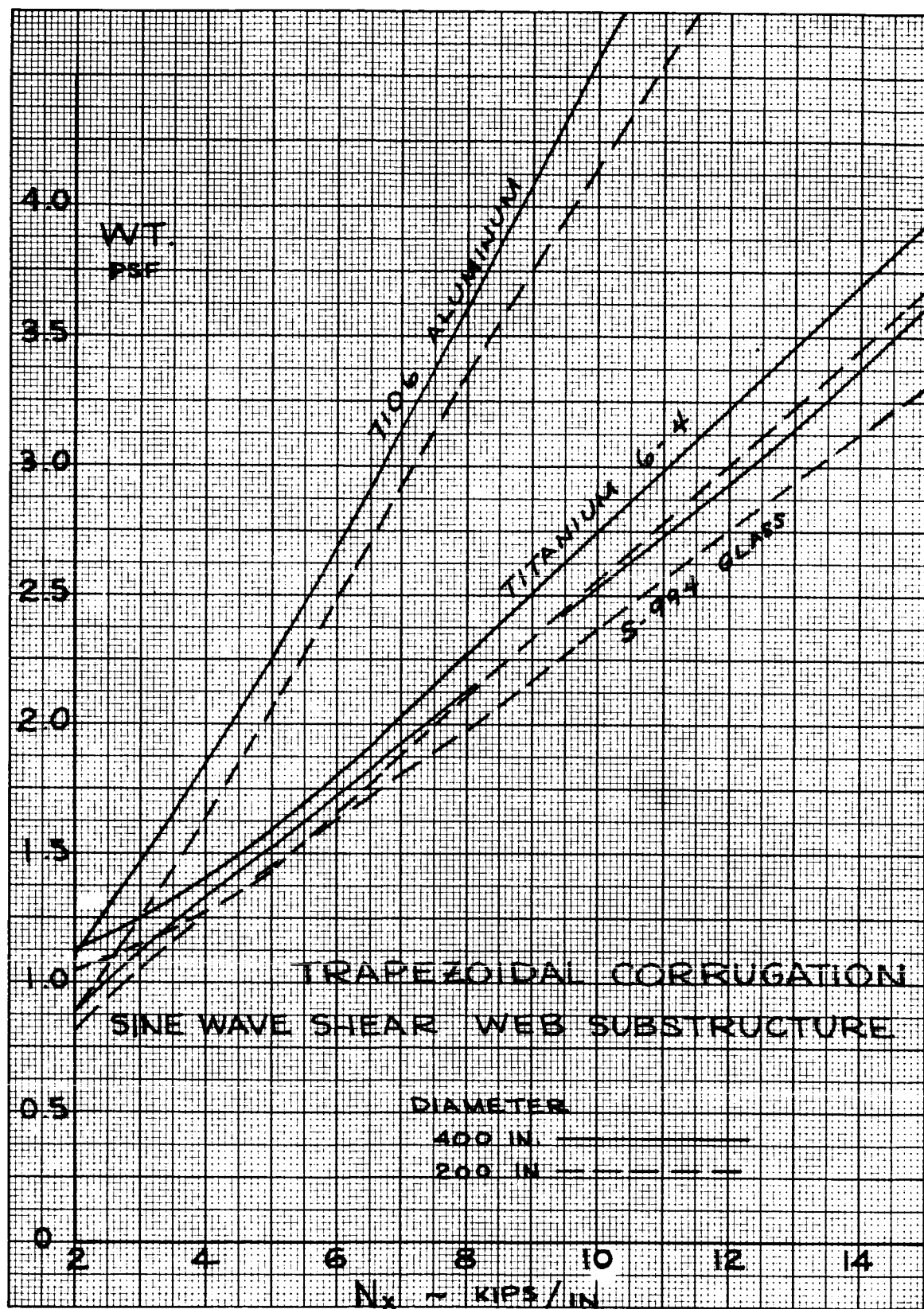


Figure 35. Panel Weight Versus Load-trapezoidal Corrugation

DOUBLE-WALL TRUSS CORE SEMISANDWICH COVER PANELS WITH TRUSS WEB SUBSTRUCTURE

The truss core semisandwich, used with the beaded truss substructure presents good design potentials in the moderate load range. The cover consists of a single sheet longitudinally reinforced by a corrugated core. The beaded truss substructure is oriented in the longitudinal direction to provide the "plate type" support structure. To facilitate fabrication, this substructure concept eliminates the requirements for transverse stiffening webs because the shell stability depends primarily upon truss action of the substructure. The three candidate materials that provide most potential for this concept consist of titanium, maraging steel, and beryllium. The titanium configuration, however, is the most producible of these three concepts. For producibility reasons, the original Phase I selection of wide column covers was altered to plate-designed covers.

The titanium truss core semisandwich cover skin gages are above the minimum requirements except at the very lowest load level considered, allowing the titanium material to operate efficiently.

Lands or pads .010 thicker than the basic face sheet are provided at all splices at substructure nodes by chem-milling. Two cover panels with longitudinal corrugations are joined to a beaded truss substructure by stitch welding through the nodes. Longitudinal cover splices are achieved by overlapping the corrugated outer panels and stitch welding to the face sheet, coupled with a flat splice sheet next to the face sheet. Circumferential cover splices are made by overlapping a corrugated splice sheet and stitch welding through all common members. Flat sheets riveted to the webs form the splices for the substructure.

The titanium truss core semisandwich is made from a corrugation fabricated on a multi-stage brake die and hot sized to establish the finished configuration. The corrugation is then spot welded to the titanium skin sheet. The skin and corrugation are heat treated before being spot welded. (Note: Titanium can be spot welded without the flat required for other alloys to prevent weld expulsion.)

Substructure to cover panel joint design of the juncture of the truss core and face sheet may cause manufacturing problems in obtaining perfect alignment. Core elements, beaded truss substructure, and face sheet, must be aligned. This concept requires development tests to increase the design confidence level and to verify the performance of the structure/cover panel composite.

The substructure is made from pure titanium for ease of forming. The beaded design of the substructure web requires that a gage of .025 be used to make the forming reasonably producible. The web is then selectively chem-milled to a constant .010 gage to reduce weight.

The substructure is attached to the covers by the use of long-reach spot welding equipment. Tooling and detail part fabrication requires careful control to provide detail parts sufficiently accurate to permit assembly spot welding of the structure.

Close adherence to standard quality control procedures for spot welding results in reliable structure which meets manned vehicle requirements. Proof pressure testing permits verification that the assembled structure meets design requirements.

Fabrication of the entire wall panel by the roll diffusion process is most attractive.

A second material chosen for this concept is 18 Ni maraging steel, which can be manufactured and assembled much as titanium by stitch welding and riveting.

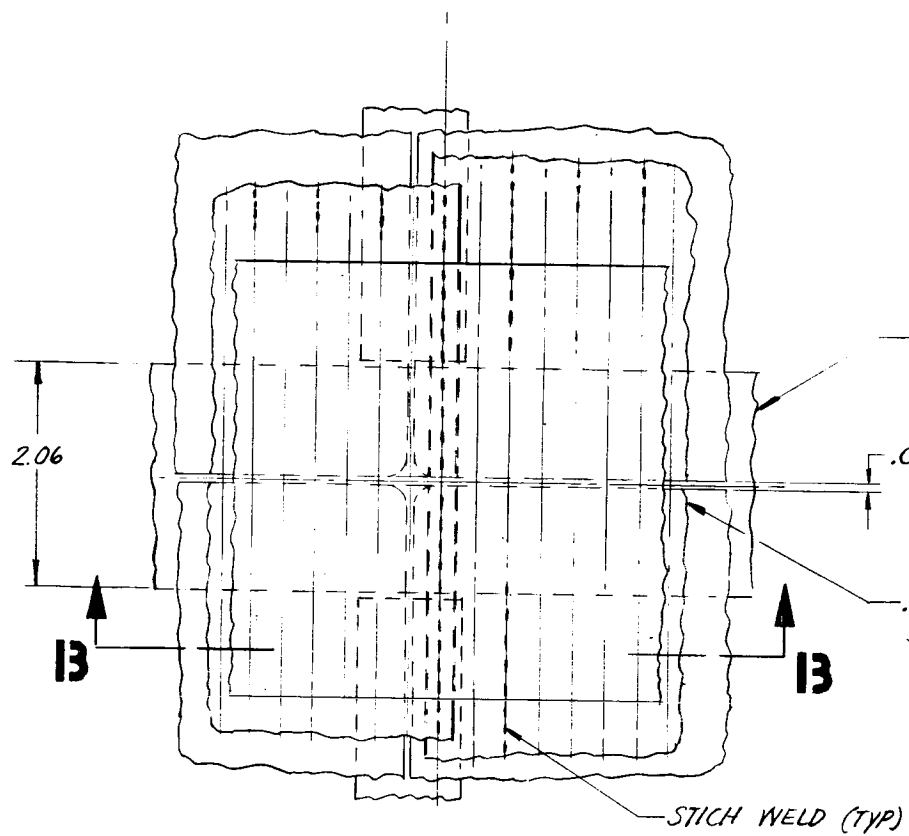
Maraging steel compression strength properties are the highest compared with all the materials considered in the study. Structural analysis of the truss core semisandwich with this high strength material results in skin gages below minimum gage at low load levels. The maraging steel material is more efficient at higher load levels where the optimum skin gage becomes unconstrained.

The 18 Ni steel configuration is produced by spot welding. Design must balance the desirable zero-width flat in the weld area to one where the weld area is wide enough to prevent weld nugget expulsion. In order to satisfy spot welding design requirements, in all probability, a weight increase is required for the steel configuration. In addition, the requirement for corrosion protection complicates welding problems.

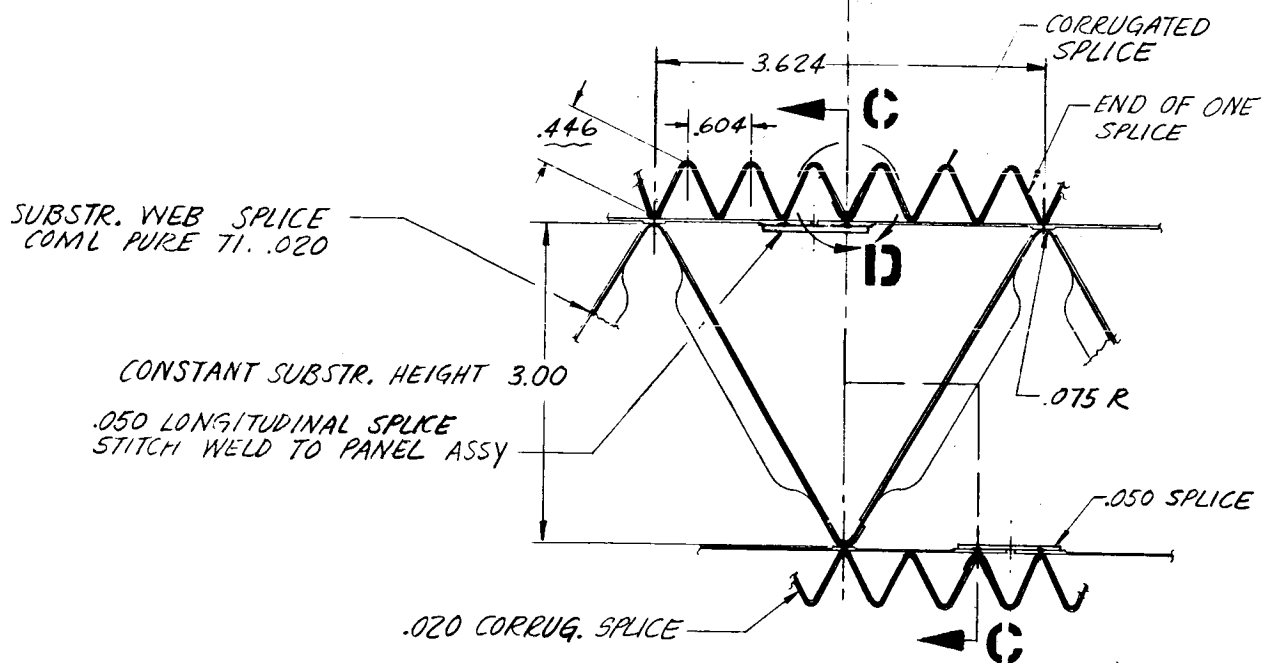
With the truss core semisandwich concept, the beryllium material becomes efficient at low load levels. At low load levels, stability requirements become more significant than strength requirements, consequently, the high stability properties of beryllium can be fully realized.

The beryllium concept has the same geometrical arrangement as the titanium concept except for the different detail dimension. Also, electron beam welding is used instead of resistance welding, and monel rivets used rather than A286 rivets. The beryllium configuration cannot be resistance welded due to basic material problems.

Production of the beryllium covers as a pure truss requires a major development program. Pressure diffusion bonding and electron beam welding appear to offer the best fabrication approaches to meet these design requirements. The attachment of covers to the substructure by resistance welding also presents the same difficulty. Again, electron beam welding appears to offer a possible solution.



DETAIL A FULL SIZE
 MTL: T1 ~ N_x = 2000 TO 15,000 LB/IN ~ 15,000 LB/IN SHOWN.
 18 NI STL & BE SIMILAR EXCEPT AS NOTED

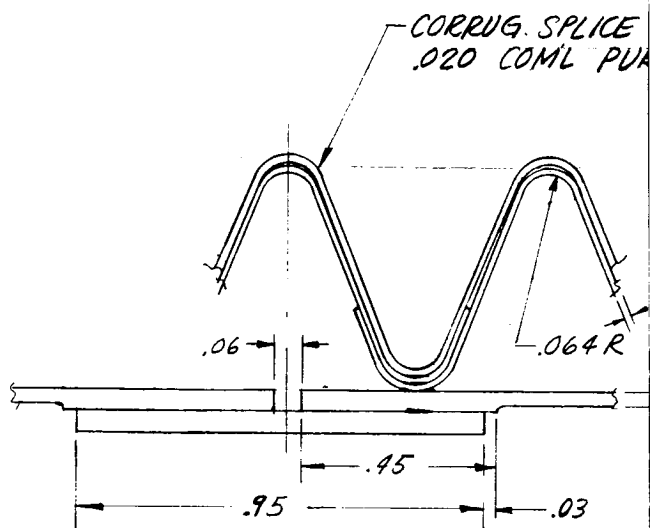


SECTION B - B

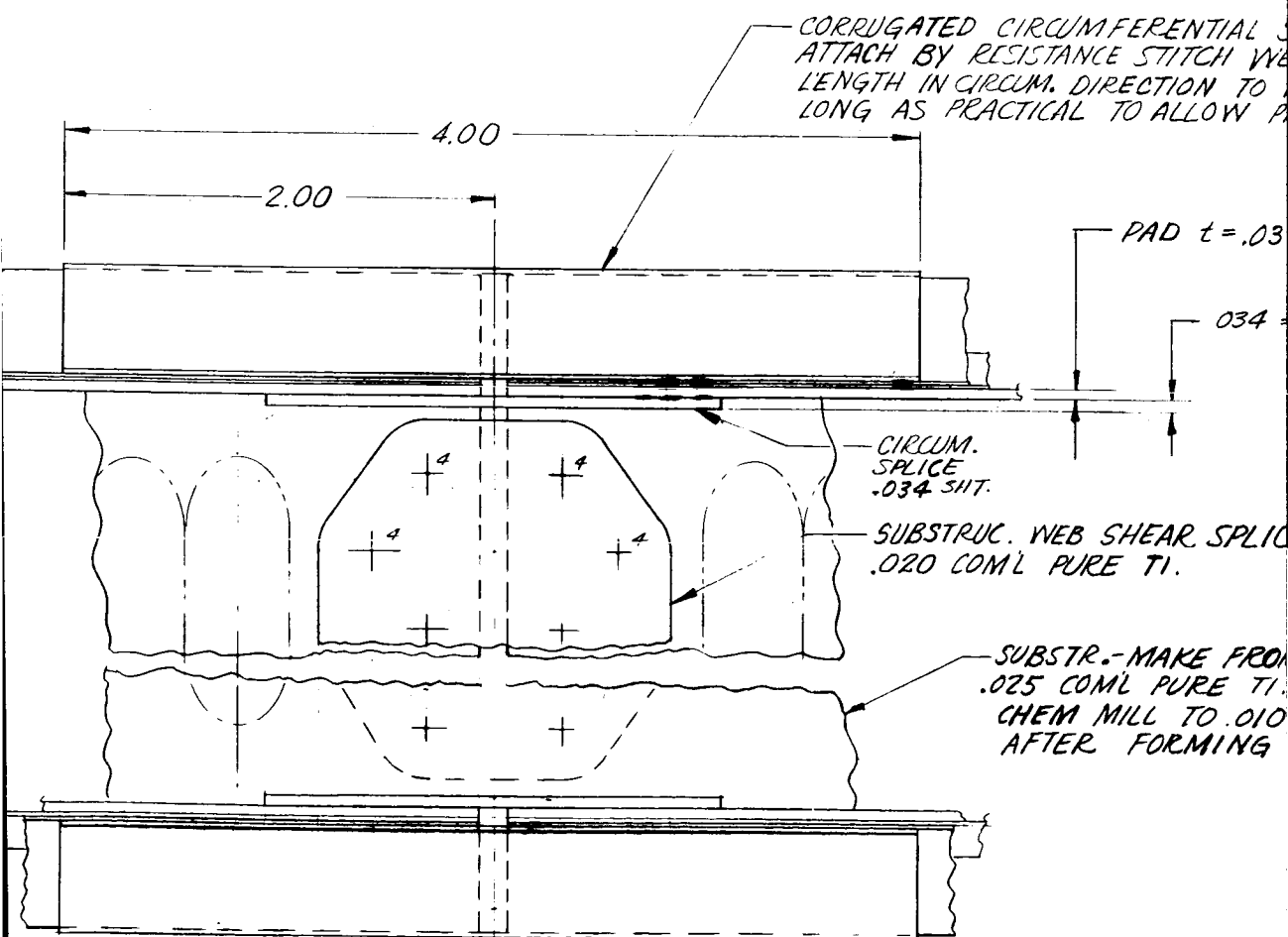
78 (1)

CIRCUM. FACE SHT. SPLICE

716 6-4 TI CORRUGATED SHEET.
STITCH WELD TO FACE SHEET.

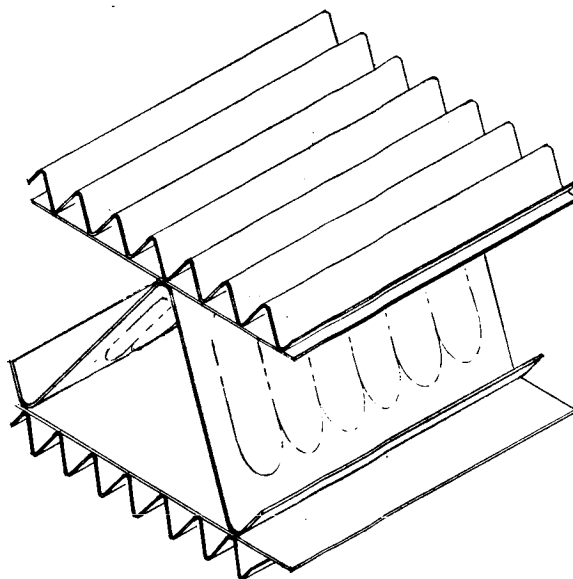


TI ~ DETAIL **D** SCALE: 4/1



SHT.
REF TI.

.016
↓
.033



SPLICE
WELDING.
BE AS
PROPER FIT.

DESIGN DWG-DOUBLE-WALL TRUSS CORE SEMI-SANDWICH

FIG. 36

$$t = t_s + .010$$

$$t = t_s + .010$$

E

1

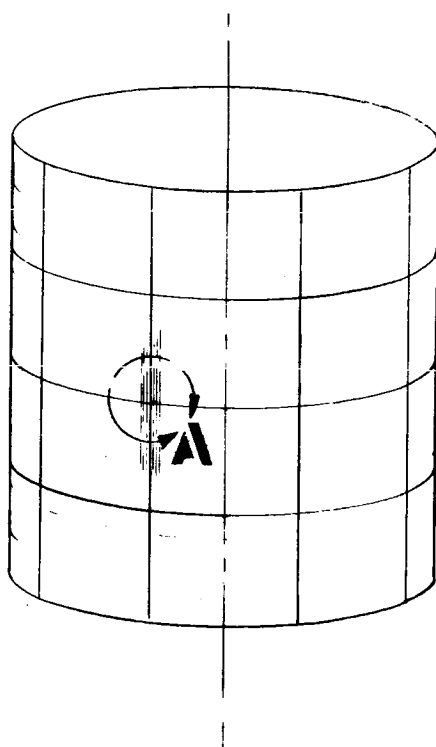
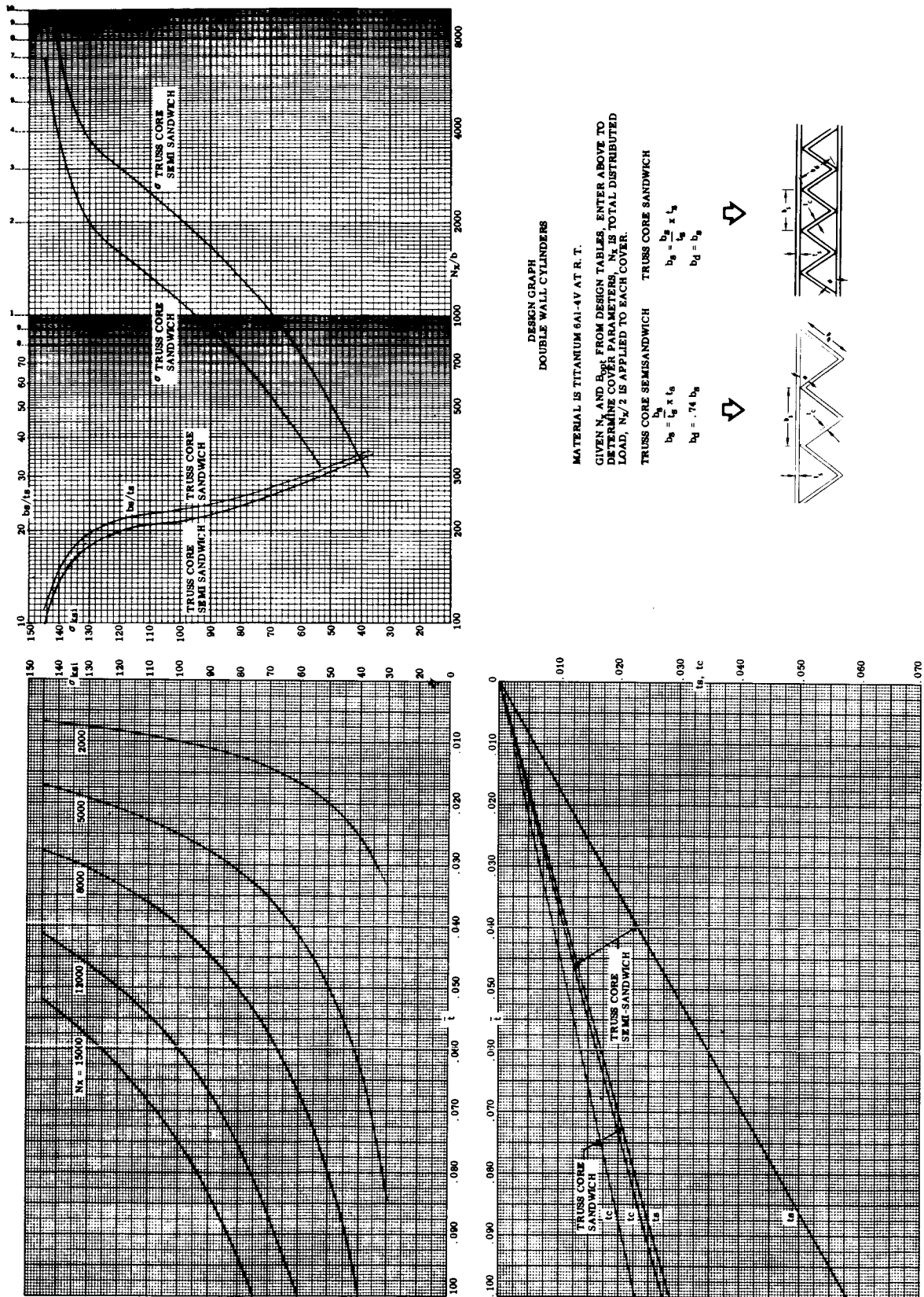


Figure 36. Design Drawing - Double-wall Truss Core Semisandwich.



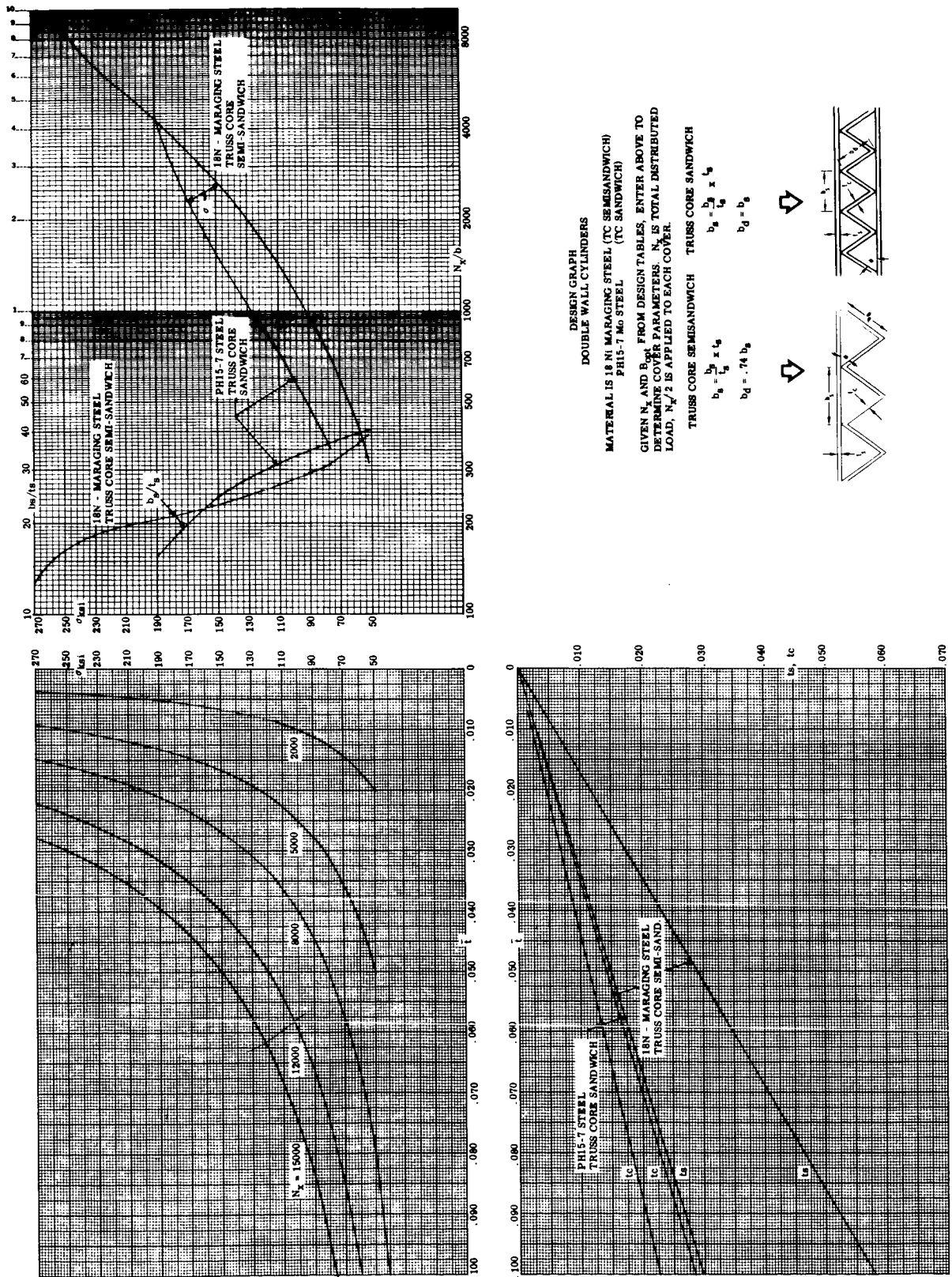


Figure 37. Design Graph - Double-wall Truss Core Semisandwich (Cont)

DESIGN GRAPH

DOUBLE WALL - TRUSS CORE SEMI-SANDWICH
BERYLLIUM AT ROOM TEMPERATURE

ALL DESIGNS OPERATING AT 47000 PSI STRESS LEVEL

$$\bar{t} = \frac{N_x}{2\sigma}$$

$$b_s/t_s = 28.5$$

$$t_s = .580 \bar{t}$$

$$t_c = .284 \bar{t}$$

$$b_d = .740 b_s$$

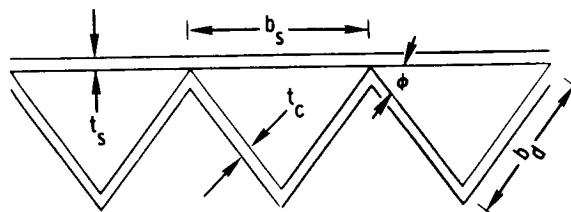


Figure 37. Design Graph - Double-wall Truss Core Semisandwich (Cont)

Table XI

TRUSS CORE SEMI-SANDWICH PLATE
TRUSS WEB SUBSTRUCTURE

MTL.	N _x LB/IN	RADIUS IN.	SUPPORT SPACING IN.	SHELL THICK. IN.	SUBSTR WEB THICK. IN.	SUBSTR WT. PSF	COVER WT. PSF	PENALTY WT. PSF	TOTAL WT. PSF
TI 6-4	2000	100	3.0	1.0	0.010	0.277	0.814	0.185	1.276
		133							
		167							
	2000	200	3.0	1.0	0.010	0.277	0.814	0.185	1.276
	5000	100	2.0	1.0	0.010	0.326	1.051	0.285	1.661
		133	2.0	1.0	0.010	0.326	1.051	0.285	1.661
		167	3.0	1.0	0.010	0.277	1.287	0.215	1.779
	5000	200	2.0	2.0	0.010	0.515	1.051	0.285	1.850
	8000	100	2.0	1.0	0.010	0.326	1.401	0.310	2.037
		133	3.0	1.0	0.010	0.277	1.628	0.247	2.152
		167	2.0	2.0	0.010	0.515	1.401	0.310	2.226
	8000	200	2.0	2.0	0.010	0.515	1.401	0.310	2.226
	12000	100	3.0	1.0	0.010	0.277	2.101	0.296	2.674
		133		2.0		0.384	2.101	0.296	2.781
		167		2.0		0.384	2.101	0.296	2.781
	12000	200	3.0	2.0	0.010	0.384	2.101	0.296	2.781
	15000	100	4.0	1.0	0.010	0.258	2.655	0.327	3.239
		133	3.0	2.0		0.384	2.543	0.334	3.261
		167	3.0	2.0		0.384	2.543	0.334	3.261
	15000	200	4.0	2.0	0.010	0.326	2.655	0.327	3.307

Table XI (Cont)

TRUSS CORE SEMI-SANDWICH PLATE
TRUSS WEB SUBSTRUCTURE

MTL.	N _x LB/IN	RADIUS IN.	SUPPORT SPACING IN.	SHELL THICK. IN.	SUBSTR WEB THICK. IN.	SUBSTR WT. PSF	COVER WT. PSF	PENALTY WT. PSF	TOTAL WT. PSF
18 Ni	2000	100	5.0	1.0	0.010	0.448	1.440	0.213	2.101
MAR-		133							
AGING		167							
STEEL	2000	200	5.0	1.0	0.010	0.448	1.440	0.213	2.101
	5000	100	2.0	1.0	0.010	0.589	1.440	0.487	2.516
		133							
		167							
	5000	200	2.0	1.0	0.010	0.589	1.440	0.487	2.516
	8000	100	2.0	1.0	0.010	0.589	1.822	0.513	2.923
		133	2.0	1.0	0.010	0.589	1.822	0.513	2.923
		167	3.0	1.0	0.010	0.500	2.231	0.387	3.119
	8000	200	2.0	2.0	0.010	0.931	1.822	0.513	3.265
	12000	100	2.0	1.0	0.010	0.589	2.243	0.549	3.380
		133	2.0	2.0	0.010	0.931	2.243	0.549	3.722
		167	2.0	2.0	0.010	0.931	2.243	0.549	3.722
	12000	200	2.0	2.0	0.010	0.931	2.243	0.549	3.722
	15000	100	2.0	1.0	0.010	0.589	2.587	0.578	3.753
		133	3.0	1.0	0.010	0.500	3.055	0.472	4.028
		167	2.0	2.0	0.010	0.931	2.587	0.578	4.095
	15000	200	2.0	2.0	0.010	0.931	2.587	0.578	4.095

Table XI (Cont)

TRUSS CORE SEMI-SANDWICH PLATE
TRUSS WEB SUBSTRUCTURE

MTL.	N _x LB/IN	RADIUS IN.	SUPPORT SPACING IN.	SHELL THICK. IN.	SUBSTR WEB THICK. IN.	SUBSTR WT. PSF	COVER WT. PSF	PENALTY WT. PSF	TOTAL WT. PSF
BE	3200	100	6.0	1.0	0.020	0.200	0.656	0.078	0.934
		133							
		167							
	3200	200	6.0	1.0	0.020	0.200	0.656	0.078	0.934
	5000	100	6.0	1.0	0.020	0.200	1.011	0.115	1.326
		133		1.0		0.200			1.326
		167		1.0		0.200			1.326
	5000	200	6.0	2.0	0.020	0.228	1.011	0.115	1.354
	8000	100	6.0	1.0	0.020	0.200	1.618	0.228	2.046
		133		1.0		0.200			2.046
		167		1.0		0.200			2.046
	8000	200	6.0	2.0	0.020	0.228	1.618	0.228	2.074
	12000	100	6.0	1.0	0.020	0.200	2.427	0.453	3.080
		133		1.0		0.200			3.080
		167		1.0		0.200			3.080
	12000	200	6.0	2.0	0.020	0.228	2.427	0.453	3.108
	15000	100	6.0	1.0	0.020	0.200	3.033	0.678	3.912
		133		1.0		0.200			3.912
		167		1.0		0.200			3.912
	15000	200	6.0	2.0	0.020	0.228	3.033	0.678	3.940

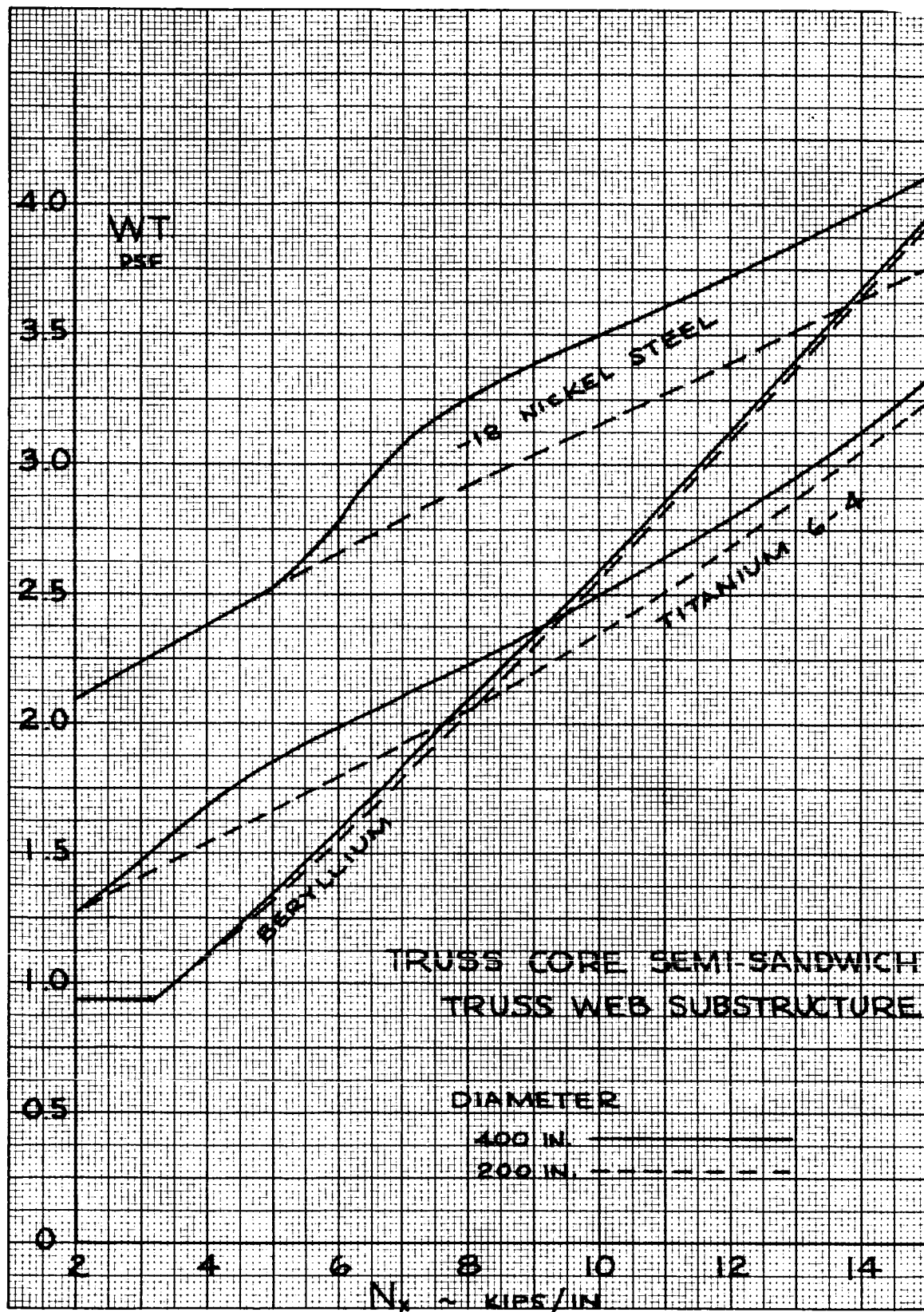


Figure 38. Panel Weight Versus Load-truss Core Semisandwich

DOUBLE-WALL INTEGRALLY STIFFENED COVER PANELS WITH TRUSS RIB SUBSTRUCTURE

This configuration consists of longitudinally stiffened panels (inner and outer) separated by circumferentially oriented beaded truss rib substructure to form a double wall cylindrical structure. 6Al-4V Ti, 7106 aluminum and S-994 glass materials are selected as most efficient materials for this configuration.

The 6Al-4V titanium cover is manufactured by static or roll diffusion bonding the stiffeners to the sheet, then chem-milling where required to provide lands or pads at all splice areas and at substructure nodes. The truss rib substructure is formed from .025 inch commercially pure titanium, then chem-milled to .010 inch. The substructure nodes are fabricated with a minimum flat and bend radius to allow the web lines of action to intersect as closely as possible to the neutral axis of the cover panel. Flat radiused strips are bonded in the node areas to provide a flat for the rivet head. Flat sheets form longitudinal splices of the covers and the substructure. Integrally stiffened sheets form the cover circumferential splice. The substructure is attached to the cover face sheet via an organic bond and blind A286 rivets.

The inner and outer panels of Ti-6Al-4V may also be fabricated by machining. For the conventionally machined concept, chemical milling is utilized after an initial machining operation to provide finished gages thinner than the minimum practical gage at which machining becomes impractical. Fully aged material is required where chemical milling is used. Subsequent to machining and chemical milling, fixturing is used during a heat treat cycle to provide the correct contour.

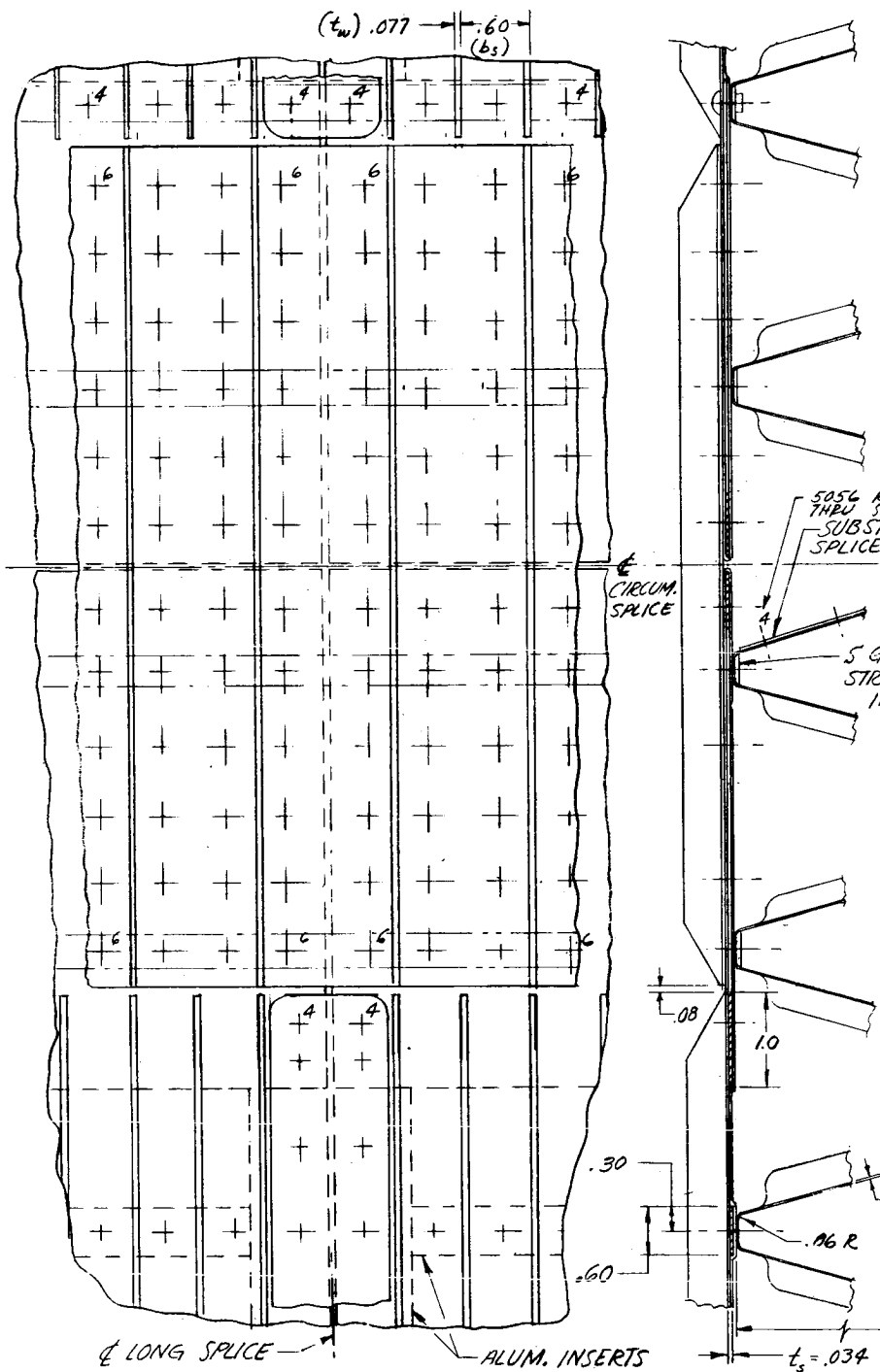
The fabrication sequence for roll diffusion bonding of the panels is similar to that described for other configurations. Less difficulty is experienced in removing the mandrels and mechanical methods of removal are successful.

The aluminum integrally stiffened concept fabrication is similar to the titanium concept except for dimensional variations. The cover is machined and chem-milled to final dimensions, and the substructure is drophammer formed from .020 inch material and chem-milled to .015 inch.

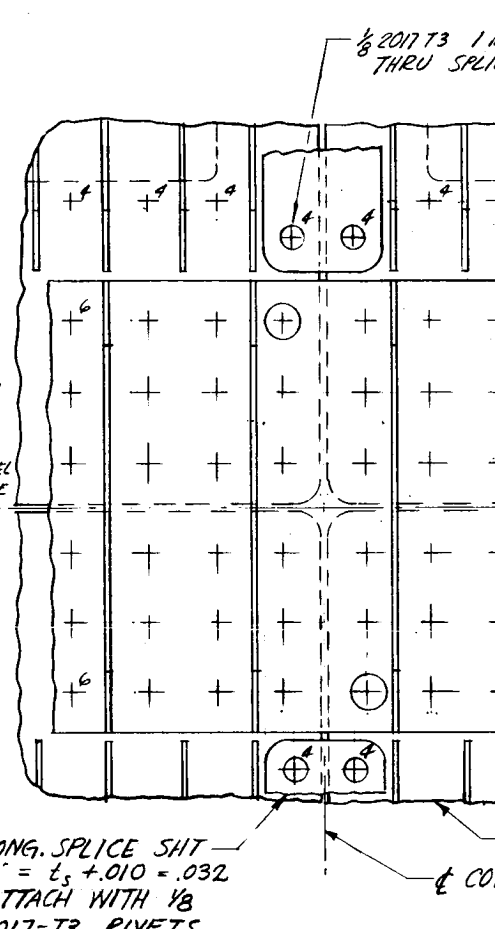
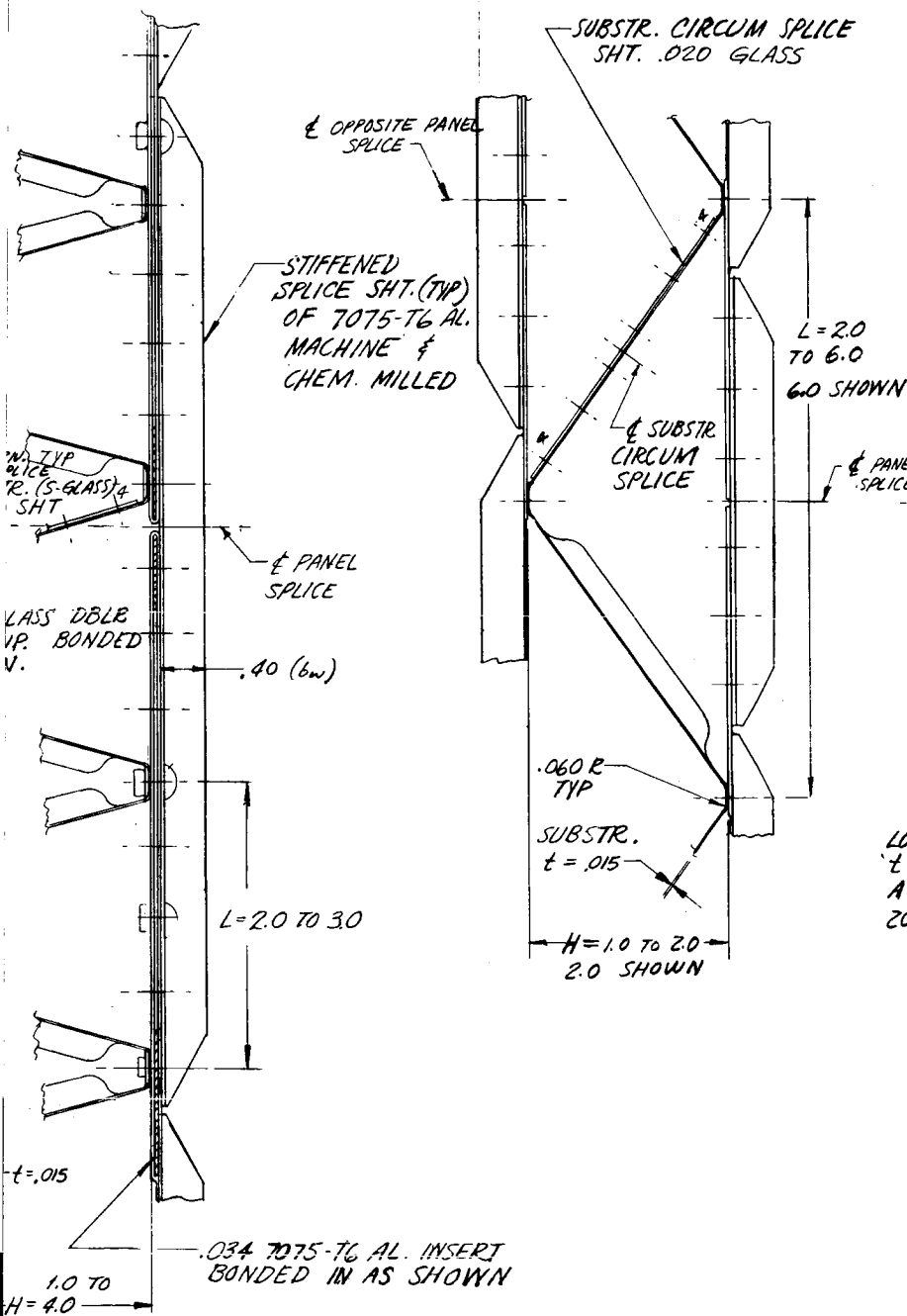
Blind fasteners are used for assembly, and all riveted joints are bonded with a room temperature curing adhesive.

S-994 glass is considered an "advanced material" because of the uncertainties and decreased reliability of a layup panel and truss rib of this type. The covers are of a 2-ply 90° orientated tape layup, with a 2024-T3 aluminum strip sandwiched in along the sides and ends. This strip increases the bearing value where the splice sheet is riveted to the edges of the cover. The substructure is bonded and riveted to the covers. All splices are bonded as well as riveted, using "soft" 5056 aluminum rivets. Radiused phenoloc strips are bonded in the nodes of the substructure for rivet lands. Where the rivet head diameter is larger, for clearance between stiffeners a phenolic block will be bonded in for the rivet to seat on.

The fabrication of two-ply 90-degree, oriented S-994 glass into integral stiffened skin concept, as defined, results in an extremely slow manufacturing process.



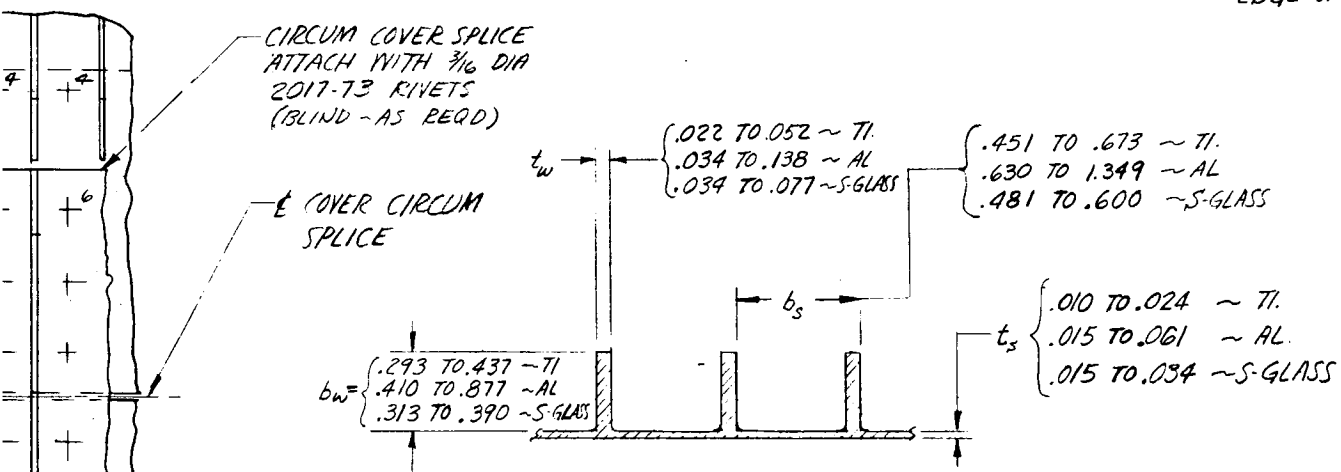
DETAIL **A₃** FULL SCALE
 MTL: S-994 GLASS ~ $N_k = 2000$ TO 15000 LB/IN ~ 15000 LB/IN SHOWN
 SIMILAR TO DETAIL A₁ EXCEPT AS NOTED
 ALL SUBSTR. TO PANEL JOINTS ADHESIVE BONDED
 AND RIVETED WITH 2117-T3 MTL. BLIND AND
 CONVENTIONAL RIVETS WHERE POSSIBLE.



DETAIL **A**₂ FULL SIZE
 MTL: 7106 AL ~ $N_t = 2000$ TO 15000 LB/IN.
 SIMILAR TO DETAIL A, EXCEPT

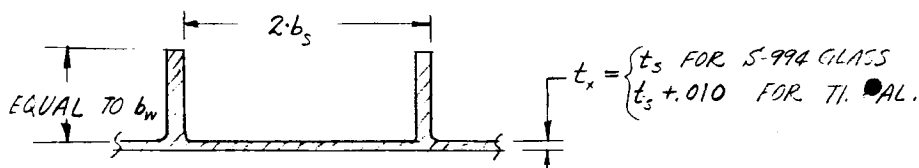
ON CTR.
E & COVER

EDGE OF CH



DETAIL OF COVER CROSS SECTION - NO SCALE

COVER
ER LONG. SPLICE

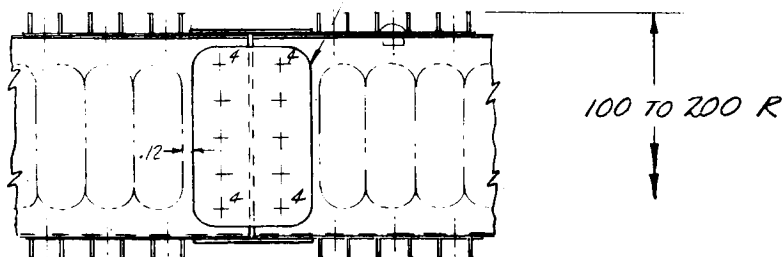


DETAIL OF COVER SPLICE CROSS SECTION - NO SCALE

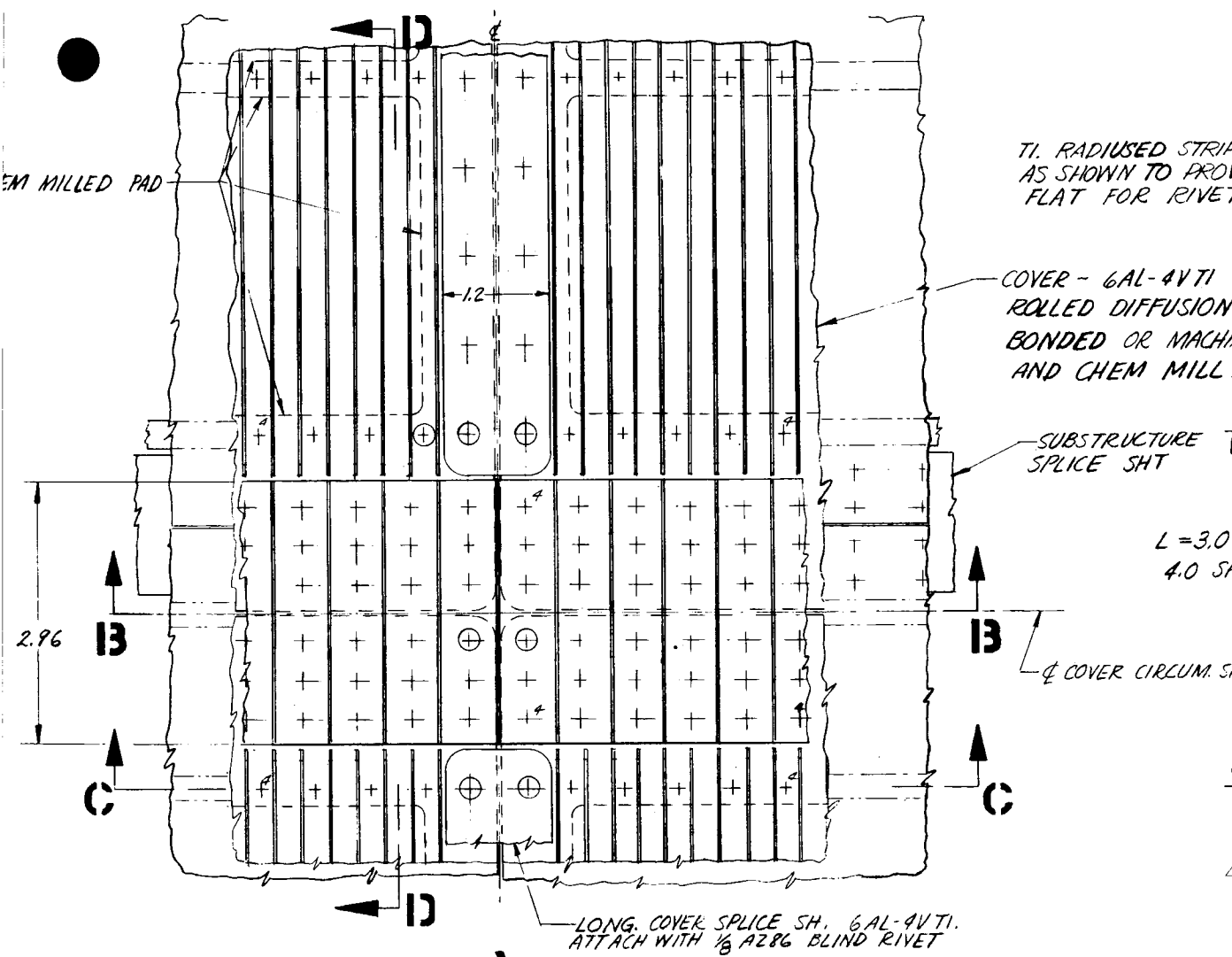
ALE
5000 LB/IN SHOWN
AS NOTED

SPLICE SHEET -.020 COML PURE
TYP WEB SPLICE AT ENDS OF
BEADED TRUSS SUBSTRUCTURE

STIFFENED CIRC

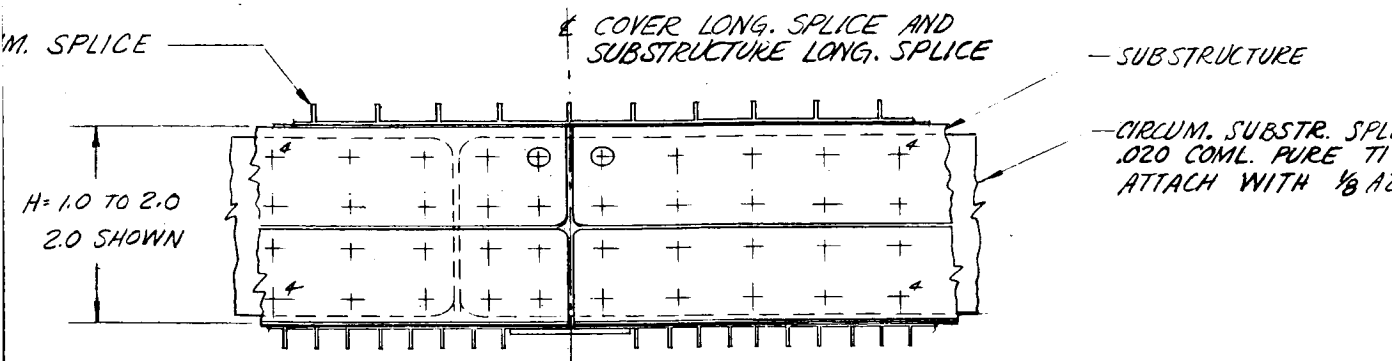


SECTION C-C FULL SCALE



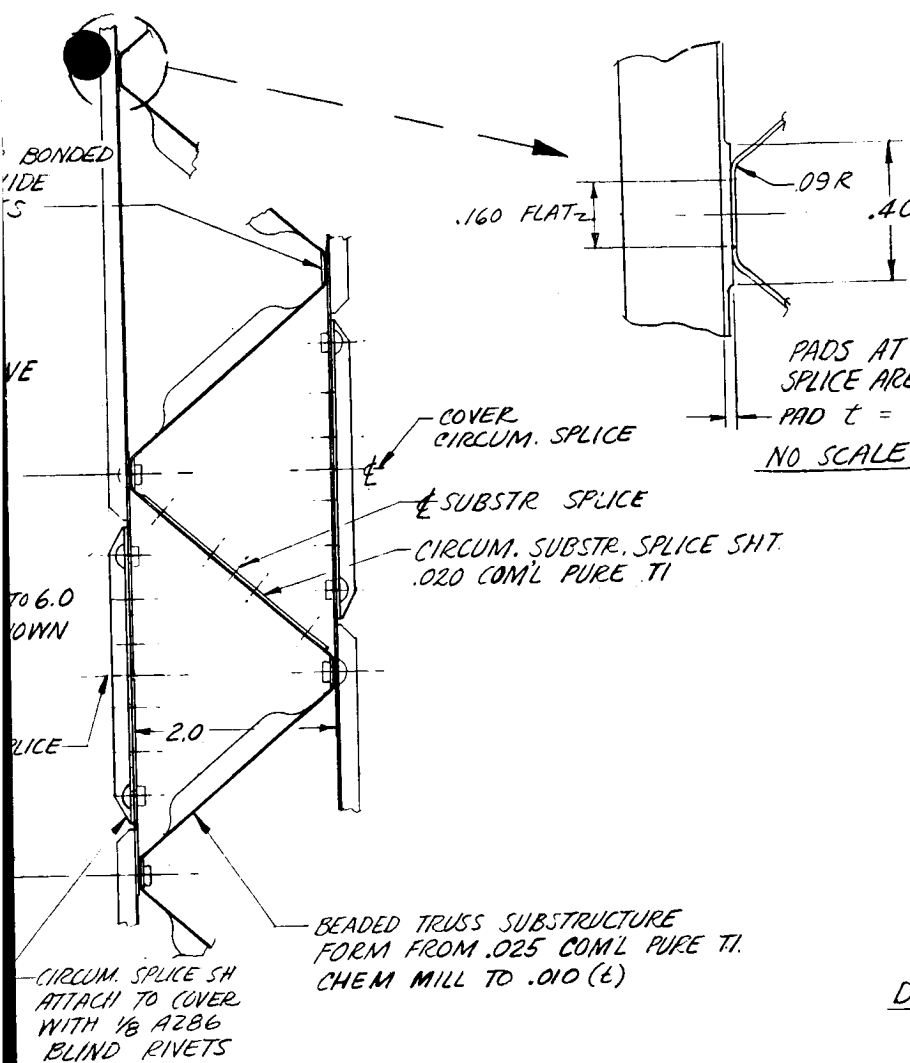
DETAIL A, FULL SCALE

MTL:TI ~ N_k = 2000 TO 15,000 LB/IN. ~ 8000 LB/IN, 200 R SHOWN



SECTION B-B FULL SCALE

88-4



SECTION D-D FULL SCALE

MAX. COVER PANEL SIZES:
FOR ROLLED DIFF BONDED: 7
FOR MACH. & CHEM MILLED: 14
FOR S-GLASS LAY-UP: 14

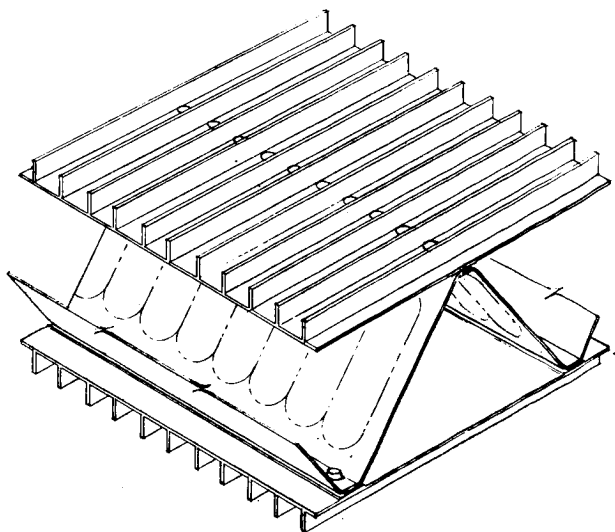
86 RIV.

48 (5)

Figure

TRUSS NODES AND
EAS CHEM MILLED

$t_s \pm .010$



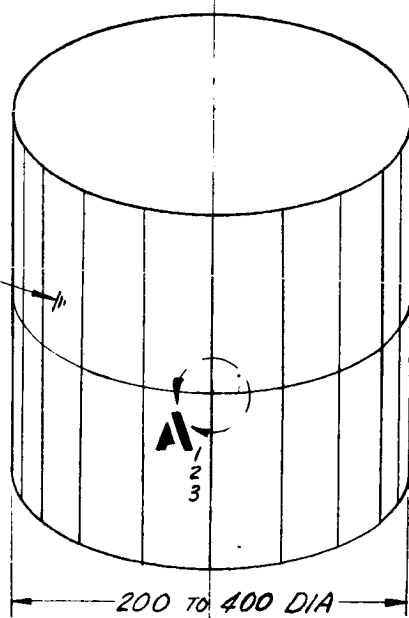
DESIGN DWG—DOUBLE-WALL INTEGRALLY STIFFENED PANEL

FIG. 39

4 W. X 200 LONG.

10 W. X 120 LONG.

6 W. X 120 LONG



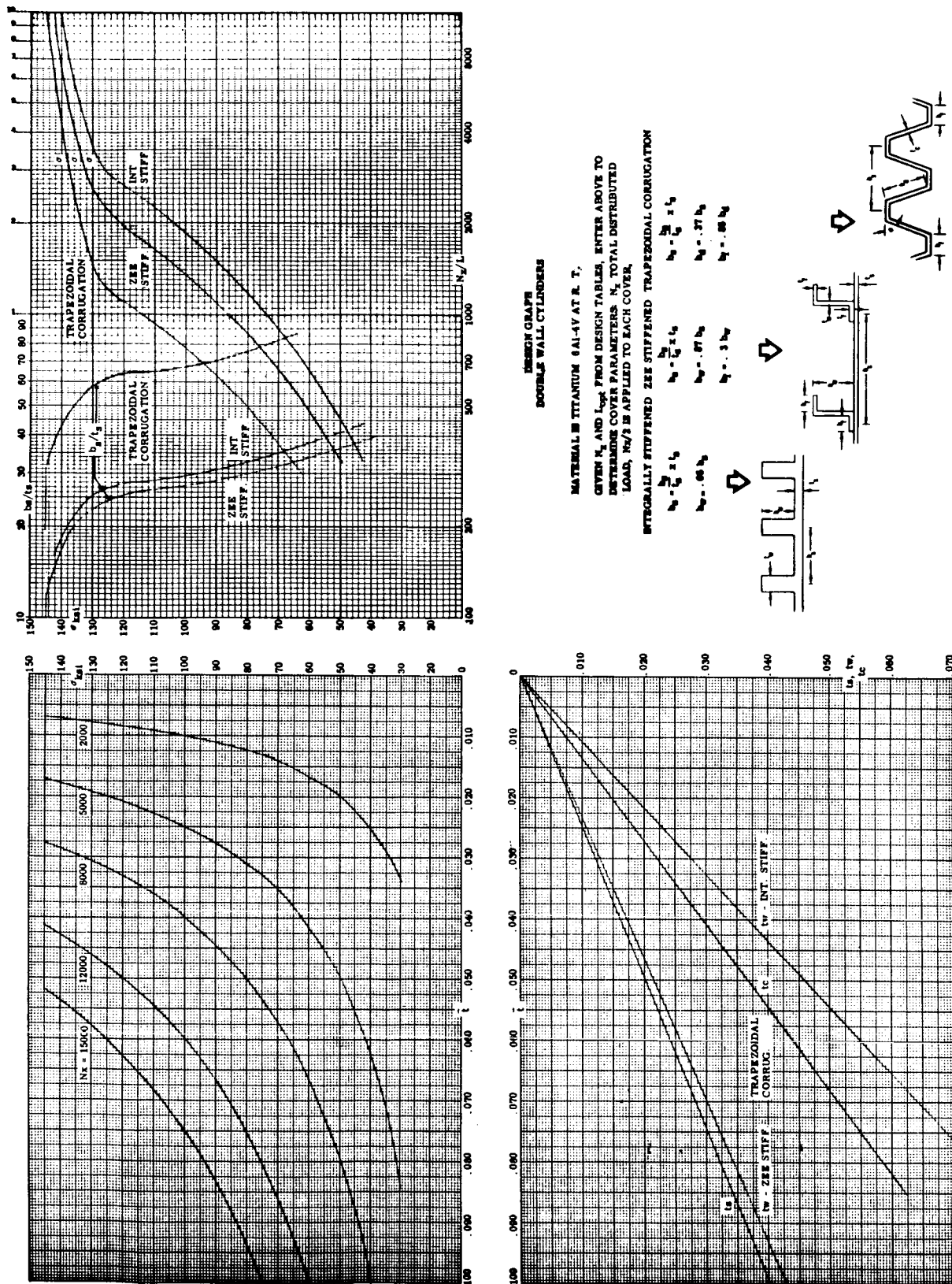


Figure 40. Design Graph - Double-wall Integrally Stiffened Panel

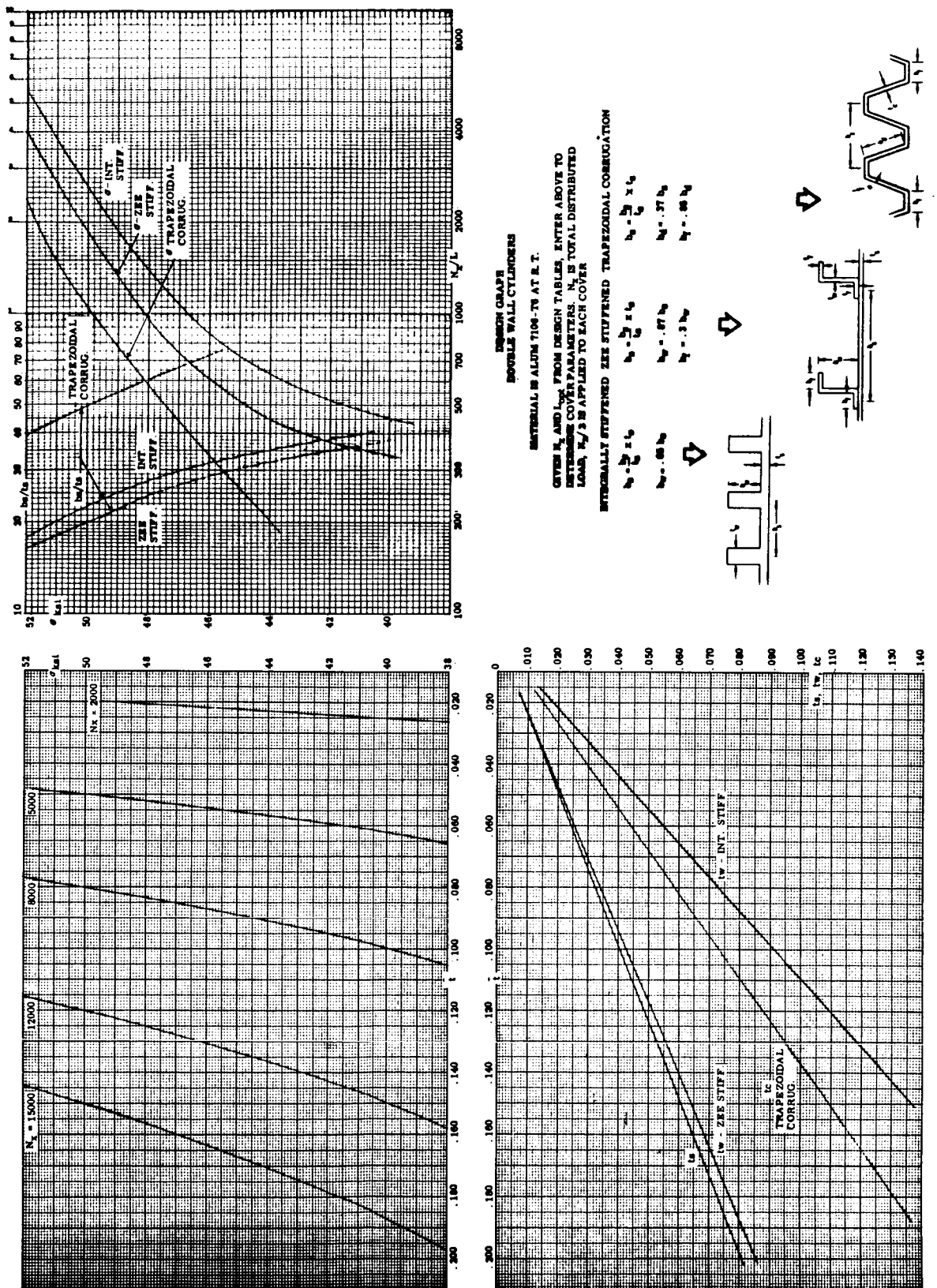
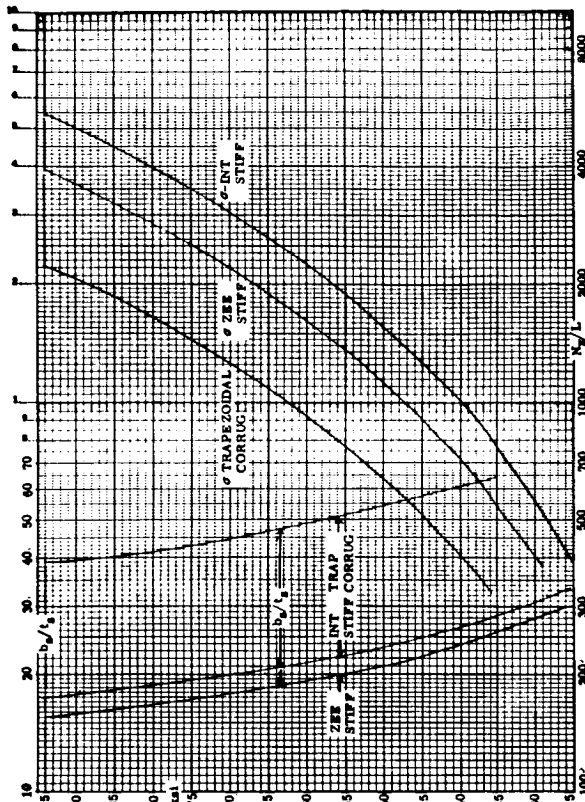


Figure 40. Design Graph - Double-wall Integrally Stiffened Panel (Cont)



DESIGN GRAPH
DOUBLE WALL CYLINDERS

MATERIAL IS 8-994 FIBERGLASS AT R. T.

ENTER N_2 AND L FROM DESIGN TABLES, ENTER ABOVE TO INTERMEDIATE COVER PARAMETERS. N_2 IS TOTAL DISTRIBUTED LOAD, $N_2/3$ IS APPLIED TO EACH COVER.

EXTERNALLY STIFFENED ZEE STIFFENED TRAPEZOIDAL CORRUGATION

$$\begin{aligned} b_0 &= \frac{L}{3} \times l_0 \\ b_0 &= \frac{L}{3} \times l_0 \\ b_0 &= .37 l_0 \\ b_0 &= .37 l_0 \end{aligned}$$

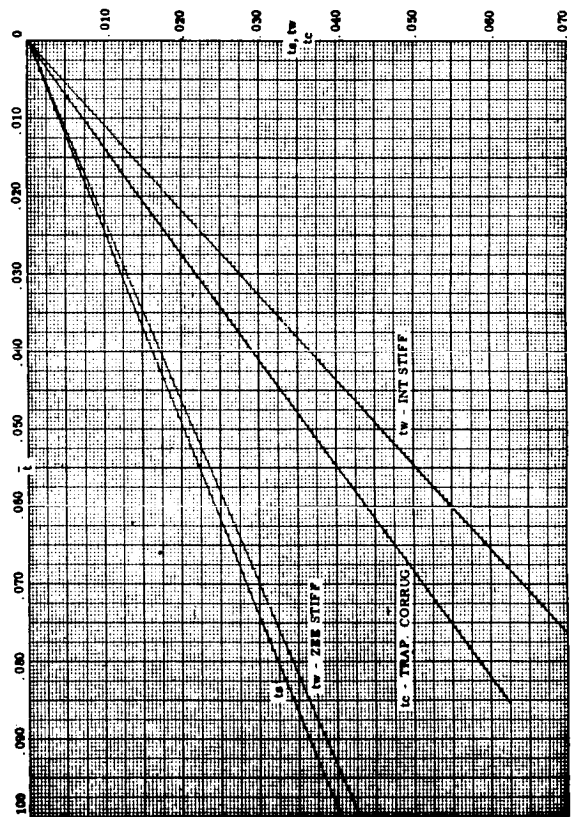
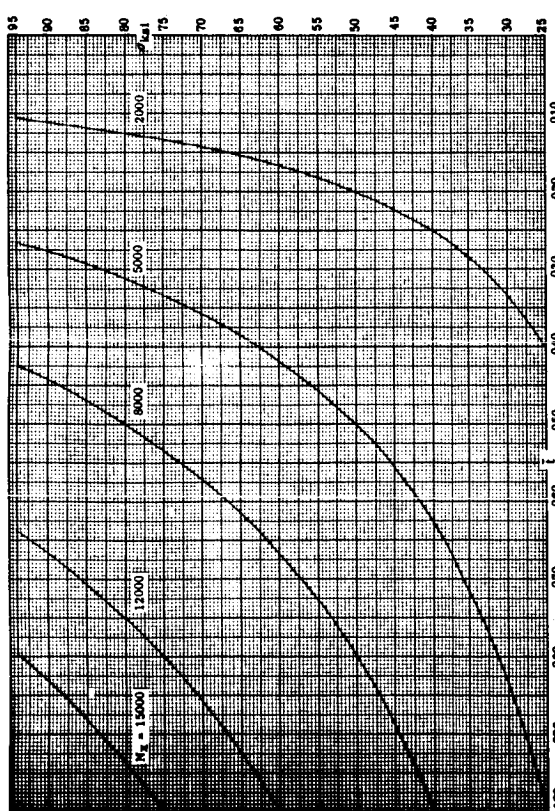
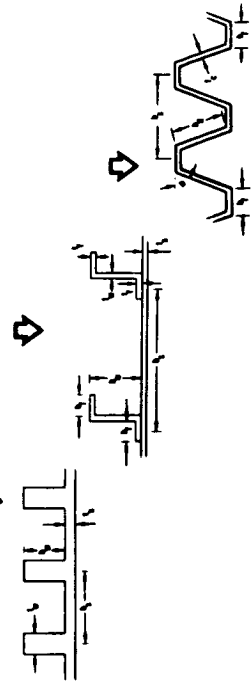


Figure 40. Design Graph - Double-wall Integrally Stiffened Panel (Cont)

Table XII

INTEGRALLY STIFFENED WIDE COLUMN
TRUSS WEB SUBSTRUCTURE

MTL.	N _x LB/IN	RADIUS IN.	SUPPORT SPACING IN.	SHELL THICK. IN.	SUBSTR WEB THICK. IN.	SUBSTR WT. PSF	COVER WT. PSF	PENALTY WT. PSF	TOTAL WT. PSF
Ti 6-4	2200	100	6.0	1.0	0.010	0.243	1.136	0.421	1.800
		137							
		163							
	2200	200	6.0	1.0	0.010	0.243	1.136	0.421	1.800
	5000	100	4.0	1.0	0.010	0.258	1.409	0.625	2.292
		137		1.0	0.010	0.258	1.409	0.625	2.292
		163		1.0	0.010	0.258	1.409	0.625	2.292
	5000	200	4.0	2.0	0.010	0.326	1.409	0.625	2.360
	8000	100	3.0	1.0	0.010	0.277	1.544	0.823	2.644
		133	4.0	1.0		0.258	1.782	0.654	2.694
		167	3.0	2.0		0.384	1.544	0.823	2.751
	8000	200	3.0	2.0	0.010	0.384	1.544	0.823	2.751
	12000	100	4.0	1.0	0.011	0.283	2.183	0.690	3.157
		133		2.0	0.010	0.326	2.183	0.690	3.199
		167		2.0	0.010	0.326	2.183	0.690	3.199
	12000	200	4.0	2.0	0.010	0.326	2.183	0.690	3.199
	15000	100	5.0	2.0	0.010	0.295	2.729	0.633	3.657
		133	5.0			0.295	2.729	0.633	3.657
		167	5.0			0.295	2.729	0.633	3.657
	15000	200	4.0	2.0	0.010	0.326	2.647	0.735	3.708

Table XII (Cont)

INTEGRALLY STIFFENED WIDE COLUMN
TRUSS WEB SUBSTRUCTURE

MTL.	N _x LB/IN	RADIUS IN.	SUPPORT SPACING IN.	SHELL THICK IN.	SUBSTR WEB THICK IN.	SUBSTR WT. PSF	COVER WT. PSF	PENALTY WT. PSF	TOTAL WT. PSF
7106	4300	100	6.0	2.0	0.010	0.171	1.403	0.340	1.914
AL ALLY		133							
		167							
	4300	200	6.0	2.0	0.010	0.171	1.403	0.340	1.914
	5000	100	5.0	1.0	0.010	0.154	1.525	0.399	2.077
		133	6.0	2.0		0.171	1.554	0.355	2.081
		167	6.0	2.0		0.171	1.554	0.355	2.081
	5000	200	6.0	2.0	0.010	0.171	1.554	0.355	2.081
	8000	100	5.0	2.0	0.010	0.183	2.353	0.495	3.031
		133	5.0	2.0		0.183	2.353	0.495	3.031
		167	5.0	2.0		0.183	2.353	0.495	3.031
	8000	200	6.0	3.0	0.010	0.202	2.381	0.455	3.037
	12000	100	5.0	2.0	0.012	0.219	3.431	0.651	4.301
		133	5.0	3.0	0.010	0.223	3.431	0.651	4.305
		167	5.0	3.0	0.010	0.223	3.431	0.651	4.305
	12000	200	6.0	4.0	0.010	0.238	3.470	0.620	4.327
	15000	100	5.0	3.0	0.010	0.223	4.243	0.795	5.260
		133	5.0	3.0	0.012	0.267	4.243	0.795	5.305
		167	5.0	4.0	0.010	0.269	4.243	0.795	5.307
	15000	200	5.0	5.0	0.010	0.277	4.289	0.773	5.339
	2800	100	6.0	2.0	0.010	0.171	1.052	0.257	1.480
	2800	200	6.0	2.0	0.010	0.171	1.052	0.257	1.480

Table XII (Cont)

INTEGRALLY STIFFENED WIDE COLUMN
TRUSS WEB SUBSTRUCTURE

MTL	N _x LB/IN	RADIUS IN.	SUPPORT SPACING IN.	SHELL THICK. IN.	SUBSTR WEB THICK. IN.	SUBSTR WT. PSF	COVER WT. PSF	PENALTY WT. PSF	TOTAL WT. PSF
S-994	2200	100	4.0	1.0	0.015	0.169	0.745	0.328	1.242
GLASS		133		1.0		0.169			1.242
		167		1.0		0.169			1.242
	2200	200	4.0	2.0	0.015	0.214	0.745	0.328	1.287
	5000	100	3.0	2.0	0.015	0.252	0.974	0.459	1.685
		133	3.0			0.252	0.974	0.459	1.685
		167	3.0			0.252	0.974	0.459	1.685
	5000	200	4.0	2.0	0.015	0.214	1.124	0.388	1.727
	8000	100	3.0	2.0	0.015	0.252	1.232	0.514	1.998
		133		2.0		0.252	1.232	0.514	1.998
		167		3.0		0.338	1.232	0.514	2.084
	8000	200	3.0	3.0	0.015	0.338	1.232	0.514	2.084
	12000	100	3.0	2.0	0.015	0.252	1.509	0.592	2.352
		133		3.0		0.338			2.438
		167		3.0		0.338			2.438
	12000	200	3.0	4.0	0.015	0.431	1.509	0.592	2.531
	15000	100	3.0	2.0	0.019	0.328	1.687	0.652	2.667
		133		3.0	0.015	0.338			2.677
		167		4.0	0.015	0.431			2.770
	15000	200	3.0	4.0	0.015	0.431	1.687	0.652	2.770

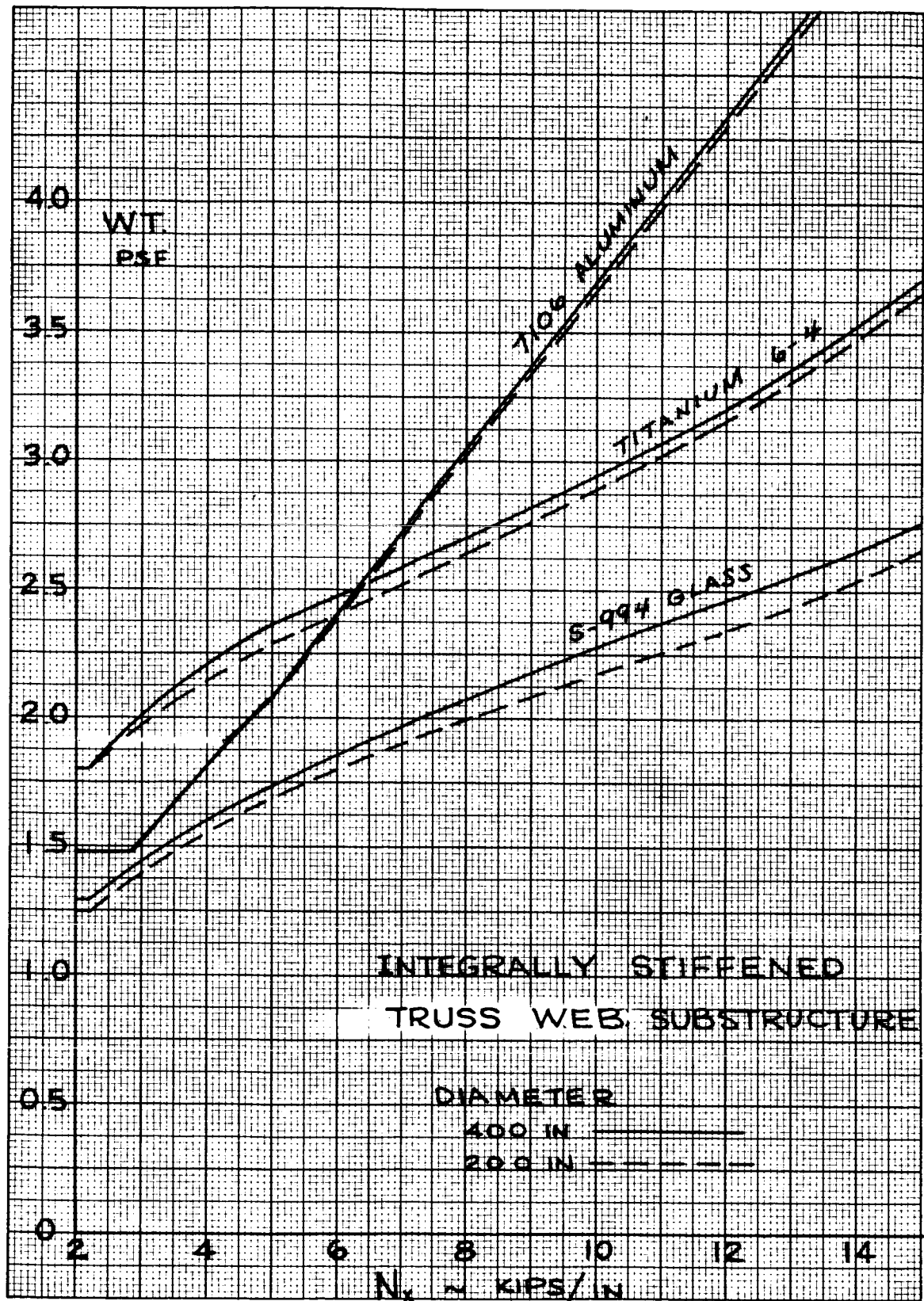


Figure 41. Panel Weight Versus Load-integrally Stiffened Panel

DOUBLE-WALL INTEGRALLY ZEE STIFFENED COVER PANELS WITH TRUSS RIB SUBSTRUCTURE

The integrally zee stiffened - beaded truss rib substructure concept is virtually identical to the integrally stiffened concept, with the exception of the cover panels. These panels have longitudinal zee shaped stiffeners rather than the simple flat stiffener. Ti-6Al-4V, 7106 aluminum, and S-994 glass are selected for structural efficiency.

Cover and substructure joint splices are similar to the integrally stiffened concept.

The inner and outer panels of Ti-6Al-4V are fabricated by roll diffusion bonding techniques. The structure is roll bonded as a double faced sandwich with subsequent machining or chem etch removal of material on one surface to provide the zee stiffened configuration. The fabrication sequence for providing a fully heat treated roll bonded structure is accomplished in the manner described previously.

In cases where a rivet head cannot clear the zee, a strip allows the rivet to seat. Where the stringer spacing dimension increases enough to allow the rivet head to fit between the upright legs. the zee portion is machined away locally as shown in the design drawing.

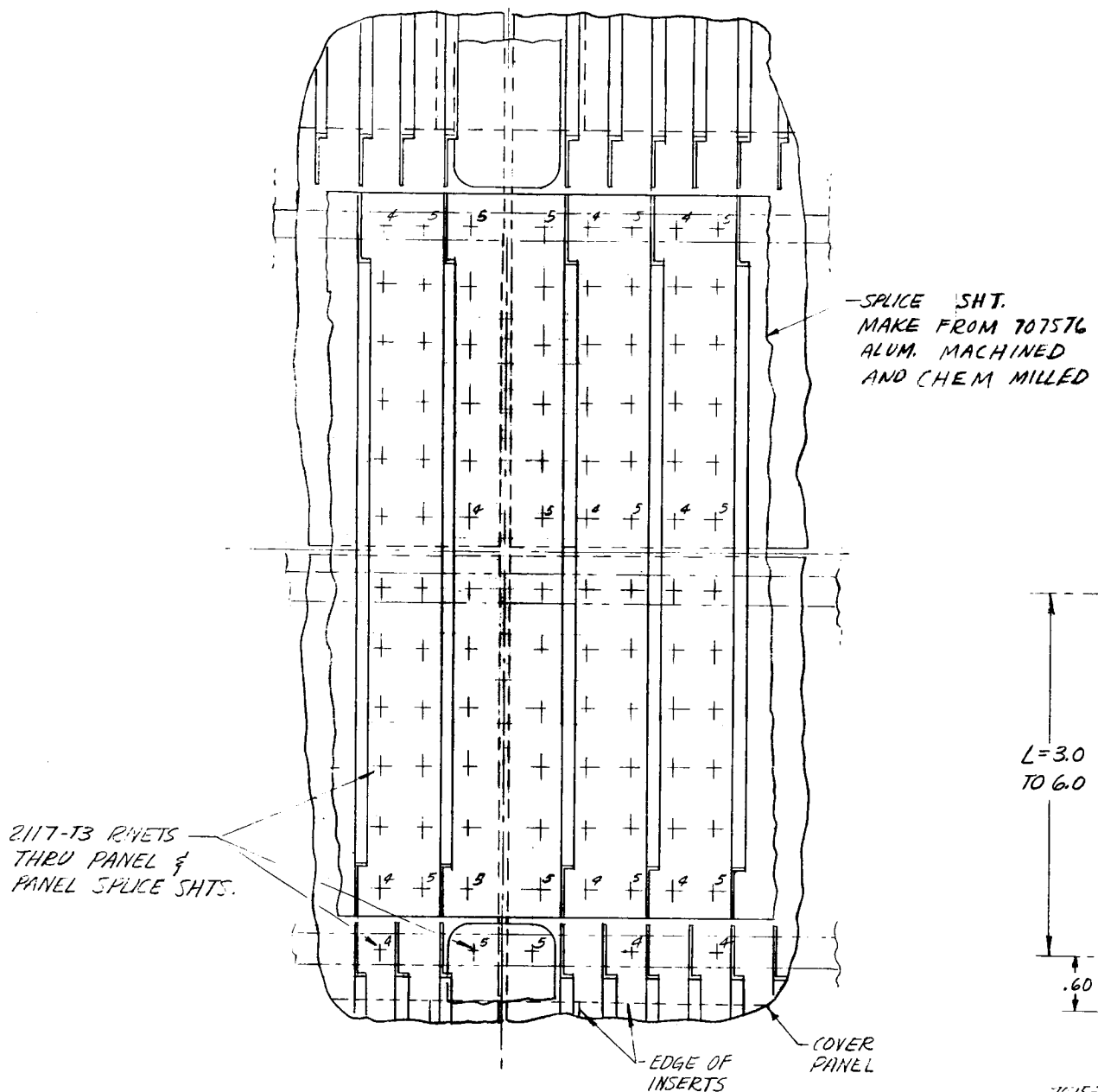
The substructure, beaded truss rib, is fabricated from commercially pure titanium sheet. Commercially pure titanium is more formable and material costs are less than for 6Al-4V titanium alloy sheet. These details are fabricated using drophammer tooling with hot sizing and subsequent stress relief operations.

Splices are fabricated as flat details and allowed to drape on assembly. Assembly is by the use of blind fasteners. Room temperature curing adhesive provides additional stiffness along all mechanical joints.

While similar in other details to the titanium, the all aluminum concept varies in production technique. For instance, the covers must be machined and chem milled, and blocks must be machined between the zees to allow rivets to be used for the lower load levels.

Panels and substructure are assembled by blind fasteners with bonding of all mechanical joints providing additional stiffness.

The S-994 glass zee stiffened concept is similar to the integrally stiffened concept having sandwiched in aluminum strips along all edges, a stiffened circumferential cover splice sheet, and flat splice sheets at other joints. Joining of all parts is accomplished by bonding and riveting, a slow and tedious process.



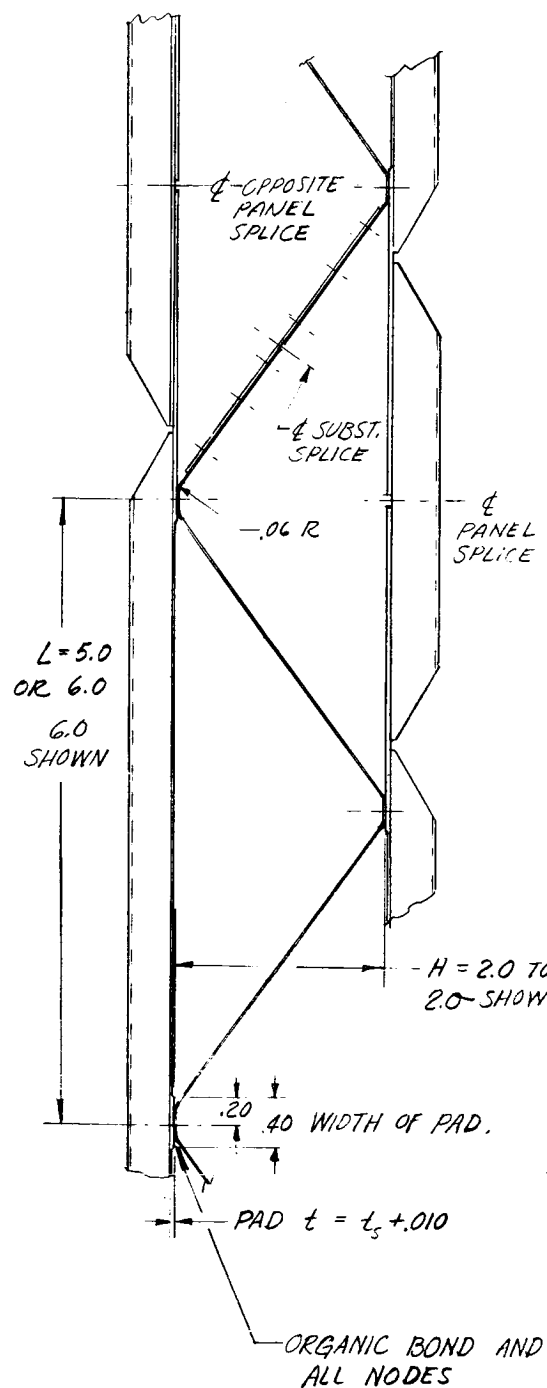
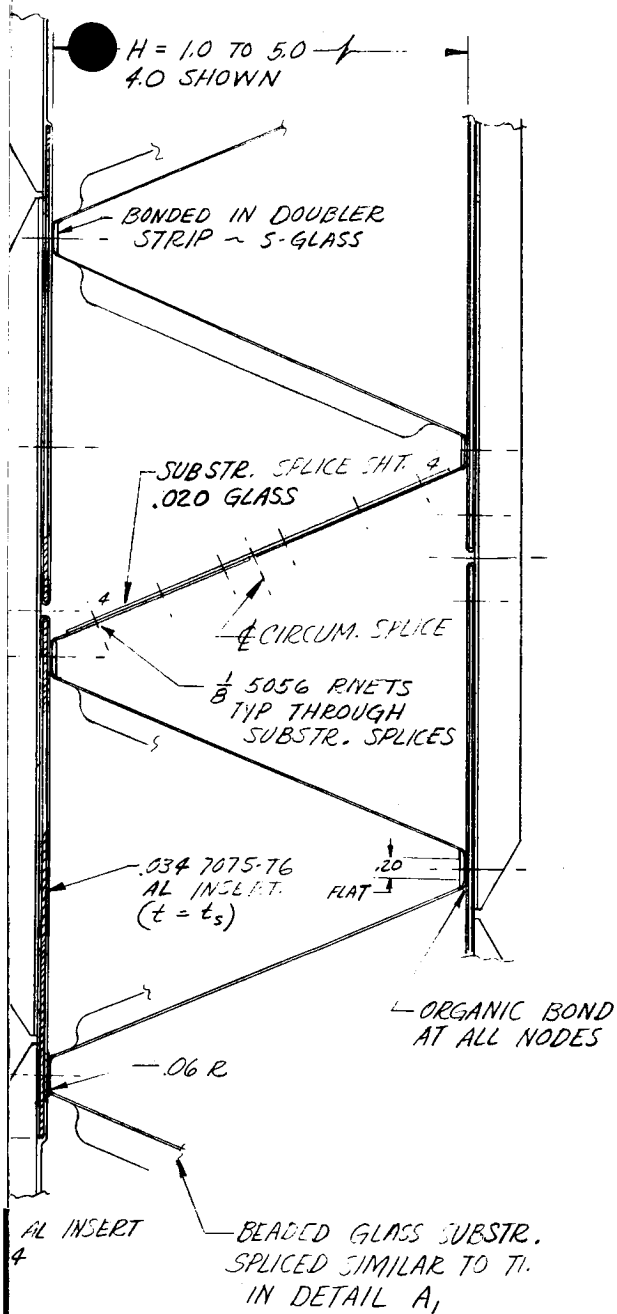
L=3.0
TO 6.0

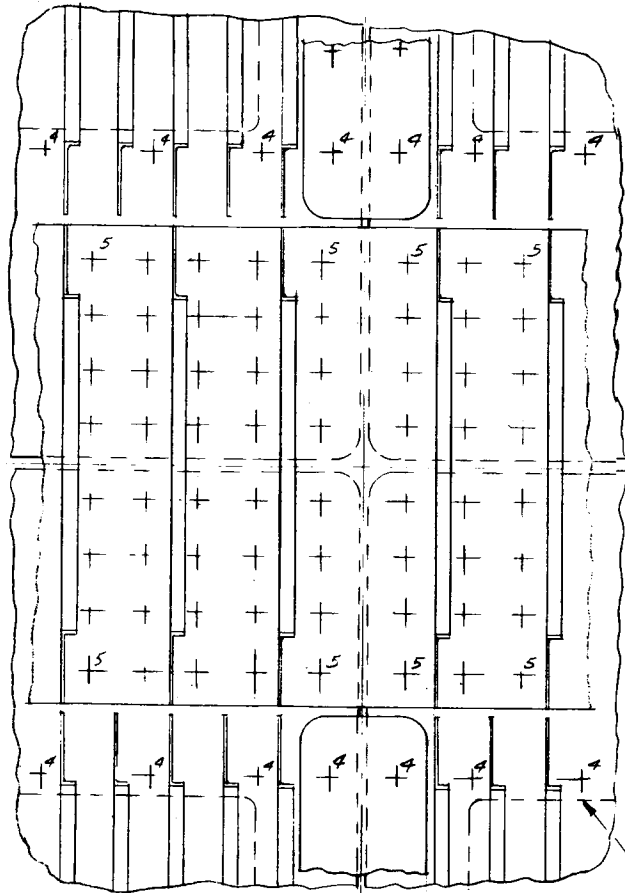
.60

7075-T6
L-.03

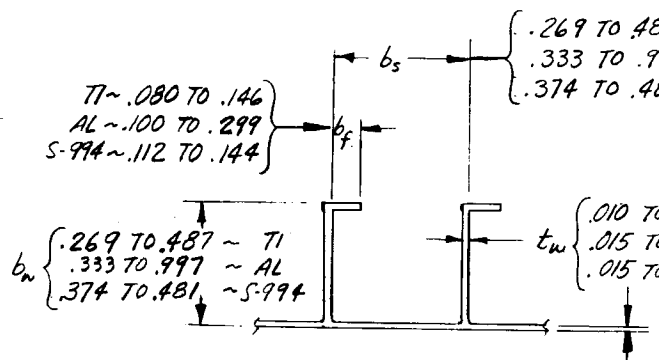
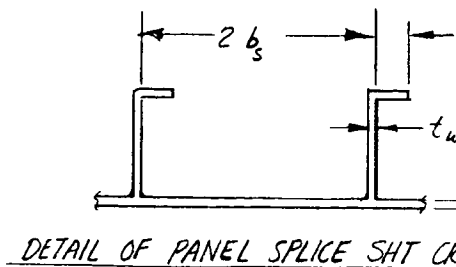
DETAIL **A**₃ FULL SCALE

MTLS: S-994 GLASS & ALUM. INSERTS AND SPICE SHT. AS NOTED
 $N_f = 2000$ TO $15,000$ LB/IN $\sim 15,000$ LB/IN, 200 R. SHOWIN
 SIMILAR TO DETAIL A, EXCEPT AS NOTED. PANEL TO
 SUBSTRUCTURE JOINTS ARE ADHESIVE BONDED AND
 RIVETED WITH 2117-T3 BLIND OR CONVENTIONAL RIVETS
 WHERE APPLICABLE.





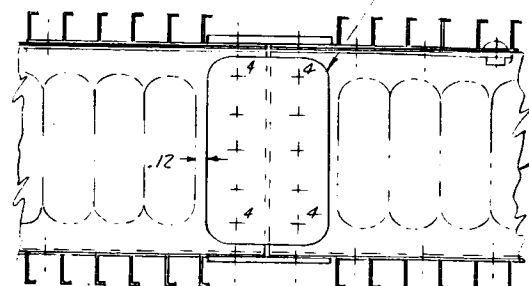
1/2 LONG. PANEL SPLICE



DETAIL A₂ FULL SCALE

MTL: 7106 AL. ~ N_x = 2000 TO 15,000 LB/IN ~ 5000 LB/IN SHOWN
SIMILAR TO DETAIL A, EXCEPT AS NOTED

RIVET



SECTION C-C FULL SCALE

b_f

t_s

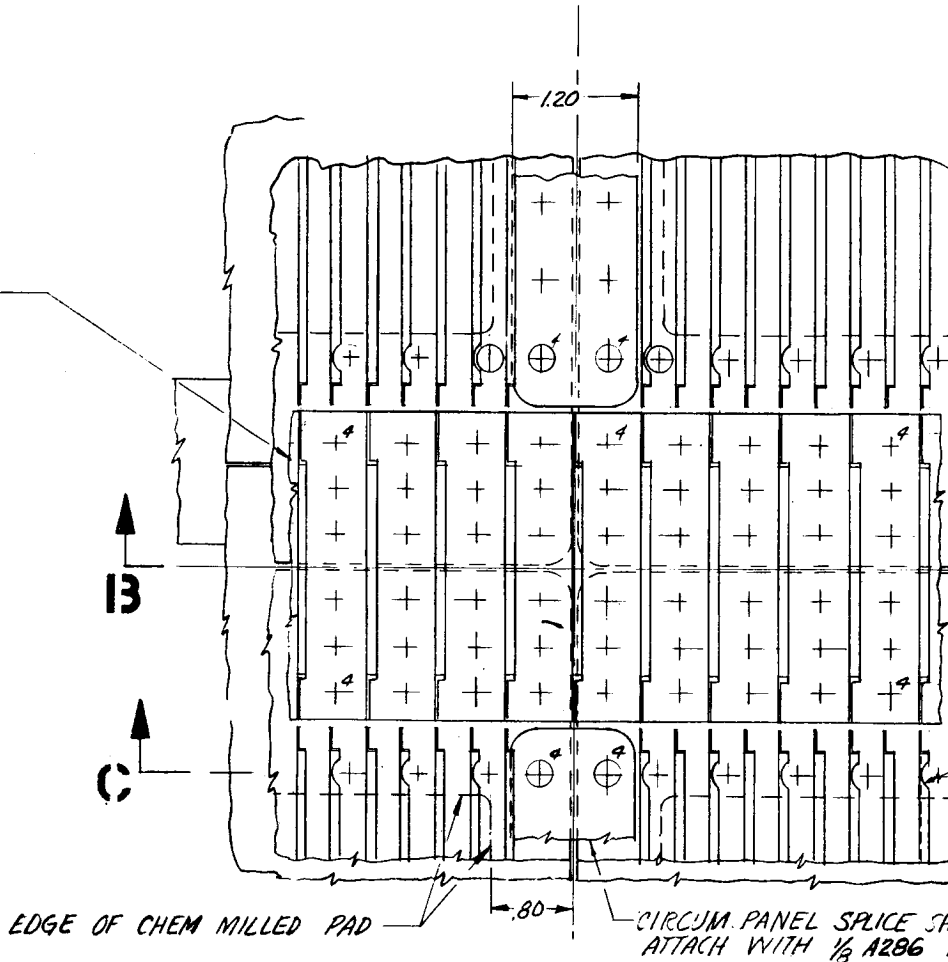
255 SECTION

CIRCUM. SPLICE SHT.
ATTACH. TO ZEE PANELS
WITH 1/8 A286 BLIND RIVETS

7 ~ TI
77 ~ AL
1 ~ S-994 GLASS

.025 ~ TI
.064 ~ AL
.035 ~ S-994

-t_s { .010 TO .025 ~ TI.
.015 TO .064 ~ AL
.015 TO .035 ~ S-994

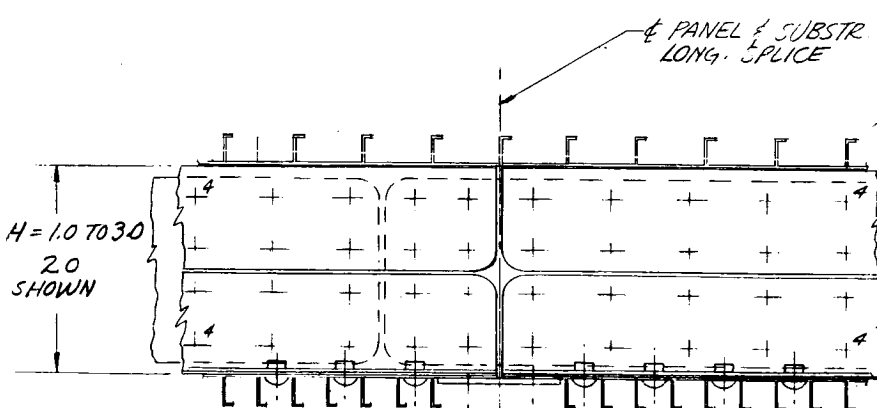


DETAIL A, FULL SCALE

MTL: TI ~ N_x = 2000 TO 15,000 LB/IN ~ 8000 LB/IN, 200

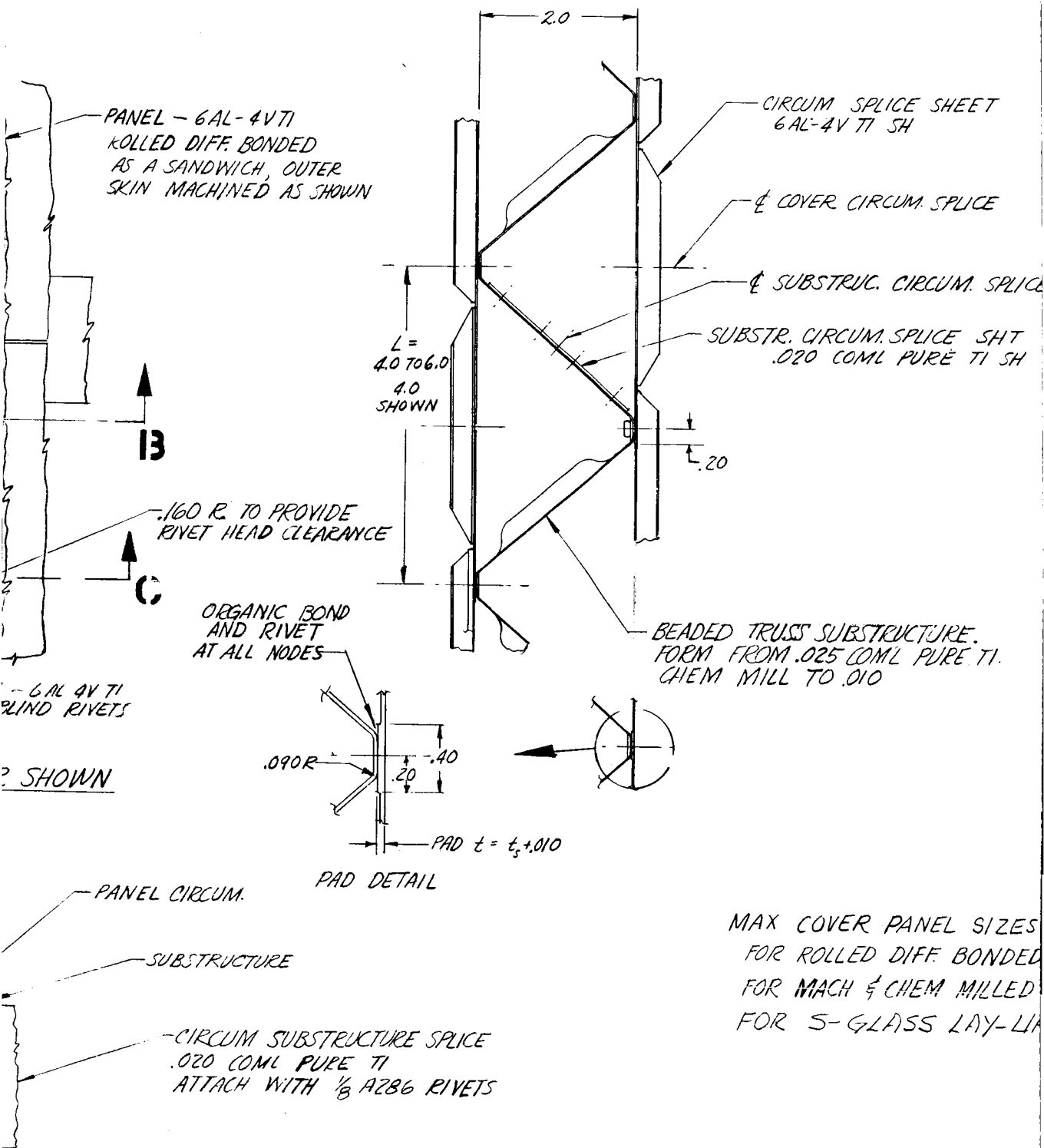
FE SHEET -- .020 COML PURE TI
WEB SPLICE AT ENDS OF
TRUSS SUBSTR.
WITH 1/8 A286 RIVETS

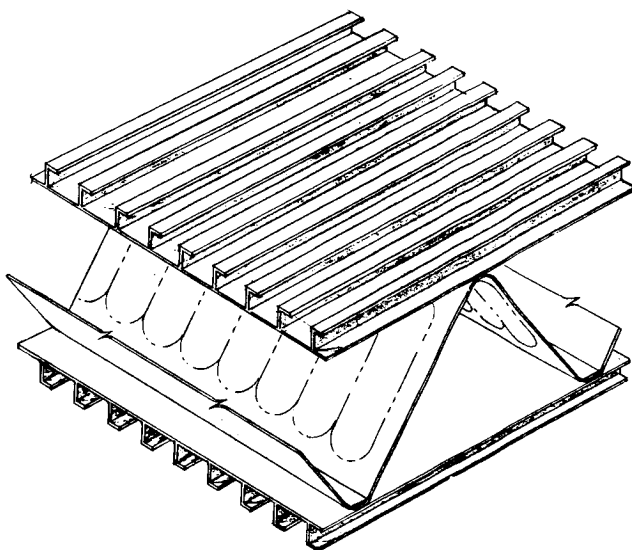
100 TO 200 R
SUBSTRUCTURE



SECTION B-B FULL SCALE

97 - (4)





DESIGN DWG - DOUBLE WALL ZEE STIFFENED PANEL
FIG 42

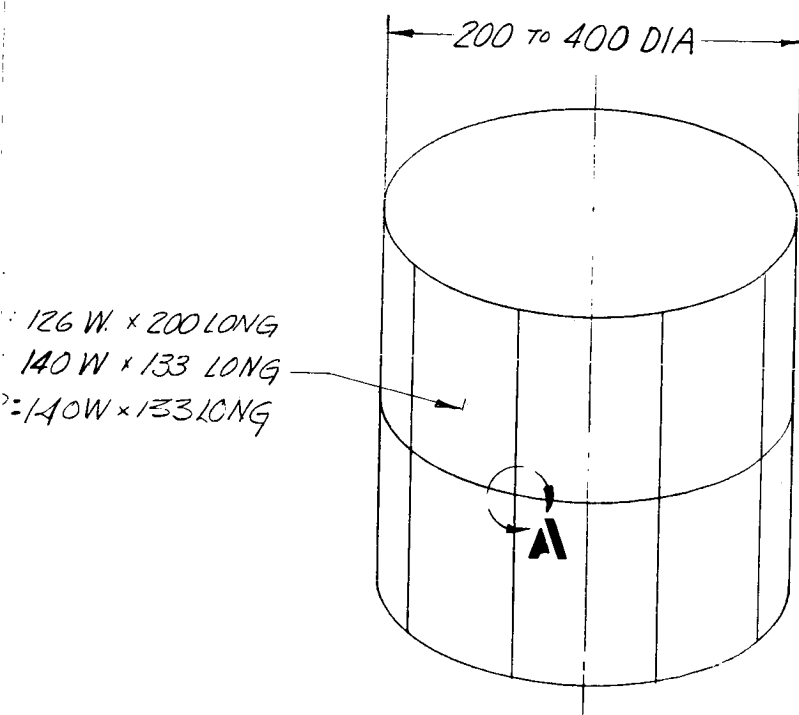


Figure 42. Design Drawing - Double-wall Zee Stiffened Panel

6

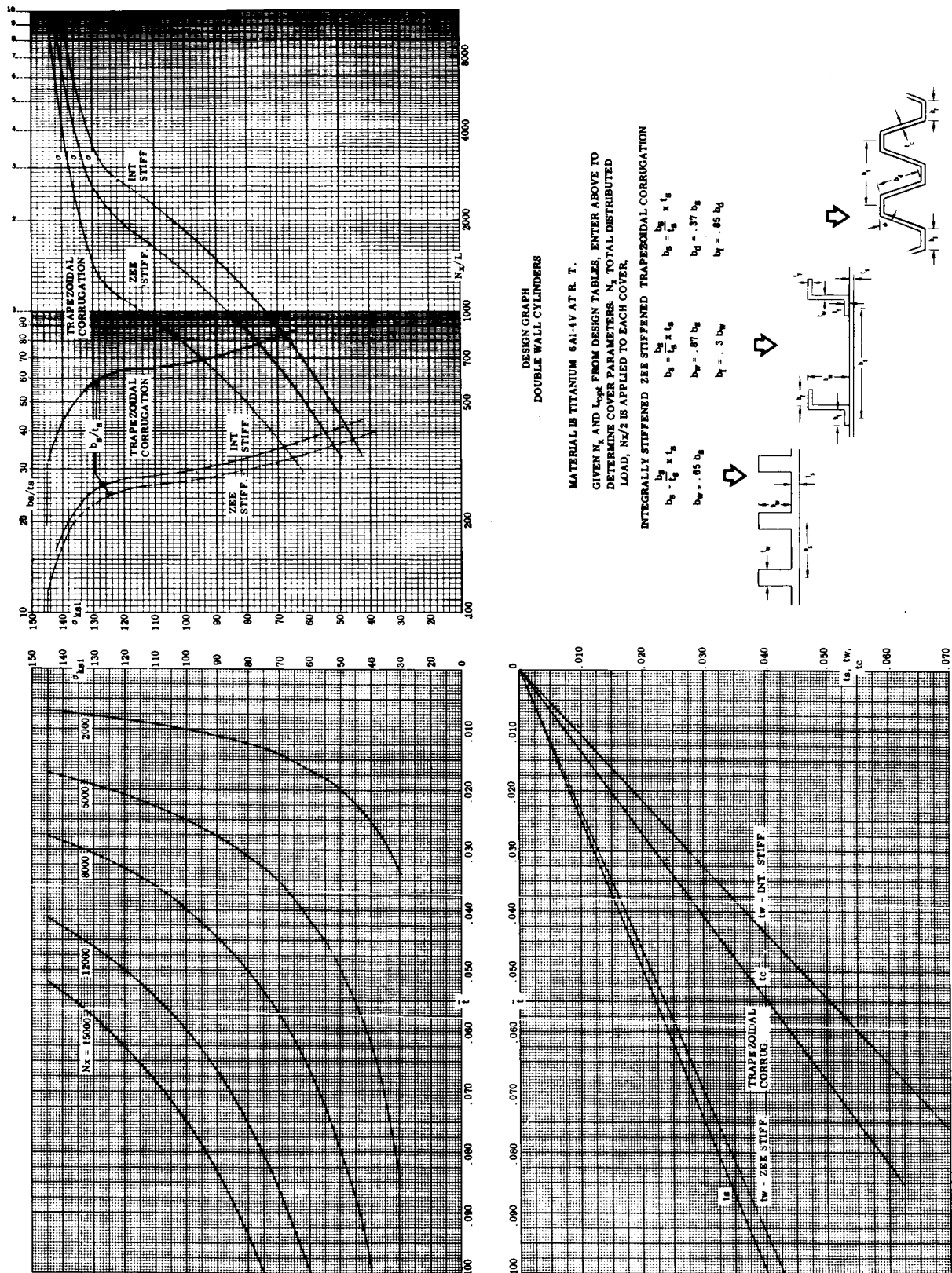
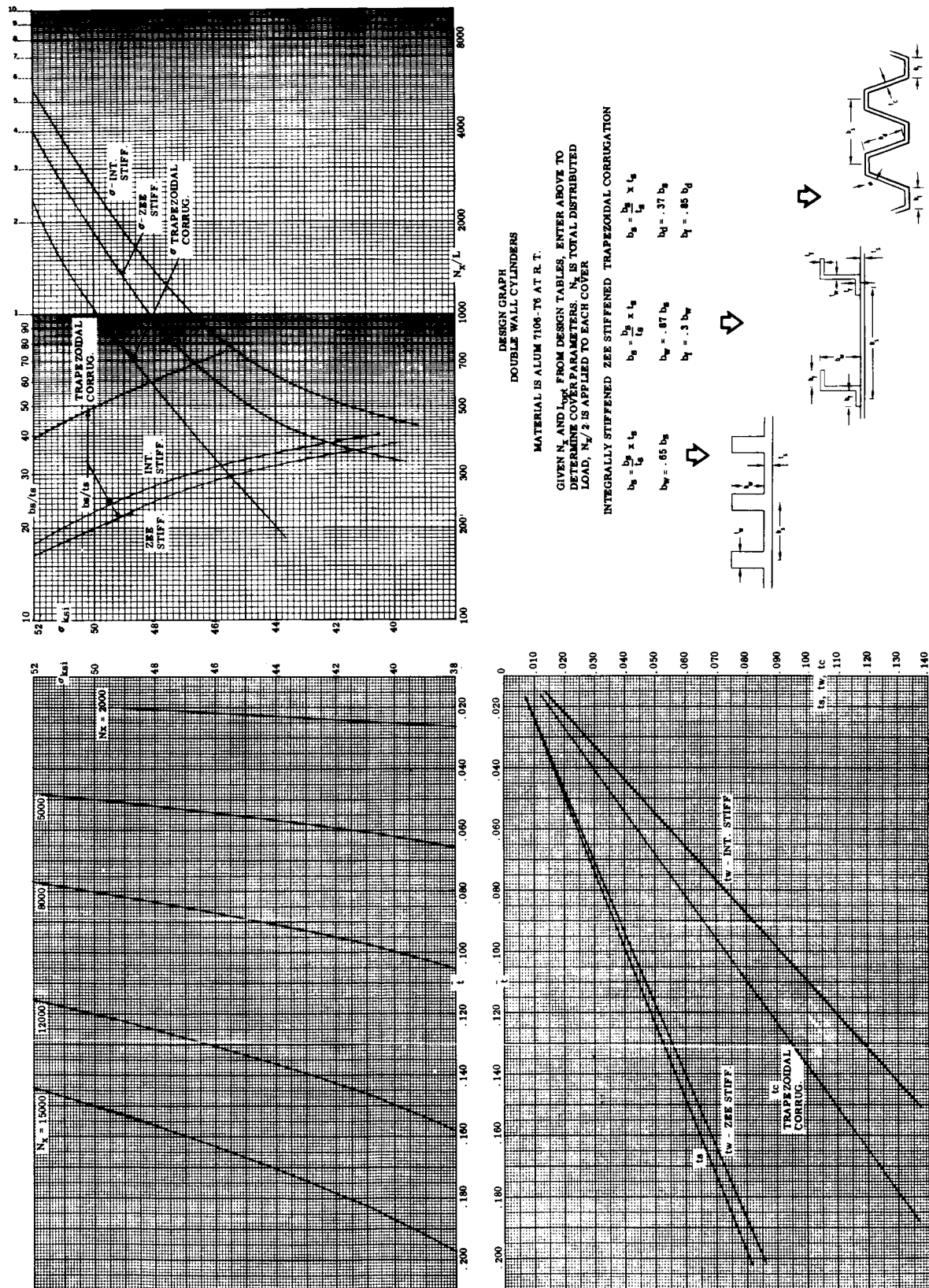


Figure 43. Design Graph - Double-wall Zee Stiffened Panel



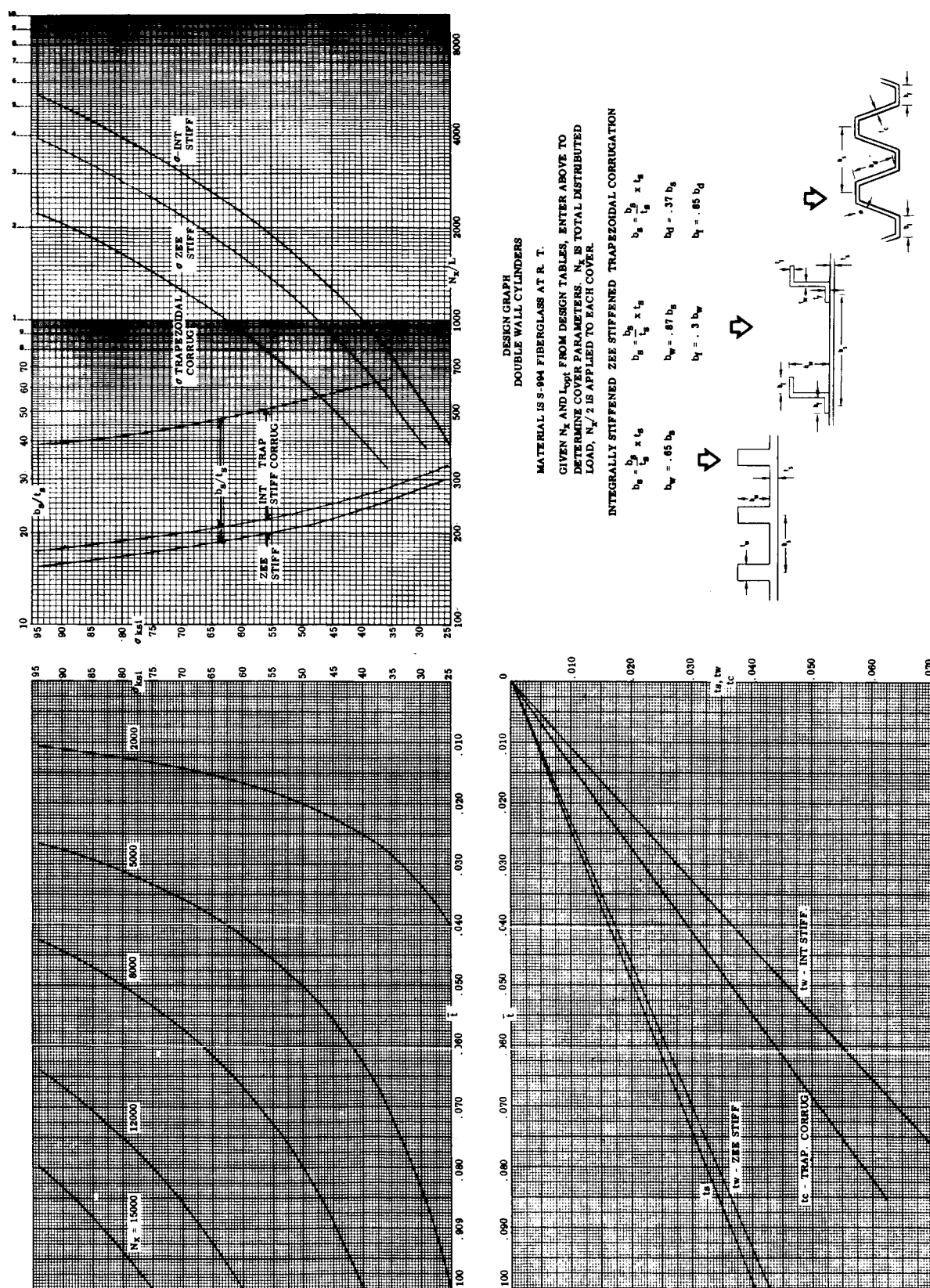


Figure 43. Design Graph - Double-wall Zee Stiffened Panel (Cont)

Table XIII
 INTEGRAL ZEE STIFFENED WIDE COLUMN
 TRUSS WEB SUBSTRUCTURE

MTL.	N _x LB/IN	RADIUS IN.	SUPPORT SPACING IN.	SHELL THICK. IN.	SUBSTR WEB THICK. IN.	SUBSTR WT. PSF	COVER WT. PSF	PENALTY WT. PSF	TOTAL WT. PSF
TI 6-4	3200	100	6.0	1.0	0.010	0.243	1.060	0.418	1.721
		133							
		167							
	3200	200	6.0	1.0	0.010	0.243	1.060	0.418	1.721
	5000	100	4.0	1.0	0.010	0.258	1.125	0.607	1.990
		133	5.0	2.0		0.295	1.257	0.503	2.055
		167	5.0	2.0		0.295	1.257	0.503	2.055
	5000	200	5.0	2.0	0.010	0.295	1.257	0.503	2.055
	8000	100	4.0	1.0	0.010	0.258	1.430	0.628	2.315
		133		2.0		0.326			2.383
		167		2.0		0.326			2.383
	8000	200	4.0	2.0	0.010	0.326	1.430	0.628	2.383
	12000	100	6.0	3.0	0.010	0.326	2.145	0.497	2.967
		133							
		167							
	12000	200	6.0	3.0	0.010	0.326	2.145	0.497	2.967
	15000	100	6.0	3.0	0.010	0.326	2.635	0.542	3.502
		133							
		167							
	15000	200	6.0	3.0	0.010	0.326	2.635	0.542	3.502

Table XIII (Cont)

INTEGRAL ZEE STIFFENED WIDE COLUMN
TRUSS WEB SUBSTRUCTURE

MTL.	N _x LB/IN	RADIUS IN.	SUPPORT SPACING IN.	SHELL THICK. IN.	SUBSTR WEB THICK. IN.	SUBSTR WT. PSF	COVER WT. PSF	PENALTY WT. PSF	TOTAL WT. PSF
7106	4300	100	6.0	2.0	0.010	0.177	1.310	0.335	1.822
AL.		133							
ALLY.		167							
	4300	200	6.0	2.0	0.010	0.177	1.310	0.335	1.822
	5000	100	6.0	2.0	0.010	0.177	1.488	0.352	2.017
		133							
		167							
	5000	200	6.0	2.0	0.010	0.177	1.488	0.352	2.017
	8000	100	5.0	2.0	0.010	0.183	2.288	0.467	2.938
		133	6.0	3.0	0.010	0.202	2.313	0.427	2.941
		167	6.0	3.0	0.010	0.202	2.313	0.427	2.941
	8000	200	6.0	3.0	0.011	0.222	2.313	0.427	2.961
	12000	100	6.0	4.0	0.010	0.238	3.376	0.563	4.177
		133		4.0		0.238			4.177
		167		5.0		0.277			4.217
	12000	200	6.0	5.0	0.010	0.277	3.376	0.563	4.217
	15000	100	5.0	4.0	0.010	0.269	4.133	0.718	5.120
		133	6.0	5.0		0.277	4.176	0.690	5.143
		167	6.0	6.0		0.319	4.176	0.690	5.185
	15000	200	6.0	6.0	0.010	0.319	4.176	0.690	5.185
	3200	100	6.0	2.0	0.010	0.177	0.983	0.300	1.46
	3200	200	6.0	2.0	0.010	0.177	0.983	0.300	1.46

Table XIII (Cont)

INTEGRAL ZEE STIFFENED WIDE COLUMN
TRUSS WEB SUBSTRUCTURE

MTL	Nx LB/IN	RADIUS IN.	SUPPORT SPACING IN.	SHELL THICK. IN.	SUBSTR WEB THICK. IN.	SUBSTR WT. PSF	COVER WT. PSF	PENALTY WT. PSF	TOTAL WT. PSF
S-994	2000	100	6.0	1.0	0.015	0.159	0.695	0.230	1.084
GLASS		133		2.0		0.182			1.106
		167		2.0		0.182			1.106
	2000	200	6.0	2.0	0.015	0.182	0.695	0.230	1.106
	5000	100	3.0	2.0	0.015	0.252	0.777	0.432	1.461
		133	3.0	2.0	0.015	0.252	0.777	0.432	1.461
		167	4.0	2.0	0.018	0.257	0.897	0.354	1.508
	5000	200	4.0	3.0	0.015	0.273	0.897	0.354	1.524
	8000	100	3.0	2.0	0.015	0.252	0.983	0.469	1.704
		133	3.0	3.0	0.015	0.338	0.983	0.469	1.790
		167	3.0	3.0	0.015	0.338	0.983	0.469	1.790
	8000	200	4.0	4.0	0.015	0.338	1.135	0.401	1.874
	12000	100	4.0	3.0	0.015	0.273	1.390	0.466	2.129
		133		3.0		0.273			2.129
		167		4.0		0.338			2.194
	12000	200	4.0	4.0	0.015	0.338	1.390	0.466	2.194
	15000	100	4.0	3.0	0.015	0.273	1.609	0.529	2.410
		133		4.0		0.338			2.476
		167		4.0		0.338			2.476
	15000	200	4.0	5.0	0.015	0.407	1.609	0.529	2.545

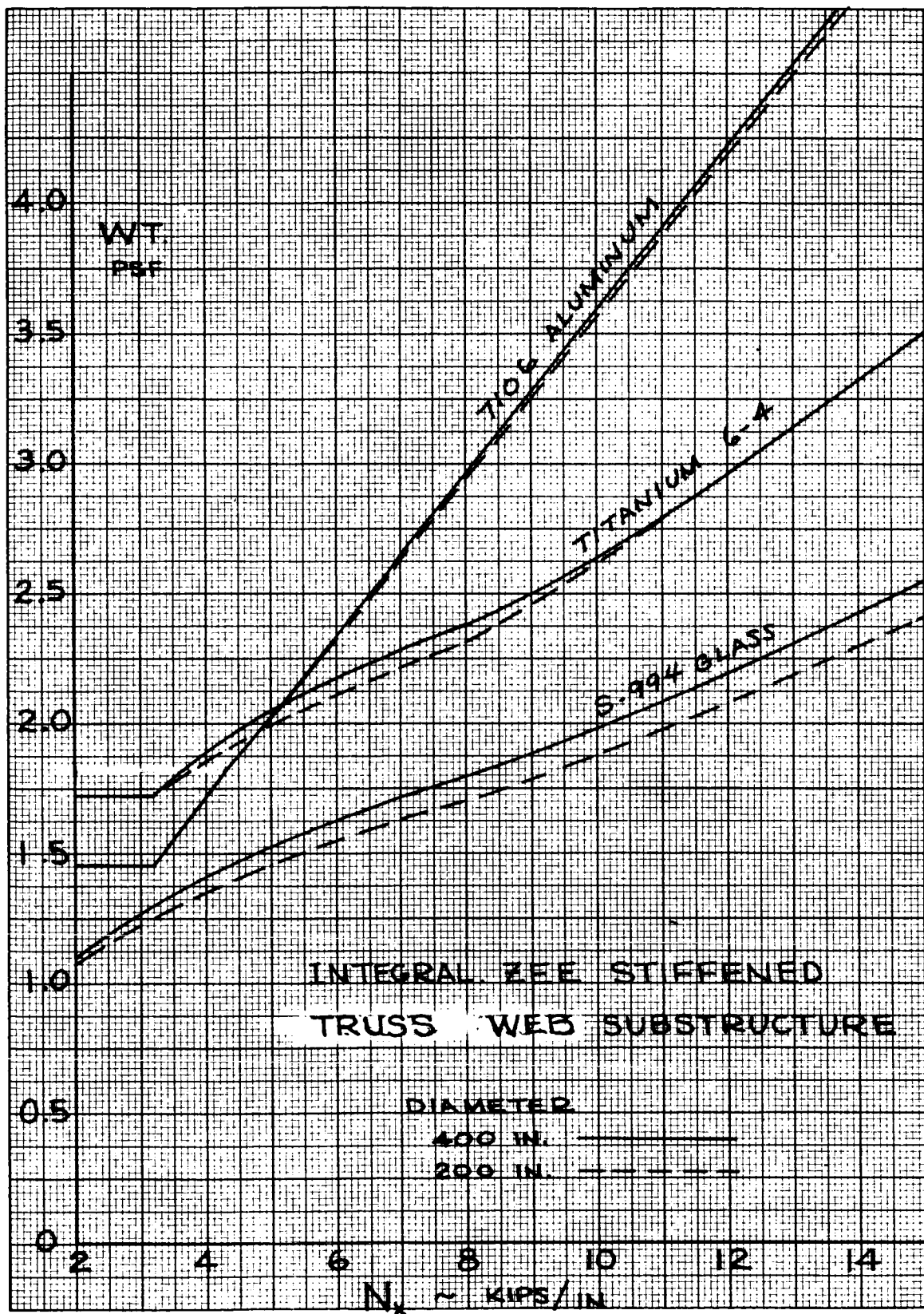


Figure 44. Panel Weight Versus Load-zee Stiffened Panel

RING STIFFENED TRAPEZOIDAL COVER CONCEPT

The ring stiffened trapezoidal corrugated configuration is fabricated from three materials: 7106 aluminum, AZ31B-H24 magnesium, and beryllium. This structure consists of load-carrying corrugated panels joined to Zee-section ring frames with mechanical attachments and bonding. The panels are spliced longitudinally with flat sheets and circumferentially with matched corrugated sheets. Separate cap sheets and web sheets splice the frames.

All attachments are made with A17ST rivets for the aluminum and magnesium materials. The beryllium structure is organically bonded and riveted together with monel rivets.

The aluminum configuration represents the simplest, most straight-forward concept. The parts are readily formed and joined using current aerospace manufacturing practice. Since there is no closeout panel, all fasteners are readily accessible making this a highly reliable structure.

For magnesium, the forming and joining applications are the same as for the aluminum configuration. However, the magnesium sheet material is formed at room or slightly elevated temperatures, depending upon the bend radius requirements, etc. Both aluminum and magnesium require protective coating to prevent corrosion.

Per currently available sheet sizes of both aluminum and magnesium sheet material, a lesser number of mechanical joints is required without necessitating fusion welding than for the beryllium concept.

Magnesium by its nature requires more care in forming and handling, and corrosion prevention is a necessity. This magnesium concept is similar to aluminum on all aspects except as noted on the design drawing.

The beryllium concept is joined in a similar manner to the aluminum and magnesium designs, except an organic bond would be used at all faying surfaces, thus reducing the number of monel rivets and the probability of cracks.

The characteristics of beryllium sheet material combined with a lack of experience in fabricating frames and corrugated panels indicates a slower rate of learning. However, a high level of reliability is predicted for assemblies of any of these materials through standard quality control methods.

All beryllium sheet material is chemically milled .002 inch per surface to improve the surface condition of the as-received material for improved fabricability. The periphery of the detail parts is produced by machining in flat pattern. Frames are formed on integrally heated two-stage form tools and subsequently sized. Corrugations are formed on integrally heated multi-stage tooling and subsequently sized. All forming is accomplished at 1000°F - 1400°F.

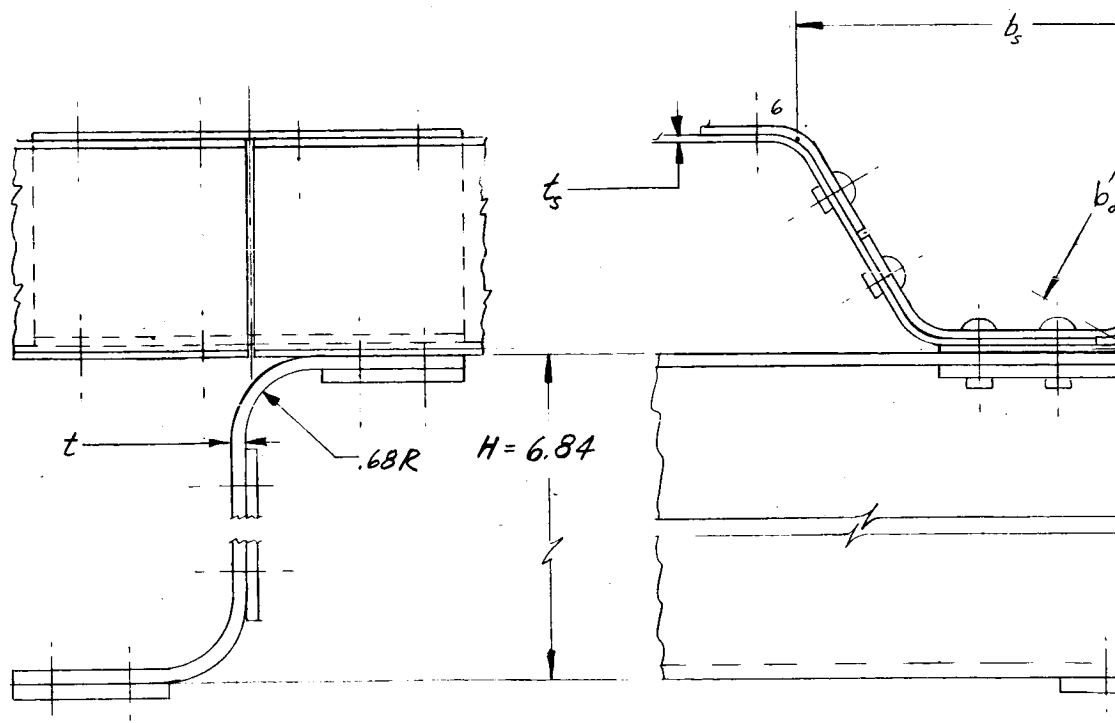
Joining is accomplished by riveting and room temperature bonding. EPON 923 is recommended for this application. However, tests are required to verify this bonding agent for beryllium structure.

TYP PANEL OVERLAP
 SPLICE ATTACH.
 RIVETS 2 IN. ON CTR.

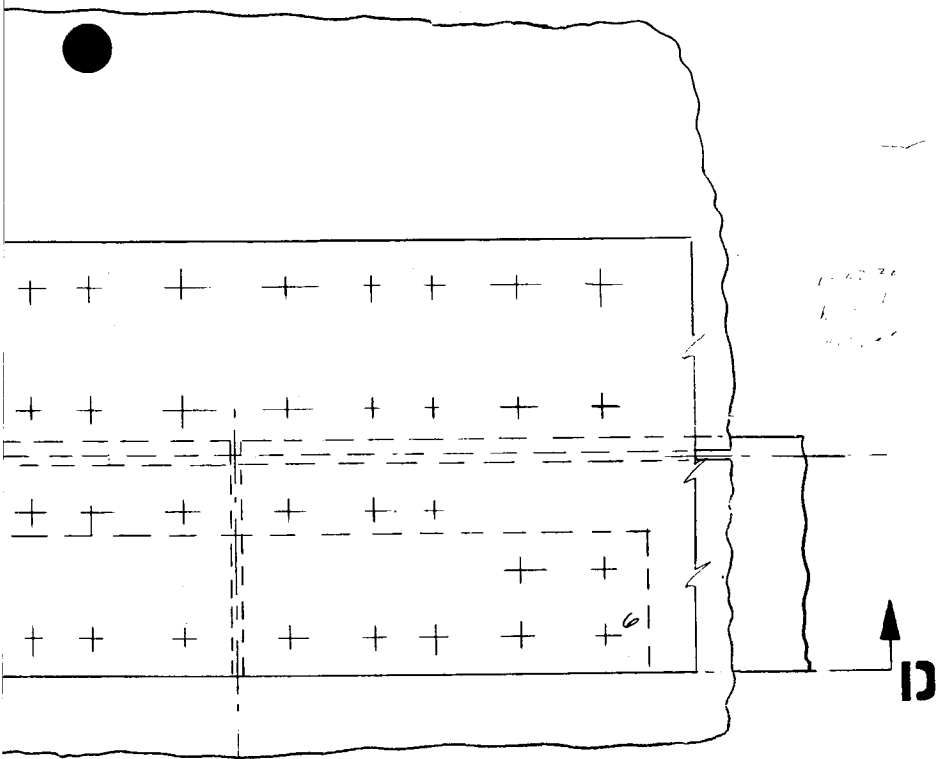
TYP FRAME SPACING (L)
 42.28

13

MTL: AZ31B-H24 MA



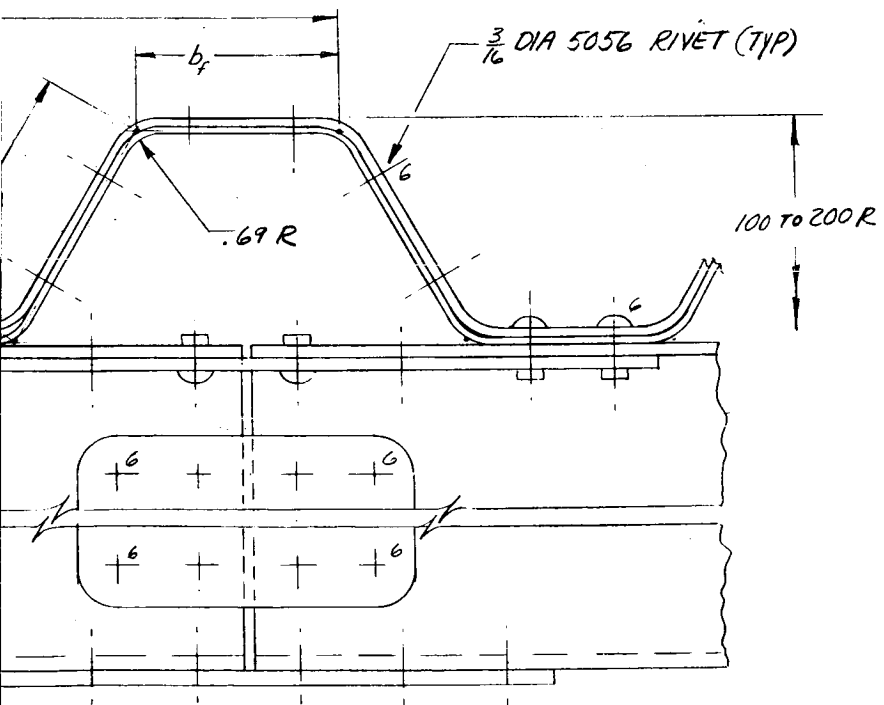
107-0



.75" STAGG
THRU OVER

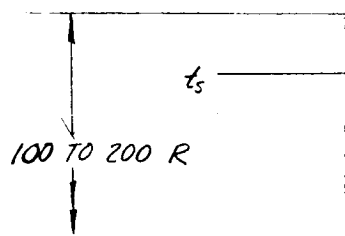
C

DETAIL **A₃** FULL SCALE
 $\bar{q} \sim N_x = 2000 \text{ TO } 15,000 \text{ LB/IN} \sim 2000 \text{ LB/IN, } 200R \text{ SHOWN}$



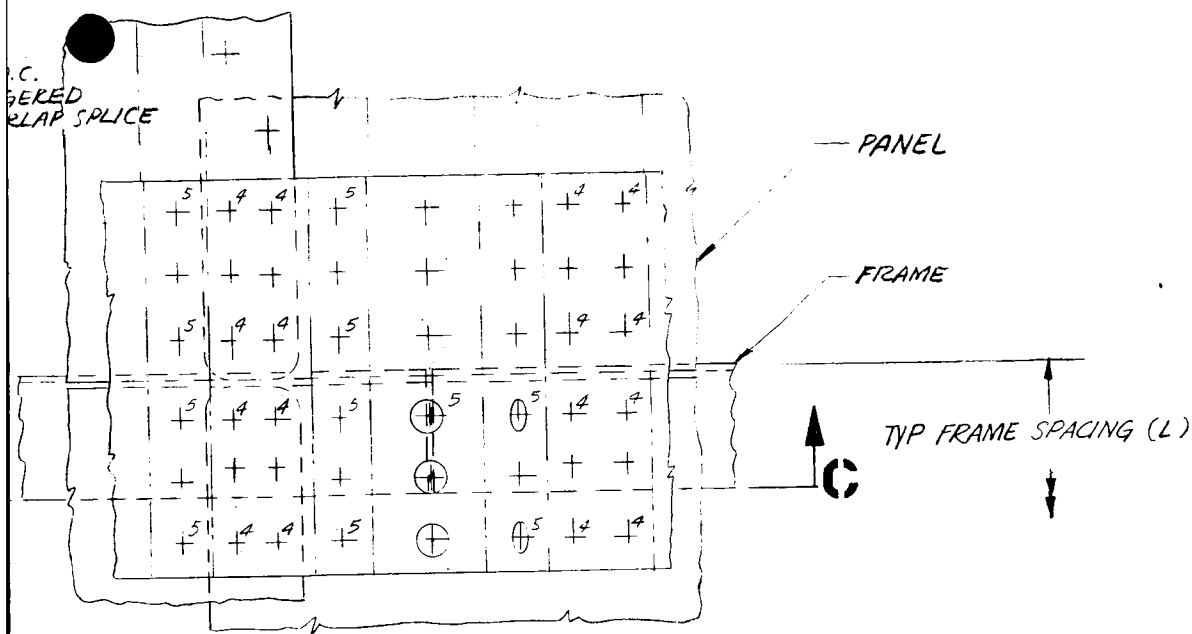
TYP OVERLAP SPLICE OF PANEL

CORRUG. PANEL SPLICE
 .040 7106 AL. SH.



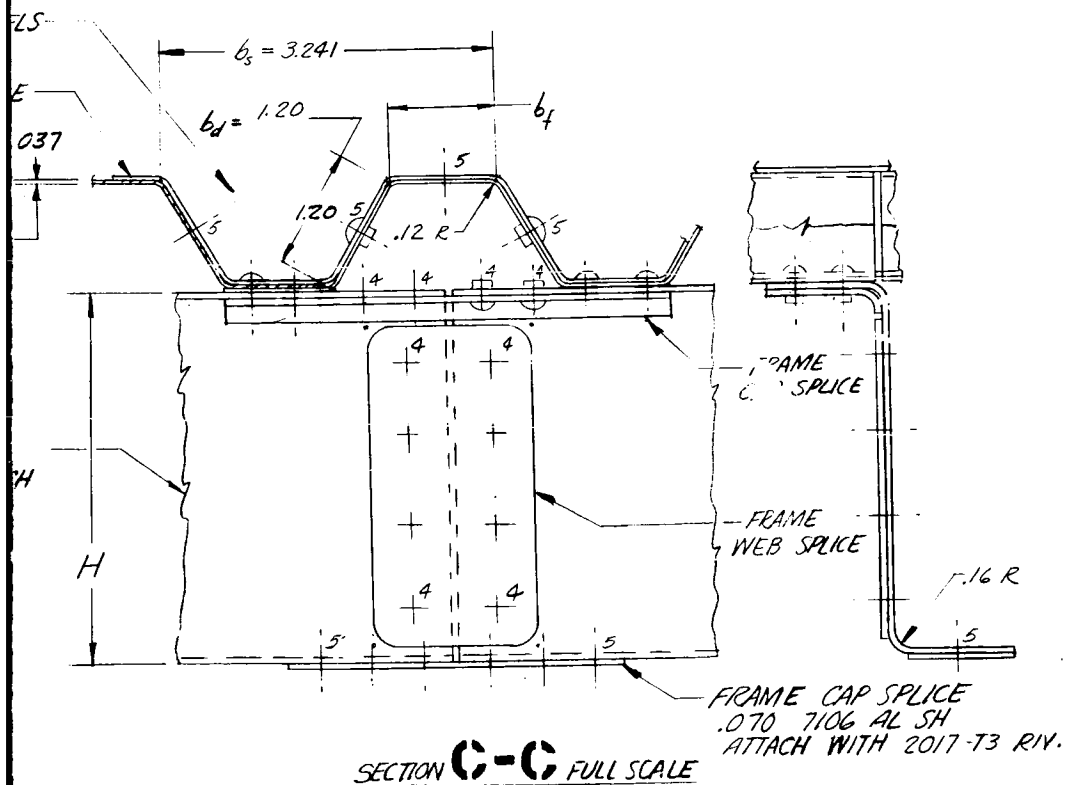
ZEE FRAME
 $t = .060 \text{ 7106 AL. S}$

SECTION **D-D** FULL SCALE

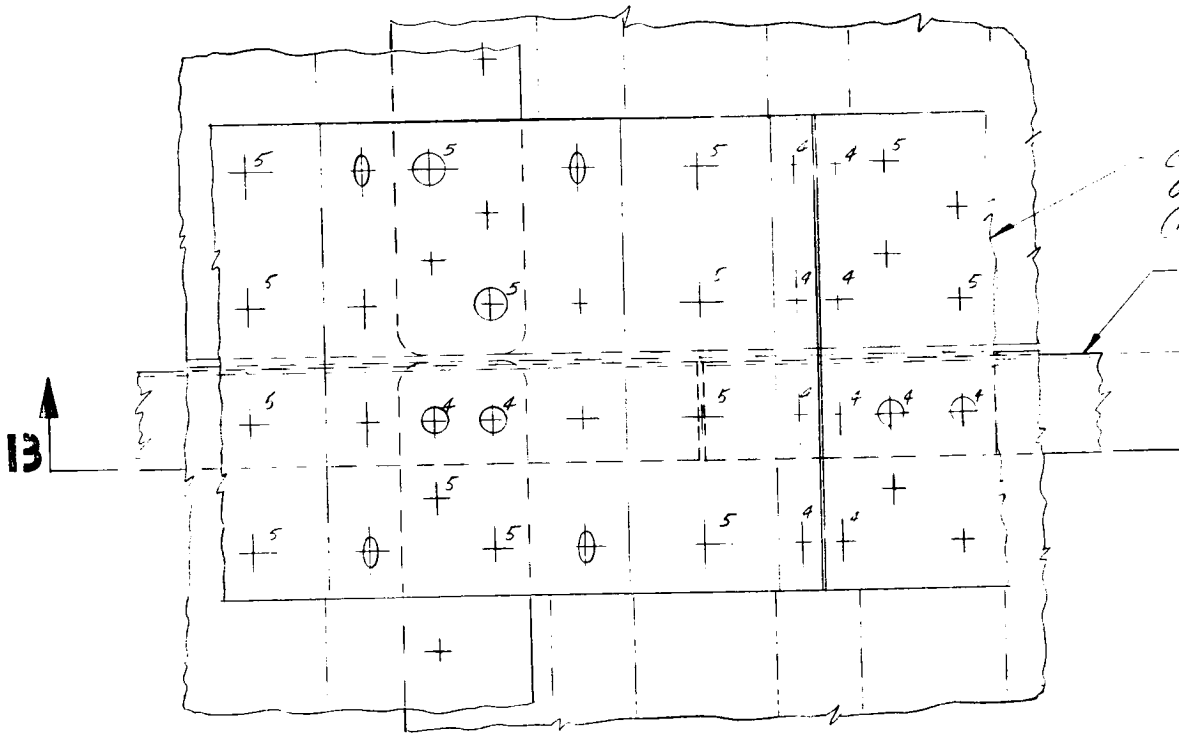


DETAIL A₂ FULL SCALE

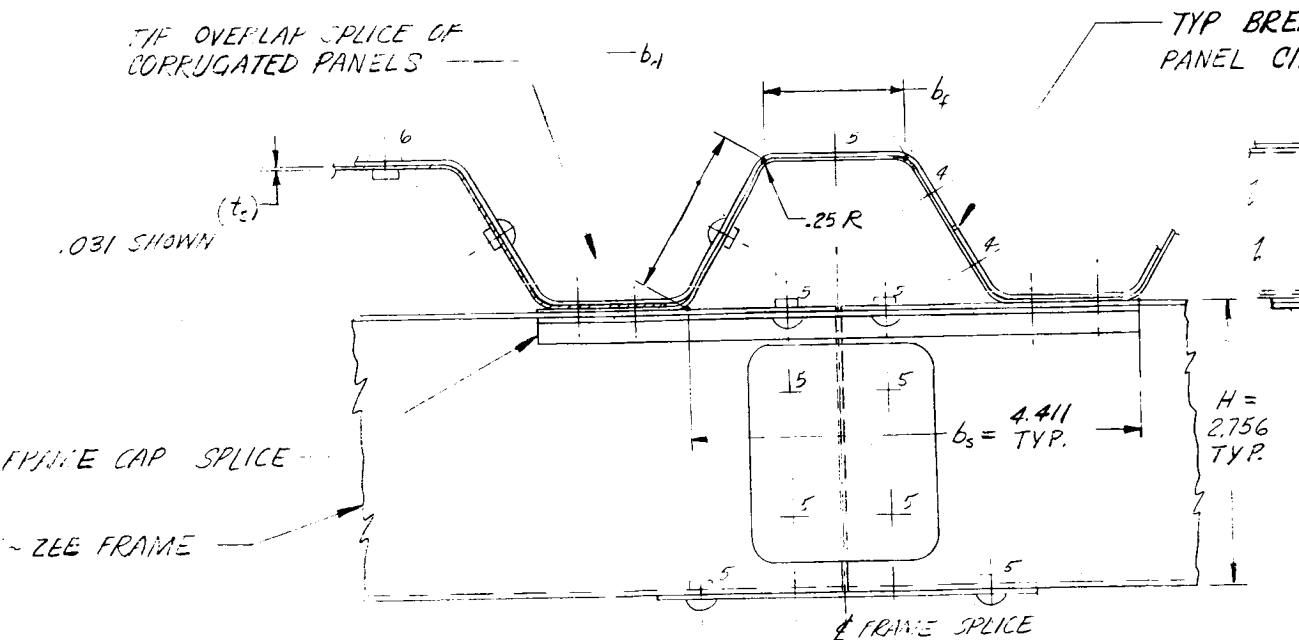
7106 AL ~ N_x = 2000 TO 15,000 LB/IN ~ 2000 LB/IN, 100 R. SHOWN



BE. SH



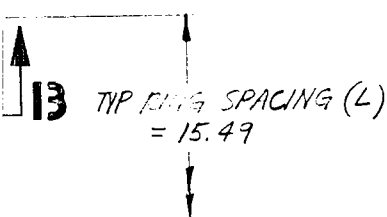
DETAIL **A1** FULL SCALE
 MTL BRILLIUM ~ $N_x = 2000$ TO 15000 LB/IN ~ 2000 LB/IN SHOWN



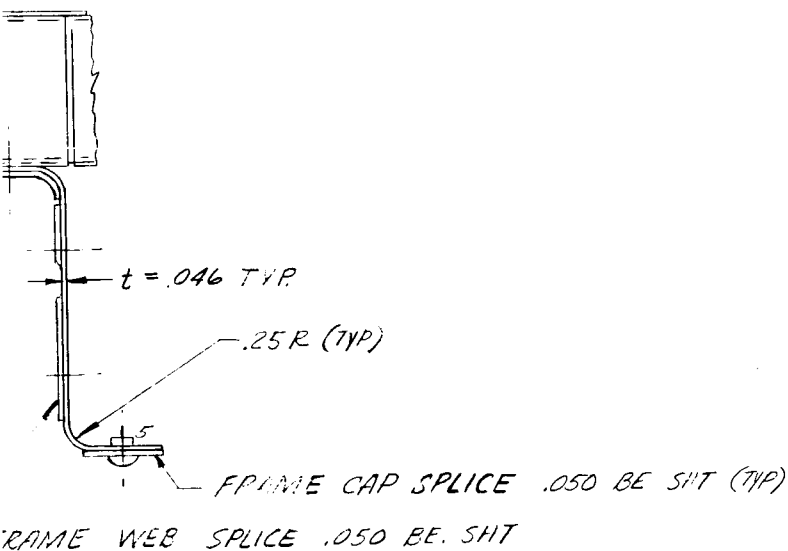
SECTION **13-13** FULL SCALE

107 (4)

VACUUM PANEL SPLICE SHIT (.040 BE. SHIT)
 ORGANIC BOND AND RIVET
 (MONEL) TO CORRUG. COVERS.
 RING FRAME

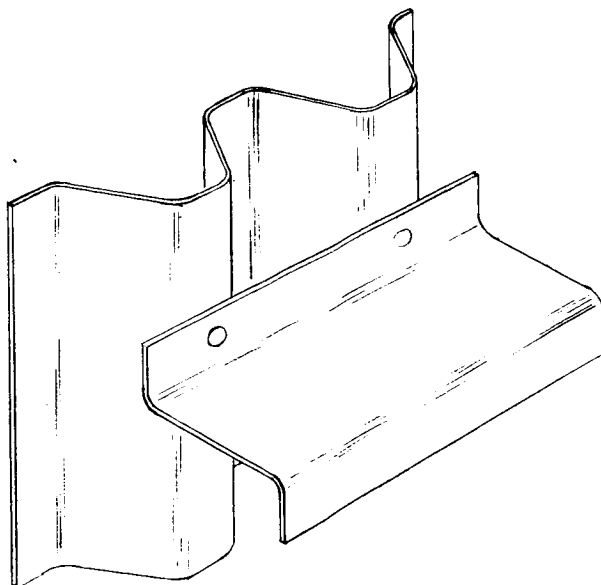


MAK IN
 VACUUM SPLICE SHIT



MAX. CORR.
 26 x

107-5



DESIGN DWG-TRAPEZOIDAL RING STIFFENED CYLINDER

FIG.

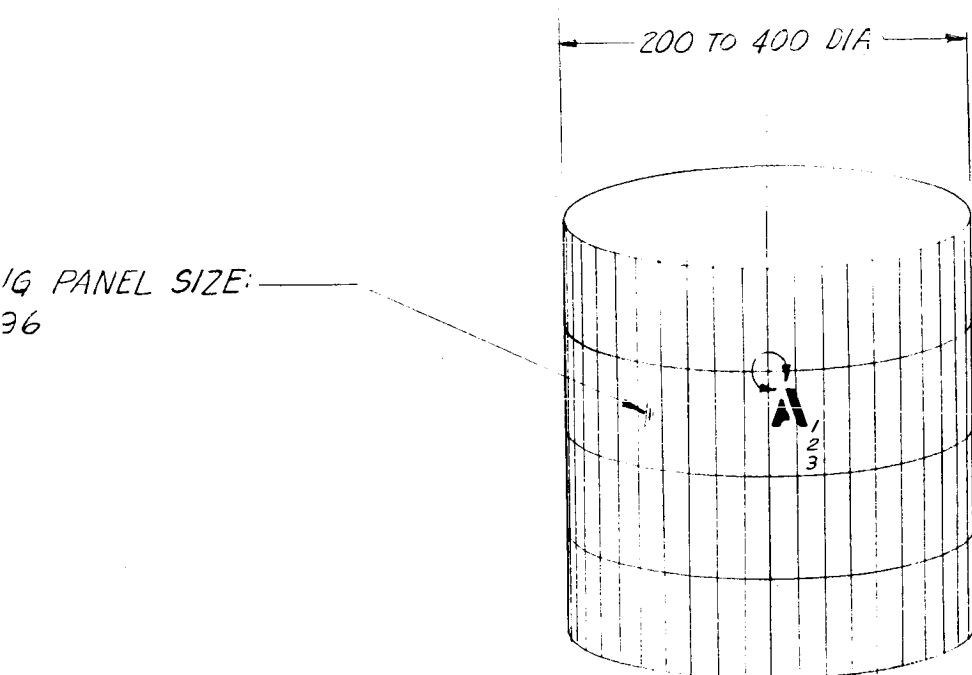


Figure 45. Design Drawing - Trapezoidal Ring Stiffened Cylinder

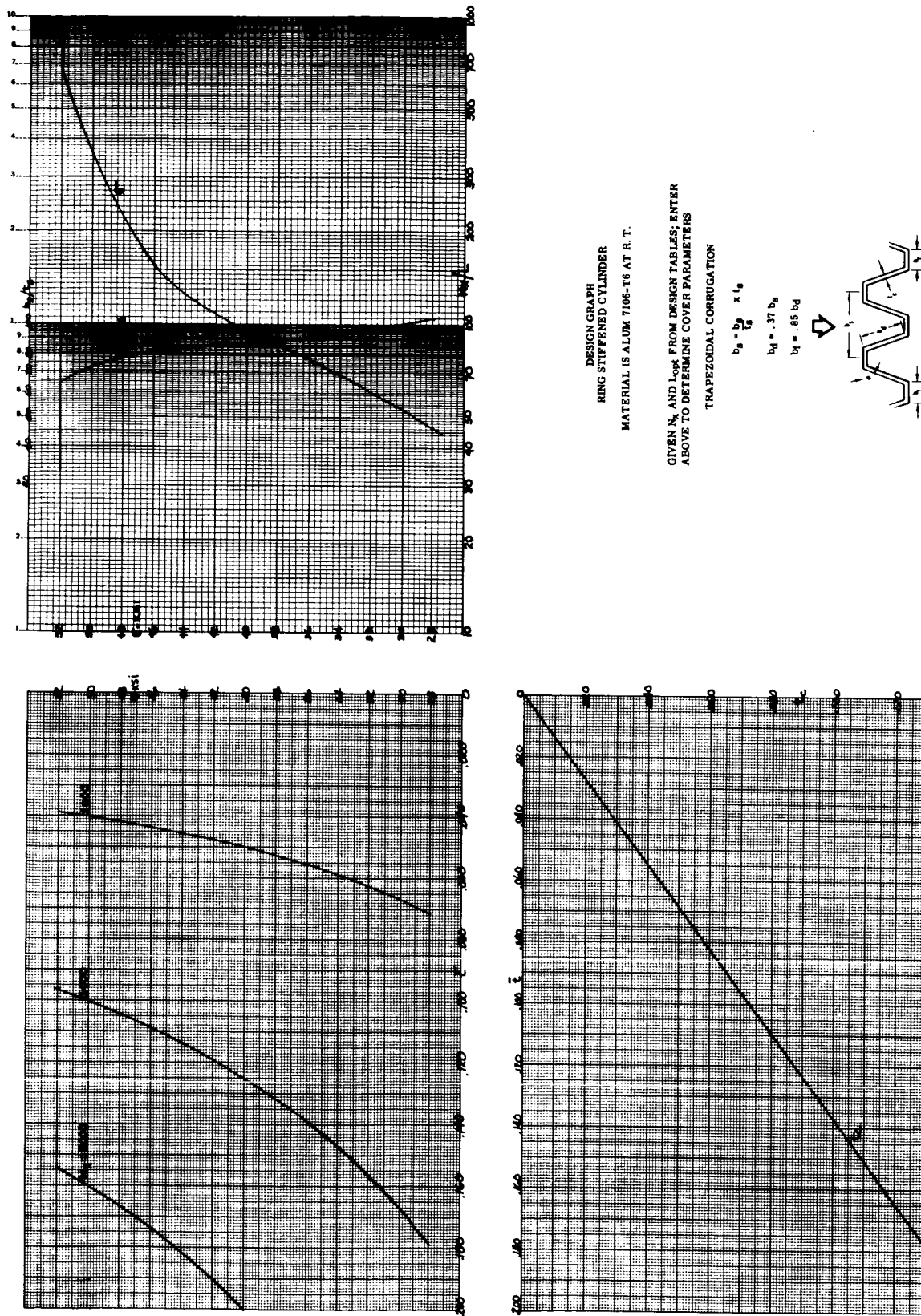


Figure 46. Design Graph - Trapezoidal Ring Stiffened Cylinder

Table XIV (Cont)

TRAPEZOIDAL CORRUGATION
RING STIFFENED
200 INCH DIAM.

[illegible]

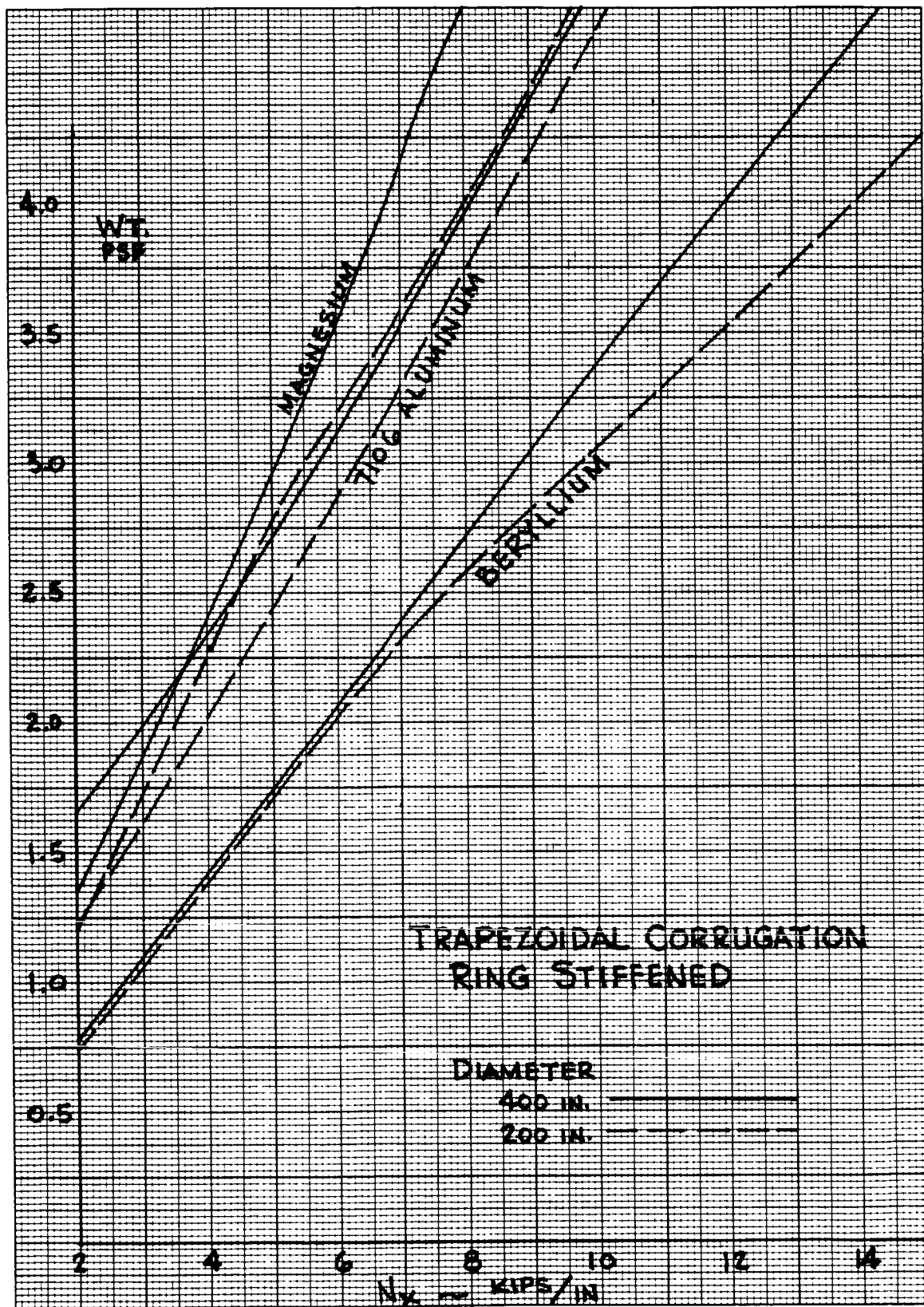


Figure 47. Panel Weight Versus Load-ring Stiffened Trapezoidal Corrugation

STRUCTURAL OPTIMIZATION ANALYSIS

RING-STIFFENED CYLINDER

Five types of ring-stiffened cylindrical shells are evaluated for minimum-weight structural design in the first phase effort. Of the eight contending design configurations in the section "Design Criteria," the honeycomb (diffusion-bonded and bonded) sandwich and the truss-core sandwich do not pertain to the ring-stiffened concept. Skin stringer types of construction analyzed are integrally stiffened stringers, "Zee" stringers, truss-core semisandwich, trapezoidal corrugation, and square grid-stiffened (0 degree to 90 degree) waffle. Circumferential "Zee" rings provide skin stringer stability at an efficient stress level.

The ring-stiffened trapezoidal corrugation is selected for detailed design in the second phase effort.

SHANLEY STABILITY CRITERION

Structural optimization of compression panel cover concepts analyzed in Reference 4 provide structural efficiency coefficients and optimum structural proportions. The stringer spacing to ring-stiffener spacing ratio is assumed to be much less than unity so that the wide-column analogy is applicable. Results of the analysis indicate this ratio to be relatively small; therefore, the assumption is valid. Optimization of the structural arrangement considers that the elastic buckling of the structural elements occurs simultaneously with the wide column buckling stress. The applied stress is equated to the wide column stress and the local plate element buckling stress as follows:

$$\sigma = \sigma_e = \sigma_{cr}$$

where

$$\sigma = \frac{N_x}{t} \quad \sigma_e = \frac{2 E}{(L/\rho)^2}$$

$$\sigma_{cr} = \frac{k_c \pi^2 \eta E}{12 (1 - \mu^2)}$$

For skin stringer design $\eta_c = (\eta_s \times \eta_t)^{1/2}$ Reference 5.

In terms of the structural efficiency coefficient and structural load index:

$$\sigma_e \sigma_{cr} \sigma^2 = \left[\frac{\pi^2 E \rho^2}{L^2} \right] \left[\frac{k_c \pi^2 \eta_c E}{12 (1 - \mu^2)} \right] \left[\frac{t}{b} \right]^2 \left[\frac{N_x}{t} \right]^2$$

resulting in the equivalent stress:

$$\sigma_O = \frac{N_X}{\bar{t}} = \left[\frac{N_X E \eta_c \epsilon}{L} \right]^{1/2}$$

where:

$$\epsilon^{1/2} = \pi \left[\frac{kc}{12 (1 - \mu^2)} \right]^{1/4} \left[\frac{\rho}{b_s} \frac{t_s}{\bar{t}} \right]^{1/2}$$

Solving for the equivalent skin thickness:

$$\bar{t} = \left(\frac{N_X L}{\epsilon E \eta_c} \right)^{1/2}$$

The transverse ring-stiffness requirements of the circumferential ring frames to provide shell stability was determined by the semi-empirical equation from Reference 6.

$$EI = \frac{C_f MD^2}{L}$$

where:

$$C_f = \frac{1}{16000}$$

Converting the equivalent bending moment, M, in terms of the axial load intensity, N_X , by conservatively assuming a linear bending stress distribution:

$$EI = \frac{N_X \pi R^2 (2R)^2}{16000L} = \frac{\pi N_X R^4}{4000L}$$

A ring shape factor of 5.4 as defined in the following relationship is used in the preliminary analysis

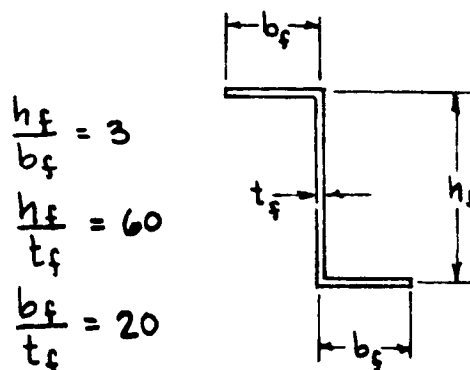
$$k_4 = \frac{I}{A^2}$$

This shape factor results in ring proportions as shown on the following page.

The equivalent frame thickness distributed over the frame spacing becomes:

$$t_{fr} = \frac{\pi R^4}{4000 k_4 L^3} \left[\frac{N_X}{E} \right]^{1/2}$$

FRAME PROPORTIONS



The total equivalent shell thickness is the sum of the skin and frame equivalent thickness:

$$\bar{t} = t + t_{fr}$$

$$t = \left[\frac{N_x L}{\epsilon E \eta_c} \right]^{1/2} + \frac{\pi R^4}{4000 k_4 L^3} \left[\frac{N_x}{E} \right]^{1/2}$$

The optimum frame spacing occurs when the total equivalent shell thickness is minimized. By performing the operation, $\partial t / \partial L = 0$, the optimum frame spacing is determined.

Arie van der Neut Stability Criterion

Orthotropic shells with buckling modes where the longitudinal half wave length is of the same order of the ring spacing; and continuous shells with discrete ring stiffeners were investigated by Arie van der Neut, References 7 and 8. Results obtained from the solution of orthotropic shell theory for the axially symmetric buckling case, indicated only a small error, (< one percent), involved by assuming more than two rings per half wave length; and therefore two rings on the half wave length was equivalent to many rings. Further analysis indicated that by increasing the ring stiffness the longitudinal half wave length decreases gradually until the number of half wave lengths equals one. The general instability has degenerated into column failure of the stringers between the rings and the equivalent ring stiffness becomes infinite. The ring stiffness required to preclude the axis symmetric buckling mode is expressed by the ring sectional area is given as:

$$A_R = 4 \pi^2 \left(\frac{R}{L} \right)^2 \left(\frac{L}{b_s} \right) \left(\frac{I_s}{L^2} \right)$$

Ring-stiffened requirements obtained by Arie van der Neut's equation as compared with Shanley's criterion indicate that an increase in total shell weight, (includes skin and stringer), would be acquired by using Arie van der Neut's criterion. This comparison was made with the trapezoidal corrugation so that the skin and ring-stiffener requirements may be completely separated since no effective skin could be used for frame area requirements. Further theoretical development of predicting ring-stiffened cylinders is needed in order to establish a firm basis for optimization studies.

SUMMARY OF RESULTS

The first phase analysis by the Shanley instability criterion shows that the trapezoidal corrugation construction provides the highest structural efficiency. The relative efficiency of competing concepts is shown by the coefficients, $\epsilon^{1/2}$, in table XV. Figures 48 and 49 show weight versus load diagrams for the five ring stiffened concepts. Figures 50 and 51 show unit weight requirements versus axial load intensity for 200-inch and 400-inch diameters, respectively. The optimum materials selected in the first phase investigation on a minimum weight basis are shown in figure 52. Two comparisons are presented indicating state-of-the-art materials and advanced materials.

Second phase results, including penalty weights, are included in figures 21 through 25 and in figure 47.

Table XV
RING STIFFENER CYLINDER COEFFICIENTS

TYPE OF CONSTRUCTION	INTEGRALLY STIFFENED	ZEE STRINGER	TRUSS CORE SEMISANDWICH	WAFFLE (0°-90°) SQUARE GRID	TRAPEZOIDAL CORRUGATION
$\epsilon^{1/2}$.810	.955	.829	.642	1.264
L	.171 R $\lambda^{1/4}$.186 R $\lambda^{1/4}$.1730 R $\lambda^{1/4}$.171 R $\lambda^{1/4}$.2137 R $\lambda^{1/4}$
t_s	.407 \bar{t}	.405 \bar{t}	.3215 \bar{t}	.407 \bar{t}	.730 \bar{t}
$t_{stiff.}$.593 \bar{t}	.595 \bar{t}	.6785 \bar{t}	1.186 \bar{t}	.270 \bar{t}
b_W	.650 b_s	.870 b_s	.766 b_s	.650 b_s	.735 b_f

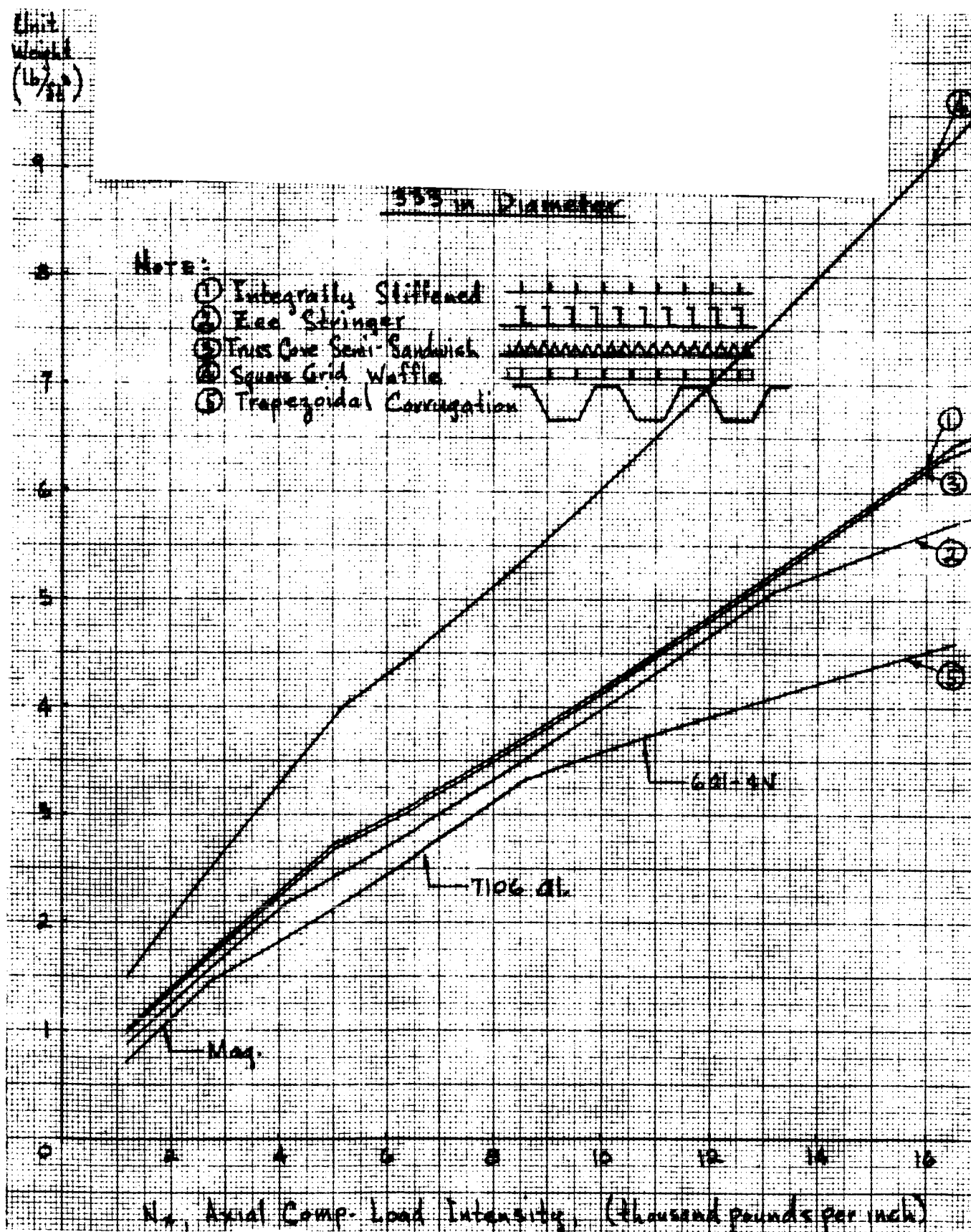


Figure 48. Ring Stiffened Construction Comparison of the Various Types of Construction Using the Selected Optimum Materials State-of-Art Materials

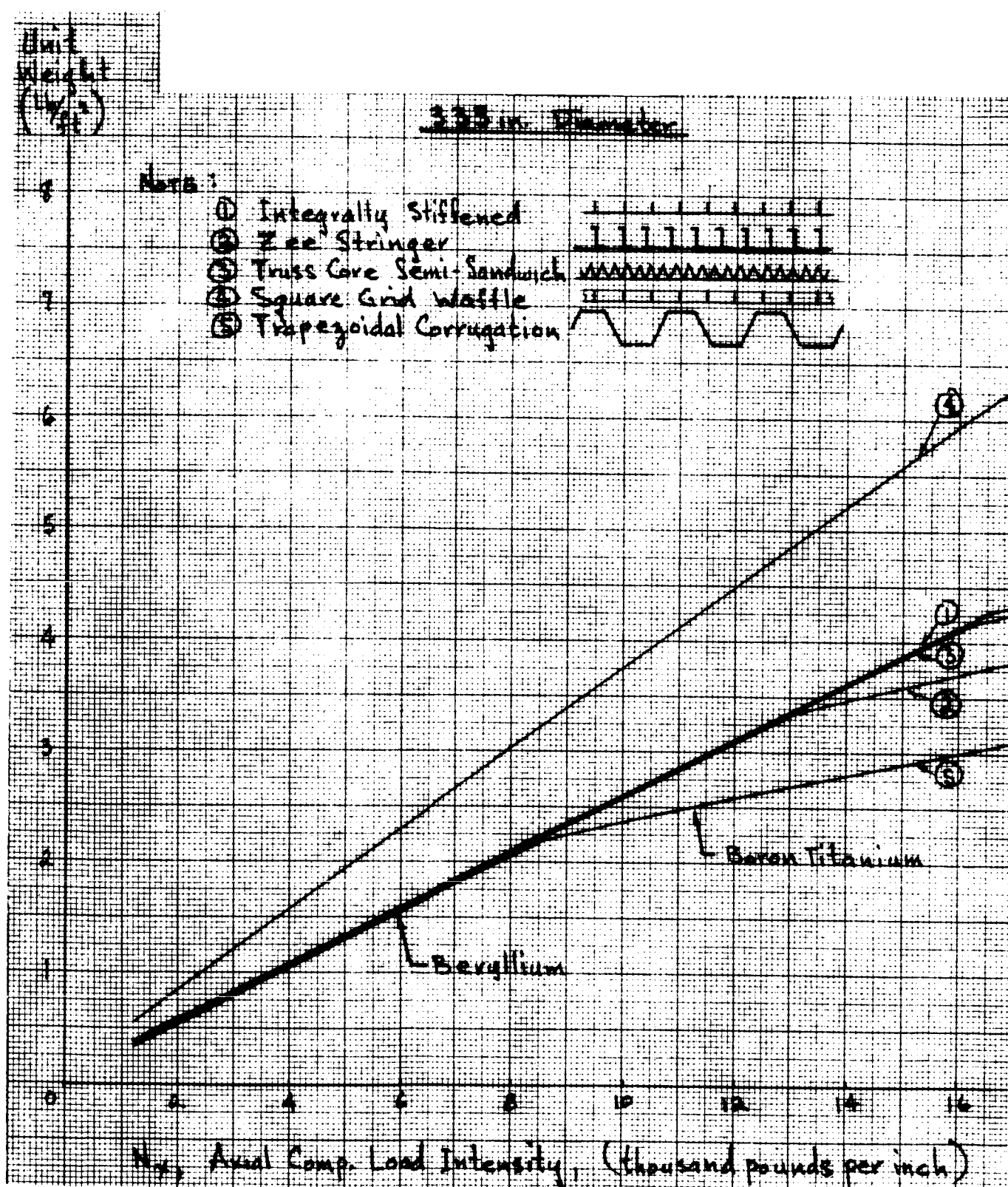


Figure 49. Ring Stiffened Construction Comparison of the Various Types of Construction Using the Selected Optimum Materials Advanced Materials

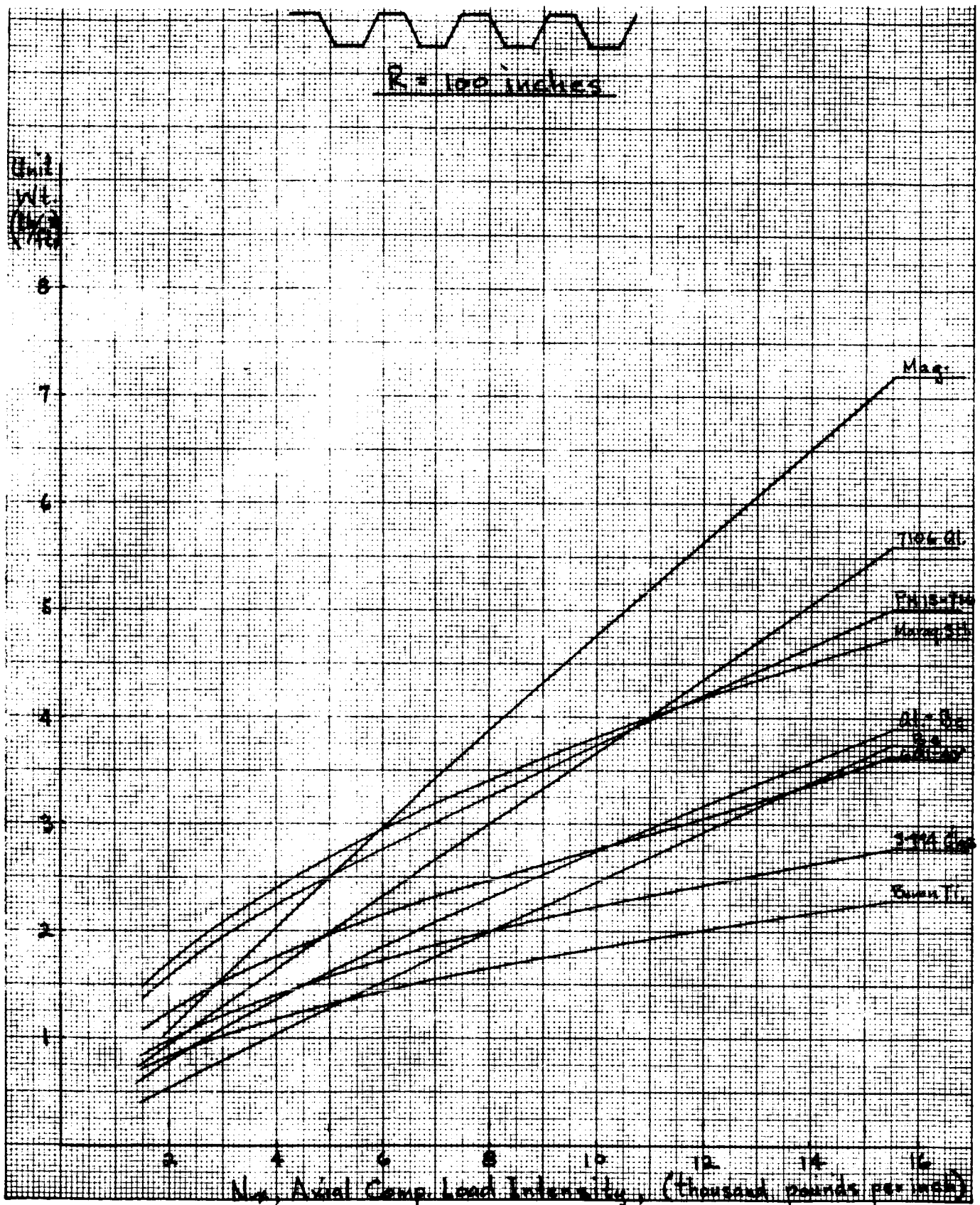


Figure 50. Ring Stiffened Trapezoidal Corrugation
($R=100$ Inches)

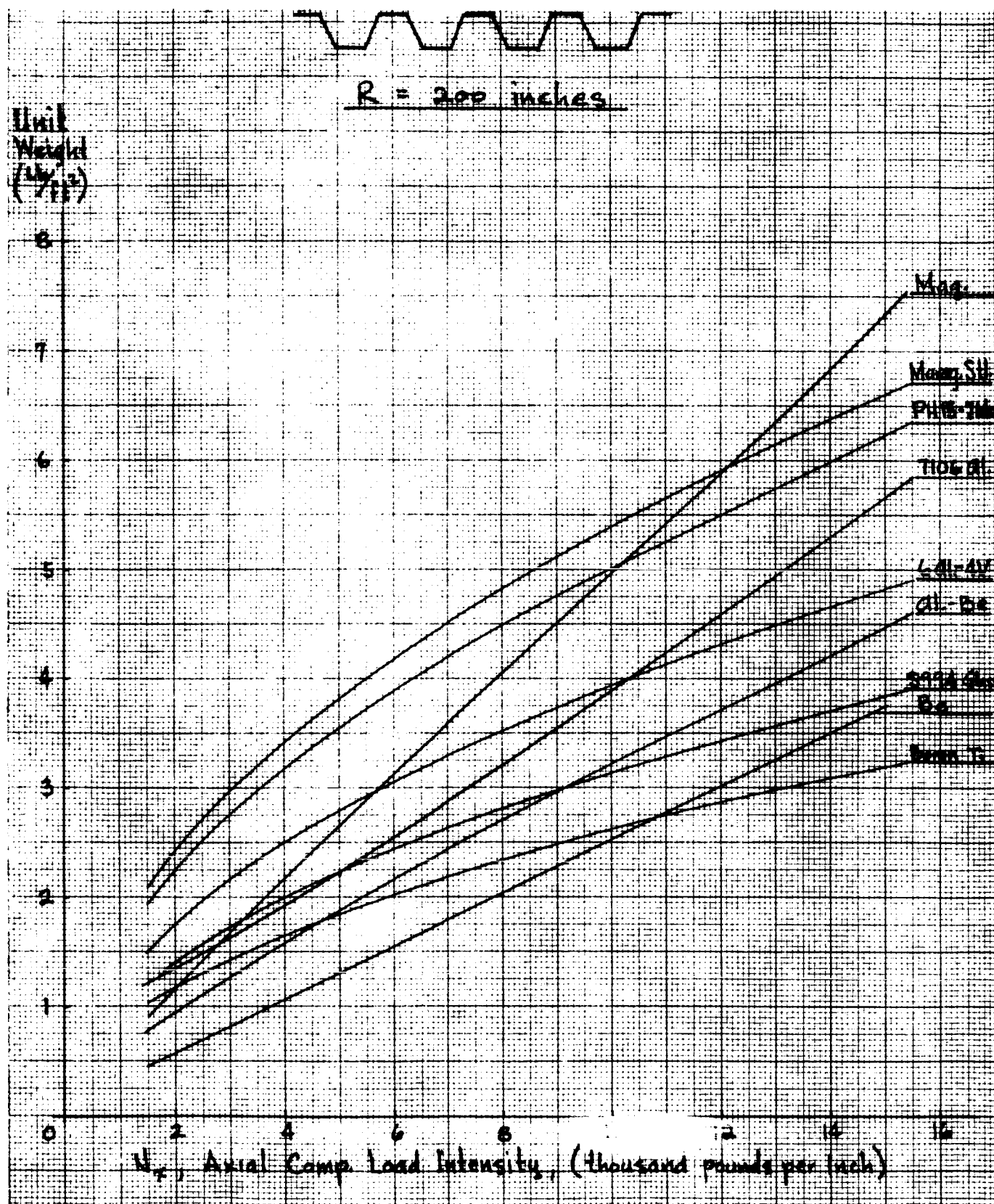


Figure 51. Ring Stiffened Trapezoidal Corrugation
($R=200$ Inches)

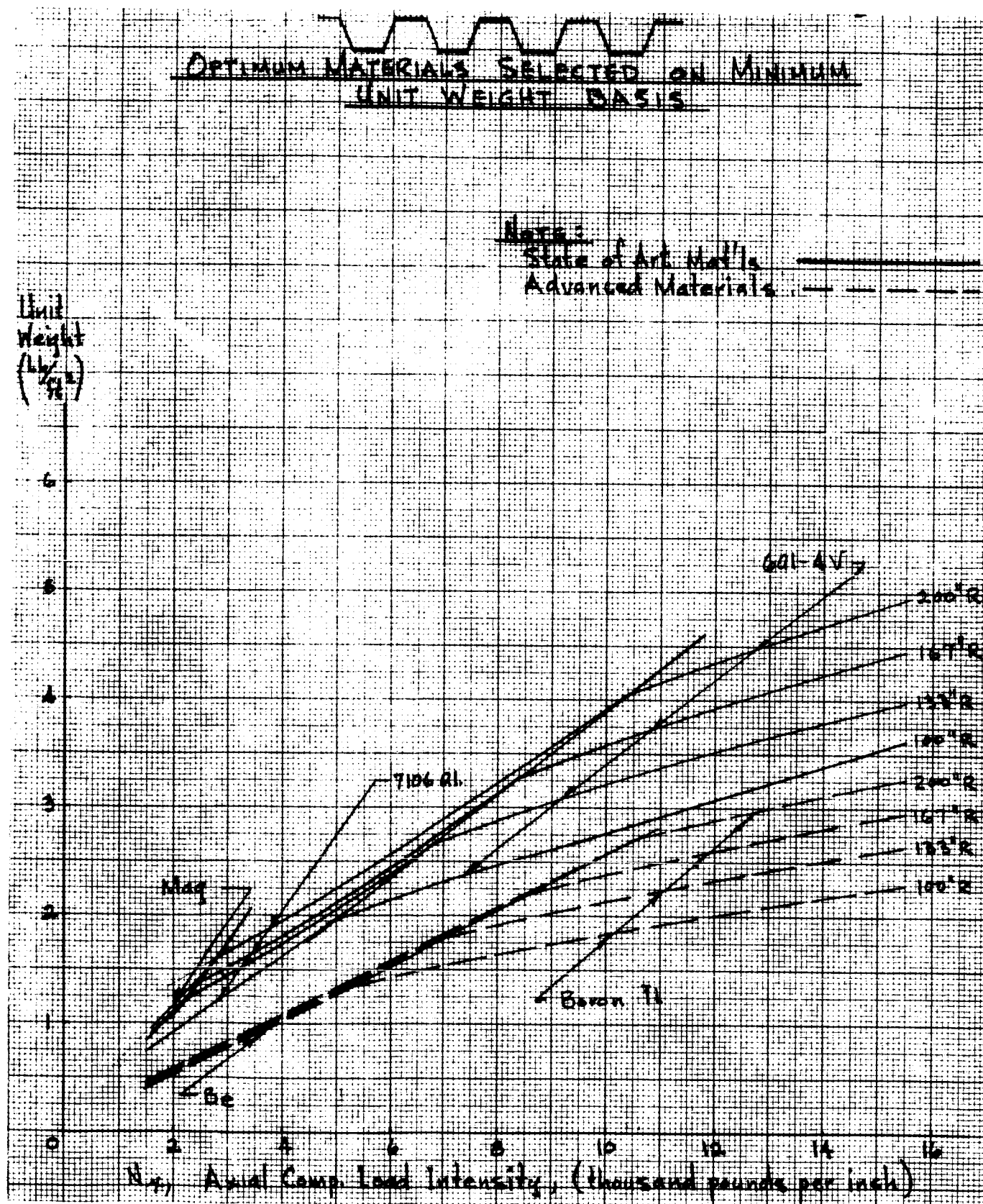


Figure 52. Ring Stiffened Trapezoidal Corrugation

DOUBLE-WALL CYLINDERS

METHOD OF ANALYSIS

Double-wall and honeycomb structural geometry and sizing is established in such a manner that all critical buckling modes occur at the design stress level. This balanced design procedure considers general cylinder stability and local stability. In the case of the double-wall concept, local stability involves cover panel buckling and buckling of the elements which make up the panel. In the case of honeycomb, intracell buckling and wrinkling stresses are evaluated. An explanation of these instability modes and equations used to predict critical stresses is included later in this section.

Equating of buckling modes for optimum design is an analytical technique established in the literature and industry-wide applications (References 4 and 6). A closed-form solution to double-wall optimization is not available. The method of analysis is, therefore, a synthesis technique.

The cover panel and the substructure properties are determined separately for varying geometry increments. The composite behavior of these elements, in general stability, is then determined to yield structural integrity with minimum weight. The evaluation of panel weight for one inch increments of panel depth and one inch increments of support spacing results in practical dimensions for the candidate concepts. The range of one to 6 inches for both of these important parameters, further, directs effort to feasible designs.

Details of the instability prediction analysis follow.

GENERAL CYLINDER STABILITY

Stability of the cylindrical shell wall requires sufficient bending and shear stiffness to prevent the formation of the buckles characteristic of this failure mode. Small deflection theory is the basic applied method of evaluating required stiffness for the double-wall concept with orthotropic core (Reference 9).

The critical buckling stress is predicted by the equation

$$f_{cr} = K E \frac{h}{r} \frac{2 \sqrt{t_1 t_2}}{\sqrt{1 - \mu^2} (t_1 + t_2)}$$

The value of the buckling coefficient, K, is found by minimizing the equation:

$$K = \frac{\eta}{(1 + \xi)^2} + \frac{(1 + \xi)^2}{4\eta} \bullet$$

$$\frac{1 + \frac{1 - \mu}{2} (\xi + \theta) \frac{V_x}{\eta}}{1 + \frac{1 - \mu}{2} (\xi + \theta) \frac{V_x}{\eta} + (1 + \xi \theta) \frac{V_x}{\eta} + \frac{1 - \mu}{2} (1 + \xi)^2 \theta \frac{V_x^2}{\eta^2}}$$

where:

$$V_x = \frac{Et_c \sqrt{t_1 t_2}}{2 \sqrt{1 - \mu^2} h r G_{xz}}$$

This minimization process is accomplished using the IBM 7094 computer. The automatic plotting capability of the cathode ray tube (CRT) is used in conjunction with the basic programs. The results of this minimization processes, showing K plotted versus V_x for various values of θ is presented in figure 53.

An example of the output necessary to calculate one value of K for a given V_x and θ is shown in figure 54.

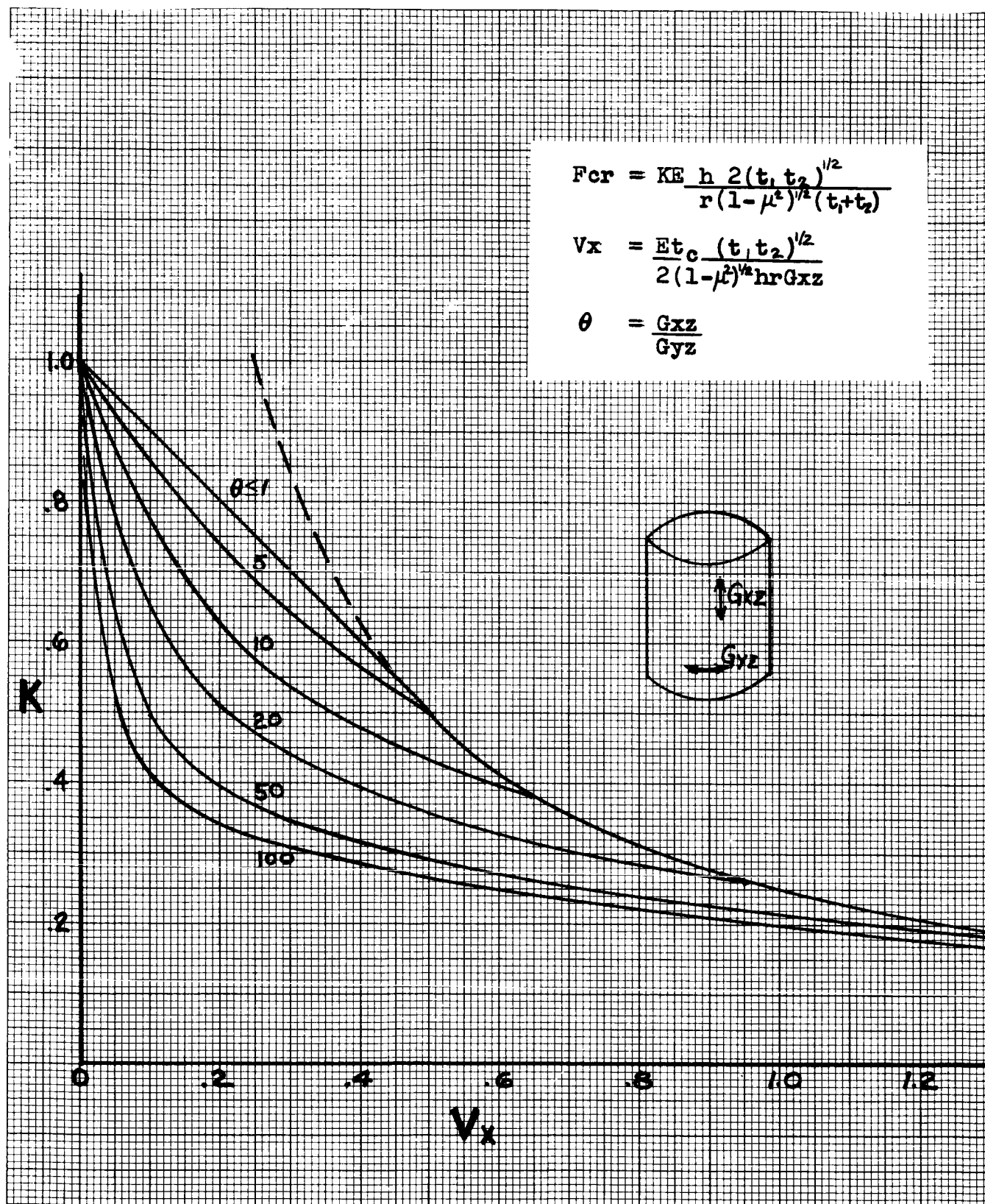


Figure 53. Buckling Coefficient for Sandwich Cylinders
With Isotropic Facings and Orthotropic Core

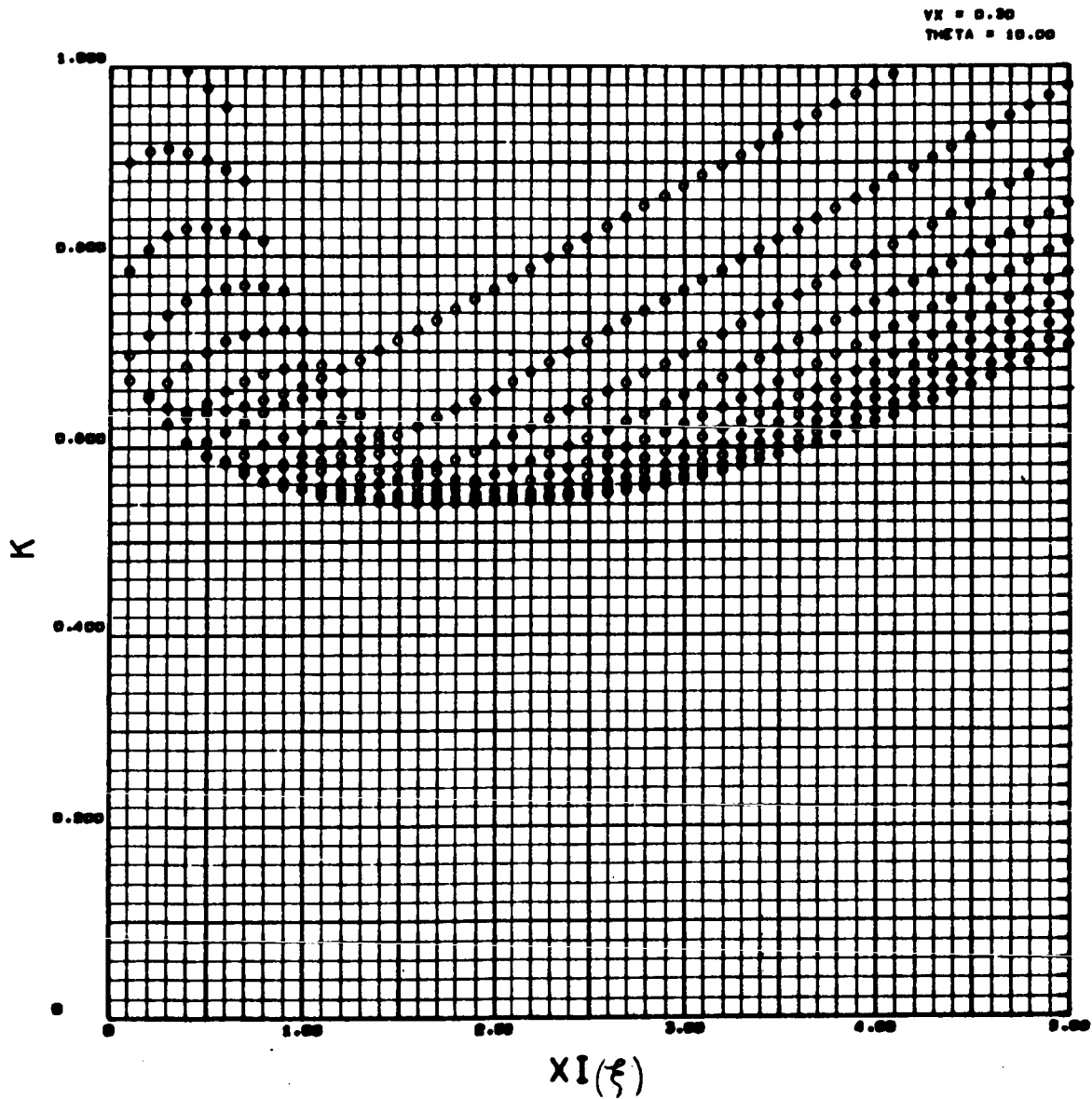


Figure 54. Minimization of Buckling Coefficient

PANEL STABILITY

Wide Columns

Efficient structural applications, under the predominantly unidirectional loading conditions, are predicted by employing wide-column theory. The optimum arrangement of structural material resulting from this design approach employs many circumferential substructure members in relation to the longitudinal stiffeners. This subdivides the cover into the panels whose width is large in comparison to length. An infinite panel width is assumed in the derivation.

The equations employed in the optimization of wide-column structural concepts are standard expressions for local stability and general stability, and the optimization expression.

Local stability (wide column)

$$\sigma_{cr} = K \frac{\pi^2 E \eta}{12 \sqrt{1 - \mu^2}} \left[\frac{t}{b} \right]^2$$

Column stability (wide column)

$$\sigma_{cr} = \frac{\pi E_t \rho^2}{L^2}$$

Optimization equation (wide column)

$$\frac{N_x}{L \bar{\eta} E} = \text{efficiency ratio} \times \left[\frac{\bar{t}}{L} \right]^2$$

The parameters in the optimization equation are derived by combining the general and local stability expressions for a particular structural concept. The efficiency factor is comprised of the geometrical relationships remaining when the loading material index $N_x/L \bar{\eta} E$ and weight index \bar{t}/L are separated from the combination of the basic stability equations. Relative efficiencies indicate most promising concepts.

Plates

The design of cover panels as plates results in high structural efficiency. The optimum arrangement of structural material resulting from this design

approach employs many longitudinal substructure members in relation to the circumferential members. This subdivides the cover into panels whose length is large in comparison to the width. An infinite panel length is assumed in the derivation.

Efficient proportioning of structural material between the skin and stringers of the cover panels is essential to the development of optimum structural configurations. The optimization is accomplished by designing the cross section to be critical in local and general stability simultaneously. The basic expressions employed are:

Local stability (plate)

$$\sigma_{cr} = K \frac{\pi^2 E}{12 (1 - \mu^2)} \left[\frac{t}{b} \right]^2$$

General stability (orthotropic plate)

$$\sigma_{cr} = K \frac{\pi^2 E}{b^2 \bar{t}} (I_x I_y)^{1/2}$$

Optimization equation (plate)

$$\frac{N_x}{b \bar{\eta} E} = \text{efficiency ratio} \times \left[\frac{t}{b} \right]^2$$

For various cross sections, the relative efficiency factors indicate concepts favorable for employment as plate structures.

VERIFICATION OF THE ATTAINMENT OF SIMPLE PANEL SUPPORT

In the preceding development of a simple support edge condition is the basis for determining double-wall cover panel sizing requirements. The substructure must provide sufficient out-of-plane stiffness to restrain the cover panel to buckle in a pattern that has zero displacement along the primary support line.

The truss-core sandwich double-wall concept was analyzed to verify the simply supported plate condition. This concept is selected since:

1. This concept is most efficient (lightest in weight)
2. The design stress level is highest for this concept
3. This concept is most competitive in the higher load range

Spot checks are made on the trapezoidal corrugation configuration.

Two methods of analysis are used. The plate configurations, typified by the double-wall truss-core sandwich design are checked by Reference 10, as shown in figure 55. The wide column configurations, typified by the double-wall trapezoidal corrugation, are checked by Reference 11, as shown in figure 56.

The truss-core sandwich buckling coefficient is minimized in a square buckle pattern. In order to achieve the design buckling coefficient required for the double-wall concept, the buckle length to be restrained is equal to the width of the truss-core sandwich panels.

The panels, which make up the shell walls, must be restrained from symmetrical and asymmetrical buckling (see figure 57). Either mode may be critical under given design conditions.

For symmetrical buckling consideration of one-half of the substructure is sufficient; stiffness is determined at the peak of the sinusoidal loading. Considering the substructure as a line support to out-of-plane unit loading results in a stiffness as follows:

$$K = \frac{AE}{PL} = \frac{1.22 t_c E}{1 (h/2)} = 2.44 \frac{t_c E}{h}$$

The antisymmetrical case must consider local cylinder wall bending and shear deformations, as well. The deflections resulting from this type of unit loading:

$$\delta = \frac{PL}{AE} + \int_0^{l/2} \frac{V}{AG} dx + \int_0^{l/2} \frac{Mm}{EI} dx$$

$$\delta = 0.205 \frac{h}{t_w E} + \frac{0.618 b^2}{h t_c E} + .01268 \frac{b^4}{EI} \quad (\text{lbs/in.})$$

The required stiffness is the inverse of this quantity.

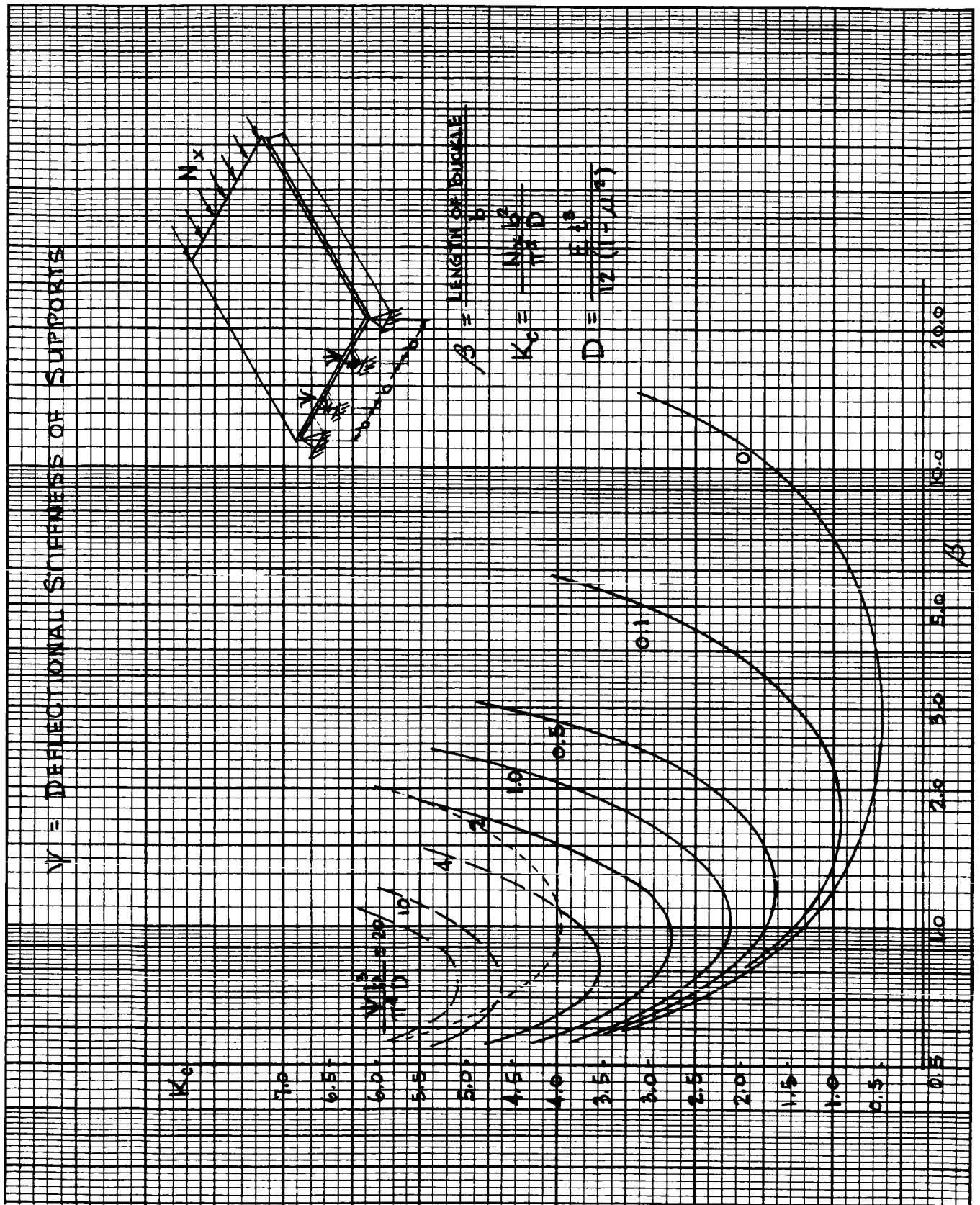


Figure 55. Stability of Three-bay Plate

BUCKLING CURVES - SPRING SUPPORTED COLUMNS

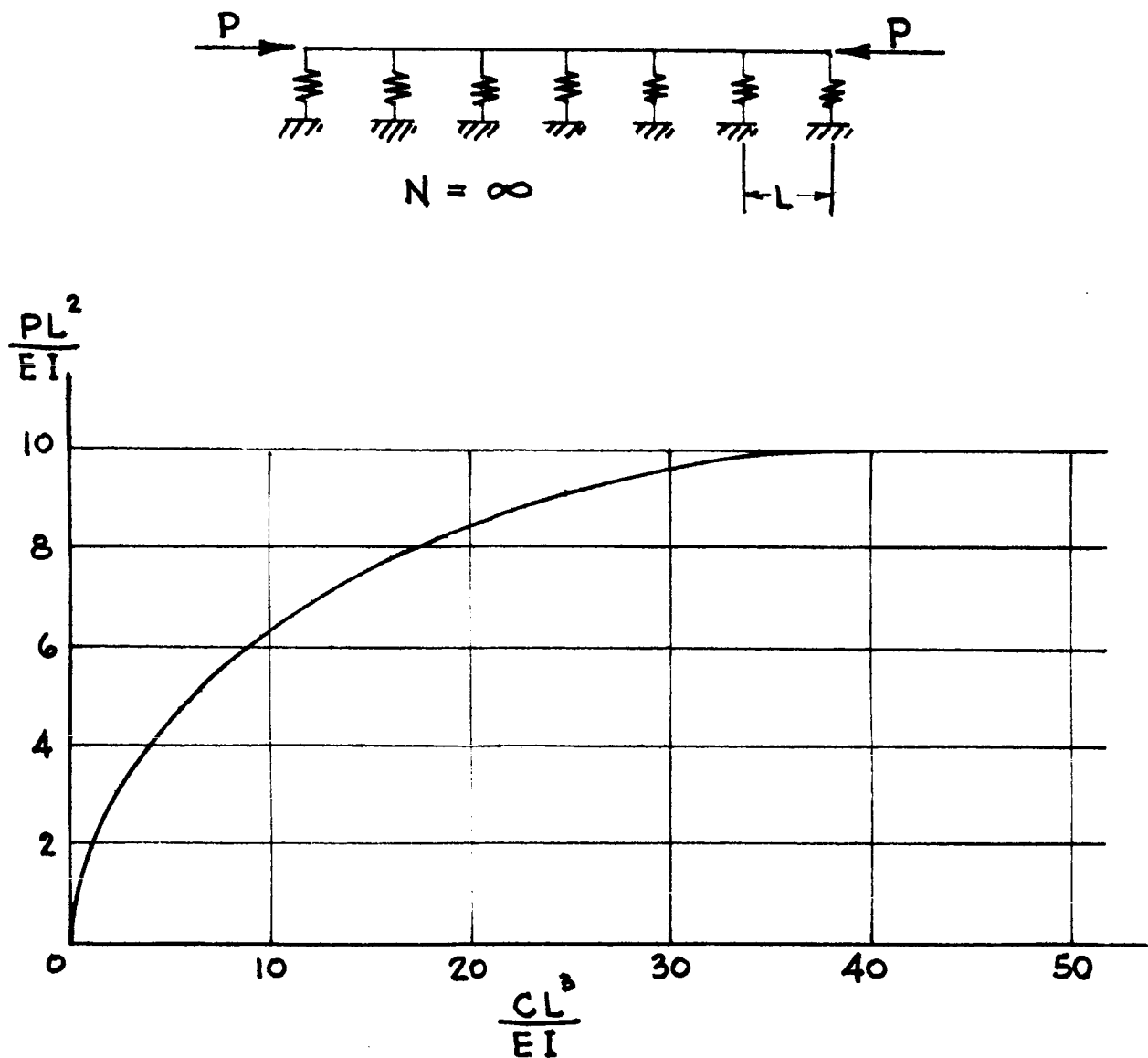
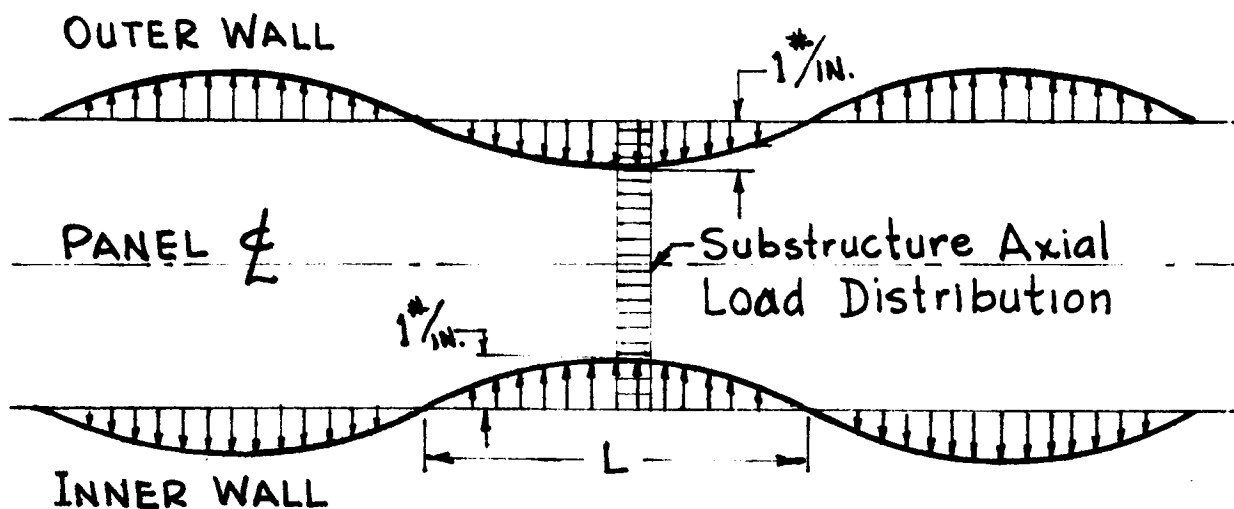
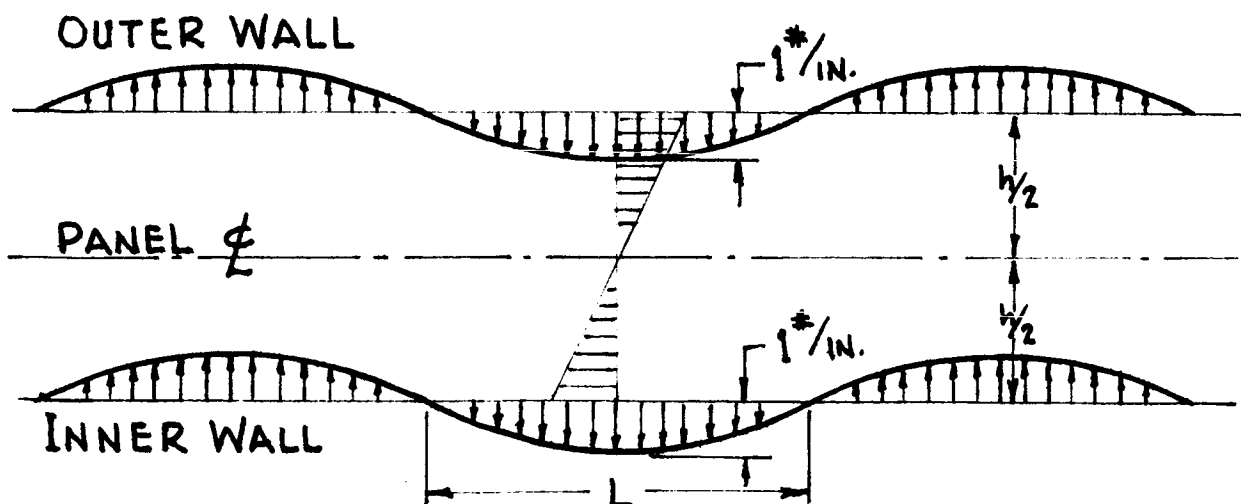


Figure 56. Buckling Curves - Spring-Supported Columns



(a) SYMMETRICAL BUCKLING



(b) ANTISYMMETRICAL BUCKLING

Figure 57. Illustration of Symmetrical and Antisymmetrical Buckling Modes

Non-Optimum Structure

In addition to the basic cover panels and substructure, non-optimum structure includes all structural weight elements necessary to construct the cylinder such that the shell will perform in accordance with the theoretical predictions. Joint splices, reinforcement pads or lands, and attachments such as rivets, bond material, and etc, are investigated to determine the weight penalty involved with each material/concept, diameter and load level. Analysis coupled with engineering design judgement, as reflected in the design drawings, is used to obtain non-optimum structural sizing. In cases of necessity, for complex detailed analyses, a conservative weight estimate is included. Test verification of such decisions is recommended.

The non-optimum weight penalty associated with each design point includes the panel splice and attachment weight, shear web cap, attachment pad and substructure attachment weight.

$$W_{pen} = W_{spl} + W_{att} + W_{cap} + W_{pad} + W_{attp} + W_{bond}$$

The splice weight includes the weight of both longitudinal and circumferential splices expressed in terms of pounds per square foot.

$$W_{spl} = \frac{(W_{LJ} + W_{CJ})}{L_p \times C} 144$$

For the double wall concepts the above expression is multiplied by a factor of 2. The weight of the longitudinal and circumferential splices is computed as follows:

$$W_{LJ} = 2L_p \times t_{spl} (W_{LJ} + A)$$

$$W_{CJ} = 2C \times t_{spl} (W_{CJ} + B)$$

Twice the diameter is used for edge distances of all attachments. The spacing between rows of attachments is designed as four times the diameter.

Balanced Design Procedure

The design approach equates general, panel, and local modes of instability to achieve optimum design. The cover panel and the substructure properties are determined separately for varying geometry increments. Cover panel and substructure properties for the design criteria investigated are tabulated in Reference 12. The results are too voluminous to present in this final report. Therefore, a typical design analysis for minimum weight is presented to illustrate the method of analysis employed and typical data generated in the performance of the investigation. In the following design example given criteria are as follows:

Material - Titanium (6Al-4V) room temperature
 Cover panel concept - Integrally stiffened, wide-column
 Substructure concept = Truss web
 Shell diameter - 400 inches
 Axial load level - 8000 lb in. (single cover load is 4000 lb/in.)

The cover panel analysis is explained first. For a substructure support spacing, L , of one to 6 inches, the cover panel concept is sized for simultaneous local buckling and column failure according to the efficiency criterion,

$$\frac{N_x}{L \bar{\eta} E} = 0.656 \left[\frac{\bar{t}}{L} \right]$$

where, $\bar{\eta} = \eta_T^{3/4}$ is the plasticity correction factor. The efficiency criterion can also be expressed in terms of stress,

$$\frac{\sigma}{\eta_T^{3/8}} = \left[0.656 E \frac{N_x}{L} \right]^{1/2}$$

Stress is related to stringer spacing, b_s , and skin thickness by the familiar expression,

$$\sigma = \frac{K \pi^2 E \eta}{12 (1 - \mu^2)} \left(\frac{t_s}{b_s} \right)^2$$

where K is a local buckling coefficient. The effective thickness, \bar{t} , of each cover panel is determined by the expression,

$$t = \frac{N_x}{2 \sigma}$$

The individual widths and thicknesses of the elements of the cross section are determined from the effective thickness and substructure spacing values.

To facilitate the determination of these parameters and dimensions, a series of design graphs have been prepared. For this particular example, the design graph of figure 40 is employed. Given the load level of 8000 lb/in., the following data are obtained from figure 40.

Table XVI

INTERGRALLY STIFFENED PANEL GEOMETRY VS COLUMN LENGTH
FOR $N_X = 8000$ LB/IN.

L	N_X/L	σ	b_s/t_s	\bar{t}	t_s	t_w	b_s	b_w
1	8,000	138,200	19.8	.0289	.012	.027	.238	.155
2	4,000	131,500	24.5	.0304	.012	.027	.294	.191
3	2,667	119,300	26.9	.0335	.014	.032	.377	.245
4	2,000	103,500	29.0	.0387	.016	.036	.464	.302
5	1,600	92,800	30.4	.0431	.018	.041	.547	.356
6	1,333	84,800	31.7	.0472	.019	.043	.603	.294

The weight of the two cover panels required for the double-wall cylinder is given as,

$$WGT = 2(144) \rho \bar{t}$$

and for the above designs results in the following weights

Table XVII

COLUMN LENGTH VS PANEL WEIGHT

L(IN.)	1	2	3	4	5	6
WT(PSF)	1.333	1.397	1.544	1.782	1.993	2.183

Substructure design analysis is presented next. For the truss web providing wide column support for the cover panels, the substructure shear moduli longitudinally and circumferentially are respectively:

$$G_{xz} = \frac{8 t_w E H}{(4H^2 + L^2)^{3/2}}$$

$$G_{yz} = \frac{t_w G (4H^2 + L^2)^{1/2}}{HL}$$

$$\Theta = G_{xz} / G_{yz}$$

$$\bar{t}_s = t_w (4H^2 + L^2)^{1/2} / L$$

Assuming a minimum substructure thickness of .010 inches for the titanium 6-4 material, and varying H from one to 6 inches for each L spacing, (also one to 6 inches), the shear moduli, theta, effective thickness, and weight are calculated. A summary sheet showing the computer output data from the substructure analysis program employed to accomplish this task is presented in table XVIII.

The shell stability equation used to determine the critical shell buckling stress is given as

$$\sigma_{CR} = K E \frac{H}{R} \bar{\eta} \frac{2 \sqrt{t_1 + t_2}}{\sqrt{1 - \mu^2} (t_1 + t_2)} = \frac{2KE\bar{\eta}H}{D(1 - \mu^2)^{1/2}}$$

Where K is a buckling coefficient dependent upon θ and the quantity V_x .

The relationship

$$V_x = \frac{E\eta t_c \sqrt{t_1 t_2}}{2\sqrt{1 - \mu^2} H R G_{xz}} = \frac{E\eta t}{D\sqrt{1 - \mu^2} G_{xz}}$$

$$\bar{\eta} = \frac{2E_T}{E + E_T} = \frac{2\eta_T}{1 + \eta_T}$$

Table XVIII

COMPUTER OUTPUT DATA - SUBSTRUCTURE WEIGHT
TRUSS WEB - WIDE COLUMNMATERIAL 6-4 Ti
GAUGE = .010 IN.

L-SPACING	H	G-XZ	G-YZ	THETA	T	WT
1.0	1.0	116633.	137965.	0.85	0.0224	0.515
	2.0	37208.	127198.	0.29	0.0412	0.950
	3.0	17382.	125102.	0.14	0.0608	1.401
	4.0	9953.	124360.	0.08	0.0806	1.858
	5.0	6423.	124015.	0.05	0.1005	2.315
	6.0	4481.	123828.	0.04	0.1204	2.774
2.0	1.0	57629.	87257.	0.66	0.0141	0.326
	2.0	29158.	68983.	0.42	0.0224	0.515
	3.0	15464.	65038.	0.24	0.0316	0.729
	4.0	9302.	63599.	0.15	0.0412	0.950
	5.0	6147.	62922.	0.10	0.0510	1.175
	6.0	4345.	62551.	0.07	0.0608	1.401
3.0	1.0	27820.	74154.	0.38	0.0120	0.277
	2.0	20864.	51417.	0.41	0.0167	0.384
	3.0	12959.	45988.	0.28	0.0224	0.515
	4.0	8363.	43930.	0.19	0.0285	0.656
	5.0	5729.	42944.	0.13	0.0348	0.802
	6.0	4134.	42399.	0.10	0.0412	0.950
4.0	1.0	14579.	68983.	0.21	0.0112	0.258
	2.0	14407.	43628.	0.33	0.0141	0.326
	3.0	10433.	37077.	0.28	0.0180	0.415
	4.0	7290.	34491.	0.21	0.0224	0.515
	5.0	5219.	33226.	0.16	0.0269	0.620
	6.0	3866.	32519.	0.12	0.0316	0.729
5.0	1.0	8350.	66453.	0.13	0.0108	0.248
	2.0	9934.	39507.	0.25	0.0128	0.295
	3.0	8211.	32126.	0.26	0.0156	0.360
	4.0	6212.	29104.	0.21	0.0189	0.435
	5.0	4665.	27593.	0.17	0.0224	0.515
	6.0	3561.	26737.	0.13	0.0260	0.599
6.0	1.0	5155.	65038.	0.08	0.0105	0.243
	2.0	6955.	37077.	0.19	0.0120	0.277
	3.0	6403.	29086.	0.22	0.0141	0.326
	4.0	5216.	25708.	0.20	0.0167	0.384
	5.0	4111.	23985.	0.17	0.0194	0.448
	6.0	3240.	22994.	0.14	0.0224	0.515

The relationship between K , θ , and V_X is as shown in figure 53. Since the design approach is to balance the local, panel, and general stability stress levels for optimum weight, the shell buckling stress is set equal to the cover panel stress level for a given L spacing. For a given diameter V_X is calculated for the range of H values, (one to 6 inches). From the substructure data shown on table XVIII, the ratio θ is seen to be always less than unity. For this case, a particularly simple relationship exists between V_X and the buckling coefficient, K .

$$\theta \leq 1 \quad K = 1 - V_X \quad (V_X \leq .50)$$

$$K = 1/4 V_X \quad (V_X > .50)$$

Knowing V_X for the assumed L spacing and H variations, K is easily determined. The actual buckling coefficient, K , is compared to the required K given by the expression

$$K_{REQ'D} = \frac{\sigma_{CR}}{\eta} D \frac{\sqrt{1-\mu^2}}{2EH}$$

Obviously, for cases where $(K)_{reqd} \leq K$, the assumed minimum gage substructure thickness, t_c , is adequate. When $(K)_{reqd} > K$, the substructure thickness is incremented upwards until the required K is attained, or a t_c of 10 times the minimum gage fails to satisfy the requirement. (In the latter case, the design is considered impossible to attain.) In this manner, six design configurations are obtained for a given substructure spacing, L , making a total combination of 36 design configurations (six substructure spacings times six shell thicknesses).

The determination of the nonoptimum weight factors is presented next. The assessed weight penalty is added to the cover and substructure weight. The weight penalty, W_{pen} , includes the panel splice and attachment weight; and shear web cap, attachment pad and substructure attachment weight.

$$W_{pen} = W_{spl} + W_{att} + W_{cap} + W_{pad} + W_{attp} + W_{bond}$$

The splice weight includes the weight of both longitudinal and circumferential splices. Thus, for the double-wall panel, the splice weight, W_{spl} , is expressed in terms of pounds per square foot as follows:

$$W_{spl} = \frac{2(W_{LJ} + W_{CJ})}{LC} \quad 144$$

Where W_{LJ} and W_{CJ} are the weight of the longitudinal and circumferential splices, respectively as follows:

$$W_{LJ} = 2 L \times t_{spl} (W_{LJ} + A)$$

$$W_{CJ} = 2 L \times t_{spc} (W_{CJ} + B)$$

Judicious design judgment was used in determining the splice widths, W and thickness, t_{sp} , as reflected in the design drawings.

The weight of the splice attachments, W_{att} , is next determined for the longitudinal and circumferential splice. Weight assessment for the longitudinal attachments was based on using 1/8-inch diameter monel rivets with 4D spacing spliced on both ends.

$$W_{attl} = 2 (\text{no. rivets}) (\text{unit wt}) = 2 \left(\frac{L}{4D} \right) .0003 = .0012L$$

Weight assessment for the circumferential attachments was based on using 1/8-inch diameter monel rivets and the critical bearing strength of the skin. Thus,

$$F_{bru} = \frac{P}{A} = \frac{N_x 4D}{2 (\text{no rows}) D t} = \frac{4 N_x}{2 (\text{no rows}) t_{sp}}$$

$$\text{Number of rows} = \frac{4 N_x}{2 F_{bru} t_{sp}}$$

$$W_{attc} = 2 (\text{no. rivets per row}) (\text{no. rows}) (\text{unit wt})$$

$$= 2 \left[\frac{L_c}{4D} \right] \left[\frac{4 N_x}{2 F_{bru} t_{sp}} \right] .0003$$

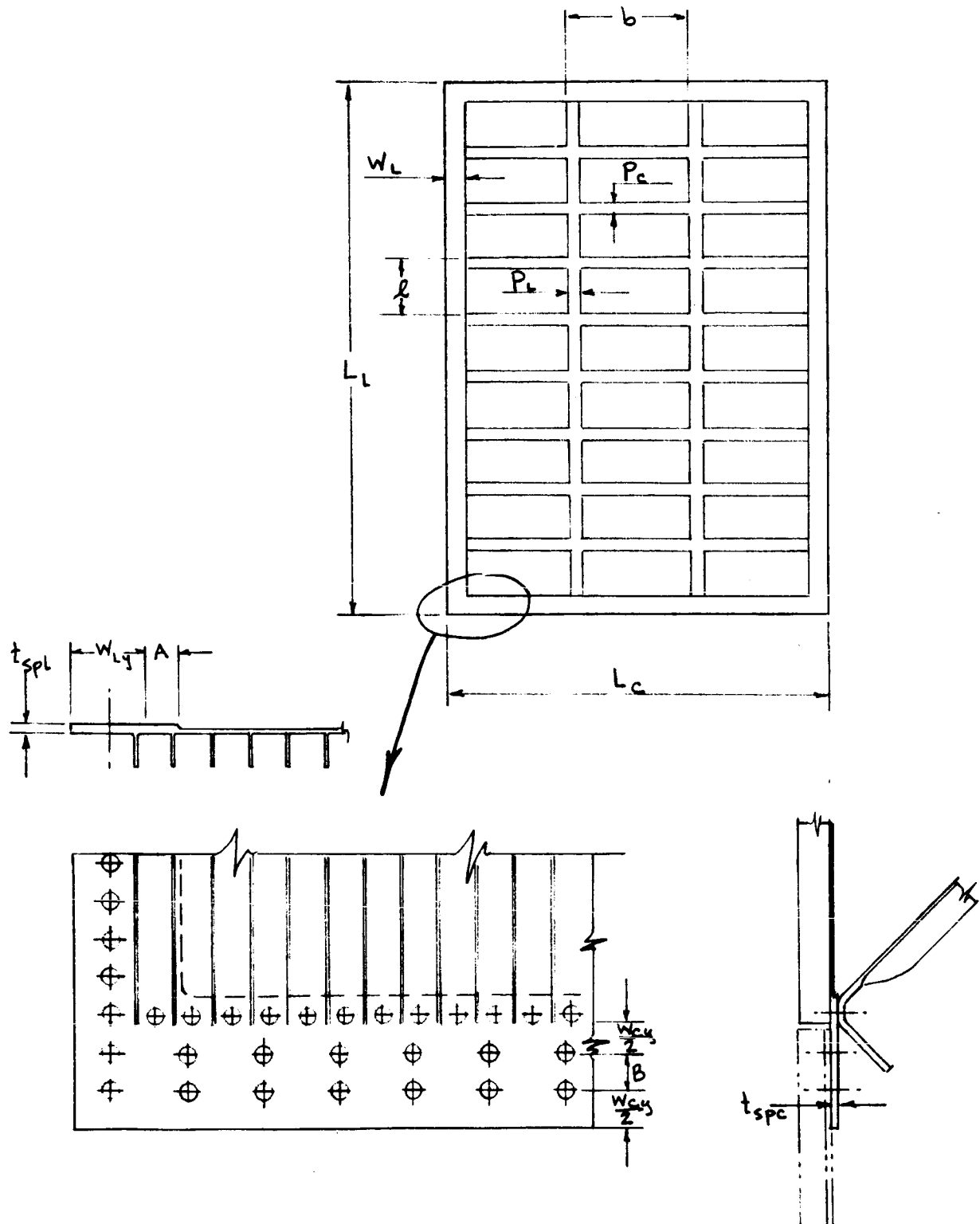


Figure 58. Definition of Geometry Terms

$$W_{attc} = 4 L_C N_X \text{ (no rows) } .0003$$

Total attachments weight in terms of pounds per square foot:

$$W_{att} = \frac{W_{att1} + W_{attc} 144}{L_C C}$$

The shear web cap used to connect the truss web substructure to the covers consists of an overlap joint to facilitate fabrication. The weight penalty resulting from the flange width and gage sizing (.375 x .040) is assessed for the cover support spacing, L:

$$W_{cap} = \frac{2 (144) (.75 \times .020) 2}{L}$$

One pad on each cover provides reinforcement for the rivet attachment to the substructure. Pad size used in weight assessment consists of:

$$W_{pad} = \frac{2 (.400 \times .010) (144)}{L}$$

Rivet attachment weight to the substructure (rivets spaced 1.75 cc)

$$W_{attp} = \frac{.0503}{L}$$

$$W_{attp} = \frac{144 (.0003) 2}{L (1.75)} = \frac{288 (.0003)}{1.75 L}$$

$$W_{attp} = \frac{.0500}{L}$$

Weight of bond to the substructure is based on the bond weight as used with honeycomb (i.e., .218 lb/ft²)

$$W = \frac{.40 (.218)}{L}$$

These nonoptimum weight increments are evaluated in the computer analysis for shell stability. For each combination of substructure spacing and shell thickness, this increment is added to the weight of the integrally stiffened covers and truss web substructure. For each L spacing, the six possible shell heights are automatically scanned in the computer program and the least total weight design is selected. When this entire procedure is repeated for each of four shell diameters, the data shown in table XIX result.

The table lists only the minimum total weight design for each L spacing and each shell diameter. The dimension shown for shell thickness (H) is that which was automatically selected as the least weight arrangement of the six possible thicknesses. Therefore, although the table shows only 24 design configurations, the actual number of designs evaluated in producing the table was 144.

A visual inspection of the table for each diameter reveals that a minimum total weight design can be realized by selecting one particular arrangement. For the design example under consideration, the data indicate that the least weight design occurs with $L = 3.0$ inches and $H = 2.0$ inches. It is noted that great variations in panel geometry are attainable with slight increases in panel weight.

As an added note of interest, considering that five loads levels were evaluated in this study for each material/design concept, permitting 5×144 results in 720 evaluations performed for each concepts.

Typical first phase calculations of panel weight vs load are summarized in figures 59 and 60 for nine materials. The full range of diameters considered, 200 inches to 400 inches, is represented in these figures. Wide column configuration potentials are shown in figures 61 and 62. Plate configuration potentials are shown in figures 63 and 64.

HONEYCOMB SANDWICH CYLINDERS

Analysis of full-depth honeycomb is performed to provide a basis for comparison in this design investigation of structures "other-than-honeycomb".

The first phase of the program considers like materials for core and facing sheets. A minimum core density corresponding to a 3/16 inch cell size and .001 core is used. Typical results of panel weight versus axial load for a 400-inch diameter are shown in figure 65 for the matrix of candidate materials. Braze or bond weight is included in these plots, but joint penalties and minimum gage restraints are not included. Figure 66 shows a full-depth honeycomb minimum weight envelope for the "state-of-the-art" materials and for the "advanced" materials. The impact of minimum gages upon honeycomb structural weight is shown in figure 67. It is seen that the advanced materials, beryllium and boron-titanium, are affected.

Table XIX
 INTEGRALLY STIFFENED - WIDE COLUMN
 TRUSS SUBSTRUCTURE

NX = 8000. LB/IN.

COVER MATERIAL 6-4 Ti

SUBSTR. MATERIAL 6-4 Ti

RADIUS	L-SPACING	H	TC	SLB WT	COV WT	PEN WT	TOT WT
100.	1.0	2.0	0.010	0.950	1.333	2.292	4.576
	2.0	1.0	0.010	0.326	1.397	1.184	2.907
	3.0	1.0	0.010	0.277	1.544	0.823	2.644
	4.0	1.0	0.010	0.258	1.782	0.654	2.694
	5.0	1.0	0.010	0.248	1.993	0.558	2.799
	6.0	2.0	0.010	0.277	2.183	0.498	2.958
133.	1.0	3.0	0.010	1.401	1.333	2.292	5.027
	2.0	2.0	0.010	0.515	1.397	1.184	3.096
	3.0	1.0	0.012	0.332	1.544	0.823	2.699
	4.0	1.0	0.010	0.258	1.782	0.654	2.694
	5.0	2.0	0.010	0.295	1.993	0.558	2.846
	6.0	2.0	0.010	0.277	2.183	0.498	2.958
167.	1.0	3.0	0.010	1.401	1.333	2.292	5.027
	2.0	2.0	0.010	0.515	1.397	1.184	3.096
	3.0	2.0	0.010	0.384	1.544	0.823	2.751
	4.0	2.0	0.010	0.326	1.782	0.654	2.762
	5.0	2.0	0.010	0.295	1.993	0.558	2.846
	6.0	2.0	0.010	0.277	2.183	0.498	2.958
200.	1.0	3.0	0.013	1.822	1.333	2.292	5.447
	2.0	2.0	0.010	0.515	1.397	1.184	3.096
	3.0	2.0	0.010	0.384	1.544	0.823	2.751
	4.0	2.0	0.010	0.326	1.782	0.654	2.762
	5.0	2.0	0.010	0.295	1.993	0.558	2.846
	6.0	2.0	0.010	0.277	2.183	0.498	2.958

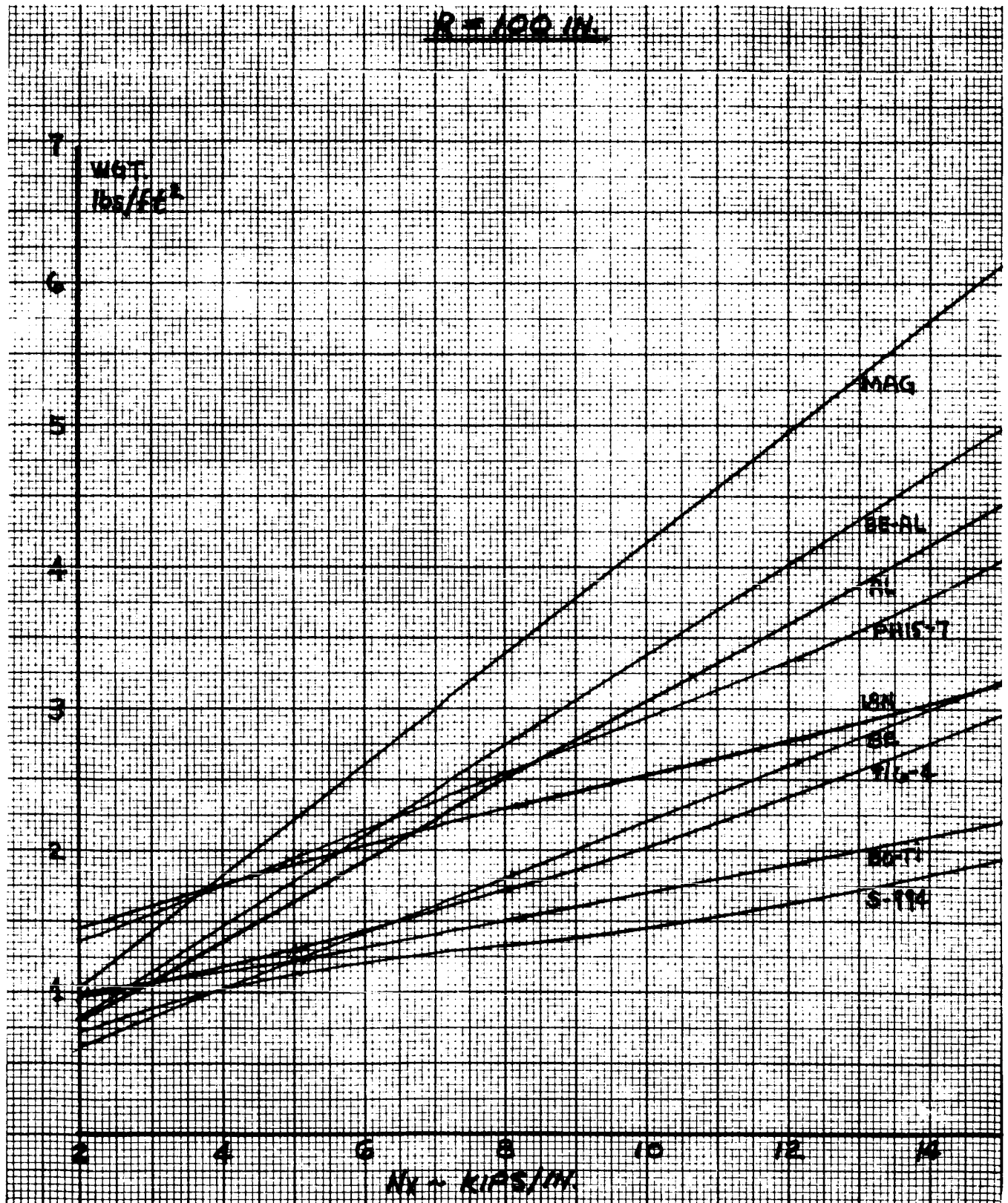


Figure 59. Integrally Stiffened Wide Column Beaded Truss Substructure

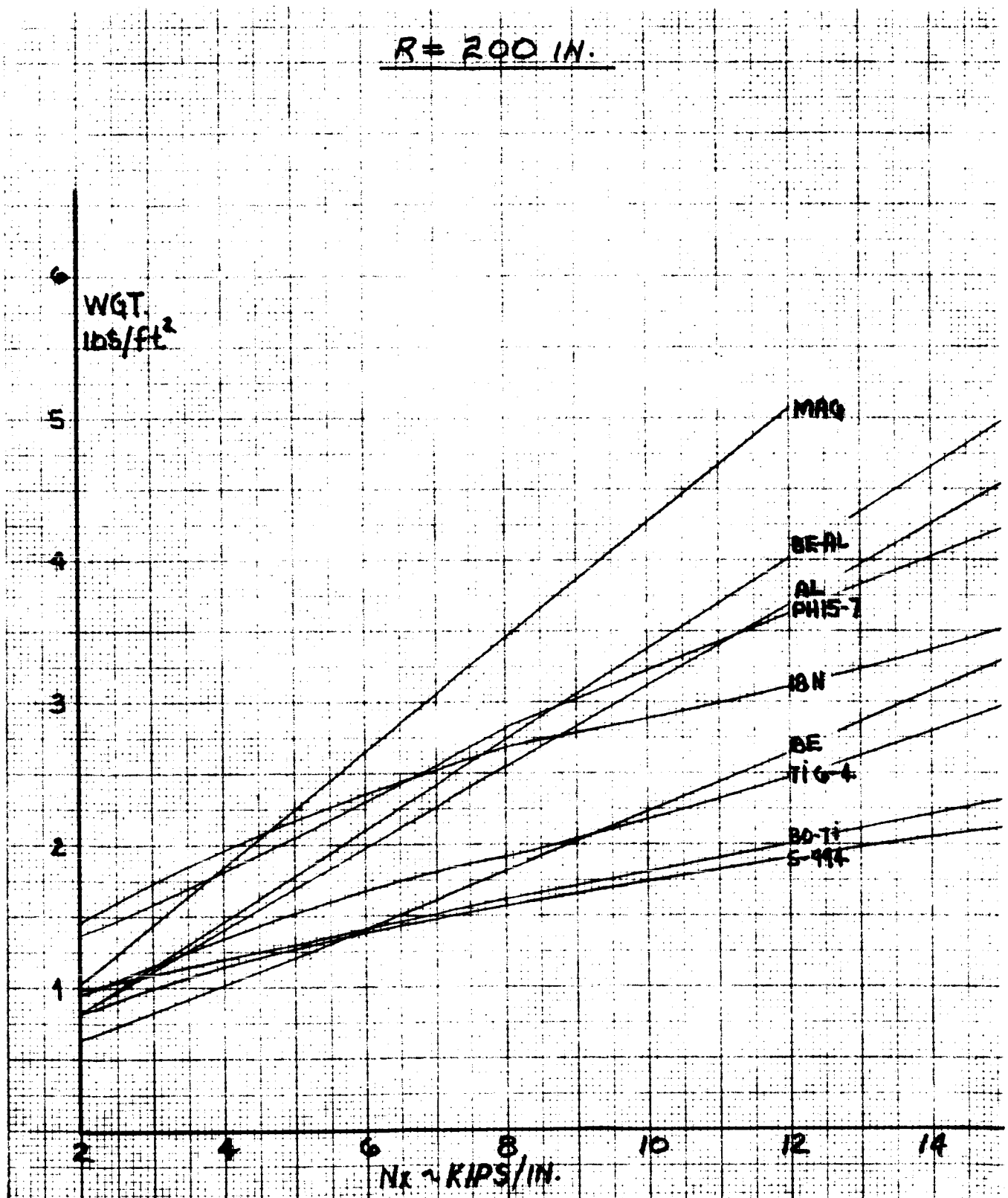


Figure 60. Integrally Stiffened Wide Column Beaded Truss Substructure

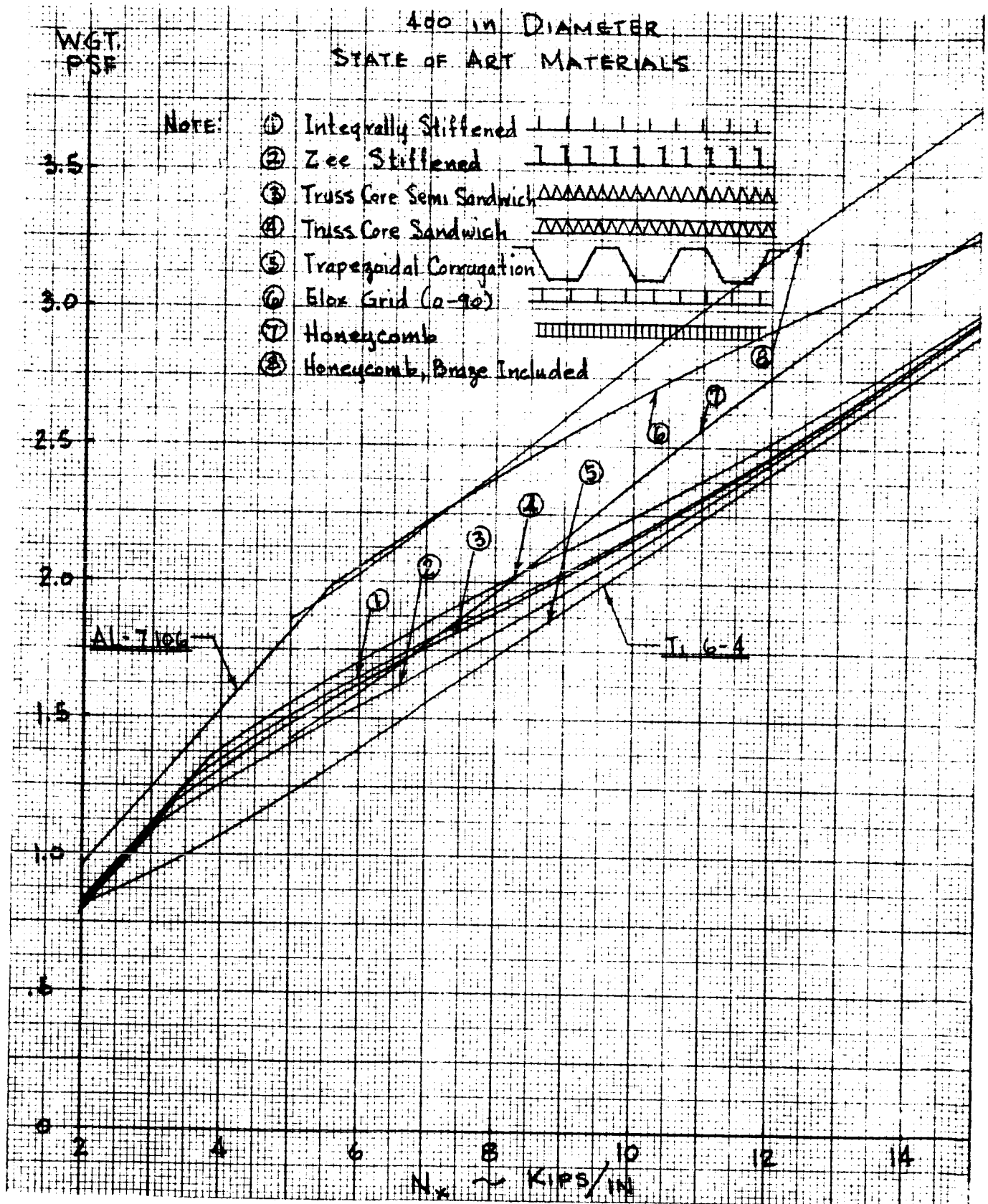


Figure 61. Double-wall Cylinders Wide Column
Bridged Truss Substructure

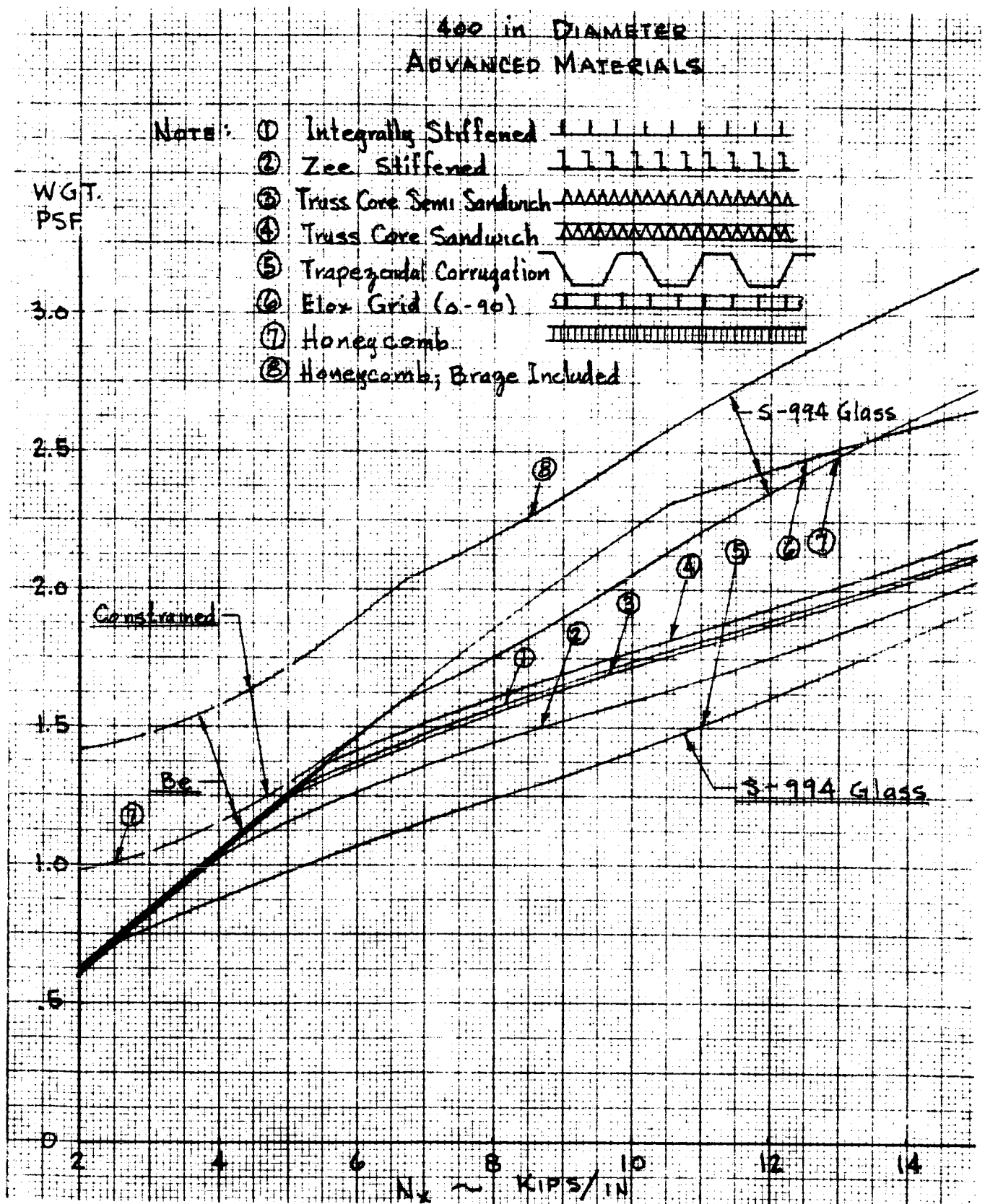


Figure 62. Double-wall Cylinders Wide Column
Beaded Substructure

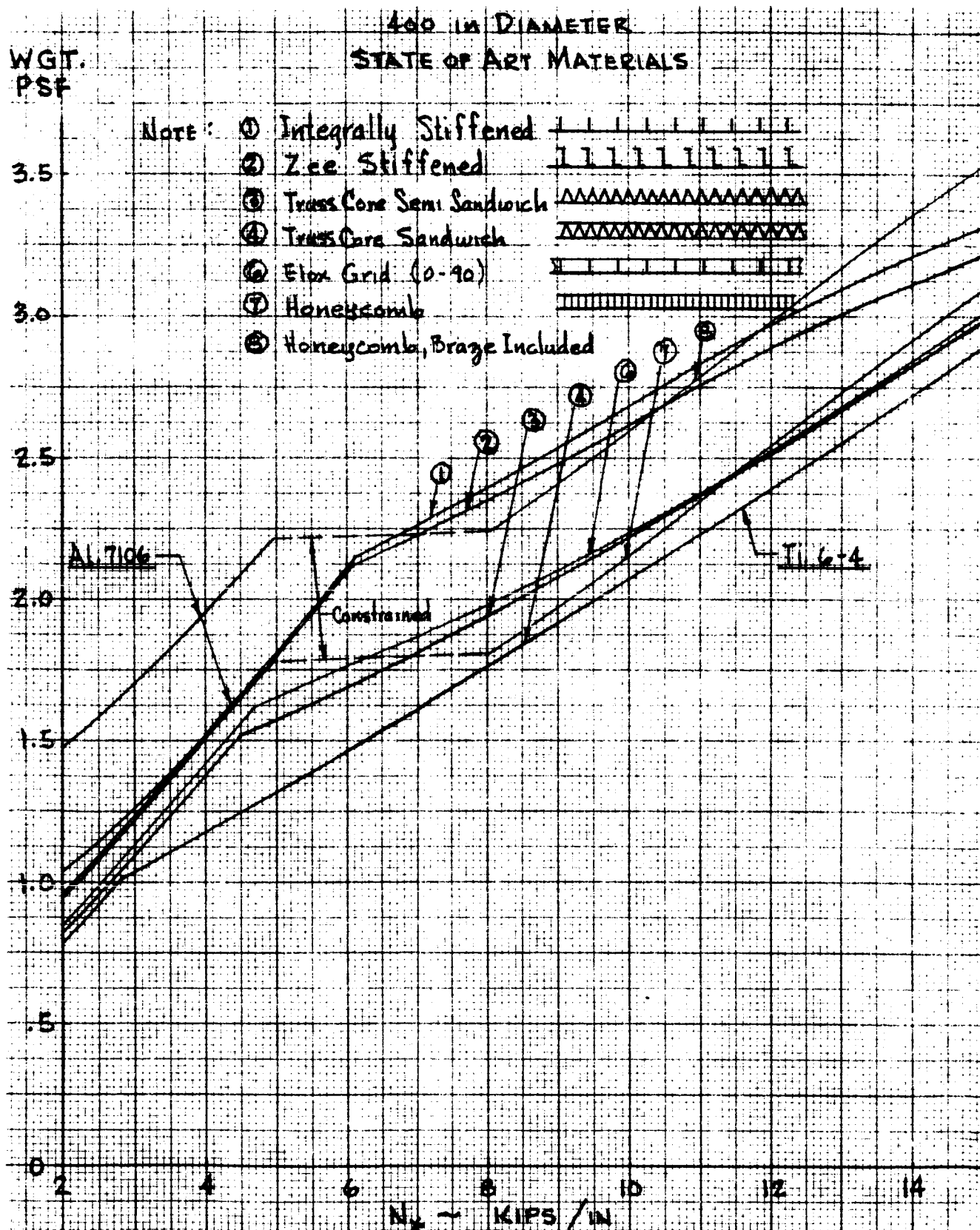


Figure 63. Double-wall Cylinders Plate - Beaded Truss Substructure

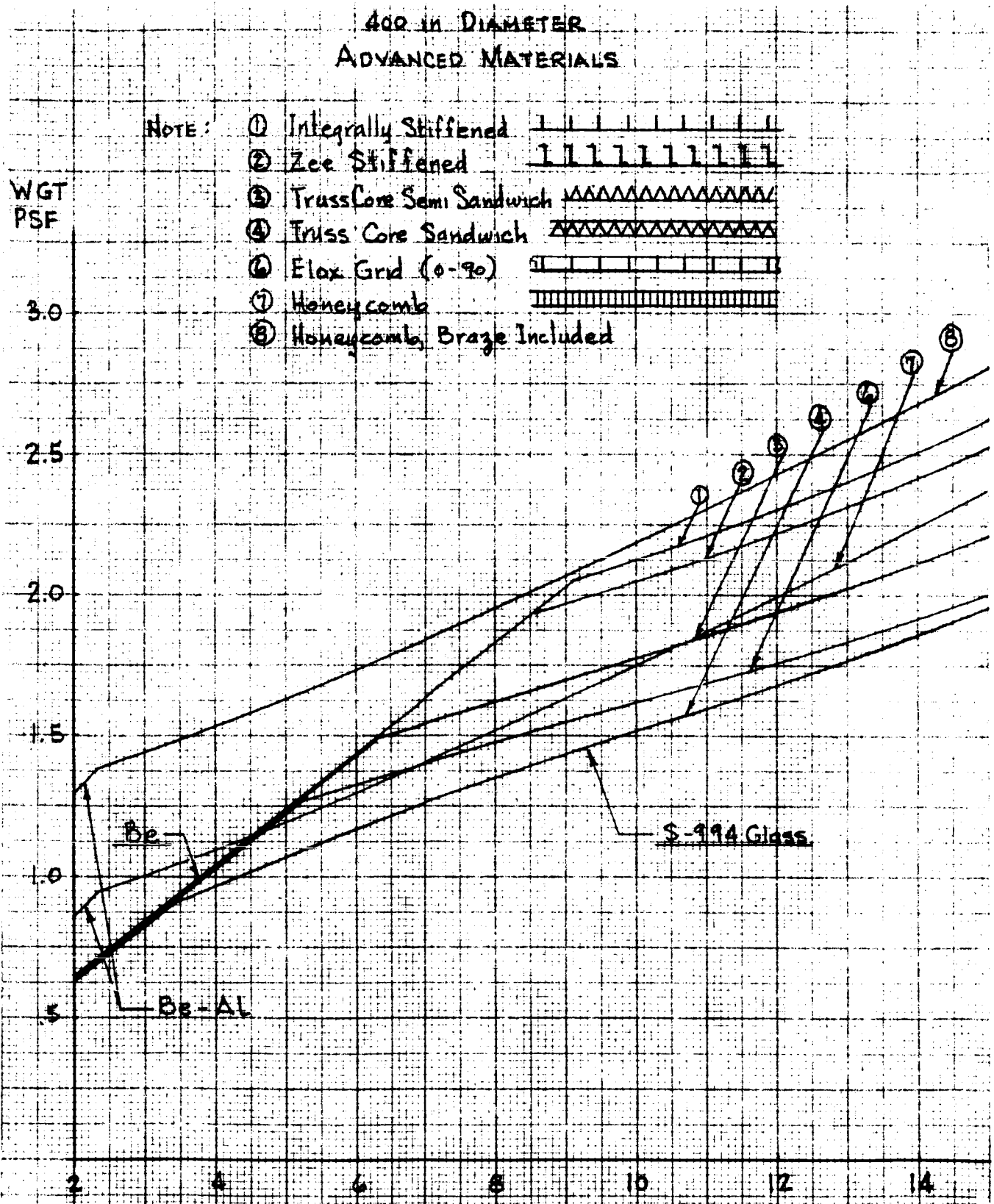


Figure 64. Double-wall Cylinders Plate - Beaded Truss Substructure

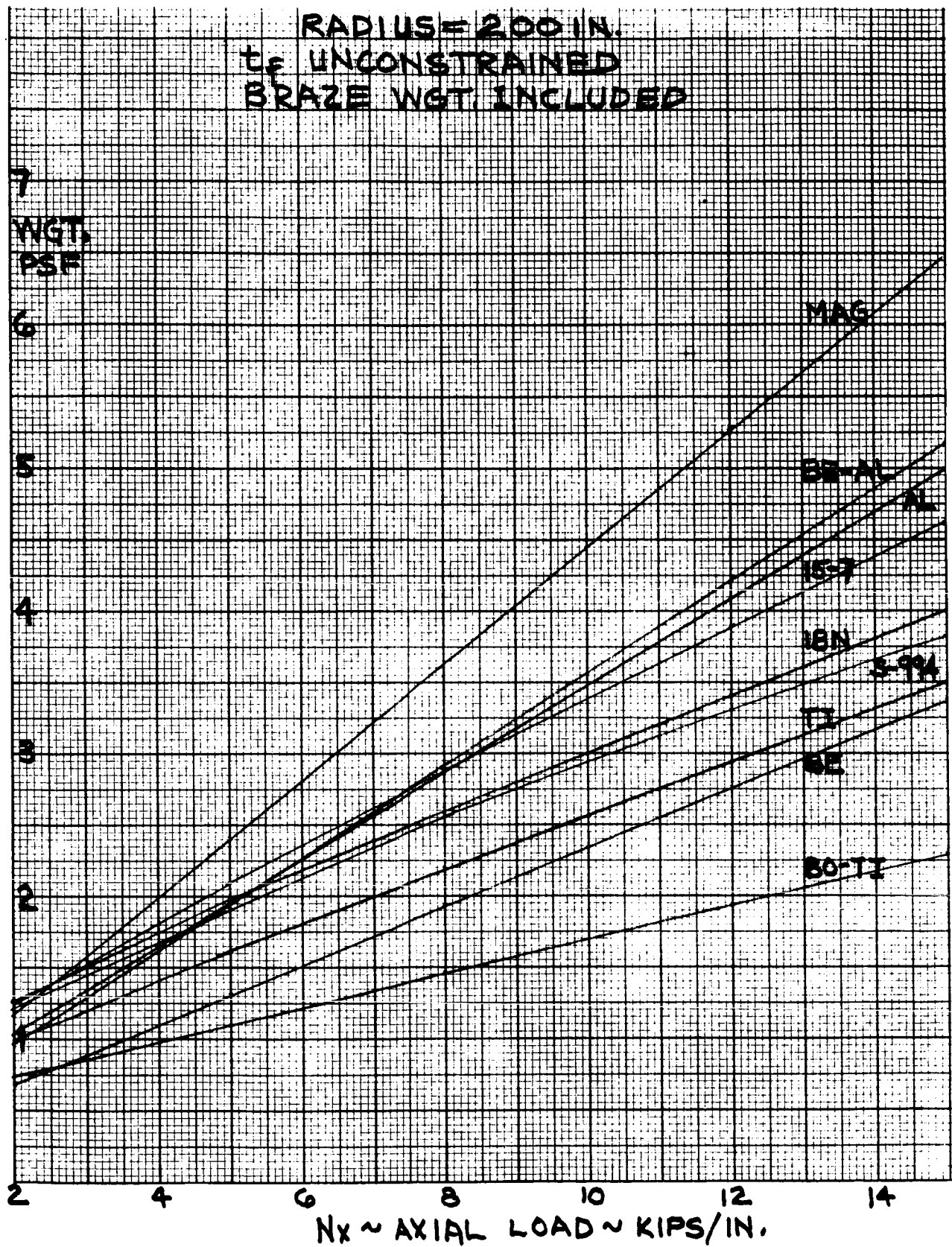


Figure 65. Full Depth Honeycomb Cylinders

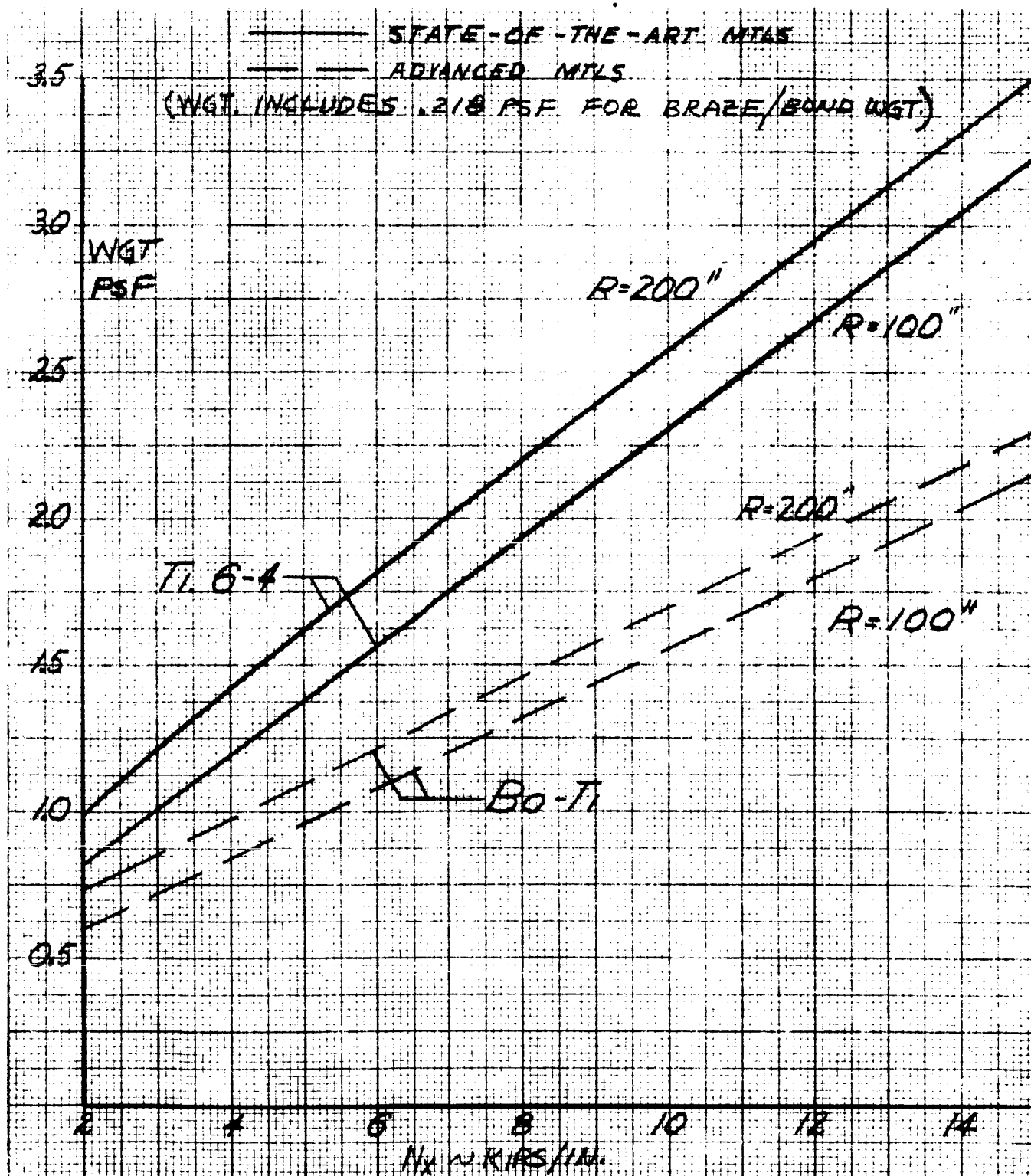


Figure 66. Full Depth Honeycomb Cylinders Optimum Materials for Minimum Weight

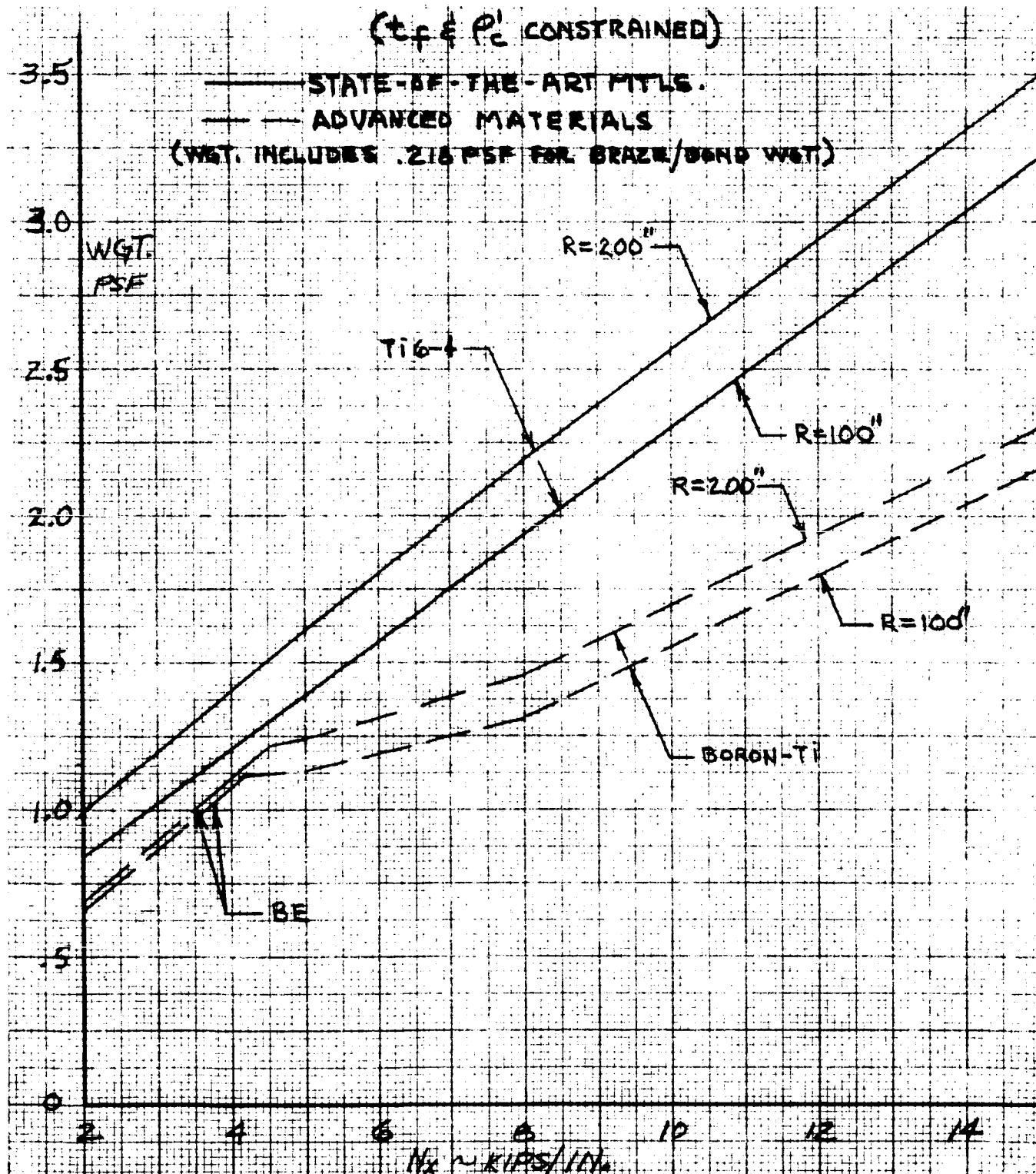


Figure 67. Honeycomb Cylinders Full Depth Core - Optimum Materials for Minimum Weight

The second phase study evaluates both minimum gage restraints and joint penalties. Summaries of these analyses are included in Tables XX through XXIV and in the figures 21 through 24 where competitive designs are compared with honeycomb. The weight values shown in the honeycomb tabulations show the basic core and facing sheet weight in the first weight column and the summation of core, facing sheet, bond, minimum gage penalty, and joint penalty in the second column. An aluminum core is used with all facing materials, except glass. Glass core is used with glass facings. In many cases increased efficiency results. In some cases, efficiency is reduced.

In the second phase study, a minimum core density of two pounds per square foot is used with the aluminum core and a minimum core density of three pounds per square foot is used with the glass core. Panel size of 10 x 0 10 feet is used to assess all shell diameters and materials. The weight penalty assessment includes a bond weight of .218 pound per square foot. Comparisons made with all face sheet materials, load levels and diameters indicate that the aluminum core provides a lighter honeycomb sandwich structure than glass core. For the state-of-the-art materials comparison, the resulting shell weight using titanium facing materials is lighter than the shell weight using aluminum facing materials; therefore, on a minimum weight basis, the titanium facing material with the aluminum core provides the full depth honeycomb comparison with other advanced material/concepts.

Table XX
FULL DEPTH HONEYCOMB CYLINDERS

SMALL DEFLECTION THEORY

$NX = 2000.$

DIAMETER	MATERIAL		WEIGHT		TF	H	CORE DENSITY	STRESS
200.	ALUMINUM 7106-T6	AL	0.716	0.936	0.022	0.537	2.00	45327.
	TITANIUM 6AL-4V	AL	0.568	0.786	0.009	0.709	2.93	116795.
	18N MARAGING STEEL	AL	0.657	0.875	0.005	0.646	3.90	185954.
	PH15-7MO STEEL	AL	0.693	0.911	0.007	0.565	3.22	147301.
	BERYLLIUM	AL	0.463	0.681	0.022	0.258	2.00	45251.
	MAGNESIUM	AL	0.913	1.131	0.045	0.537	2.00	22388.
	S-944 GLASS	GL	0.569	0.787	0.017	1.244	2.20	59076.
	BERYLLIUM-ALUMINUM	AL	0.727	0.945	0.029	0.499	2.00	34000.
267.	BORON-TITANIUM	AL	0.413	0.631	0.007	0.568	3.22	153604.
	ALUMINUM 7106-T6	AL	0.745	0.963	0.022	0.696	2.00	45327.
	TITANIUM 6AL-4V	AL	0.623	0.841	0.009	0.936	2.93	116795.
	18N MARAGING STEEL	AL	0.723	0.941	0.006	0.783	3.54	169307.
	PH15-7MO STEEL	AL	0.740	0.958	0.007	0.663	2.93	137959.
	BERYLLIUM	AL	0.473	0.691	0.022	0.316	2.00	45251.
	MAGNESIUM	AL	0.935	1.153	0.046	0.558	2.00	21898.
	S-944 GLASS	GL	0.643	0.861	0.017	1.646	2.20	59076.
333.	BERYLLIUM-ALUMINUM	AL	0.751	0.969	0.029	0.646	2.00	34000.
	BORON-TITANIUM	AL	0.454	0.672	0.007	0.689	2.93	139853.
	ALUMINUM 7106-T6	AL	0.771	0.989	0.022	0.854	2.00	45327.
	TITANIUM 6AL-4V	AL	0.669	0.887	0.009	1.062	2.66	106339.
	18N MARAGING STEEL	AL	0.778	0.996	0.006	0.971	3.54	169307.
	PH15-7MO STEEL	AL	0.778	0.996	0.007	0.819	2.93	137959.
	BERYLLIUM	AL	0.482	0.700	0.023	0.259	2.00	43292.
	MAGNESIUM	AL	0.955	1.173	0.046	0.682	2.00	21898.
400.	S-944 GLASS	GL	0.715	0.933	0.018	1.930	2.20	55780.
	BERYLLIUM-ALUMINUM	AL	0.776	0.994	0.029	0.791	2.00	34000.
	BORON-TITANIUM	AL	0.488	0.706	0.008	0.783	2.66	127333.
	ALUMINUM 7106-T6	AL	0.798	1.016	0.022	1.015	2.00	45327.
	TITANIUM 6AL-4V	AL	0.711	0.929	0.010	1.164	2.42	96820.
	18N MARAGING STEEL	AL	0.825	1.043	0.008	1.064	3.22	154150.
	PH15-7MO STEEL	AL	0.817	1.035	0.007	0.978	2.93	137959.
	BERYLLIUM	AL	0.488	0.706	0.023	0.294	2.00	43292.
	MAGNESIUM	AL	0.976	1.194	0.046	0.807	2.00	21898.
	S-944 GLASS	GL	0.766	0.984	0.023	1.825	2.00	43665.
	BERYLLIUM-ALUMINUM	AL	0.800	1.018	0.029	0.939	2.00	34000.
	BORON-TITANIUM	AL	0.519	0.737	0.009	0.859	2.42	115933.

Table XXI
FULL DEPTH HONEYCOMB CYLINDERS
SMALL DEFLECTION THEORY

$NX = 5000.$

DIAMETER	MATERIAL		WEIGHT		TF	H	CORE DENSITY	STRESS
200.	ALUMINUM 7106-T6	AL	1.636	1.854	0.052	0.894	2.00	47934.
	TITANIUM 6AL-4V	AL	1.126	1.344	0.019	0.850	3.22	128279.
	18N MARAGING STEEL	AL	1.251	1.469	0.011	0.798	4.72	221942.
	PH15-7MO STEEL	AL	1.476	1.694	0.015	0.787	3.90	163486.
	BERYLLIUM	AL	1.116	1.334	0.054	0.509	2.00	46085.
	MAGNESIUM	AL	2.159	2.466	0.110	0.769	2.00	22693.
	S-944 GLASS	GL	1.047	1.354	0.035	1.532	2.66	71264.
	BERYLLIUM-ALUMINUM	AL	1.712	2.019	0.074	0.617	2.00	34000.
	BORON-TITANIUM	AL	0.786	1.093	0.015	0.653	3.54	168707.
267.	ALUMINUM 7106-T6	AL	1.676	1.983	0.052	1.136	2.00	47934.
	TITANIUM 6AL-4V	AL	1.197	1.503	0.019	1.112	3.22	128279.
	18N MARAGING STEEL	AL	1.352	1.658	0.011	1.054	4.72	221942.
	PH15-7MO STEEL	AL	1.543	1.850	0.016	0.889	3.54	155699.
	BERYLLIUM	AL	1.127	1.433	0.054	0.573	2.00	46085.
	MAGNESIUM	AL	2.189	2.497	0.111	0.843	2.00	22489.
	S-944 GLASS	GL	1.151	1.459	0.039	1.857	2.42	64884.
	BERYLLIUM-ALUMINUM	AL	1.734	2.042	0.074	0.750	2.00	34000.
	BORON-TITANIUM	AL	0.845	1.152	0.015	0.852	3.54	168707.
333.	ALUMINUM 7106-T6	AL	1.710	2.017	0.053	1.164	2.00	47032.
	TITANIUM 6AL-4V	AL	1.266	1.574	0.019	1.371	3.22	128279.
	18N MARAGING STEEL	AL	1.445	1.753	0.012	1.188	4.29	203871.
	PH15-7MO STEEL	AL	1.604	1.912	0.016	1.095	3.54	155699.
	BERYLLIUM	AL	1.137	1.445	0.055	0.523	2.00	45251.
	MAGNESIUM	AL	2.217	2.525	0.111	1.007	2.00	22489.
	S-944 GLASS	GL	1.239	1.547	0.039	2.291	2.42	64884.
	BERYLLIUM-ALUMINUM	AL	1.757	2.065	0.074	0.888	2.00	34000.
	BORON-TITANIUM	AL	0.903	1.210	0.015	1.048	3.54	168707.
400.	ALUMINUM 7106-T6	AL	1.743	2.051	0.053	1.367	2.00	47032.
	TITANIUM 6AL-4V	AL	1.336	1.644	0.021	1.433	2.93	116795.
	18N MARAGING STEEL	AL	1.528	1.835	0.012	1.419	4.29	203871.
	PH15-7MO STEEL	AL	1.661	1.969	0.017	1.144	3.22	147301.
	BERYLLIUM	AL	1.145	1.452	0.055	0.566	2.00	45251.
	MAGNESIUM	AL	2.242	2.550	0.112	1.049	2.00	22288.
	S-944 GLASS	GL	1.314	1.621	0.042	2.512	2.20	59076.
	BERYLLIUM-ALUMINUM	AL	1.781	2.089	0.074	1.031	2.00	34000.
	BORON-TITANIUM	AL	0.960	1.268	0.016	1.150	3.22	153604.

Table XXII
 FULL DEPTH HONEYCOMB CYLINDERS
 SMALL DEFLECTION THEORY

$NX = 8000.$

DIAMETER	MATERIAL		WEIGHT		TF	H	CORE DENSITY	STRESS
200.	ALUMINUM 7106-T6	AL	2.536	2.844	0.081	1.317	2.00	49232.
	TITANIUM 6AL-4V	AL	1.677	1.985	0.031	0.895	3.22	128279.
	18N MARAGING STEEL	AL	1.799	2.256	0.017	0.913	5.19	237182.
	PH15-7MO STEEL	AL	2.212	2.668	0.023	0.964	4.29	170811.
	BERYLLIUM	AL	1.760	2.215	0.085	0.821	2.00	46841.
	MAGNESIUM	AL	3.390	3.749	0.174	1.132	2.00	23033.
	S-944 GLASS	GL	1.434	1.793	0.047	1.847	3.22	85967.
	BERYLLIUM-ALUMINUM	AL	2.708	6.716	0.118	0.725	2.20	34000.
267.	BORON-TITANIUM	AL	1.154	1.543	0.024	0.693	3.54	168707.
	ALUMINUM 7106-T6	AL	2.584	2.974	0.082	1.434	2.00	48633.
	TITANIUM 6AL-4V	AL	1.747	2.136	0.031	1.154	3.22	128279.
	18N MARAGING STEEL	AL	1.923	2.312	0.018	1.075	4.72	221942.
	PH15-7MO STEEL	AL	2.298	2.687	0.024	1.065	3.90	163486.
	BERYLLIUM	AL	1.776	2.135	0.086	0.770	2.20	46512.
	MAGNESIUM	AL	3.427	3.787	0.175	1.137	2.00	22770.
	S-944 GLASS	GL	1.577	1.937	0.051	2.239	2.93	78271.
333.	BERYLLIUM-ALUMINUM	AL	2.724	3.084	0.118	0.893	2.00	34000.
	BORON-TITANIUM	AL	1.212	1.572	0.024	0.889	3.54	168707.
	ALUMINUM 7106-T6	AL	2.625	2.986	0.083	1.511	2.00	48049.
	TITANIUM 6AL-4V	AL	1.816	2.176	0.031	1.411	3.22	128279.
	18N MARAGING STEEL	AL	2.021	2.382	0.018	1.327	4.72	221942.
	PH15-7MO STEEL	AL	2.377	2.737	0.024	1.308	3.90	163486.
	BERYLLIUM	AL	1.786	2.147	0.086	0.865	2.00	46299.
	MAGNESIUM	AL	3.460	3.821	0.177	1.225	2.00	22642.
400.	S-944 GLASS	GL	1.696	2.056	0.056	2.545	2.66	71264.
	BERYLLIUM-ALUMINUM	AL	2.744	3.104	0.118	1.011	2.00	34000.
	BORON-TITANIUM	AL	1.269	1.629	0.024	1.084	3.54	168707.
	ALUMINUM 7106-T6	AL	2.665	3.025	0.084	1.577	2.00	47479.
	TITANIUM 6AL-4V	AL	1.886	2.246	0.031	1.673	3.22	128279.
	18N MARAGING STEEL	AL	2.122	2.482	0.018	1.582	4.72	221942.
	PH15-7MO STEEL	AL	2.445	2.805	0.026	1.338	3.54	155699.
	BERYLLIUM	AL	1.799	2.159	0.087	0.826	2.00	45769.
400.	MAGNESIUM	AL	3.491	3.852	0.177	1.410	2.00	22642.
	S-944 GLASS	GL	1.803	2.164	0.056	3.029	2.66	71264.
	BERYLLIUM-ALUMINUM	AL	2.766	3.126	0.118	1.144	2.00	34000.
	BORON-TITANIUM	AL	1.328	1.688	0.024	1.282	3.54	168707.

Table XXIII
 FULL DEPTH HONEYCOMB CYLINDERS
 SMALL DEFLECTION THEORY

$NX = 12000.$

DIAMETER	MATERIAL		WEIGHT		TF	H	CORE DENSITY	STRESS
200.	ALUMINUM 7106-T6	AL	3.716	4.077	0.120	1.705	2.00	49845.
	TITANIUM 6AL-4V	AL	2.399	2.878	0.045	1.028	3.54	131965.
	18N MARAGING STEEL	AL	2.512	3.051	0.025	0.940	5.19	237182.
	PH15-7MO STEEL	AL	3.160	3.716	0.035	1.001	4.29	170811.
	BERYLLIUM	AL	2.611	3.039	0.127	1.076	2.20	47244.
	MAGNESIUM	AL	5.015	5.443	0.258	1.559	2.00	23256.
	S-944 GLASS	GL	1.918	2.346	0.070	1.902	3.22	85967.
	BERYLLIUM-ALUMINUM	AL	4.036	4.606	0.176	0.709	2.93	34000.
	BORON-TITANIUM	AL	1.646	2.103	0.036	0.753	3.54	168707.
267.	ALUMINUM 7106-T6	AL	3.777	4.234	0.122	1.728	2.00	49031.
	TITANIUM 6AL-4V	AL	2.481	2.939	0.047	1.215	3.22	128279.
	18N MARAGING STEEL	AL	2.636	3.193	0.025	1.228	5.19	237182.
	PH15-7MO STEEL	AL	3.266	3.839	0.035	1.298	4.29	170811.
	BERYLLIUM	AL	2.631	3.060	0.128	1.082	2.20	46875.
	MAGNESIUM	AL	5.063	5.492	0.260	1.624	2.00	23077.
	S-944 GLASS	GL	2.074	2.502	0.070	2.483	3.22	85967.
	BERYLLIUM-ALUMINUM	AL	4.054	4.625	0.176	0.950	2.42	34000.
	BORON-TITANIUM	AL	1.702	2.168	0.036	0.943	3.54	168707.
333.	ALUMINUM 7106-T6	AL	3.828	4.294	0.123	1.864	2.00	48633.
	TITANIUM 6AL-4V	AL	2.550	3.015	0.047	1.469	3.22	128279.
	18N MARAGING STEEL	AL	2.759	3.335	0.025	1.512	5.19	237182.
	PH15-7MO STEEL	AL	3.366	3.957	0.037	1.349	3.90	163486.
	BERYLLIUM	AL	2.648	3.239	0.129	1.223	2.00	46659.
	MAGNESIUM	AL	5.104	5.533	0.262	1.646	2.00	22901.
	S-944 GLASS	GL	2.228	2.657	0.070	3.058	3.22	85967.
	BERYLLIUM-ALUMINUM	AL	4.069	9.973	0.176	1.241	2.00	34000.
	BORON-TITANIUM	AL	1.759	2.234	0.036	1.135	3.54	168707.
400.	ALUMINUM 7106-T6	AL	3.875	4.350	0.124	1.976	2.00	48242.
	TITANIUM 6AL-4V	AL	2.619	3.094	0.047	1.729	3.22	128279.
	18N MARAGING STEEL	AL	2.883	3.358	0.027	1.611	4.72	221942.
	PH15-7MO STEEL	AL	3.446	3.921	0.037	1.595	3.90	163486.
	BERYLLIUM	AL	2.662	3.137	0.129	1.307	2.00	46659.
	MAGNESIUM	AL	5.140	5.615	0.263	1.757	2.00	22814.
	S-944 GLASS	GL	2.364	2.839	0.077	3.354	2.93	78271.
	BERYLLIUM-ALUMINUM	AL	4.086	4.360	0.176	1.338	2.00	34000.
	BORON-TITANIUM	AL	1.817	2.292	0.036	1.332	3.54	168707.

Table XXIV
FULL DEPTH HONEYCOMB CYLINDERS
SMALL DEFLECTION THEORY

$NX = 15000.$

DIAMETER	MATERIAL		WEIGHT		TF	H	CORE DENSITY	STRESS
200.	ALUMINUM 7106-T6	AL	4.597	5.072	0.150	1.840	2.00	49845.
	TITANIUM 6AL-4V	AL	2.935	3.465	0.057	1.072	3.54	131965.
	18N MARAGING STEEL	AL	3.035	3.634	0.030	1.090	5.71	248018.
	PH15-7MO STEEL	AL	3.846	4.471	0.042	1.225	4.72	177813.
	BERYLLIUM	AL	3.246	3.725	0.158	1.324	2.20	47468.
	MAGNESIUM	AL	6.227	6.706	0.321	1.804	2.00	23328.
	S-944 GLASS	GL	2.281	2.761	0.087	1.946	3.22	85967.
	BERYLLIUM-ALUMINUM	AL	5.028	5.687	0.221	0.745	3.22	34000.
267.	BORON-TITANIUM	AL	2.017	2.524	0.044	0.773	3.90	170000.
	ALUMINUM 7106-T6	AL	4.662	5.169	0.151	2.062	2.00	49516.
	TITANIUM 6AL-4V	AL	3.020	3.580	0.057	1.359	3.54	131965.
	18N MARAGING STEEL	AL	3.171	3.790	0.032	1.248	5.19	237182.
	PH15-7MO STEEL	AL	3.977	4.616	0.044	1.326	4.29	170811.
	BERYLLIUM	AL	3.270	3.750	0.159	1.349	2.20	47170.
	MAGNESIUM	AL	6.282	6.763	0.323	1.914	2.00	23184.
	S-944 GLASS	GL	2.437	2.918	0.087	2.525	3.22	85967.
333.	BERYLLIUM-ALUMINUM	AL	5.050	5.708	0.221	0.998	2.66	34000.
	BORON-TITANIUM	AL	2.072	2.588	0.044	0.989	3.54	168707.
	ALUMINUM 7106-T6	AL	4.720	5.236	0.152	2.237	2.00	49191.
	TITANIUM 6AL-4V	AL	3.101	3.618	0.058	1.516	3.22	128279.
	18N MARAGING STEEL	AL	3.294	3.934	0.032	1.532	5.19	237182.
	PH15-7MO STEEL	AL	4.082	4.742	0.044	1.620	4.29	170811.
	BERYLLIUM	AL	3.289	3.770	0.160	1.351	2.20	46875.
	MAGNESIUM	AL	6.328	6.809	0.325	1.971	2.00	23041.
400.	S-944 GLASS	GL	2.590	3.071	0.087	3.098	3.22	85967.
	BERYLLIUM-ALUMINUM	AL	5.067	5.726	0.221	1.166	2.42	34000.
	BORON-TITANIUM	AL	2.127	2.654	0.044	1.177	3.54	168707.
	ALUMINUM 7106-T6	AL	4.773	5.300	0.153	2.382	2.00	48871.
	TITANIUM 6AL-4V	AL	3.170	3.697	0.058	1.774	3.22	128279.
	18N MARAGING STEEL	AL	3.419	4.083	0.032	1.820	5.19	237182.
	PH15-7MO STEEL	AL	4.188	4.871	0.046	1.827	3.90	163486.
	BERYLLIUM	AL	3.306	3.989	0.161	1.342	2.20	46584.
400.	MAGNESIUM	AL	6.370	7.053	0.326	2.112	2.00	22971.
	S-944 GLASS	GL	2.747	3.430	0.087	3.681	3.22	85967.
	BERYLLIUM-ALUMINUM	AL	5.084	5.748	0.221	1.533	2.00	34000.
	BORON-TITANIUM	AL	2.185	2.723	0.044	1.571	3.54	168707.

SIGNIFANCE OF LENGTH/DIAMETER

BACKGROUND

The objective of this investigation, the design of lightweight structural wall concepts, is based upon the selection of candidate concepts/materials with minimum weight potential. Since the nonpressurized sections of boosters comprise a significant proportion of total structural weight, efficient design practice strives to reduce these sections to minimum length. The analytical basis of this investigation is the assumption that the critical buckling load is independent of cylinder length. This assumption is valid for long cylinders. However, in short cylinders the tank sections provide support to the shell. The validity of the "long" cylinder assumption and the potential weight savings resulting from tank support are investigated in this section.

The design of attractive configurations places emphasis upon detailed design of cover panels, substructure, cover panel to substructure attachment, and longitudinal and circumferential wall splices. In this manner a representative section of the cylinder is designed and evaluated. A generally valid comparison is made between concepts/materials without the limiting consideration of boundary conditions imposed by contiguous tank sections.

It is shown that the range of L/D ratios established in the section "Design Criteria" are in the long cylinder range. The L/D ratios investigated range from 0.50 to 2.50. These ratios combined with the four diameters under consideration yield the cylinder lengths shown in table XXV.

Table XXV

CYLINDER LENGTHS
(Units of L and D = inches)

L/D	D = 200	D = 266	D = 333	D = 400
.50	100	133	167	200
1.00	200	266	333	400
1.50	300	400	500	600
2.00	400	532	667	800
2.50	500	665	835	1000

RING STIFFENED CYLINDER ANALYSIS

The shortest cylinder length is obtained at the lowest L/D and smallest diameter. A cylinder length of 100 inches offers the most likely geometry for potential weight savings. Typical calculations are shown for a length of 100 inches with the maximum load level of 15,000 lbs/in. for the trapezoidal corrugation configuration. A simple support is assumed to exist at each end of the 100-inch length wall section. For 6Al-4V titanium the effective thickness of the cover is given by the equation:

$$\bar{t}_{\text{cover}} = \frac{1}{\alpha} \left(\frac{N_x L}{E \eta} \right)^{1/2} = \frac{1}{1.264} \left[\frac{15000(100)}{16.3 \times 10^6 (1)} \right]^{1/2} = .240 \text{ in.}$$

The corresponding stress level is:

$$\sigma_o = \frac{15000}{.240} = 62500 \text{ lb/in.}^2$$

Cover unit weight is determined by the equation:

$$W = \bar{t} \rho (144) = 0.24 (.16)(144) = 5.54 \text{ lb/ft.}^2$$

The results of the analysis from the IBM program with optimum ring spacing is presented below for comparison.

$$\bar{t} = \bar{t}_{\text{cover}} + \bar{t}_{\text{frame}} = .115 + .0379 = .1529 \text{ in.}$$

$$W = .1529 (.16)(144) = 3.52 \text{ lb/ft.}^2$$

Thus, the end supported wide column is 2.02 lb/ft.² heavier than the optimum ring-stiffened cylinder.

It is concluded that for an L/D range of 0.5 to 2.5 structural model of a simply-supported column supported at the ring-frames applies. No significant weight savings can be attained by considering end effects for the trapezoidal corrugation configuration.

DOUBLE-WALL CYLINDER ANALYSIS

Analysis of a typical double-wall design point is conducted to determine the influence of cylinder length on the buckle pattern formed at the critical compression stress level. The example chosen for this analysis is as follows:

Shell covers - truss core sandwich
 Shell substructure - sine-wave shear webs
 Shell diameter - 400 inches
 Axial load level - 15,000 lb/in.
 Material - titanium 6-4 at room temperature

For various cylinder lengths from 200 inches to 1000 inches, the theoretical buckling patterns are determined from the analysis of Reference 9. The theoretical buckling coefficient of Reference 9 is given by the expression:

$$K = \frac{\eta}{(1 + \xi)^2} + \frac{(1 + \xi)^2}{4\eta} \left[\left(1 + \frac{1 - \mu}{2} (\xi + \theta) \frac{V_x}{\eta} \right) / \left(1 + \frac{1 - \mu}{2} (\xi + \theta) \frac{V_x}{\eta} + (1 + \xi \theta) \frac{V_x}{\eta} + \frac{1 - \mu}{2} (1 + \xi)^2 \frac{V_x^2}{\eta^2} \right) \right]$$

where:

$$\eta = \frac{a^2 (1 - \mu)^2}{m \pi^2 r h} \quad (\text{for shells with equal facing thicknesses})$$

$$\xi = \left(\frac{na}{m\pi r} \right)^2$$

A graph of the buckling coefficient, K , versus V_x for various values of θ is shown in figure 53. Each K value on this graph is determined by varying η and ξ for a given θ and V_x , and determining the minimum resulting coefficient. Figure 54 shows a typical point on the buckling coefficient graph. The graph

illustrates that several combinations of η and ξ can result in buckling coefficients which are quite similar, hence the question arises as to the sensitivity of the critical buckle pattern for combinations of the η and ξ parameters above and below the minimum K combination.

For the particular design example chosen, a stability analysis shows the optimum configuration to be:

$$\begin{aligned} h &= 3.0 \text{ inches (shell thickness)} \\ b &= 6.0 \text{ inches (substructure spacing axially)} \\ L &= 20.0 \text{ inches (substructure spacing circumferential)} \\ \theta &= 3.33 \\ V_x &= .200 \end{aligned}$$

Utilizing these values of V_x and θ , an analysis is performed using a computer program to determine the variation of the buckling coefficient, K, with various values of the η and ξ parameters. The resulting minimum K values for each combination of η and ξ are tabulated as follows:

Table XXVI

MINIMUM K VALUES
 $V_x = .200 \quad \theta = 3.33$

η	ξ	K
.4	.2	.7846
.6	.4	.7809 (Minimum)
.8	.6	.7836
1.0	.8	.7887

The data shows that the minimum buckling coefficient, K, occurs with the combination of $\eta = .6$ and $\xi = .4$, with slight variations in K for the other combinations listed (see figure 68). In order to determine what effect each of these combinations has on the cylinder buckle pattern, the data are analyzed further.

It can be shown that the number of waves circumferentially is given by the expression:

⊙ K_{MIN} FOR A GIVEN η FAMILY OF POINTS

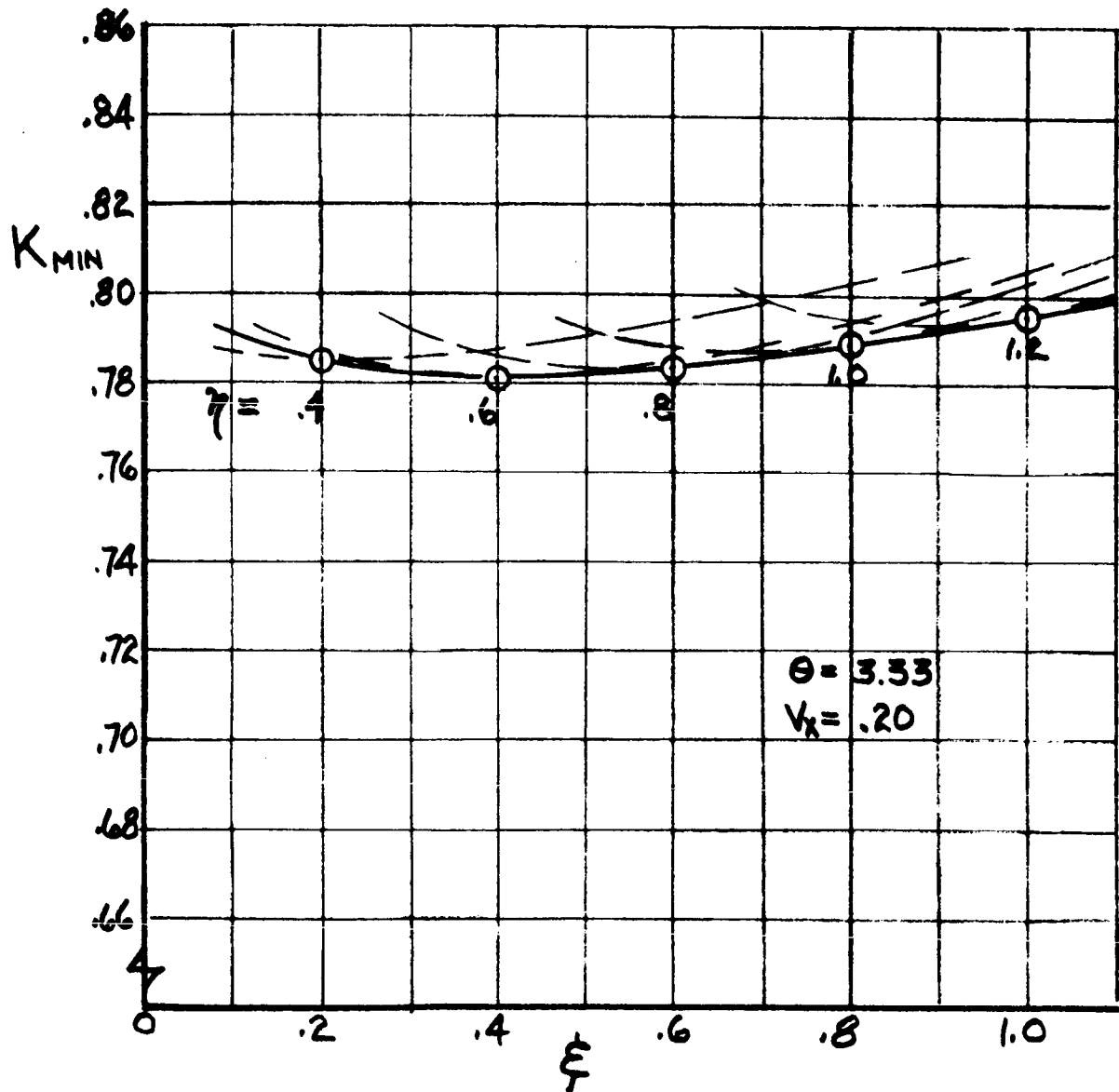


Figure 68. Variation of K_{MIN} With Shell Buckling Parameters

$$n = \left[\frac{\xi(1 - \mu^2)}{\eta h} r \right]^{1/2}$$

which for this particular example reduces to

$$n = 7.98 \left(\frac{\xi}{\eta} \right)^{1/2}$$

For the values of ξ and η listed previously, the number of waves circumferentially are shown as follows:

Table XXVII
CIRCUMFERENTIAL HALF-WAVE LENGTHS

η	ξ	n	n'	\bar{C}
.4	.2	5.60	5	125.6
.6	.4	6.50	6	104.5
.8	.6	6.88		
1.0	.8	7.10	7	89.5

Since the number of circumferential waves must be an integer, the values of n' were assumed to represent these integers. The quantity \bar{C} is the circumference of a 400-inch diameter cylinder divided by $2n$, or the length of each half-wave circumferential buckle.

The relationship between the parameters m and η can be expressed as:

$$m = \left[\frac{a^2 (1 - \mu^2)}{\pi^2 r h \eta} \right]^{1/2}$$

For this particular example, this expression reduces to

$$m = \frac{a}{79\eta^{1/2}}$$

The variation of m , the number of half-waves axially, for various assumed cylinder lengths, a , is tabulated as follows:

Table XXVIII

NUMBER OF LONGITUDINAL HALF-WAVES
 $m(1/2 \text{ waves axially, rounded-off to nearest half wave})$

η	$a = 200$	$a = 400$	$a = 600$	$a = 800$	$a = 1000$
.4	4.0	8.0	12.0	16.0	20.0
.6	3.5	6.5	10.0	13.0	16.5
.8	3.0	5.5	8.5	11.5	14.0
1.0	2.5	5.0	7.5	10.0	12.5

Converting these values to the length of each buckle ($\bar{L} = a/m$).

Table XXIX

LONGITUDINAL HALF WAVE LENGTHS

	$a = 200$	$a = 400$	$a = 600$	$a = 800$	$a = 1000$
η	Inches	Inches	Inches	Inches	Inches
.4	50.0	50.0	50.0	50.0	50.0
.6	57.1	61.5	60.0	61.5	60.6
.8	66.6	72.7	70.0	69.5	71.4
1.0	80.0	80.0	80.0	80.0	80.0

The tabulated data indicate that the length of the buckle half-wave axially is quite insensitive to the cylinder length at a given combination of the η and ξ parameters.

For a given cylinder length, the expected buckle length would be approximately 60 inches regardless of cylinder length, (K_{\min} occurs at $\eta = .6$). Maximum limits for the buckle length is between 50 and 80 inches. This shows that the circumferential shear web spacing of 20 inches is a reasonable figure for design.

COMPARISON OF STRUCTURAL STIFFNESS OF OPTIMUM CONCEPTS

Primary bending stiffness comparison of the selected ring stiffened and double-wall material/concepts was made with honeycomb construction. In the longitudinal direction of the cylinder, continuous stringer and skin elements become fully effective with non-buckled skin criterion, therefore, the total thickness of the covers, \bar{t} , is used in the moment of inertia computation. The bending stiffness comparison was based on the following equation:

$$EI = E \pi R_c^3 \bar{t}_{\text{cover}}$$

For the double-wall the nominal \bar{t}_{cover} is multiplied by two to include both covers.

LARGE DEFLECTION ANALYSIS

INTRODUCTION

Typical experiments conducted to determine the buckling stress of thin isotropic cylindrical shells are reported in Reference 13. In contrast to experience gained with other thin structural elements, e.g., plates and bars, the tests show appreciable differences from theoretical predictions by classical theory. The average buckling stress is only approximately 20 to 30 percent of the classical buckling stress (Reference 13). In addition to the disagreement in buckling stresses the test results show unusually large scatter.

The discrepancy between theory and tests has been attributed to several factors. Some interrelated factors are:

1. Initial imperfections
2. End support conditions
3. Difficulty in formulating the mathematically complex problem
4. Test machine flexibility
5. Post-buckling behavior.

Reference 14 provides an excellent account of post-buckling theory. Additional terms providing even greater theoretical accuracy are shown in Reference 15. End condition evaluation for unreinforced isotropic cylinders is developed in Reference 16. Typical post-buckling behavior shows sharply reduced load capacity after buckling occurs (Reference 17). It is postulated that initial imperfections have a significant effect upon the actual initial buckling stress, as shown in figure 71.

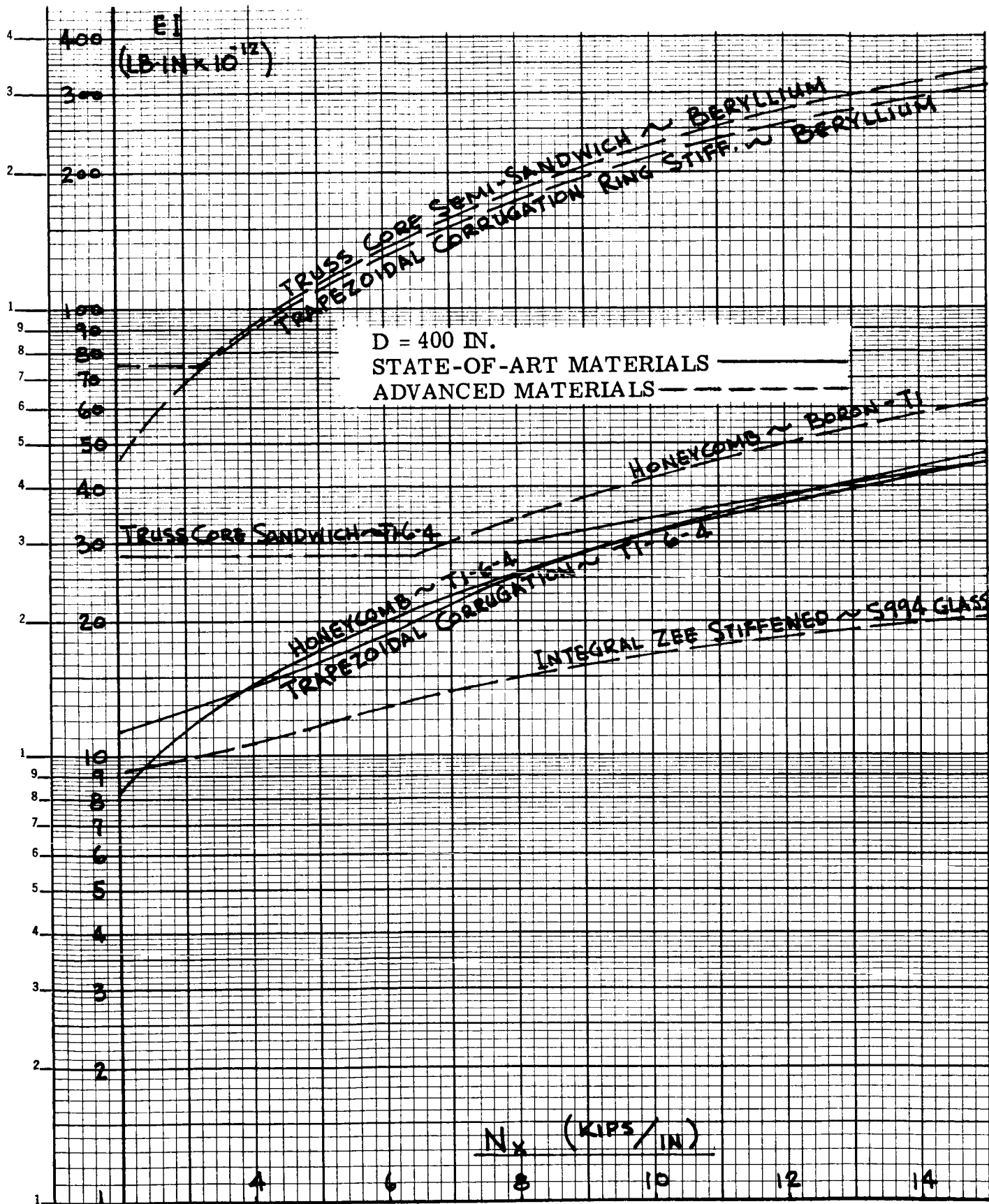


Figure 69. Comparison of Primary Bending Stiffness of Selected Concepts to Honeycomb ($D = 400$)

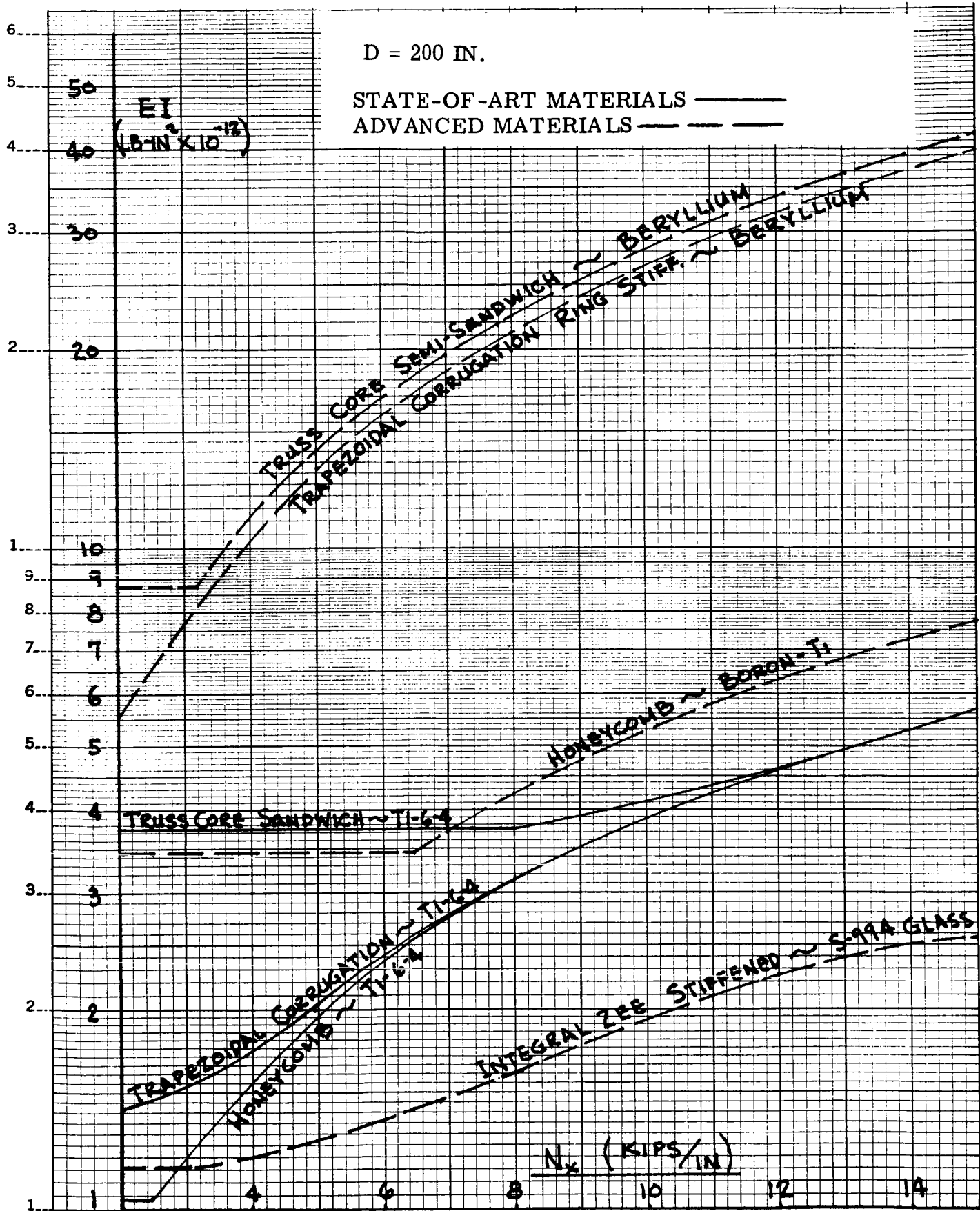


Figure 70. Comparison of Primary Bending Stiffness of Selected Concepts to Honeycomb ($D = 200$)

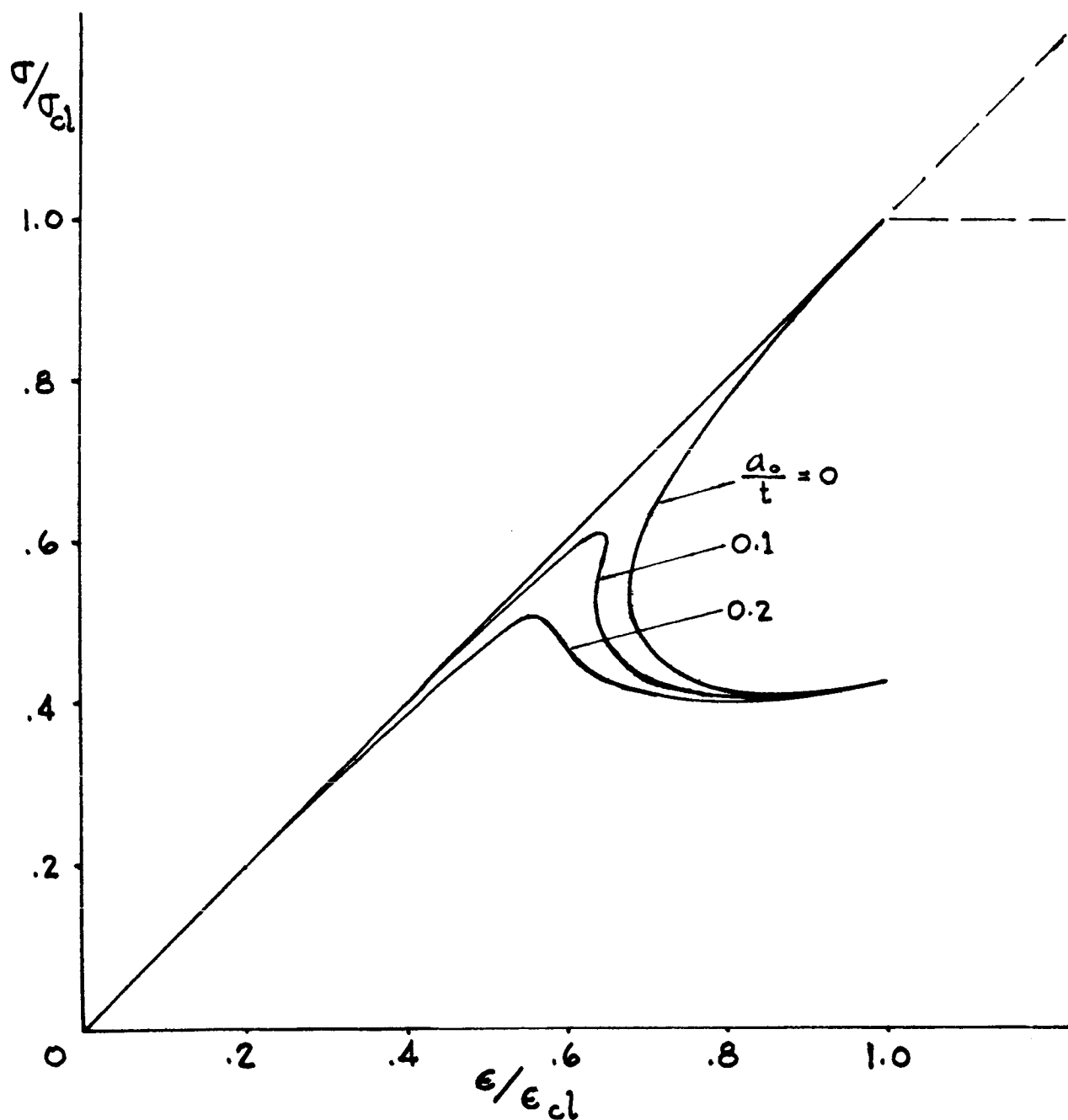


Figure 71. Postbuckling Response of Isotropic Cylinders With Initial Imperfections

Fortunately, the ring-stiffened cylinder, honeycomb cylinder, and the double-wall cylinder concepts are much more amenable to classical theoretical prediction than the thin isotropic shells. These particular cases are discussed later in this section.

Attempting to profit from the problems encountered in predicting thin shell buckling stresses, the designer asks, "What is the best design procedure to prevent premature failures? What is the weight penalty?" One method is to use large deflection theory. Another method is to assign an arbitrary safety factor to the questionable general stability margin of safety. Thus, cylinder general stability sizing is based upon effective load greater than the design load.

Both of these approaches lead to a more conservative design than the basic small deflection theory.

The large deflection analysis in this study, therefore, stresses two primary facets of the design problem.

1. Structural weight penalty of accommodating a design based on a more conservative general stability criterion.
2. Geometrical changes called for by the large deflection criterion.

HONEYCOMB AND DOUBLE-WALL CYLINDERS

Honeycomb and double-wall cylinder configurations have inherent characteristics that tend to preclude the disagreement found between theory and isotropic shell tests. Important factors are:

1. "Thick" versus "thin" shells
2. "Weak" core
3. Plastic range versus elastic range.

Tests show that the variation between theoretical predictions and test buckling stress is a function of R/t . As the shell wall thickness is increased for a given diameter, the difference between theory and test is decreased (Reference 17).

For shell configurations having flexible core tests show greater predictability (Reference 18).

Designs that fail in the plastic range tend to buckle in the pattern consistent with classical theory. Theory and test compare favorably (Reference 19).

A measure of each of these factors is found in the optimum design configurations. The need to design according to the more conservative large deflection analysis is, therefore, of much less consequence than in the case of isotropic cylinders.

Analysis of selected honeycomb and double-wall configurations for large deflection analysis is based upon Reference 20.

The mean cylinder buckling stress, σ , is predicted by the familiar equation:

$$\frac{\sigma}{\eta} = K E_x \frac{H}{R}$$

The value of K , as derived in Reference 20, is given by:

$$K = \frac{64}{z^2} \left(\frac{\gamma_3}{\eta} - \frac{9\gamma_2}{32\gamma_1\eta} + \gamma_4\eta \right)$$

where z and η are measures of the size of the buckling pattern. z and η are varied through a series of potential values to determine the minimum value of K .

As an illustration of the interdependence of the variables in the buckling phenomenon, the equations for γ_1 , γ_2 , γ_3 , and γ_4 follow:

$$\begin{aligned} \gamma_1 = & \frac{z^4}{4096} + \frac{E_y}{4096 E_x} + \frac{z^4}{512 \left(z^4 \frac{E_x}{E_y} + 81 + \frac{9z^2 E_x}{\mu_{xy}} - 18\sigma_{xy} z^2 \right)} \\ & + \frac{z^4}{512 \left(81z^4 \frac{E_x}{E_y} + 1 + 9z^2 \frac{E_x}{E_y} - 18\sigma_{xy} z^2 \right)} + \frac{17z^4}{2048 \left(z^4 \frac{E_x}{E_y} + 1 + \frac{z^2 E_x}{\mu_{xy}} - 2\sigma_{xy} z^2 \right)} \end{aligned}$$

$$\gamma_2 = \frac{E_y}{512 E_x} + \frac{z^4}{32 \left(z^4 \frac{E_x}{E_y} + 1 + \frac{z^2 E_x}{\mu_{xy}} - 2\sigma_{xy} z^2 \right)}$$

$$\gamma_3 = \frac{E_y}{256 E_x} + \frac{z^4}{32 \left(z^4 \frac{E_x}{E_y} + 1 + \frac{z^2 E_x}{\mu_{xy}} - 2\sigma_{xy} z^2 \right)}$$

$$y_4 = \frac{T}{32\lambda h (f_1 + f_2)} \left[\frac{I + \frac{I}{K_4} (d_1 d_3 - d_2^2) \frac{\eta}{E_x} \left(\frac{S_x}{z^2} + S_y \right)}{1 + \frac{\eta d_1 S_x}{E_x z^2} + \frac{\eta d_3 S_y}{E_x} + \frac{\eta (d_1 d_3 - d_2^2) S_x S_y}{E_x^2 z^2}} + I_f \right]$$

The peak value of K for the case of infinite core shear rigidity by this theory is 0.4. This value compares to the value of K = 1.0 for the small deflection theory. With assumptions comparable to those used in the basic small deflection analysis, the preceding equations are converted into the K vs V_x plot shown in figure 72.

RESULTS OF LARGE-DEFLECTION ANALYSIS

Results of first phase large deflection analysis for full depth honeycomb are shown in Table XXX. Weight vs load for the integrally stiffened double-wall concept is shown in figure 73 and Table XXXI. Weight increases and geometry changes necessary to satisfy the more conservative large deflection criterion is shown visually. First phase results indicate that the double-wall concept is affected to a much lesser extent than the honeycomb sandwich. The weight difference between theories for the sandwich cylinder is twice that for the double-wall concept. This is largely the result of an increased core weight for the sandwich cylinder, due to the increased core height necessitated by the more conservative theory.

Results of the second phase large deflection analysis for full depth honeycomb are shown in Table XXXII. Panel weight versus load for the truss core sandwich double-wall concept is shown in figure 74. A weight and geometry comparison is shown in Table XXXIII. Panel weight versus load for the truss core semisandwich double-wall concept is shown in figure 75. A weight and geometry summary is shown in Table XXXIV.

It is noted that the use of aluminum core in the honeycomb cylinder results in alleviating the impact of the large deflection analysis. This effect is most pronounced in the lower load region. Similarly, the sinewave shear web weight differential is much less than the first phase truss web weight differential.

INCREASED GENERAL STABILITY SAFETY FACTOR

The design of composite cylinders involves buckling of local elements as well as general cylinder instability. Experience in design permits a different confidence level in each category of instability. The buckling of local panel elements can be calculated with high reliability. Actually, a large post-buckling strength reserve is likely. General instability is the type of failure that so often fails to meet theoretical predictions.

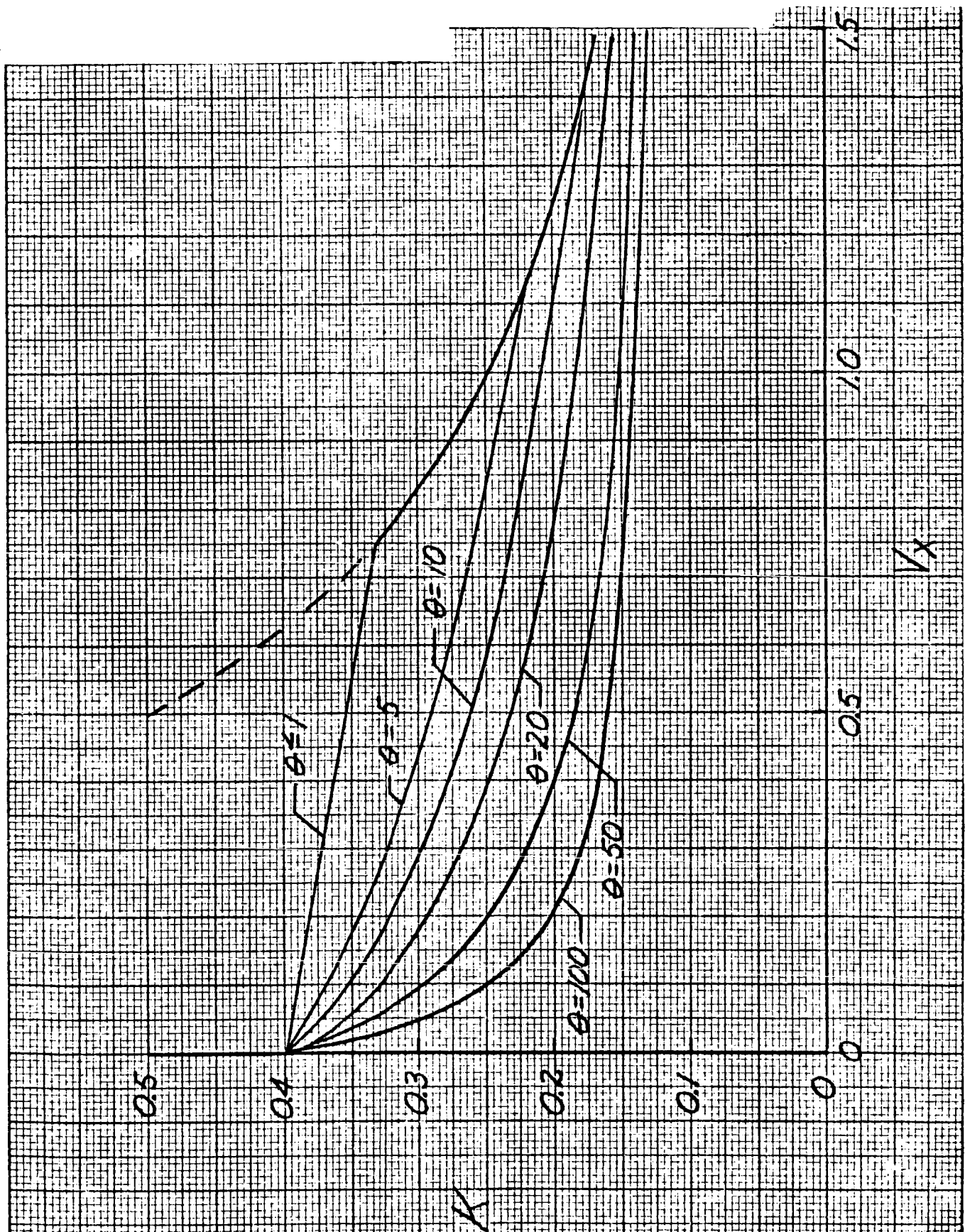
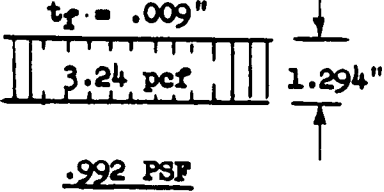
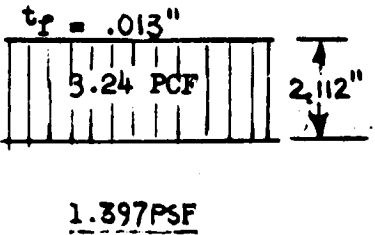
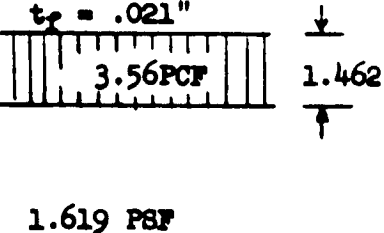
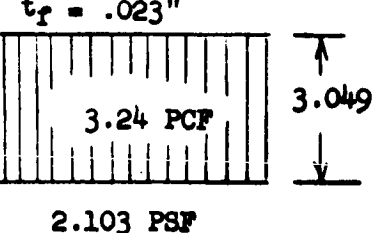
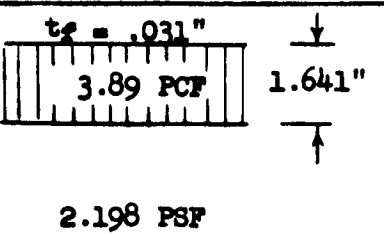
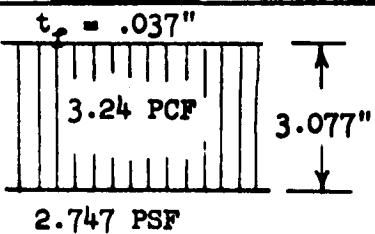
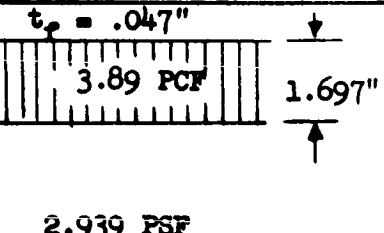
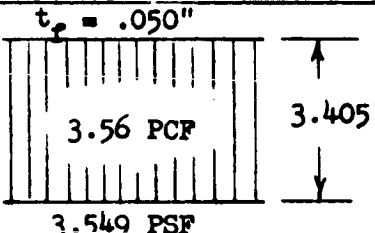
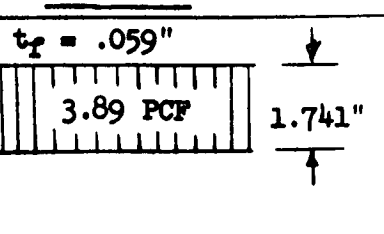
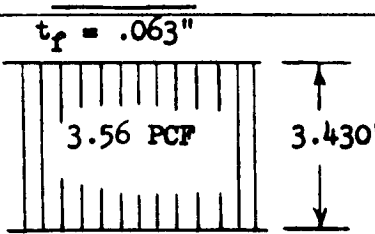
Figure 72. K Versus V_x for Large Deflection Analysis

Table XXX

WEIGHT AND CONFIGURATION COMPARISON
FULL DEPTH HONEYCOMB SHELL

DIAM = 400 INCHES TITANIUM 6-4 MATERIAL

N_x	SMALL DEFLECTION THEORY	LARGE DEFLECTION THEORY	WGT INCREASE RATIO
2000	$t_f = .009"$  <u>.992 PSF</u>	$t_f = .013"$  <u>1.397 PSF</u>	1.41
5000	$t_f = .021"$  <u>1.619 PSF</u>	$t_f = .023"$  <u>2.103 PSF</u>	1.30
8000	$t_f = .031"$  <u>2.198 PSF</u>	$t_f = .037"$  <u>2.747 PSF</u>	1.25
12000	$t_f = .047"$  <u>2.939 PSF</u>	$t_f = .050"$  <u>3.549 PSF</u>	1.21
15000	$t_f = .059"$  <u>3.497 PSF</u>	$t_f = .063"$  <u>4.137 PSF</u>	1.18

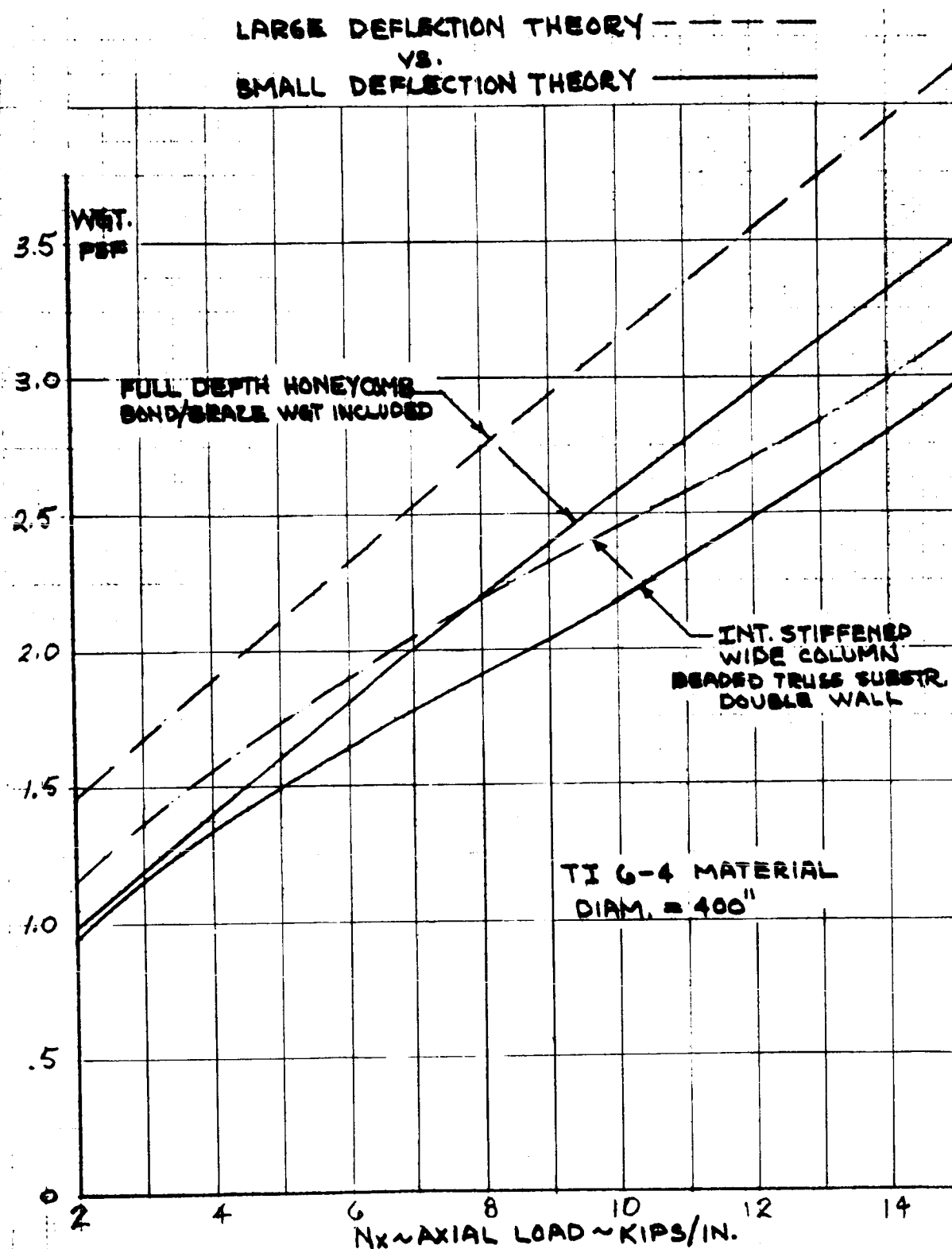


Figure 73. Weight Comparison Large Deflection Theory Versus Small Deflection Theory

Table XXXI

WEIGHT AND CONFIGURATION COMPARISON
INTEGRALLY STIFFENED WIDE COLUMN-BEADED TRUSS SUBSTRUCTURE











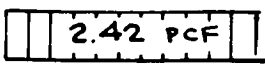
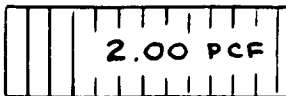
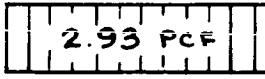
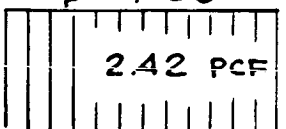
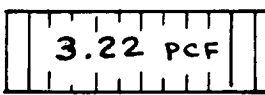
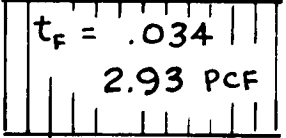
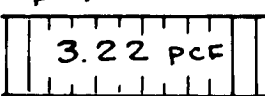
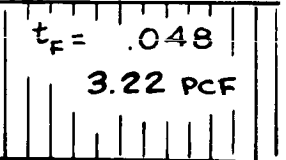
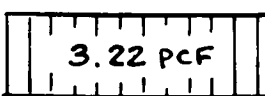
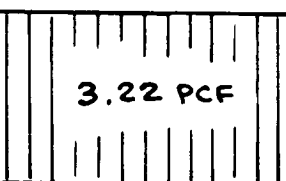
DIAM = 400 INCHES		TITANIUM 6-4 MATERIAL	
N_x	SMALL DEFLECTION THEORY	LARGE DEFLECTION THEORY	WGT INCREASE RATIO
2000	 .956 PSF	 1.156 PSF	1.22
5000	 1.512 PSF	 1.735 PSF	1.15
8000	 1.912 PSF	 2.197 PSF	1.15
12000	 2.479 PSF	 2.698 PSF	1.09
15000	 2.973 PSF	 3.164 PSF	1.065

Table XXXII

WEIGHT AND CONFIGURATION COMPARISON
FULL DEPTH HONEYCOMB SANDWICH SHELLALUMINUM CORE - TITANIUM 6-4 FACE
DIAM. = 400 IN. MATERIAL

N_x LB/IN	SMALL DEFLECTION THEORY	LARGE DEFLECTION THEORY	WEIGHT INCREASE RATIO
2000	$t_F = .010$ IN.  0.929 PSF	$t_F = .012$ IN.  1.167 PSF	1.26
5000	$t_F = .021$  1.644 PSF	$t_F = .026$  2.050 PSF	1.25
8000	$t_F = .031$  2.246 PSF	$t_F = .034$  2.745 PSF	1.22
12000	$t_F = .047$  3.094 PSF	$t_F = .048$  3.612 PSF	1.17
15000	$t_F = .058$  3.697 PSF	$t_F = .058$  4.211 PSF	1.14

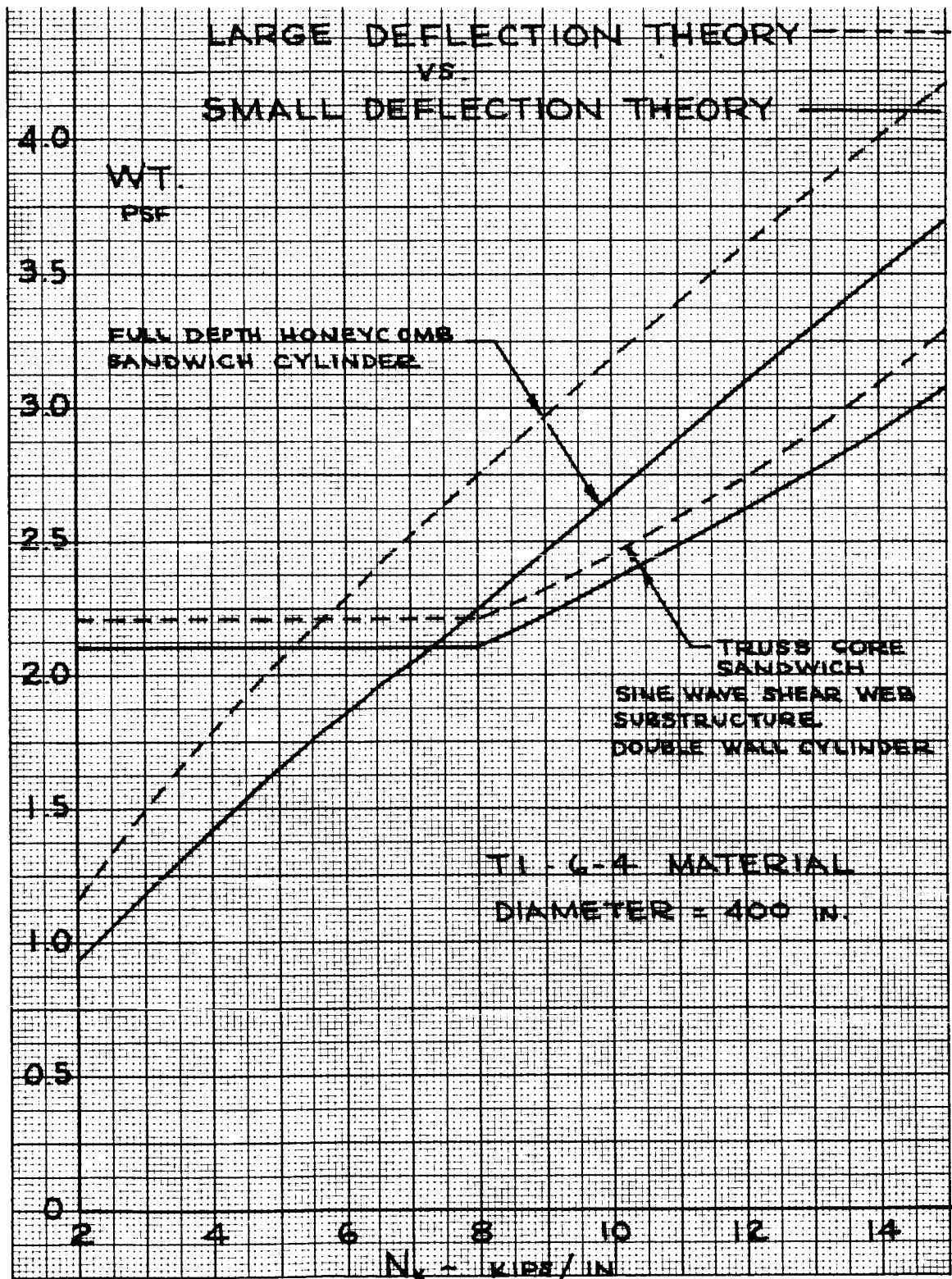
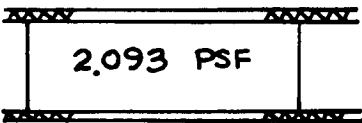
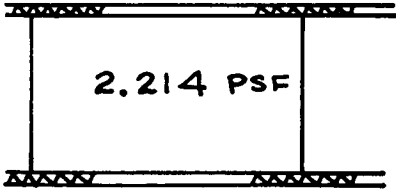
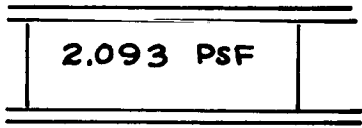
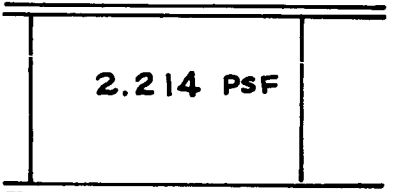
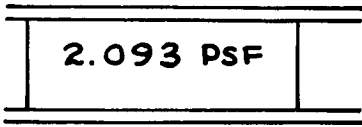
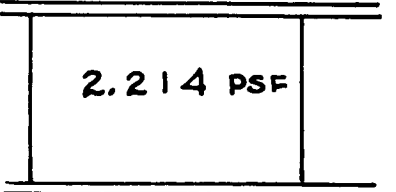
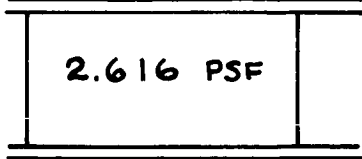
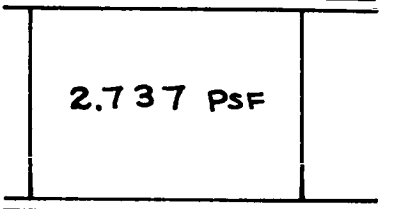
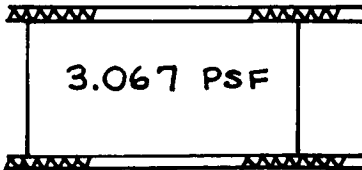
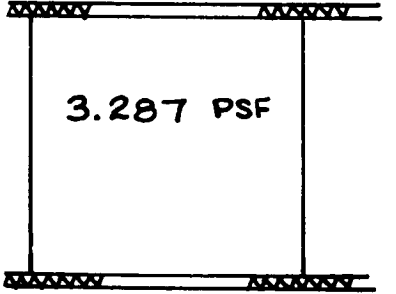


Figure 74. Weight Comparison Large Deflection Theory
Versus Small Deflection Theory

Table XXXIII

WEIGHT AND CONFIGURATION COMPARISON
 SINE WAVE SHEAR WEB SUBSTRUCTURE
 DIAM. = 400 IN. TITANIUM 6-4 MATERIAL

N_x LB./IN	SMALL DEFLECTION THEORY	LARGE DEFLECTION THEORY	WEIGHT INCREASE RATIO
2000	 2.093 PSF	 2.214 PSF	1.06
5000	 2.093 PSF	 2.214 PSF	1.06
8000	 2.093 PSF	 2.214 PSF	1.06
12000	 2.616 PSF	 2.737 PSF	1.05
15000	 3.067 PSF	 3.287 PSF	1.07

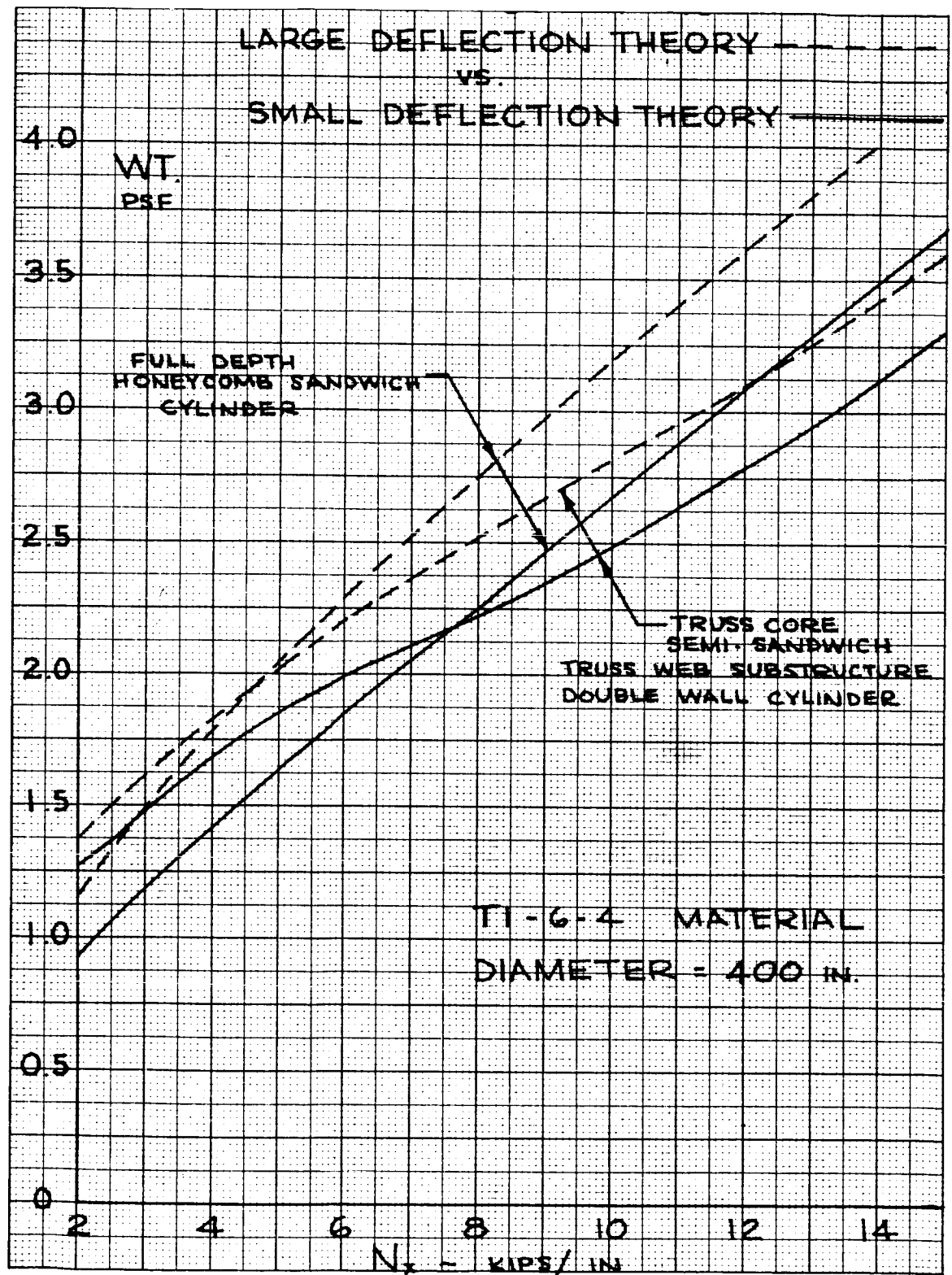
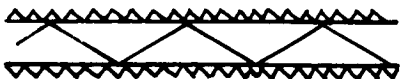
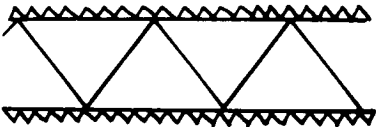
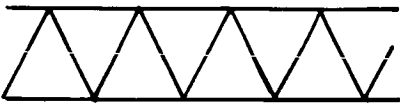
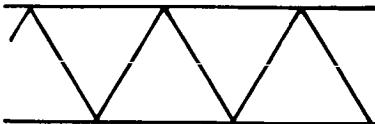
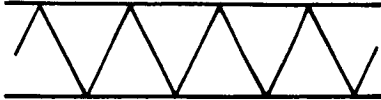
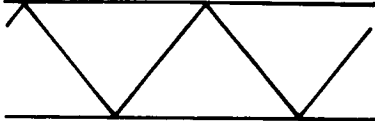
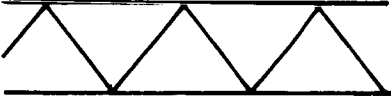
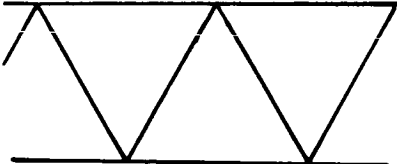
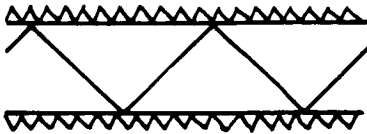
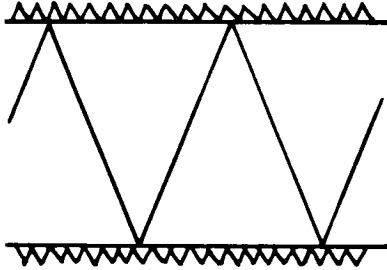


Figure 75. Weight Comparison Large Deflection Theory
Versus Small Deflection Theory

Table XXXIV

WEIGHT AND CONFIGURATION COMPARISON
 TRUSS CORE SEMI-SANDWICH PLATE COVER
 TRUSS WEB SUBSTRUCTURE
 DIAM. = 400 IN. TITANIUM 6-4 MATERIAL

N_x LB/IN	SMALL DEFLECTION THEORY	LARGE DEFLECTION THEORY	WEIGHT INCREASE RATIO
2000	 1.276 PSF	 1.387 PSF	1.09
5000	 1.850 PSF	 2.017 PSF	1.09
8000	 2.226 PSF	 2.519 PSF	1.13
12000	 2.781 PSF	 3.098 PSF	1.11
15000	 3.307 PSF	 3.601 PSF	1.09

A method of design that is investigated in this section takes account of this variation in confidence level. Local and panel stability predictions are based on the nominal design load. General stability is calculated with margins of safety of 0.00, 0.25, and 0.50. The resulting design, therefore, has a realistically high margin in general stability, while the local and panel stability criteria are designed with zero margin. The recognition of the true problem area and application of conservative design to this critical facet of the total problems offers the potential of design integrity with a low weight penalty.

Ring Stiffened Cylinders

The general stability equation used in the ring stiffened skin-stringer analysis is investigated to determine the structural weight increase for margins of safety of 0.0, 0.25, and 0.50. The margins of safety are not applied to the elastic buckling stress equation of the local structural elements; therefore, only the frame pitch "L" and radius of gyration " ρ " is affected in the following general stability equation:

$$\sigma_e = \frac{\pi^2 E}{(L/\rho)^2}$$

An abbreviation for the safety factor, (S.F.), is used. The reduced allowable general stability stress is given by the equation:

$$\sigma_{eR} = \frac{\pi^2 E}{(S.F.) (L/\rho)^2} \quad \therefore \sigma_e = \sigma_{eR} (S.F.)$$

Substitution of the reduced allowable general stability stress in the equivalent optimized stress equation yields:

$$\sigma_{oR} = \left[\frac{\sigma_e}{(S.F.)} \sigma_{cR}^2 \right]^{1/4}$$

$$\sigma_{oR} = \frac{\sigma_o}{(S.F.)^{1/4}}$$

The cover equivalent thickness is modified to include the margin of safety on general stability. The adjusted cover equivalent thickness, $\bar{t}_{M.S.}$, is obtained from the reduced equivalent stress relationship.

$$\frac{N_x}{\bar{t}_{M.S.}} = \frac{N_x}{\bar{t}_{cover} (S.F.)^{1/4}}$$

The total equivalent shell thickness, including the safety factor, is expressed as:

$$t = \bar{t}_{M.S.} + \bar{t}_{frame}$$

$$t = \bar{t}_{cover} (S.F.)^{1/4} + \bar{t}_{frame}$$

The cover and frame equivalent thickness distribution is then determined by adding the safety factor to the basic equation:

$$t = \frac{(S.F.)^{1/4}}{\alpha} \left[\frac{N_x L}{E \eta} \right]^{1/2} + \left[\frac{\pi R^4}{4000 k_4 L^3} \left(\frac{N_x}{E} \right) \right]^{1/2}$$

The optimum frame spacing for the trapezoidal corrugation, ($L = .2137 R^{1/4}$), is substituted into the preceding equation resulting in Reference 2:

$$t = (.2137 \eta^{1/4})^{1/2} \left[\frac{(S.F.)^{1/4} \left(\frac{N_x R}{E \eta} \right)^{1/2}}{1.264} + \left(\frac{\pi}{4000 (5.4) (.2137)^4} \right)^{1/2} \left(\frac{N_x R}{E \eta} \right)^{1/2} \right]$$

or

$$t = .462 \eta^{1/8} \left[.791 (S.F.)^{1/4} + .265 \right] \left(\frac{N_x R}{E \eta} \right)^{1/2}$$

The percentage increase in unit weight above zero margins of safety or safety factor of one:

$$\Delta\% = 1 - \left[\frac{.791 (S.F.)^{1/4} + .265}{.791 (1.00)^{1/4} + .265} \right]$$

$$\Delta\% = 1 - [.75 (S.F.)^{1/4} + .25]$$

The preceding equation is evaluated for the margins of safety under investigation in Table XXXV.

Table XXXV
WEIGHT INCREMENTS CAUSED BY VARIATION IN M.S.

M.S.	S.F.	(S.F.) ^{1/4}	.75(S.F.) ^{1/4}	.75(S.F.) ^{1/4} + .25	Δ%
0	1.00	1.00	.75	1.00	0
.25	1.25	1.059	.795	1.045	4.5
.50	1.50	1.107	.831	1.081	8.1

Double-Wall Cylinders

The general stability equation used in the double-wall analysis is investigated to determine the structural weight increase for margins of safety of 0.00, 0.25, and 0.50. The margins of safety are not applied to the buckling of structural elements.

For a given cover panel concept and material, the local stress level is established by specifying the axial load, N_x , and L, substructure spacing. The shell general instability design stress level is then established by multiplying the local allowable, σ_L , times the factor of safety, F.S. For local and general instability stress levels in the elastic range for a particular material

$$(F.S.) \times \sigma_L = \sigma_G = \frac{2KEH}{D(1-\mu^2)^{1/2}}$$

Solving for the product KH, we have

$$KH = (F.S.) \frac{D(1-\mu^2)^{1/2}}{2} \left(\frac{\epsilon}{E}\right)^{1/2} \left(\frac{N_x}{L}\right)^{1/2}$$

This relationship indicates that the KH product is directly proportional to the factor of safety. The relationship between the buckling coefficient, K, and shell height, H, is such that K and H are not independent. As H is increased, holding L **constant**, K is decreased at a slower rate. The KH product is primarily influenced by variations in core height, H. As the factor of safety is increased, increasing H proportionally has the effect of adding a minimum of weight to the cross section. This results because substructure weight is generally small in comparison to total weight.

The following example illustrates this effect. Consider an integrally stiffened, wide column concept with the beaded truss substructure. The material is titanium 6-4, and the diameter is 400 inches. With an axial load level of 5000 pounds per inch, and a substructure spacing of four inches, all stresses are elastic. From the shell stability, analysis at zero margin for the concept, the optimum shell height was found to be two inches. Increasing the height by the factors of safety of 1.25 and 1.50 results in the following conservative estimates for weight increase:

Table XXXVI

WEIGHT INCREASE VERSUS PANEL HEIGHT FOR VARYING M.S.

H	Weight Increase Ratio
2.0	1.0
2.5	1.05
3.0	1.08

A greater weight increase would result if the shell stability stress levels exceeded the proportional limit. Figure 76 shows the variation in weight penalty associated with a range of safety factors and shell stress levels for aluminum 7106 material. Depending on the desired safety factor, a weight increase of 12 to 20 percent results if the shell stress level is compression yield. This increase drops rapidly with decreasing stresses until a 5 to 8 percent increase is indicated for stress levels below the proportional limit.

It is emphasized that these percentage increases reflect comparisons of cross sections at equal load index values (N_x/L), where only the shell height has been altered to produce the required margin on shell instability.

The significance of including a margin of safety in the general stability margin offers increases in reliability for small weight increases. For optimum designs operating in the elastic range, the weight penalty is small. As the design stress level increases into the inelastic range the penalty increases.

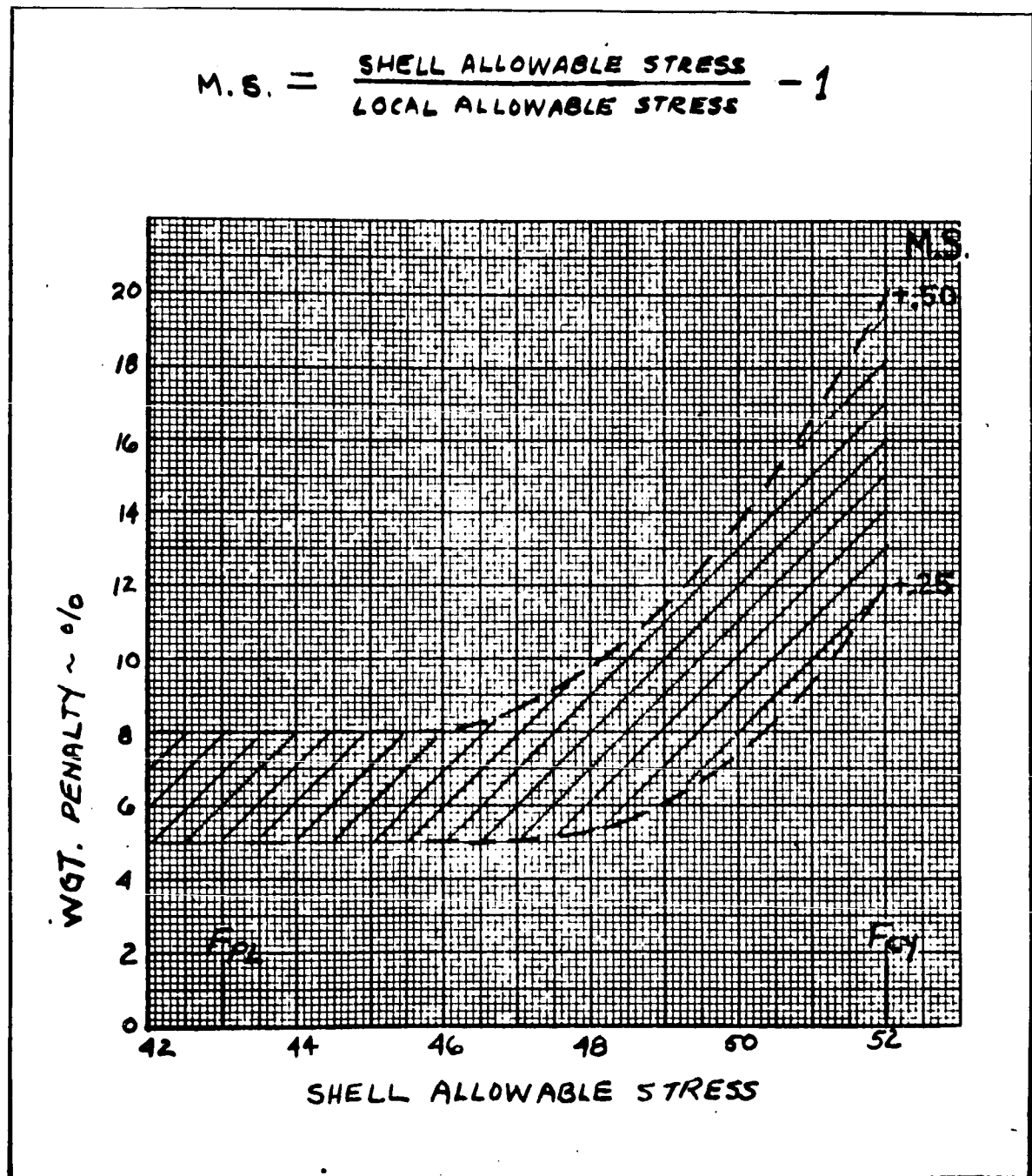


Figure 76. Margin of Safety Effect Integrally Stiffened Wide Column Beaded Truss Substructure Aluminum X7106

COST ANALYSIS

Six configurations, with two load levels per configuration and one type of material, are selected for cost evaluation. The configurations selected are producible and structurally effective. The purpose of the evaluation is to provide cost-weight relationships as a guide to selection of the more cost-weight effective configurations.

Two load levels are analyzed for each configuration to show a cost-load level effect. Except for an all-beryllium structure analyzed for 2000 lbs/in. and 5000 lbs/in. load levels, all configurations are analyzed at 5000 lbs/in. and 15,000 lbs/in. load levels.

Material, labor and burden, and tooling costs are given for each concept. Material costs include a rework, rejection, and procurement cost allowance. Labor and burden costs are based upon corporate-wide labor standards and reflect learning curve effects for quantities. Tooling costs are based upon quantity requirements for producing one shell structure per month. Costs given are engineering trade costs and do not include equipment and facilities items, engineering costs, profit, etc., normally utilized in establishing B and P or firm pricing quotes.

Because the wide range of potential structural sizes investigated would result in such a profusion, a single set of costs, the following parameters are selected. The shell structure is 400 inches in diameter and 400 inches long. Another condition established is that the substructure and inner and outer panels be of the same type of material. Additionally, all mechanical joints are required to be bonded with a room temperature curing adhesive, EPON 923, to provide additional stiffness at the joint.

Summary cost sheets give material, labor and burden, and tooling costs for each configuration and load level. (Reference figures 77 through 81.) Detail and assembly costs are given for quantities of fifty on total, per-square-foot, and per-pound basis. Additionally, the distribution of costs by percent of total cost is shown for all elements of cost. The per-square-foot values are based upon an area of 3490.7 square feet, which represents the surface area of the structure considered.

Curves depicting the effect of quantity on total cost, by configuration and load level, are given in figures 77, 78, and 79.

Figures 80 and 81 show a plot of the cost-weight effectiveness of each configuration by load level. The ring stiffened trapezoidal corrugation concept for the 2000 lbs/in. load level, is not represented as there is no competitive configuration that has been cost analyzed. The abscissa is cost per-square-foot of structure; the ordinate is weight per-square-foot of structure. By this chart, weight and weight saving can easily be cost related. If a line is drawn between the points representing any two configurations, the slope of that line represents the incremental cost per pound to change from one configuration to the other and save weight. Upon selecting a dollar value for saving a pound of weight, the configuration closest to the origin that is intersected by a slope line that represents the value of saving a pound of weight, is the optimum weight-cost effective configuration.

The truss-core semisandwich shows the best cost per-square-foot for both load levels, based upon requirements for 50 units. Reference figures 78 and 79. Based on lesser quantities, the trapezoidal corrugation is least expensive. Too, the trapezoidal corrugation could be cost-weight competitive with the truss-core semisandwich at 50 units at some nominal cost allowance for saving a pound of weight. Reference figure 80.

The integrally stiffened wide column concept is costed for machining the inner and outer panels, contributing to the relatively high cost per square foot. Compared to the panel design for truss-core sandwich, the integrally stiffened panels fabricated in a roll diffusion bonded concept would be of a simpler design, and would appear in a more favorable cost relationship than indicated in this analysis.

As all mechanical joints **are** also bonded, complete or partial elimination of either riveting or bonding requirements would reduce costs.

For a further cost reduction, alternate substructure concepts to the arc seam welded frames could be designed. For instance, "Zee" channels with flanged lightening holes, could be utilized at reduced costs.

A mix of substructure and cover materials could produce a more cost effective design. However, the cost-weight relationship would require analysis.

In summary, the number of units required, their cost and weight, and the amount of dollars that can be spent to save a pound of weight, are all important factors for making an effective design decision.

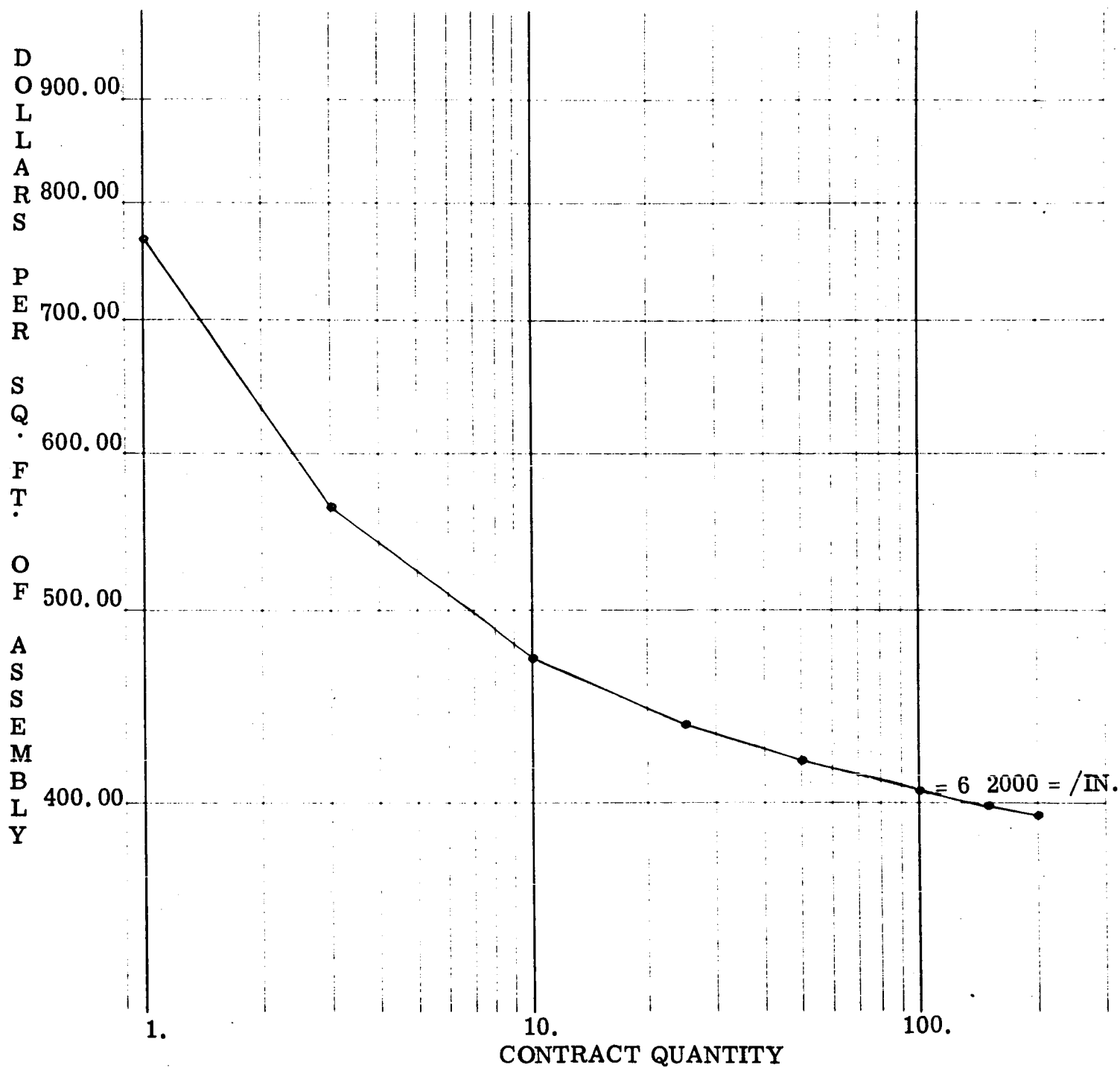


Figure 77. Effect of Quantity on Cost of Various Design Concepts
($P=2000 \text{ lb/in}$)

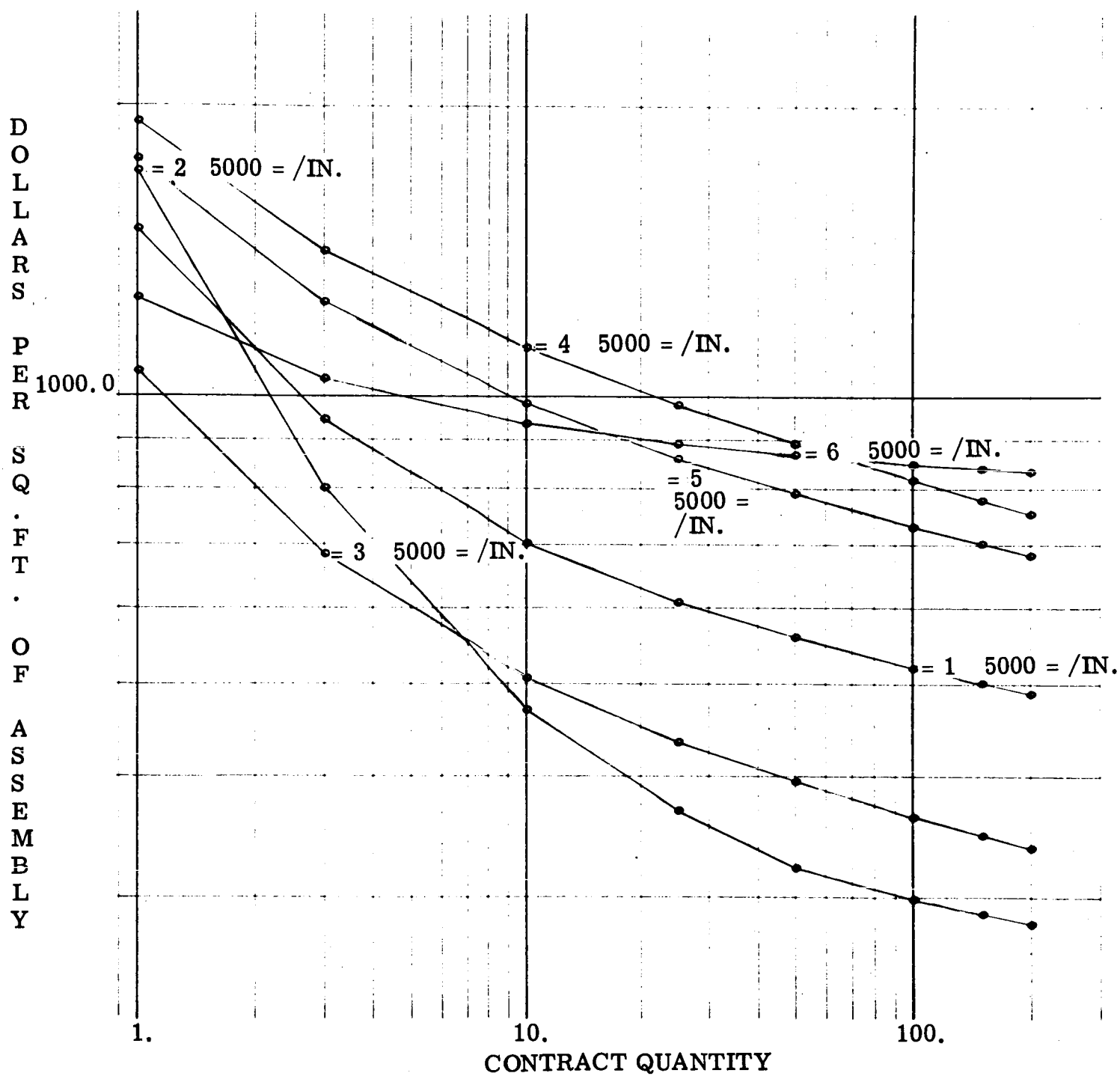


Figure 78. Effect of Quantity on Cost of Various Design Concepts

$$(P=5000 \text{ lb/in})$$

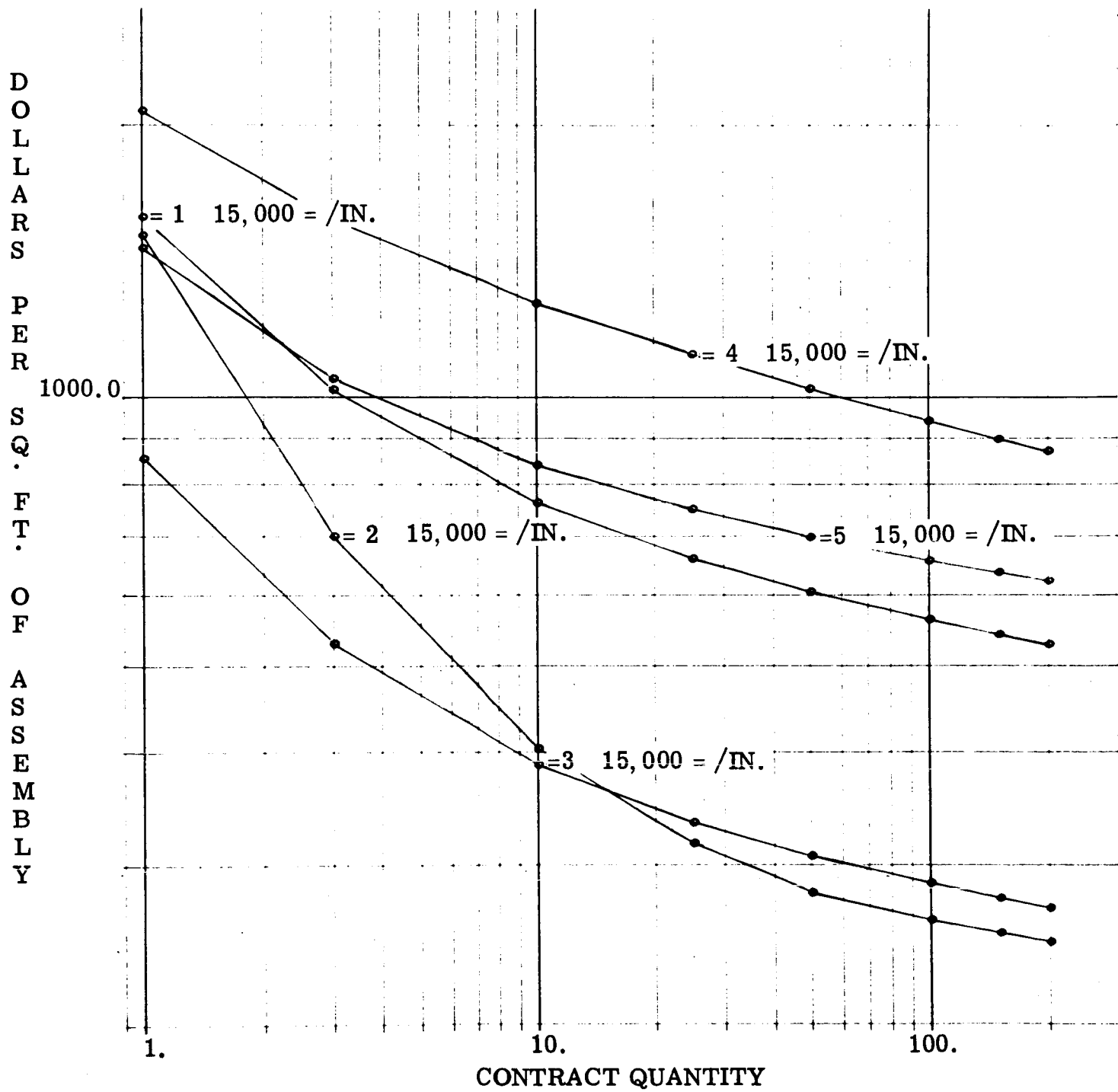


Figure 79. Effect of Quantity on Cost of Various Design Concepts

$$(P=15000 \text{ lb/in})$$

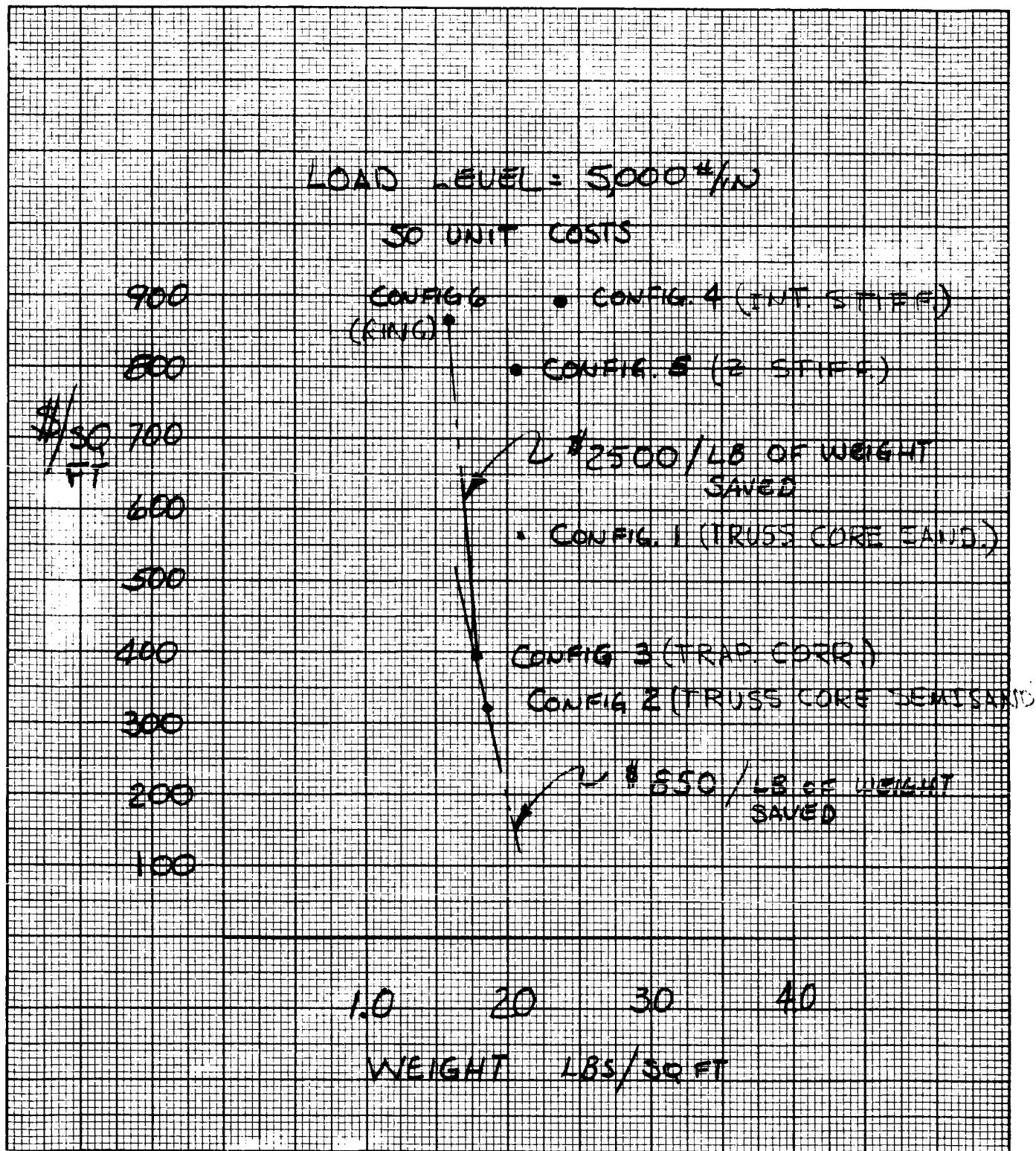


Figure 80. Cost/Weight Trade Study Chart

(P=5000 $\frac{\text{lb}}{\text{in}}$)

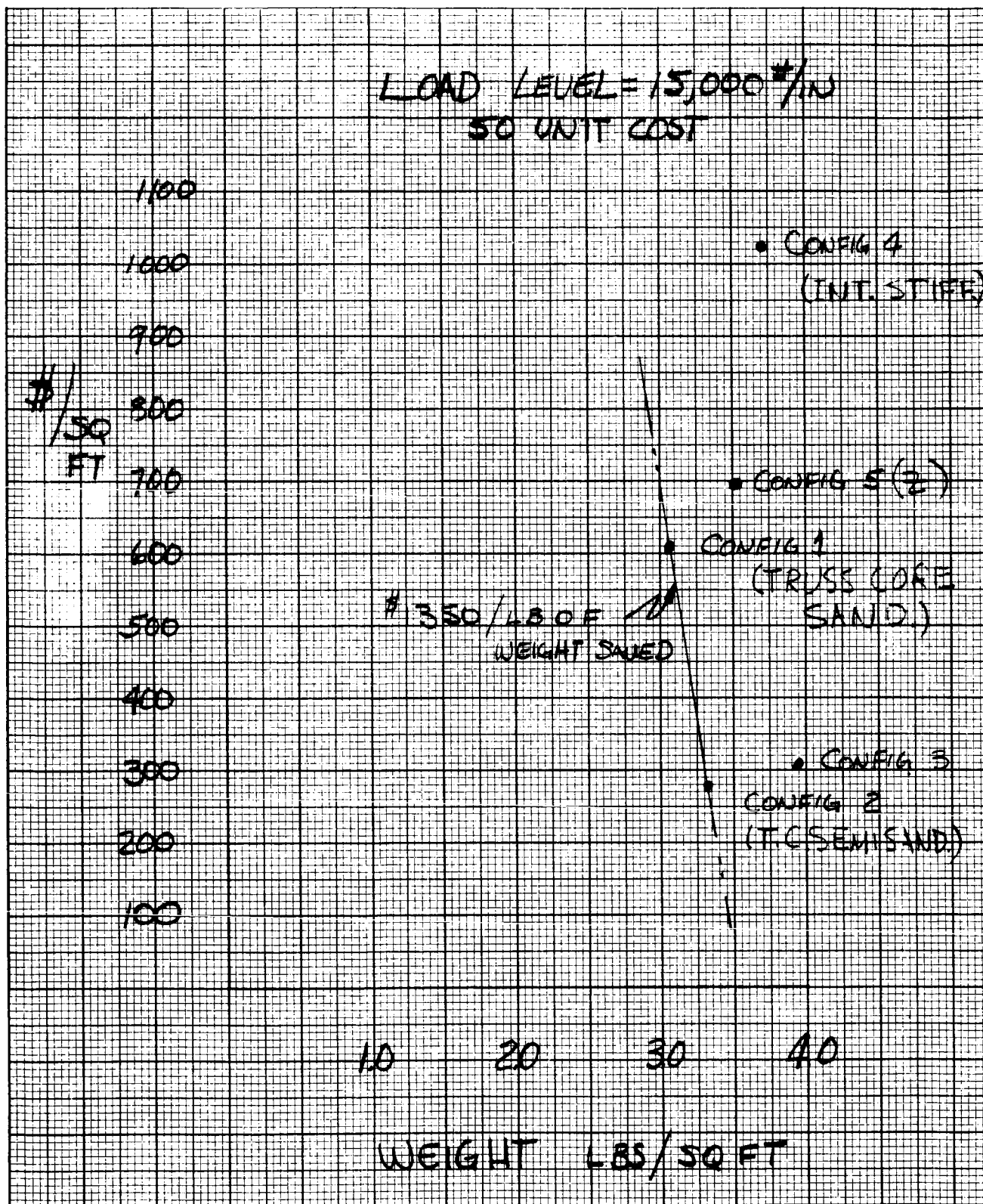


Figure 81. Cost/Weight Trade Study Chart

(P=15,000 lb/in)

Table XXXVII

SUMMARY OF DASH NUMBERED PARTS IN ASSEMBLY =1 5000=/IN -
TRUSS CORE, SINE WELD

DASH NUMBER	PART NAME	QUANTITY PER ASSY	UNIT COST	COST PER SQ. FT.	PERCENT COST OF ASSEM.
-3	SKINS-TRUSS	136	567.56	22.11	3.96
-5	CORE-TRUSS	844	6.06	1.46	0.26
-7	SKINS-TRUSS	136	567.56	22.11	3.96
-9	CORE-TRUSS	844	6.06	1.46	0.26
-13	CAP-SPAR	008	7.93	2.29	0.41
-15	WEB-SPAR	520	29.22	21.10	3.78
-17	CAP-FRAME	518	0.77	1.00	0.18
-19	WEB-FRAME	259	1.62	1.05	0.19
-23	SPLICE-LOT.	68	33.91	0.66	0.12
-25	SPLICE-TRNV.	34	19.57	0.19	0.03
-27	SPLICE-DBLR	34	3.42	0.03	0.01
-29	CLIPS	036	0.72	1.85	0.33
-33	COVER-RETORT	272	191.42	14.92	2.67
-35	YOKE-RETORT	136	427.36	16.65	2.98
-37	FILLERS-RTRT	272	6.95	0.54	0.10
-39	MANDRELS	392	0.75	12.36	2.21
-43	MANDRELS	392	0.16	2.61	0.47
-45	TUBE	136	18.30	0.71	0.13
-1	ASSEMBLY	1	519617.83	435.33	77.95

FINAL COST OF ASSEMBLY=1 5000=/IN	1949374.59	
FINAL COST PER SQ.FT. OF ASSEMBLY	558.45	
TOTAL MATERIAL COST PER ASSEMBLY	682390.36	PERCENT ASSEMBLY COST 35.01
TOTAL FABRICATION COST PER ASSEMBLY	1225989.56	PERCENT ASSEMBLY COST 62.89
TOTAL PRORATED TOOLING COST PER ASSEMBLY	40994.83	PERCENT ASSEMBLY COST 2.10

Table XXXVIII

SUMMARY OF DASH NUMBERED PARTS IN ASSEMBLY =1 15000=/IN -
TRUSS CORE, SINE WELD

DASH NUMBER	PART NAME	QUANTITY PER ASSY	UNIT COST	COST PER SQ. FT.	PERCENT COST OF ASSEM.
-3	SKINS-TRUSS	136	567.56	22.11	3.65
-5	CORE-TRUSS	616	7.06	1.25	0.21
-7	SKINS-TRUSS	136	567.56	22.11	3.65
-9	CORE-TRUSS	616	7.06	1.25	0.21
-13	CAP-SPAR	260	7.93	2.86	0.47
-15	WEB-SPAR	150	26.25	23.69	3.91
-17	CAP-FRAME	652	0.73	1.18	0.19
-19	WEB-FRAME	826	1.47	1.19	0.20
-23	SPLICE-LOT.	66	33.91	0.66	0.11
-25	SPLICE-TRNV.	34	19.57	0.19	0.03
-27	SPLICE-DBLR	34	3.42	0.03	0.01
-29	CLIPS	304	0.71	2.31	0.38
-33	COVER-RETORT	272	191.42	14.92	2.46
-35	YOKE-RETORT	136	427.36	16.65	2.75
-37	FILLERS-RTRT	272	6.95	0.54	0.09
-39	MANDRELS	568	0.25	3.00	0.50
-43	MANDRELS	568	0.25	3.00	0.50
-45	TUBE	136	16.64	0.73	0.12
-1	ASSEMBLY	1	705103.05	488.47	80.59

FINAL COST OF ASSEMBLY=1 15000=/IN
FINAL COST PER SQ.FT. OF ASSEMBLY
TOTAL MATERIAL COST PER ASSEMBLY
TOTAL FABRICATED COST PER ASSEMBLY
TOTAL PRORATED TOOLING COST PER
ASSEMBLY

2115866.09
606.14
743205.30
1331666.11
40994.83

PERCENT ASSEMBLY COST 35.13
PERCENT ASSEMBLY COST 62.94
PERCENT ASSEMBLY COST 1.94

Table XXXIX

SUMMARY OF DASH NUMBERED PARTS IN ASSEMBLY =2 5000=/IN -
SEMI-SAND, BEAD TRUSS

DASH NUMBER	PART NAME	QUANTITY PER ASSY	UNIT COST	COST PER SQ. FT.	PERCENT COST OF ASSEM.
-3	FACE SHEET	36	1765.38	18.21	5.66
-5	CORRUGATION	216	565.93	35.02	10.90
-7	FACE SHEET	36	1765.38	18.21	5.66
-9	CORRUGATION	216	217.24	13.44	4.18
-11	TRUSS	180	600.98	30.99	9.64
-13	SPLICT-LGT.	72	17.19	0.35	0.11
-15	SPLICE-TRVU.	54	36.14	0.56	0.17
-17	SPLICE-DBLR	54	1.89	0.03	0.01
-1	ASSEMBLY	1	714190.13	204.60	63.66

FINAL COST OF ASSEMBLY=2 5000=/IN	1121928.88		
FINAL COST PER SQ.FT. OF ASSEMBLY	321.41		
TOTAL MATERIAL COST PER ASSEMBLY	267457.91	PERCENT ASSEMBLY COST	23.84
TOTAL FABRICATION COST PER ASSEMBLY	787046.84	PERCENT ASSEMBLY COST	70.15
TOTAL PRORATED TOOLING COST PER ASSEMBLY	87424.15	PERCENT ASSEMBLY COST	6.01

Table XL

SUMMARY OF DASH NUMBERED PARTS IN ASSEMBLY =2 15000=/IN -
SEMI-SAND, BEAD TRUSS

DASH NUMBER	PART NAME	QUANTITY PER ASSY	UNIT COST	COST PER SQ. FT.	PERCENT COST OF ASSEM.
-3	FACE SHEET	36	3324.08	34.28	12.26
-5	CORRUGATION	216	327.01	20.23	7.24
-7	FACE SHEET	36	3324.08	34.28	12.26
-9	CORRUGATION	216	327.01	20.23	7.24
-11	TRUSS	180	597.46	30.81	11.02
-13	SPLICE-LGT.	72	17.19	0.35	0.13
-15	SPLICE-TRNV.	54	99.97	1.55	0.55
-17	SPLICE-DBLR.	54	1.89	0.03	0.01
-1	ASSEMBLY	1	481236.39	137.86	49.30

FINAL COST OF ASSEMBLY=2 15000=/IN
FINAL COST PER SQ.FT. OF ASSEMBLY

976121.52
279.63

TOTAL MATERIAL COST PER ASSEMBLY
TOTAL FABRICATION COST PER ASSEMBLY
TOTAL PRORATED TOOLING COST PER
ASSEMBLY

389472.07 PERCENT ASSEMBLY COST 39.90
519225.32 PERCENT ASSEMBLY COST 53.19
67424.15 PERCENT ASSEMBLY COST 6.91

Table XLI

SUMMARY OF DASH NUMBERED PARTS IN ASSEMBLY =3 5000=/IN -
TRAP. CORE-SINE WELD

DASH NUMBER	PART NAME	QUANTITY PER ASSY	UNIT COST	COST PER SQ. FT.	PERCENT COST OF ASSEM.
-3	TRAP. CORE	192	515.43	28.35	7.18
-5	TRAP. CORE	192	515.43	28.35	7.18
-7	CAP-SPARS	256	4.53	0.33	0.08
-9	WEB-SPARS	200	1.94	1.78	0.45
-13	CAP-FRAMES	464	5.18	9.59	2.43
-15	WEB-FRAMES	232	42.21	39.08	9.90
-17	SPLICE-TRNV.	66	10.03	0.19	0.05
-19	SPACERS	152	0.11	3.05	0.77
-23	CLIPS	928	0.90	3.32	0.84
-25	SPLICE-SPAR	96	0.78	0.02	0.01
-1	ASSEMBLY	1	979576.15	280.62	71.10

FINAL COST OF ASSEMBLY=3 5000=/IN 1377723.73
FINAL COST PER SQ.FT. OF ASSEMBLY 394.68

TOTAL MATERIAL COST PER ASSEMBLY	159902.65	PERCENT ASSEMBLY COST	11.61
TOTAL FABRICATION COST PER ASSEMBLY	1193271.11	PERCENT ASSEMBLY COST	86.61
TOTAL PRORATED TOOLING COST PER ASSEMBLY	24550.00	PERCENT ASSEMBLY COST	1.78

Table XLII

SUMMARY OF DASH NUMBERED PARTS IN ASSEMBLY =3 15000=/IN -
TRAP. CORE-SINE WELD

DASH NUMBER	PART NAME	QUANTITY PER ASSY	UNIT COST	COST PER SQ. FT.	PERCENT COST OF ASSEM.
-3	TRAP. CORE	144	776.63	32.04	10.43
-5	TRAP. CORE	144	776.63	32.04	10.43
-7	CAP-SPARS	256	20.30	1.49	0.48
-9	WEB-SPARS	200	2.75	2.52	0.82
-13	CAP-FRAMES	288	11.71	14.39	4.68
-15	WEB-FRAMES	144	43.52	26.73	8.70
-17	SPLICE-TRNV.	66	52.20	0.99	0.32
-19	SPACERS	328	0.04	0.96	0.31
-23	CLIPS	576	1.06	2.60	0.85
-25	SPLICE-SPAR	96	0.90	0.02	0.01
-1	ASSEMBLY	1	674907.00	193.34	62.96

FINAL COST OF ASSEMBLY=3 15000=/IN 1072029.61
FINAL COST PER SQ.FT. OF ASSEMBLY 307.11

TOTAL MATERIAL COST PER ASSEMBLY	259553.66	PERCENT ASSEMBLY COST	24.21
TOTAL FABRICATION COST PER ASSEMBLY	787925.70	PERCENT ASSEMBLY COST	73.50
TOTAL PRORATED TOOLING COST PER ASSEMBLY	24550.27	PERCENT ASSEMBLY COST	2.29

Table XLIII

SUMMARY OF DASH NUMBERED PARTS IN ASSEMBLY =4 5000-/IN -
INTEGRAL SKIN-SINE 2

DASH NUMBER	PART NAME	QUANTITY PER ASSY	UNIT COST	COST PER SQ. FT.	PERCENT COST OF ASSEM.
-3	SKIN-UPPER	84	11453.85	275.62	30.88
-5	SKIN-LOWER	84	11453.85	275.62	30.88
-7	SINE ZEE	188	160.37	54.58	6.11
-8	SINE-ZEE	188	160.37	54.58	6.11
-9	SPLICE-LONG.	54	29.95	0.46	0.05
-13	SPLICE-ZEE	376	0.93	0.63	0.07
-15	SPLICE-TRNV.	36	29.58	0.31	0.03
-1	ASSEMBLY	1	605431.25	230.74	25.85

FINAL COST OF ASSEMBLY=4 5000-/IN 3115590.06
FINAL COST PER SQ.FT. OF ASSEMBLY 892.54

TOTAL MATERIAL COST PER ASSEMBLY	906615.88	PERCENT ASSEMBLY COST	29.10
TOTAL FABRICATION COST PER ASSEMBLY	2187552.25	PERCENT ASSEMBLY COST	70.21
TOTAL PRORATED TOOLING COST PER ASSEMBLY	21422.05	PERCENT ASSEMBLY COST	0.69

Table XLIV

SUMMARY OF DASH NUMBERED PARTS IN ASSEMBLY=4 15000=/IN -
INTEGRAL SKIN-SINE 2

DASH NUMBER	PART NAME	QUANTITY PER ASSY	UNIT COST	COST PER SQ. FT.	PERCENT COST OF ASSEM.
-3	SKIN-UPPER	84	15712.46	378.10	36.94
-5	SKIN-LOWER	84	15712.46	378.10	36.94
-7	SINE-ZEE	900	167.39	43.16	4.22
-8	SINE-ZEE	900	167.39	43.16	4.22
-9	SPLICE-LONG.	54	42.26	0.65	0.06
-13	SPLICE-ZEE	800	0.93	0.48	0.05
-15	SPLICE-TRNV.	36	91.53	0.94	0.09
-1	ASSEMBLY	1	624736.39	178.97	17.48

FINAL COST OF ASSEMBLY=4 15000=/IN 3572992.06
FINAL COST PER SQ.FT. OF ASSEMBLY 1023.57

TOTAL MATERIAL COST PER ASSEMBLY	1047324.65	PERCENT ASSEMBLY COST	29.31
TOTAL FABRICATION COST PER ASSEMBLY	2504245.53	PERCENT ASSEMBLY COST	70.09
TOTAL PRORATED TOOLING COST PER ASSEMBLY	21422.05	PERCENT ASSEMBLY COST	0.60

Table XLV

SUMMARY OF DASH NUMBERED PARTS IN ASSEMBLY=5 5000-/IN -
ZEE STIFF, SINE ZEE

DASH NUMBER	PART NAME	QUANTITY PER ASSY	UNIT COST	COST PER SQ. FT.	PERCENT COST OF ASSEM.
-3	SKINS-STIFF	136	573.82	22.36	2.83
-5	CORE-STIFF	308	7.27	0.64	0.08
-7	SKINS-STIFF	136	19.54	0.76	0.10
-9	CORE-STIFF	308	7.27	0.64	0.08
-13	WEB-FRAME-RH	261	142.44	92.26	11.68
-15	WEB-FRAME-LH	261	142.44	92.26	11.68
-17	SPLICE-LGT	68	44.75	0.87	0.11
-19	SPLICE-TRNV.	34	33.72	0.33	0.04
-23	SPLICE-WEB	522	0.81	1.05	0.13
-25	COVER-RETORT	272	191.42	14.92	1.89
-27	YOKE-RETORT	136	427.36	16.65	2.11
-29	FILLERS-RTRT	272	6.95	0.54	0.07
-33	MANDRELS	332	0.76	4.42	0.56
-35	MANDRELS	332	0.76	4.42	0.56
-37	TUBE	136	18.84	0.73	0.09
-1	ASSEMBLY	1	874552.80	537.01	67.99

FINAL COST OF ASSEMBLY = 5 5000-/IN.

2757217.94

FINAL COST PER SQ. FT. OF ASSEMBLY

789.88

TOTAL MATERIAL COST PER ASSEMBLY

1063668.14

PERCENT ASSEMBLY COST 38.58

TOTAL FABRICATION COST PER ASSEMBLY

1668845.23

PERCENT ASSEMBLY COST 60.53

TOTAL PRORATED TOOLING COST PER ASSEMBLY

24704.73

PERCENT ASSEMBLY COST 0.90

Table XLVI

SUMMARY OF DASH NUMBERED PARTS IN ASSEMBLY =5 15000=/IN -
ZEE STIFF, SINE ZEE

DASH NUMBER	PART NAME	QUANTITY PER ASSY	UNIT COST	COST PER SQ. FT.	PERCENT COST OF ASSEM.
-3	SKINS-STIFF	136	646.93	25.21	3.61
-5	CORE-STIFF	172	7.66	0.38	0.05
-7	SKINS-STIFF	136	646.93	25.21	3.61
-9	CORE-STIFF	172	7.66	0.38	0.05
-13	WEB-FRAME-RH	360	150.31	58.56	8.38
-15	WEB-FRAME-LH	360	150.31	58.56	8.38
-17	SPLICE-LGT	68	44.75	0.87	0.12
-19	SPLICE-TRNV	34	33.72	0.33	0.05
-23	SPLICE-WEB	720	0.62	0.64	0.09
-25	COVER-RETORT	272	191.42	14.92	2.14
-27	YOKE-RETORT	136	427.36	16.65	2.38
-29	FILLERS-RTRT	272	2.86	0.22	0.03
-33	MANDRELS	696	2.68	9.00	1.29
-35	MANDRELS	696	2.68	9.00	1.29
-37	TUBE	136	18.84	0.73	0.11
-1	ASSEMBLY	1	668134.69	477.88	68.41

FINAL COST OF ASSEMBLY-5 15000-/IN 2438352.59
FINAL COST PER SQ.FT. OF ASSEMBLY 698.53

TOTAL MATERIAL COST PER ASSEMBLY	1248688.89	PERCENT ASSEMBLY COST	51.21
TOTAL FABRICATION COST PER ASSEMBLY	1164959.13	PERCENT ASSEMBLY COST	47.78
TOTAL PRORATED TOOLING COST PER ASSEMBLY	24704.73	PERCENT ASSEMBLY COST	1.01

Table XLVII

SUMMARY OF DASH NUMBERED PARTS IN ASSEMBLY #6 2000-/IN -
RING STIFF TRAPEZOID

DASH NUMBER	PART NAME	QUANTITY PER ASSY	UNIT COST	COST PER SQ. FT.	PERCENT COST OF ASSEM.
-3	CORRUGATION	245	3417.49	239.86	57.16
-5	RING FRAME	154	2529.60	111.60	26.59
-7	SPLICE-FRAME	154	22.02	0.97	0.23
-9	SPLICE-LONG.	245	224.20	15.74	3.75
-13	SPLICE-CAP	308	11.02	0.97	0.23
-15	SPLICE-TRNV.	196	264.83	14.87	3.54
-1	ASSEMBLY	1	124454.92	35.65	8.50

FINAL COST OF ASSEMBLY-6 2000-/IN 1464920.48
 FINAL COST PER SQ.FT. OF ASSEMBLY 419.66

TOTAL MATERIAL COST PER ASSEMBLY	1097346.31	PERCENT ASSEMBLY COST	74.91
TOTAL FABRICATION COST PER ASSEMBLY	350997.79	PERCENT ASSEMBLY COST	23.96
TOTAL PRORATED TOOLING COST PER ASSEMBLY	16576.44	PERCENT ASSEMBLY COST	1.13

Table XLVIII

SUMMARY OF DASH NUMBERED PARTS IN ASSEMBLY-6 5000-/IN -
RING STIFF TRAPEZOID

DASH NUMBER	PART NAME	QUANTITY PER ASSY	UNIT COST	COST PER SQ. FT.	PERCENT COST OF ASSEM.
-3	CORRUGATION	300	6208.20	533.55	61.41
-5	RING FRAME	240	3165.08	217.61	25.05
-7	SPLICE-FRAME	240	28.69	1.97	0.23
-9	SPLICE-LONG.	300	483.66	41.57	4.78
-13	SPLICE-CAP	480	30.38	4.18	0.48
-15	SPLICE-TRNV.	240	322.68	22.19	2.55
-1	ASSEMBLY	1	166508.49	47.70	5.49

FINAL COST OF ASSEMBLY=6 5000=/IN 3032598.44
 FINAL COST PER SQ.FT. OF ASSEMBLY 868.77

TOTAL MATERIAL COST PER ASSEMBLY	2516872.84	PERCENT ASSEMBLY COST	82.99
TOTAL FABRICATION COST PER ASSEMBLY	499149.25	PERCENT ASSEMBLY COST	16.46
TOTAL PRORATED TOOLING COST PER ASSEMBLY	16576.44	PERCENT ASSEMBLY COST	0.55

FOLLOW-ON TESTING PROGRAM

Introduction

The analytical and design effort reported herein has resulted in efficient and feasible structural concepts for uniaxially loaded, double-wall cylinders. The design concepts selected as optimum, producible versions for lightweight shell structures have been signified in previous sections of this report. This study has revealed that the selected double-wall concepts represent practical designs which will significantly reduce the weight of similar structural portions of Saturn V designed with conventional ring-frame concepts.

In view of these findings, a follow-on test program is recommended to provide experimental verification of the strength and weight analyses reported in this document. In addition to supporting the strength and weight conclusions, the follow-on effort will provide additional insight into the pertinent cost factors involved in the manufacture of the optimum double-wall design concepts, and will establish the practicality and inherent reliability of the optimum cost-weight concept. It is believed that only through the actual fabrication and testing of the optimum design details can a true realization of the outstanding potential of the double-wall cylinder concepts be attained.

Proposed Follow-On Program Plan

The proposed follow-on program is divided into categories as follows:

1. Program Plan and Definition
2. Design and Analysis
3. Specimen Fabrication
4. Structural Testing
5. Data Reduction and Correlation
6. Final Report

It is anticipated that this follow-on program will be of ten months duration, including presentation of the final report. See Reference 21 for a display of the time and effort phasing of the proposed plan.

Test Program Scope

The most promising configurations, as determined by the design investigation, are recommended for test evaluation.

In order to obtain a maximum of significant test data, as expeditiously and economically as possible, the proposed program places emphasis on both the cover panel concepts and the substructure concepts.

Short Column Tests

Short column test specimens of the selected cover panel concepts will provide test verification for local and panel compression allowables, and provide checks on the strength, weight, and cost data for the axial load-carrying material. The compression allowables for local and panel stability provide the most meaningful data for comparison of structural efficiency.

From the analyses shown in previous sections of this report, it can be shown that the comparative efficiency factors for various cover panel concepts are of prime importance to the attainment of the minimum weight indicated by double-wall design concepts. For instance, the effective thickness, (and hence, weight), of a given cover panel concept is given by the expression,

$$\bar{t} = \left[\frac{N_x L}{\epsilon \eta E} \right]^{1/2}$$

Where ϵ is the efficiency factor for the given cover panel concept. The efficiency factor is determined from a simultaneous mode optimization analysis, and, for wide column concepts, is dependent upon the local buckling coefficient and the shape factor for the cross section. Considering the equation for effective thickness previously noted, a divergence of the actual efficiency from the analytical efficiency produces an undesirable effect on weight. One of the aspects of the efficiency factor that can be verified experimentally with short column specimens is the local buckling effect. Demonstration of the validity of the assumed local buckling characteristics of the optimum cover panel concepts is essential before general stability tests are performed.

The proposed short column test program for verification of local buckling characteristics is for specimens, each approximately 4 inches long in the direction of loading, and 6 inches to 8 inches wide. The total number of specimens is determined by permuting the following design parameters:

- 2 materials (Titanium and one other are suggested)
- 3 cover concepts (Truss core sandwich, truss core semi-sandwich, and trapezoidal corrugation are suggested)
- 4 load levels
- 2 replicates
- 48 (total recommended)

A four inch column length is considered practical, since the end fixity of the test platens will eliminate column failure. The width of 6 inches of 8 inches will provide a sufficient lateral dimension to include several pitches of the skin-stiffener combinations. The two optimum materials of construction will be determined from the weight-strength analyses of the double-wall concepts, and will be state-of-the-art materials. (Titanium and one other are suggested.) The three cover concepts selected will be the first, second, and third best designs based on the weight-strength analyses, and the selected load levels will be compatible with those selections. (Truss core sandwich, truss core semi-sandwich, and trapezoidal corrugation are suggested.) At least two replicates of each material/design concept are necessary to demonstrate a measure of concept reliability and lend credence to the test results. Appropriate load-deformation data will demonstrate the local stability characteristics of the selected material/design concepts by providing data on buckling and ultimate stress levels. See Figure 82 for a pictorial representation of the short column test program and a typical expected data-theory comparison graph. All tests will be conducted at room temperature. No strain gage instrumentation is considered necessary for these tests. Recordings will be made of actual panel dimensions, weight, buckling load, and failure load. Photographs are to be taken of the completed panels and the failed specimens.

An associated product of this effort will be a comparative evaluation of the cost and weight data of the selected concepts. The cost data will, of necessity, reflect the limited production quantity of the contemplated program. However, the cost information can be quite beneficial in highlighting major cost considerations associated with each particular design, and in suggesting potentially favorable cost-weight trade-off avenues.

Panel Tests

Panel tests are recommended to ascertain the general stability characteristics of the selected optimum cover panel concepts. The number, 48, and the suggested concepts and materials, are intentionally designed to match the short column test program specimens determined by permitting 2 materials, 4 load levels, 3 cover panel concepts, and two replicates of each.

The panel test specimens are expected to be approximately 6 inches by 24 inches in size. The test conditions will be for simply supported plates and wide column specimens, where the support conditions will be provided by appropriate fixturing around each specimen. All specimens will be tested to failure at room temperature and load-deformation recorded.

This general stability data, coupled with the local stability information on identical specimens, will provide the basis for comparison of the theoretical structural efficiency values with the actual test demonstrations. Depending on the outcome of these results, appropriate adjustments in the predicted weight-strength variations of the three selected cover concepts will be made. These data will also be used as the basis for succeeding selections of optimum design concepts to be fabricated into larger, double-wall structural test specimens.

Local Stability Tests

2 Materials
3 Cover Concepts
4 Load Levels
2 Replicates

} 48 Specimens

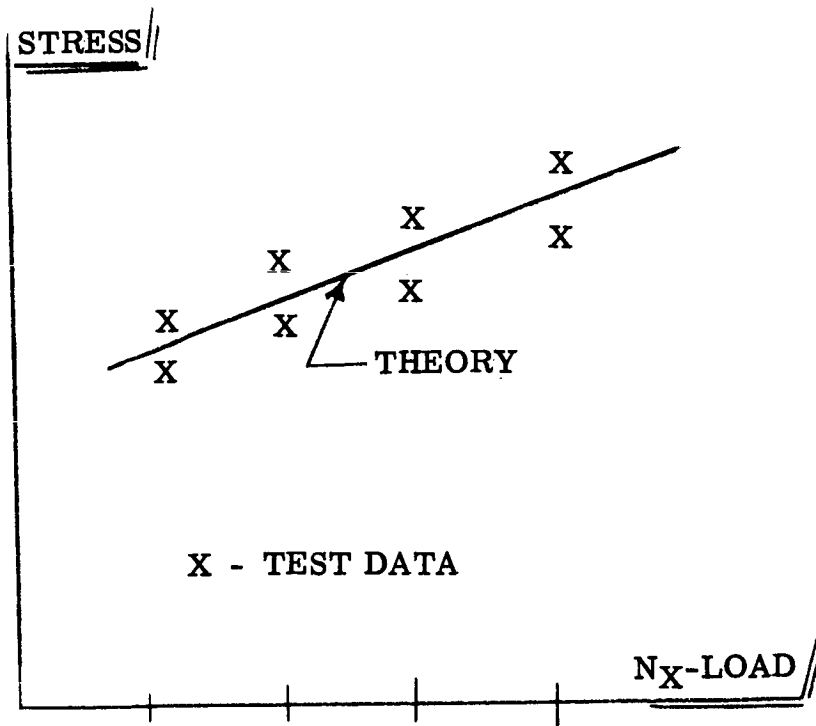
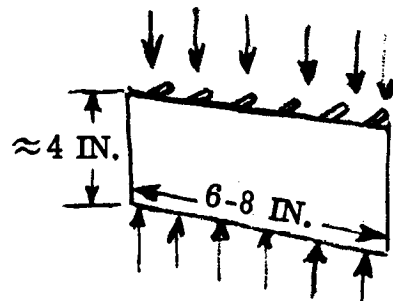


Figure 82. Test Values Versus Theory

Substructure Tests

A minimum of twelve substructure test specimens are recommended for: follow-on effort, three specimens of each of the two optimum types of substructure for two materials. These substructure specimens are essential to the overall demonstration of the stability characteristics of the double wall shell concept. Due to the complex nature of the possible failure modes of the double-wall shell, the substructure separating the load-carrying facing sheets must be subjected to various out-of-plane loads. It is necessary to demonstrate that the actual shear stiffness of the substructure concepts will meet the analytical shear stiffness values determined in this program. Also, since the optimum substructures to be considered are bi-directional in nature, both circumferential and longitudinal, out-of-plane shear stiffnesses must be determined. The importance of these substructure specimens cannot be over emphasized. The total substructure stiffness is significantly affected by various local stiffnesses which are difficult to predict analytically. These local stiffnesses are influenced by design and fabrication details that are difficult to predict beforehand. Therefore, the most expedient solution to the determination of these substructure stiffnesses is to fabricate and test representative designs. A judicious combination of analytical optimization coupled with illuminating test data will provide the necessary substructure design insight so vital to the double-wall shell concept.

The recommended program for substructure stiffness verification consists of thirty six test specimens. The number of specimens required is determined by permitting the following design parameters:

- 2 materials (titanium and aluminum are suggested)
 - 3 cover panel concepts
 - 2 substructure concepts (sine-wave shear web and truss web are suggested)
 - 3 design variations
 - 1 load index
- 36 specimens

It is contemplated that the two materials of construction will be state-of-the-art materials, (titanium and aluminum are suggested), and the substructure concepts will be the two leading candidates from the initial weight-strength analyses, (sine-wave shear web and truss web are suggested). Each basic substructure concept will be designed in three variations, including such criteria as gages, lands, eccentricities, fastening concepts, fabrication procedures, and the like. It is expected that manufacturing cost considerations will be an important aspect of this effort. Stiffness considerations will also be of prime importance.

Each material/design substructure concept will be designed to provide the shear and support stiffnesses required for an appropriate shell design load level and support spacing criterion. Each design will be subjected to three different loading conditions; tests to determine shear stiffnesses longitudinally and circumferentially, and out-of-plane tension and compression tests to determine the influence of the local design. An appropriate cover panel will be attached to each substructure material/design concept to insure that the proper

detail effects are included in the tests. The overall size of these specimens will vary with the particular design considerations involved, but should not exceed approximately three feet by three feet in size. All testing will be at room temperature, and load-deflection diagrams will be recorded. Suitable photographic records of the tests will be maintained.

It is contemplated that the cover panels used in these tests, the short column, and the general stability specimens would all be taken from common larger assemblies for economy in fabrication.

Joint Tests

Joint structural test specimens are recommended for design, fabrication, and test in column compression to verify analytical and test predictions.

Each of the specimens will be fabricated from approximately 12 x 18 inch cover panels of selected optimums. These specimens will be tested at room temperature in a universal testing machine, and the failure load recorded. No strain gage instrumentation is proposed.

The total number of specimens is determined by permuting the following design parameters:

- 4 Cover/joining design concepts
- 2 Materials
- 3 Load levels

24 (Approximate number of specimens)

The cover/joint design concepts will be selected from the leading weight-strength shell concepts of the original double-wall optimization analyses. A cover/joint design is considered to encompass both cover panel and joint design variations. Two leading material candidates will be selected, and the load levels for design and test will be compatible with the structural/material concept being evaluated.

Double-Wall Concept Tests

NAA recommends fabrication of several double-wall structural compression panels of approximately six by six feet. The specimens will include the cover panels and supporting substructure and will include a circumferential and longitudinal splice joint. The completed specimens will be delivered to NASA for feasibility demonstration. The specimens for selection will be based upon the original optimization and design analyses.

Final Report

A final report is recommended to summarize both the analytical program and the testing data, with modified summary design curves where indicated by test results. The inclusion of the testing data into the analytical

portion of the overall program is considered of prime importance to the demonstration of the useful and practical applications of the double-wall shell concept to all future space hardware programs.

Alternate Experimental Analyses

The previous discussions and recommendations were concerned primarily with test specimens of small to moderate proportions. Demonstration of general stability characteristics requires large test specimens and is dependent upon manufacturing tolerances and end conditions. As an alternate to such a full-scale test program for these promising double-wall shell concepts, NAA/LAD recommends an analysis of the optimum configurations to determine the benefits of scale model fabrication and testing. A discussion of scale models is presented below:

Objectives of Experimental Analyses

The recent development of advanced structural concepts for aerospace structures requires growth in both design technology and experimental methods. As vehicle sizes are increased, and as test facility requirements become more complex, the testing of reduced-size models becomes more feasible. Considerable expense and calendar time can be saved through the study of full size structural behavior by use of model analysis.

The objective of experimental analysis, therefore, is to investigate specific behavioral characteristics of full-scale structures through the selection of significant parameters, application of similitude techniques, and experimental study of scale models.

Alternate Approaches to Experimental Analysis

The following candidate types of experimental models are available for consideration:

1. Unity-scale models subjected to simulated environments.
2. Reduced-scale models, subjected to scaled environments.
3. Unity scale segments, subjected to simulated boundary conditions, test loads and temperatures.
4. Experimental determination of elastic constants of structural concept segments, followed by computer evaluation of full-scale structure based upon experimentally determined elastic constants.

In the recommended follow-on test program, a study will be made of the relative values of the models indicated above. With regard to Model Class 2, for instance, the effects of scale-reduction will be presented in a manner so that expected parameter fidelity may be assessed in terms of decreasing model size.

REFERENCES

1. Blumrich, J.F., "A Rising Tide of Structural Problems", Astronautics and Aeronautics, pp 54-57, June 1965.
2. Mellin, S.C., "Design Investigation of Cylindrical Structures Other Than Honeycomb - Quarterly Report" NA-65-502, North American Aviation, Inc., Los Angeles, September 1965.
3. Cimino, R.V., "Producibility and Cost Analysis Quarterly Report in Support of Contract No. NAS8-20009, Design Investigation of Cylindrical Structures Other Than Honeycomb", North American Aviation, Inc., TFD-65-590, September 1965.
4. Emero, D.H., Spunt, L., "Optimization of Multiribs and Multiweb Wing Box Structure Under Shear and Moment Loads", AIAA, 1965.
5. Gerard, G., "Structural Stability Theory", McGraw-Hill Book Co., Inc., New York, 1962.
6. Shanley, "Weight/Strength Analysis", Dover Book Co.
7. Arie van der Neut, "The General Instability of Stiffened Cylindrical Shells Under Axial Compression", Report 314, National Aeronautical Research Institute, Amsterdam; in Reports and Transactions Vol. XIII, 1947, pg 557-584.
8. Arie van der Neut, "General Instability of Orthogonally Stiffened Cylindrical Shells", NASA TN1510, pg 309-321.
9. Zahn, J. and Kuenzi, E., "Classical Buckling of Cylinders of Sandwich Construction in Axial Compression - Orthotropic Cores", U.S. Forest Service Research Note FPL-018, November 1963.
10. Johnson, A., Charts Relating to the Compressive Shear and Buckling Stresses of Longitudinally Supported Plates to the Effective Deflectional Stiffness of the Supports", NACA TN 4188, February 1958.
11. Budiansky, B. Deide, P., and Weinberger, R., "The Buckling of A Column on Equally Spaced Deflectional and Rotational Springs", NACA TN 1519, March 1948.
12. Emero, D.H., "Tabulation of Cover Panel, and Substructure Data for Design Investigation", NA-65-502-1, September 1965.
13. Gerard, George, "Handbook of Structural Stability, Part IV - Failure of Plates and Composite Elements", August 1957, p 5.

14. Thielmann, W.F., "New Developments in The Non-Linear Theories of Buckling of Thin Cylindrical Shells", Aeronautics and Astronautics, Proceeding of the Durant Centennial Conference, pp 76-121, Pergamm Press, 1960.
15. Almroth, B.O., "Post Buckling Behavior of Orthotropic Cylinders Under Axial Compression", AIAA Journal, Vol. 2, No. 10, October 1964.
16. Rehfield, L.W., "Further Study of the Effect of Edge Restraint on the Buckling of Axially-Compressed Circular Cylindrical Shells", SUDAER No. 237, Stanford University, May 1965.
17. Timoshenko, S., "Theory of Elastic Stability", New York, McGraw-Hill Book Co., Inc., 1952, pp 430-453.
18. Anderson, Roger A., "Structures Technology - 1964", Astronautics and Aeronautics, December 1964, pp 16-17.
19. Gerard, George, "Compressive Stability of Orthotropic Cylinders", Journal of the Aerospace Sciences, October 1962, pp 1177-1178.
20. March, H.W. and Kuenzi, E.W., "Buckling of Cylinders of Sandwich Construction in Axial Compression", Forest Products Laboratory Report No. 1830, December 1957.